ABSTRACT

Title of Dissertation: BIODEPOSITION AND BIOGEOCHEMICAL PROCESSES IN SHALLOW, MESOHALINE SEDIMENTS OF CHESAPEAKE BAY

Rebecca R. Holyoke, Doctor of Philosophy, 2008

Directed By: Research Associate Professor Jeffrey C. Cornwell
Marine Estuarine Environmental Science

Stocks of the eastern oyster, *Crassostrea virginica*, have been declining in Chesapeake Bay since the late 19th century, and current strategies involve restoring culture of *C. virginica* on-bottom and in devices suspended within the water column. Subtidal suspension culture of *C. virginica* in Chesapeake Bay occurs mostly in sheltered inlets and tidal creeks and, thereby, has the potential to influence shallow water biogeochemical processes. To assess the influence of *C. virginica* biodeposits and benthic microalgae on sediment nitrogen and phosphorus exchange, field studies with *C. virginica* held in aquaculture floats and laboratory experiments were conducted. Enhanced organic nitrogen deposition from *C. virginica* biodeposits led to gradual increases in surface sediment nitrogen and pore water ammonium concentrations; however, modifications to pore water concentrations were not always expressed at the sediment-water interface.

Benthic microalgae often modulated the influence of biodeposits on sediment nitrogen exchange but, as observed in laboratory experiments, the supply of nitrogen from *C. virginica* biodeposits may exceed their biological demand. Organic carbon from biodeposits had varying influences on aerobic respiration but consistently stimulated anaerobic metabolism. Shifts in net phosphorus exchange were driven by this anaerobic remineralization and concentrations of iron and manganese oxy(hydr)oxides, with transitions in fluxes coinciding with changes in benthic photosynthesis and oxidation of surface sediments. Manganese and iron oxy(hydr)oxides from biodeposits supported incorporation of added phosphorus and prevented exchange at the sediment-water interface in the absence of iron-sulfide mineral formation. Differences in the response of shallow water sediments to *C. virginica* biodeposits were due to the quality and quantity of biodeposits supplied, as well as the spatial and temporal variability within these sediments. Initial conditions and corresponding reference sediments illustrated the potential for sediment biogeochemistry and nutrient exchange from tidal creek sediments to vary spatially and temporally on relatively small scales. Factors influencing variability within tidal creek sediments were related to shifts in riverine freshwater inputs, macroalgal blooms, nutrient concentrations in overlying waters, and bioirrigation from the clam, *Macoma balthica*.

BIODEPOSITION AND BIOGEOCHEMICAL PROCESSES IN SHALLOW, MESOHALINE SEDIMENTS OF CHESAPEAKE BAY

By

Rebecca R. Holyoke

Dissertation submitted to the Faculty of the Graduate School of the
University of Maryland, College Park, in partial fulfillment
of the requirements for the degree of
Doctor of Philosophy
2008

Advisory Committee:

Professor Jeffrey C. Cornwell, Chair
Professor Roger I. E. Newell
Professor Lawrence P. Sanford
Professor Roberta L. Marinelli
Professor George W. Luther, III, University of Delaware
Professor Patrick C. Kangas, Dean's Representative

Dedication

Eva Marie and Elissa Corinne

May you also be fortunate enough to receive strength, encouragement, and compassion from your family and friends . . . for these are the gifts that make any dream attainable

Acknowledgements

Throughout my dissertation, I have been fortunate enough to receive an immense amount of guidance, enlightenment, support and love from a whole host of individuals – ranging from family and friends to faculty, technicians, and staff. My journey over the last . . . dare I say 5 ½ years . . . never would have been possible without the scientific and personal network I made during my time in Cambridge. As I reflect back on this process, I just hope that each of you know just how much appreciation I have for you and all that you helped me accomplish. A complete dissertation . . . at least in my eyes . . . is not something achieved by a single individual but all those who were along for the ride.

I would first like to express my appreciation and respect for my dissertation examining committee: Jeffrey C. Cornwell, Roger I. E. Newell, Lawrence P. Sanford, Roberta L. Marinelli, George W. Luther, III, and Patrick C. Kangas. Your advice throughout this process has been irreplaceable; individually and collectively you have helped me polish my dissertation research into chapters that I am proud to present to the scientific community. I have the utmost appreciation and respect for my advisor, Jeff Cornwell, who has guided me through this dissertation process with much patience. He has supported me throughout all my wavering and confusion, as a friend and mentor, and for that I am truly thankful. I offer special thanks to Roger Newell for always knowing how to motivate me, for supporting me through my rollercoaster emotions, and most importantly, for introducing me to interdisciplinary science (e.g., eastern oysters, erosion of biodeposits). I am grateful to Larry Sanford for educating me on sediment resuspension and erosion microcosms; without his support, I would still be shy of

becoming a proper sediment biogeochemist. I am grateful to Roberta Marinelli for continually motivating me to address the ecological relevance of my research. Always pushing me to ask the questions: What does this mean? And what influence does this have down the line? I offer my thanks to George Luther for introducing me to the intimate details of marine inorganic chemistry, particularly oxidation-reduction reactions and molecular orbital theory, and for supporting me financially during revisions. Concurrent with Roberta's emphasis on how biology affects chemistry was always George's perspective on how chemistry affects biology. And to my Dean's Representative, Patrick Kangas, I thank you for your unending enthusiasm; it was refreshing being able to discuss my interests with a scientist engaged in similar research.

I have much appreciation for all those in the Cornwell laboratory: Michael Owens, Erica Kiss, Christopher Chick, Theresa Coley, Jessica Burton Evans, Eric Nagel, Jennifer O'Keefe, Sara Rhoades, and Jessica Nagel (honorary member). I have depended on each of you for your knowledge, advice, and physical support with laboratory experiments and analyses, but most of all, I just wanted to say thank you for always sharing in my frustrations. I would especially like to thank Mike Owens for offering so much of his time to helping me hash out my experimental designs and always assisting with data analyses and equipment construction. Somehow you always know how to fix the problem (with your magic touch) and what to say to put my thoughts into perspective. I would also like to thank Steve Suttles and Patrick Dickhudt, with whom I conducted the 2006 and 2003 erosion microcosm experiments. I am most appreciative of your assistance with equipment design and construction, MatLab programming, and paired-

core analyses. Additional gratitude goes out to Elizabeth North, Raleigh Hood, and Jiangtao Xu for discussions on the importance of these experiments.

I am extremely grateful to Stephanie Alexander, Don Meritt, Ben Parks, Angela Padeletti, Chris Markin, Bob Carey, and the Oyster Recovery Partnership (and crew) for providing *Crassostrea virginica*. I especially thank Don Meritt and Clarissa Rounsaville for assistance with collection of *C. virginica* biodeposits, and Melissa Radcliffe and Angela Padeletti for chlorophyll, temperature, and salinity data. I thank Vincent Adams and the Radiation Facility at the University of Maryland College Park for irradiating homogenized biodeposits, and Mohamad Al-Sheikhly for granting me permission to use this facility. I thank Vic Kennedy and Stephanie Hurder for identifying and determining biomass of the clam, *Macoma balthica*, and Stephanie for her long hours at the microscope counting fluorescent particles for preliminary dispersal analyses. Off-bottom aquaculture of *C. virginica* and sediment core collection never would have been possible without Bill Boicourt, Posey Boicourt, and Mr. and Mrs. Donald Kerstetter. Thank you for granting me access to La Trappe Creek via your properties.

I thank Todd Kana for the use of his membrane-inlet mass spectrometer for dissolved gas analyses, and David Weiss for technical support with this instrument. I am grateful to Analytical Services, especially Lois Lane, Crystal Thomas, Laurie Van Heukelem, and Sara Rhoades, for analyzing samples for carbon, nitrogen, chlorophyll *a* and $NO_2^- + NO_3^-$ concentrations. I also thank Erin Markin and Andy Lazur for use of their Teklight light bank, and Bahram Momen, Howard Townsend, and David Kimmel for their assistance with statistics. An additional thank you goes out to David Kimmel for helping me locate stream flow data for the Greensboro water gauge station. I am grateful

for the presentation and graphical assistance that I received from Tim Carruthers, Tom Fisher, Greg Radcliffe, Anne Gustafson, Maureen Brooks, and the Integration and Application Network.

I would like to thank the maintenance staff at Horn Point Laboratory, especially Blaise Brown, Gordy Dawson, James (Bear) Kampmeyer, Ralph Kimes, and Richie Long, for their field and laboratory assistance. I truly appreciate your willingness to lend a hand whether it was to prep the boats or as simple as cutting PVC for new standpipes. I thank everyone in the HPL business office, especially Jane Gilliard for her willingness to search for a solution. I appreciate the technical and audio visual support of Patrick Maloney, Shoujun Fan, and Anne Willey. I am grateful to Darlene Windsor for always doing whatever it takes to locate the book or article that you just have to have that minute. And a very special thank you goes to Jack Seabrease! Jack, you are the best machinist I have ever met, and I have no idea how I am going to develop an experiment without you. You had to have designed and constructed almost every piece of equipment I used while at Horn Point.

Financial support for this dissertation was provided through the Maryland Sea Grant program, the Dr. Nancy Foster Scholarship Program, and the Keith Campbell Foundation. Additional funding came from the Horn Point Education Committee and Marine Estuarine Environmental Science Program in the form of small grants, travel grants, and educational support. With each of these awards came tremendous support from various individuals and offices. I would especially like to thank Fredrika Moser, Jonathan Kramer, Theresa Lee, Susan Leet, Erica Goldman, Ruth Moore, Priti Brahma, Haja Bah, Kadija Baffoe-Harding, Arlene Simpson Porter, Amy Sipps, Nancy Jones,

Phyllis Rhoades, Patricia Dekker, Mike Roman, Pat Glibert, Diane Stoecker, Evamaria Koch, Ken Paynter, and Debbie Morrin-Nordlund.

Lastly to my family and friends . . . without hesitation each of you has stood beside me throughout this trying process. All of you have in your own way given me strength, encouragement and compassion, and for that I am truly grateful. Your support has ranged from everyday chats or moments of tears to standing in the midst of a hurricane just to prevent me from losing a summer of work. I hope you all know how special you are to me, and that I wish you all the success you have helped me achieve. I owe the greatest thank you to all of you . . . The Holyoke's – Mom, Dad, Brother, Yvonne, Eva, and Elissa, Joe Filipowicz, the rest of the Filipowicz's, Twix, Carrie (Brock) Schmid, Mike Owens, Ralph Kimes, Kevin Rosemary, the VFW and Canvasback crews, Jeremy Testa, Jessie Burton Evans, Jess Nagel, Eric Nagel, Clarissa Rounsaville, Erica Kiss, Angela Padeletti, Shannon Freeman, Jennifer O'Keefe, and Steve Suttles. And to the one who loves me unconditionally, I love you too!

Table of Contents

Dedication ii
Acknowledgements iii
Table of Contents viii
List of Tables xii
List of Figures xiv

Chapter 1: Introduction and Overview 1
Introduction 2
Objectives and Hypotheses 5
Synopsis 7
Chapter 2 7
Chapter 3 8
Chapter 4 10
Chapter 5 11
Conclusions 12
Figure Legends 14

Chapter 2: Variability in Sediment Biogeochemistry and Nutrient Exchange within Tidal Creeks of Mesohaline Chesapeake Bay, USA 27
Abstract 28
Introduction 29
Materials and Methods 31
Study sites 31
Sediment core collection and aerobic incubations 32
Nutrient flux incubations 33
Bioirrigation by benthic infauna 35
Surface sediment, pore water, and solid-phase collection 35
Analyses 37

Results and Discussion 39
Characterization of surface sediments 39
Factors influencing sediment oxygen consumption 41
Deviations in benthic oxygenic photosynthesis 44
Shifts in nutrient exchange at the sediment-water interface 45
Temporal variability in pore water profiles and bioirrigation 48
Summary and Conclusions 51
Acknowledgements 53
Figure Legends 59

Chapter 3: Biogeochemical Responses of Shallow Water Sediments to Small-scale Aquaculture of the Eastern Oyster, *Crassostrea virginica* 75
Abstract 76
Introduction 77
Materials and Methods 80
Study sites 80
Sedimentation traps 81
Sediment core collection and incubations 82
Surface sediment, pore water, and solid-phase collection 85
Results 87
Deposition 87
Surface sediments 88
Net ecosystem metabolism 90
Pore water NH_4^+ profiles 91
Nitrogen fluxes 93
Sedimentary sulfur 95
Discussion 97
Acknowledgements 106
Figure Legends 114

Chapter 4: Temporal Variation in Sediment Nitrogen and Phosphorus Fluxes as Mediated by the Interactions of Benthic Microalgae and Organic Deposition 132
Abstract 133
Introduction 134
Materials and Methods 139
Sediment core collection 139
Sediment core incubations 140
Analyses 143
Results 146
Initial conditions 146
Benthic microalgal biomass 147
Temporal variations in measured fluxes 148
Discussion 153
Sediment metabolism and benthic photosynthesis 153
Net ecosystem metabolism and the trophic classification of sediments 156
Influence of sediment metabolism and benthic photosynthesis on nutrient cycling 158
Transitions in nitrogen and phosphorus exchange: Disconnect with trophic status 164
Conclusions 168
Acknowledgements 169
Figure Legends 184

Chapter 5: Dynamic Response of Pore Water and Solid-phase Constituents to Perturbations in Benthic Photosynthesis and Organic Matter Deposition 195
Abstract 196
Introduction 197
Materials and Methods 201
Sediment core collection and incubation 201
Pore water and solid-phase sectioning 203
Analyses 204
Results 208

Initial conditions 208
Biodeposits 210
Surface sediments 211
Pore water profiles 212
Solid-phase profiles 216
Microelectrodes 218
pH 220
Discussion 220
Acknowledgements 230
Figure Legends 238

Appendix A: Critical erosion threshold of eastern oyster (*Crassostrea virginica*, Gmelin) biodeposits: influence of feces, pseudofeces, and incorporation within sediments 252
Objectives and Hypotheses 253
Materials and Methods 253
Sandpaper 1-6 (BDR03-08) 253
Sediment 1-15 (BDR09-23) 255
Field validation with benthic microalgae (Sediment 16-17, Trap 1-4) 258
Modified-Gust microcosm 258
Statistical analyses 259
Acknowledgements 260
Figure Legends 263

Appendix B: Raw data (mean ± standard deviation) and the comparison of least squares means for significant ($P < 0.05$) main effects, and additional figures for Appendix A 276
Figure Legends 289

References 300

List of Tables

(Abbreviated)

2.1 Water column and surface sediment (0-1 cm) characteristics for locations within the tidal reaches of La Trappe Creek

2.2 Percent organic content (550°C) and concentrations of sediment chlorophyll *a* for the 0-1 cm depth interval of sediment

3.1 Sample logistics and water column and surface sediment characteristics for three sampling locations in the upper, mesohaline portion of La Trappe Creek, Maryland, USA

3.2 Quantitative description of small-scale aquaculture of *Crassostrea virginica* (eastern oyster) at three sampling locations in a tidal creek of the Choptank River, Chesapeake Bay, Maryland, USA

3.3 Deposition of total nitrogen and surface sediment concentrations of total nitrogen and chlorophyll *a* from Oyster and Reference sites in Lowry Cove, Mainstem, and Pier

4.1 Physical and chemical properties of the location of sediment core collection within the main-stem of La Trappe Creek (38° 39.223' N, 076° 05.267' W), a tributary of the Choptank River sub-estuary (Chesapeake Bay, USA), on 31 August 2005 between approximately 12 pm and 3 pm

4.2 Summary statistics for nutrient (O_2, N_2, NH_4^+, SRP) flux incubations and sediment (0-1 cm) chlorophyll *a*

4.3 Sediment chlorophyll *a*, as a proxy for benthic microalgal biomass, for the initial state of La Trappe Creek sediments and four treatments developed from two surface sediment irradiances and two biodepositional loadings

4.4 Sediment exchange of N_2 and $NO_3^- + NO_2^-$ from HL, HH, LL, and LH sediment cores initially and after 4, 10, 13, and 19 days of treatment

4.5 Trophic status for HL, HH, LL, and LH sediment cores initially and after 4, 10, 13, and 19 days of treatment

4.6 Fluctuations in the direction of nitrogen and phosphorus exchange at the sediment-water interface during dark and light sediment core incubations prior to and after 4, 10, 13 and 19 days of particulate organic matter loading

5.1 Solid-phase concentrations of total C, N, and P and HCl-extractable Mn and Fe collected from subsamples of eastern oyster (*Crassostrea virginica*) biodeposits

added to laboratory-incubated sediment cores and the total concentration of these nutrients added over 19 days for the two experimental loadings

5.2 Depth-integrated (0-1 cm) solid-phase and pore water concentrations for the initial condition of La Trappe Creek sediments and the four experimental treatments after 19 days of loading

5.3 Depth-integrated (0-10 cm) solid-phase and pore water concentrations for the initial condition of La Trappe Creek sediments and the four experimental treatments after 19 days of loading

5.4 Mean ratios of total carbon, nitrogen, and phosphorus within surface sediments from La Trappe Creek initially and after 19 d of treatment exposure

A.1 Cumulative eroded mass at critical shear stress values of 0.10, 0.20, and 0.30 Pa for sediment cores collected from La Trappe Creek

B.1 Background total suspended solid concentrations determined for replacement water pumped through sandpaper cores

B.2 Cumulative eroded mass for each combination of treatment, volume, and defined critical shear stress established in Sandpaper experiments 1-6 (BDR03-08), and the comparison of least squares means for significant main effects

B.3 Loss on ignition at 450°C for each combination of treatment, volume, and applied shear stress established in Sandpaper experiments 1-6 (BDR03-08), and the comparison of least squares means for significant main effects

B.4 Cumulative eroded mass for each combination of treatment, time, and defined critical shear stress established in Sediment core experiments 1-15 (BDR09-23), and the comparison of least squares means for significant main effects

B.5 Loss on ignition at 450°C for each combination of treatment, time, and applied shear stress established in Sediment core experiments 1-15 (BDR09-23), and the comparison of least squares means for significant main effects

List of Figures
(Abbreviated)

1.1 Annual landings of *Crassostrea virginica* in Maryland and Virginia from 1950 through 2006 and the number of market *C. virginica* sold by Virginia aquaculturists in 2005, 2006, and predicted for 2007

1.2 Conceptual diagram of the potential influence of *Crassostrea virginica* biodeposits on nitrogen removal through burial of particulate organic nitrogen and enhancement of coupled nitrification-denitrification

1.3 Conceptual diagram of the potential influence of benthic photosynthesis and microalgal assimilation on regeneration and exchange of nitrogen from added *Crassostrea virginica* biodeposits

1.4 Conceptual diagram of the potential influence of benthic microalgae and *Crassostrea virginica* biodeposits on phosphorus exchange across the sediment-water interface

1.5 Conceptual diagram of the influence of *Crassostrea virginica* biodeposits on surface sediment concentrations of particulate organic nitrogen and N_2-N fluxes

1.6 Conceptual diagram of the influence of *Crassostrea virginica* biodeposits on nitrogen regeneration and exchange

1.7 Conceptual diagram of the combined influence of benthic microalgae and particulate organic matter from *Crassostrea virginica* biodeposits on nitrogen and soluble reactive phosphorus fluxes

1.8 Conceptual diagram of the influence of benthic microalgae and particulate organic matter from *Crassostrea virginica* biodeposits on soluble reactive phosphorus exchange and associated oxidation-reduction processes

1.9 Conceptual diagram of the influence of *Crassostrea virginica* aquaculture on shallow water sediments supporting benthic microalgal communities

2.1 Location of study sites within La Trappe Creek, a tributary of the Choptank River, Chesapeake Bay, Maryland, USA

2.2 Surface sediment concentrations of total nitrogen versus total carbon and HCl-extractable iron versus inorganic phosphorus for cores collected at study sites located within Oyster bar, Lowry Cove, Pier, and Mainstem

2.3 Medians, first and third quartiles, and ranges for dark O_2 fluxes, light O_2 fluxes, gross primary productivity, and net ecosystem metabolism for cores collected at study sites located within Oyster bar, Lowry Cove, Pier, and Mainstem.

2.4 Mean dark O_2 fluxes and rates of net ecosystem metabolism for study sites revisited in Lowry Cove, Pier, and Mainstem in 2002 and 2003

2.5 Monthly and daily stream flow for the Greensboro water gauge station, Choptank River, Chesapeake Bay, Maryland versus dark O_2 fluxes for sediment cores collected within Oyster bar, Lowry Cove, Pier, and Mainstem

2.6 Mean dark N_2-N fluxes for cores collected at study sites located within Oyster bar, Lowry Cove, Pier, and Mainstem

2.7 Mean light N_2-N fluxes for cores collected at study sites located within Oyster bar, Lowry Cove, Pier, and Mainstem

2.8 Mean dark $NO_3^- + NO_2^-$ fluxes for cores collected at study sites located within Oyster bar, Lowry Cove, Pier, and Mainstem

2.9 Mean light $NO_3^- + NO_2^-$ fluxes for cores collected at study sites located within Oyster bar, Lowry Cove, Pier, and Mainstem

2.10 Mean fluxes of O_2 versus NH_4^+ and soluble reactive phosphorus for dark and light incubations of sediment cores collected within Oyster bar, Lowry Cove, Pier, and Mainstem

2.11 Mean pore water concentrations of NH_4^+ and Br^- measured or modeled within sediment cores from sites revisited in Pier and Mainstem

3.1 Deposition of total nitrogen and surface sediment concentrations of total nitrogen and chlorophyll *a* on sampling dates (July – September 2002) for Lowry Oyster and Reference sites

3.2 Deposition of total nitrogen and surface sediment concentrations of total nitrogen and chlorophyll *a* on sampling dates (July – September 2003) for Mainstem Oyster and Reference sites

3.3 Deposition of total nitrogen and surface sediment concentrations of total nitrogen and chlorophyll *a* on sampling dates (May – July 2003) for Pier Oyster and Reference sites

3.4 Mean percent organic content for material collected in sedimentation traps (deposition) and surface sediments retrieved from Lowry, Mainstem, and Pier

3.5 Mean ratios of total carbon to nitrogen for material collected in sedimentation traps (deposition) and surface sediments retrieved from Lowry, Mainstem, and Pier

3.6 Mean rates of net ecosystem metabolism, determined from dark and light O_2 fluxes, for Oyster and Reference sites on sampling dates at Lowry, Mainstem, and Pier

3.7 Mean pore water NH_4^+ concentrations in sediment cores collected from Oyster and Reference sites at Mainstem, Lowry, and Pier

3.8 Mean NH_4^+ flux during dark and light incubations for Oyster and Reference sites on sampling dates

3.9 Mean N_2-N flux during dark and light incubations for Oyster and Reference sites sampled at Lowry, Mainstem, and Pier

3.10 Mean pore water concentrations of total dissolved sulfide in sediment cores collected from Oyster and Reference sites at Mainstem, Lowry, and Pier

3.11 Pore water concentration ratios of sulfate to chloride in sediment cores collected from Oyster and Reference sites at Lowry, Mainstem, and Pier

3.12 Solid-phase profiles of acid-volatile sulfide and chromium-reducible sulfide in duplicate sediment cores from Mainstem Oyster and Reference on 23 July and 25 September 2003

3.13 Relationship of benthic biomass to shell length for the clam, *Macoma balthica*, and biomass present in cores collected from Pier Oyster and Reference

4.1 Schematic of the systematic arrangement of sediment cores and incubation tanks held in a temperature-controlled chamber at 28 °C under a diel cycle of 14 h of light and 10 h of darkness

4.2 Mean O_2 flux during dark and light incubations for four treatments (HL, HH, LL, LH) developed from two surface sediment irradiances and two biodepositional loadings

4.3 Mean estimates of gross primary productivity and net ecosystem metabolism for four treatments (HL, HH, LL, LH) developed from two surface sediment irradiances and two biodepositional loadings

4.4 Mean NH_4^+ flux during dark and light incubations for four treatments (HL, HH, LL, LH) developed from two surface sediment irradiances and two biodepositional loadings

4.5 Mean soluble reactive phosphorus flux during dark and light incubations for four treatments (HL, HH, LL, LH) developed from two surface sediment irradiances and two biodepositional loadings

4.6 Measured gross and net daily N_2-N + NH_4^+ and soluble reactive phosphorus fluxes versus predicted fluxes determined from stoichiometric conversions of gross and net ecosystem metabolism

4.7 Photographs illustrating the progression of benthic microalgal mat thickness in a representative high light, high loading (HH) and low light, high loading (LH) sediment core initially and after 6-12 d of POM additions

5.1 Pore water profiles of NH_4 and SO_4^{2-} to Cl^- ratios for the initial state of La Trappe Creek sediments and four treatments developed from two surface sediment irradiances and two biodepositional loadings

5.2 Pore water profiles of soluble reactive phosphorus, total dissolved iron, sulfate, and total dissolved sulfide

5.3 Solid-phase profiles of HCl-extractable Mn, HCl-extractable Fe, acid-volatile sulfide, and iron oxy(hydr)oxides

5.4 Dissolved O_2 and pH profiles for the initial state of La Trappe Creek sediments and four treatments developed from two surface sediment irradiances and two biodepositional loadings

5.5 ΣH_2S profiles within surface sediments of incubated cores prior to the first and 19th addition of POM, as determined with amperometric microsensors for $H_2S_{(g)}$ and pH

5.6 Pore water NH_4^+ and soluble reactive phosphorus concentrations versus the corresponding SO_4^{2-} concentrations measured initially and upon conclusion of the experiment

5.7 Calculated pore water upward fluxes of NH_4^+ and soluble reactive phosphorus versus the corresponding sediment fluxes measured in the dark upon conclusion of the experiment, after 19 days of loading

5.8 Dissolved inorganic carbon fluxes estimated from stoichiometric conversions of net ecosystem metabolism for four treatments developed from two surface sediment irradiances and two biodepositional loadings

5.9 Potential interactions of oxidized and reduced forms of iron, manganese, and sulfur species and their combined influence on the retention and mobility of phosphorus within sediments

A.1 Schematic of the experimental design for Sandpaper 1-6 (BDR03-08), conducted from 09 May through 11 May 2006

A.2 Schematic of the experimental design for Sediment 1-15 (BDR09-23), conducted from 25 May through 04 June 2006

A.3 Schematic of the modified-Gust microcosms (9.525 cm I.D.) used to expose *Crassostrea virginica* biodeposits and sediment cores to defined shear stresses

A.4 Erosion rates in time for Control and Treatment sediment cores from a representative Sediment experiment (Sediment 14, BDR16)

A.5 Cumulative eroded mass for each volume of feces and pseudofeces positioned on 320A grit (36 μm) wet-dry silicon carbide abrasive paper in Sandpaper 1-6 (BDR03-08) and cumulative eroded mass of feces and pseudofeces at 0.05 and 0.10 Pa

A.6 Cumulative eroded mass versus the age of biodeposits at three defined critical shear stresses for Treatment and Control cores combined

A.7 Loss on ignition at 450°C for applied shear stresses and the age of biodeposits for Treatment and Control cores combined (Sediment 1-15 (BDR09-23))

A.8 Profiles of critical shear stress with cumulative eroded mass for Treatment and Control cores from Sediment 8 (BDR10) and La Trappe Creek (Sediment 17, Trap2-4)

B.1 Cumulative eroded mass in kg and kg m^{-2} for each volume of feces and pseudofeces positioned on 320A grit (36 μm) wet-dry silicon carbide abrasive paper in Sandpaper 1-6 (BDR03-08) experiments

B.2 Erosion rates in time for 2.5 ml of feces and pseudofeces positioned on abrasive paper in a representative Sandpaper experiment (Sandpaper 2, BDR04)

B.3 Erosion rates in time for 10.6 ml of feces and pseudofeces positioned on abrasive paper in a representative Sandpaper experiment (Sandpaper 5, BDR07)

B.4 Comparison of critical shear stresses for Sandpaper 1-6 (BDR03-08) as determined with a modified version of the erosion formulation of Sanford and Maa (2001) and a new formulation, which assumes a constant critical shear stress, and the relationship of β/df and the cumulative eroded mass of feces and pseudofeces

B.5 Photographs illustrating eastern oysters (*Crassostrea virginica*) in submerged holding trays; pseudofecal material within a graduated pipette; a dual O-ring PVC disc covered with 320A (36 μm) waterproof abrasive paper; an adjustable PVC

disc used to level the sediment or sandpaper surface within cores; the erosion microcosm system; and the filtering rigs for 47 and 142 mm GF/F filters

B.6 Photographs illustrating pseudofeces and of feces within cores prior to the start of the 0.01 Pa flushing interval (Sandpaper 3, BDR05), and during the 0.10 Pa, 0.15 Pa, 0.20 Pa, and 0.30 Pa step intervals

B.7 Photographs illustrating Control and Treatment cores from Sediment 4 (BDR21) prior to the 0.01 Pa flushing interval and during the 0.20 Pa step interval

B.8 Photograph of a Treatment core (Sediment 1, BDR18) when an polychaete emerged from its burrow and consumed a proportion of added biodeposits

Chapter 1: Introduction and Overview

Introduction

Standing stocks of the eastern oyster, *Crassostrea virginica* (Gmelin 1791), have been declining in Chesapeake Bay since the late 19th century (Kennedy and Breisch 1981). Declines in *C. virginica* abundance have stemmed from oyster harvesting and the resulting loss of oyster reef habitats (Rothschild et al. 1994, Smith et al. 2003) and been exacerbated by mortalities from the protozoan parasites, *Perkinsus marinus* (Dermo) and *Haplosporidium nelsoni* (MSX, Ford and Tripp 1996). Continuous declines in the annual landings of *C. virginica* (Figure 1.1) and reductions in the potential for these suspension feeders to exert partial top-down control on phytoplankton and to enhance benthic-pelagic coupling (Newell 1988, Newell et al. 2005) have prompted efforts to restore stocks of *C. virginica* 10-fold from a 1994 baseline (http://www.chesapeakebay.net/agreement.htm, 19 June 2007). Current restoration strategies involve increasing stocks through the placement of hatchery-reared spat on existing oyster bars and increasing sub-tidal suspension (i.e., off-bottom) operations for growth (National Research Council 2004). Increases in *C. virginica* aquaculture have already been observed in Virginia, USA (Murray et al. 2007), with aquaculture comprising up to 69% of annual landings in 2005 through 2007 (Figure 1.1).

Off-bottom aquaculture of *C. virginica* in Chesapeake Bay typically occurs within sheltered inlets and tidal creeks, at relatively shallow water depths. Although these types of shallow waters constitute a large proportion of Chesapeake Bay, relatively few studies on sediment biogeochemistry have been conducted in shallow water sediments supporting benthic microalgal communities. Previous research has focused primarily on sandy sediment (Rizzo and Wetzel 1985, Murray and Wetzel 1987, Simon 1988, Rizzo

1990), and studies, including measurements of dissolved oxygen and nutrient fluxes, have been limited to single sites or individual sampling dates within seasons (Rizzo 1990, Reay et al. 1995). Lack of an understanding of these shallow water environments makes it difficult to discern what influence *C. virginica* biodeposits (feces and pseudofeces) may have on shallow water biogeochemistry, and ultimately, if increases in *C. virginica* aquaculture will serve as one means of restoring the ecological benefits of *C. virginica* to Chesapeake Bay.

The ecological function of *C. virginica* has been studied largely from the perspective of the influence of these suspension feeders on water column concentrations of nitrogen and reductions or increases in phytoplankton biomass (e.g., Dame et al. 1989, Dame et al. 1992, Dame and Libes 1993, Nelson et al. 2004). Increased water column concentrations and excretion of NH_4^+ have been used to suggest that *C. virginica* recycle nitrogen rapidly and, thereby, enhance water column production (Dame et al. 1984, Pietros and Rice 2003). Filtering and packaging of phytoplankton as biodeposits, however, has the potential to redirect particulate organic nitrogen (PON) to sediments and photosynthesis in shallow waters to benthic microalgae (Porter et al. 2004). The influence of PON from biodeposits on sediment nitrogen cycling, particularly nitrogen burial and denitrification, remains unclear (Newell et al. 2004, Newell et al. 2005). No measurements of denitrification, or N_2-N loss, have been conducted for sediments receiving *C. virginica* biodeposits or other shallow water sediments within Chesapeake Bay. Greater denitrification potentials have been observed in sediments beneath long-lines of *Crassostrea gigas* (Gilbert et al. 1997) and on culture ropes in New Zealand mussel farms (Kaspar et al. 1985).

Nitrogen exchange in shallow water sediments, outside of Chesapeake Bay, have been shown to vary with the assimilatory uptake of NH_4^+ and NO_3^- by benthic microalgae and associated competition between benthic photoautotrophs, nitrifiers, and denitrifiers (Sundback and Miles 2000, Risgaard-Petersen et al. 2004). Penetration of dissolved oxygen into sediments has varying effects on nitrogen fluxes at the sediment-water interface since it contributes to increases or decreases in coupled nitrification-denitrification (Tiedje et al. 1989, Risgaard-Petersen et al. 1994, Rysgaard et al. 1995, An and Joye 2001, Dalsgaard 2003) and decreases in direct denitrification (Rysgaard et al. 1995). Accumulation of biodeposits on surface sediments may further alter the influence of benthic microalgae on nitrogen retention and transformations through burial of the photoautotrophs or increased nutrient availability for growth (Gibbs et al. 2005).

Although *C. virginica* and benthic microalgae have both been shown to be important mediators in nitrogen cycling, less emphasis has been placed on understanding the influence of *C. virginica* biodeposits and benthic microalgae on sediment phosphorus exchange. Influences of benthic microalgae on phosphorus cycling have often been inferred from flux measurements (Graneli and Sundback 1985, Sundback and Graneli 1988, Rizzo 1990, Reay et al. 1995), deviations in nutrient stoichiometry, and the current understanding of phosphorus retention in near shore and continental margin sediments (e.g., Krom and Berner 1981; Sundby et al. 1992; Thamdrup et al. 1994; Slomp et al. 1996; McManus et al. 1997; Anschutz et al. 1998).

Studies in shallow, illuminated sediments have been compartmentalized to include only a portion of the interactions among dissolved oxygen, phosphorus, manganese, iron and sulfur species (e.g., Kostka and Luther 1995; Epping et al. 1998;

Rozan et al. 2002; Ma et al. 2006), and as such, it is unclear if the mineralization of organic phosphorus or the reduction of iron oxy(hydr)oxides is responsible for the availability of phosphorus for exchange at the sediment-water interface. Concurrent measurements of dissolved oxygen profiles and phosphorus fluxes have not been conducted in shallow water sediments, and yet, oxidation of iron (II) from benthic photosynthesis is thought to be responsible for phosphorus retention through chemical precipitation of iron oxy(hydr)oxides and associated adsorption of phosphate. For sediments positioned beneath *C. virginica* aquaculture, enhanced deposition has the potential to influence sediment phosphorus exchange through mineralization of non-refractory organic phosphorus (Ingall and Jahnke 1997). Rates of decomposition and supply of this labile organic matter are also relevant to the reduction of iron oxy(hydr)oxides and associated release of bound inorganic phosphorus. Production of dissolved sulfide from sulfate reduction may increase phosphorus effluxes even to shallow, oxygenated waters through the reduction of iron oxy(hydr)oxides and associated production of iron-sulfides (Rozan et al. 2002).

Objectives and Hypotheses

Throughout this dissertation, I addressed how biodeposits (feces and pseudofeces) from the eastern oyster, *Crassostrea virginica*, and benthic microalgae influence biogeochemical processes in shallow water sediments of Chesapeake Bay. Research was conducted to evaluate the individual and interacting influences of benthic microalgal assimilation, photosynthesis, and *C. virginica* biodeposits on nitrogen and phosphorus exchange at the sediment-water interface. Field and laboratory studies were performed

with tidal creek sediments (La Trappe Creek, Chesapeake Bay, Maryland) supporting benthic microalgae, as determined from sediment chlorophyll *a*, and reference sediments served to further the understanding of shallow water (<2 m) sediments within Chesapeake Bay. Specific attention was given to determining rates of net denitrification (N_2-N loss), NH_4^+ regeneration, and soluble reactive phosphorus (SRP) fluxes, and measurements of pore water and solid-phase constituents were used to infer the mechanisms responsible for exchange. Research presented in Chapters 2-5 offered insight into whether increasing *C. virginica* aquaculture in tidal creeks may be beneficial to the ecological restoration of Chesapeake Bay, and ultimately, how improving water clarity at existing oyster bars may alter nutrient cycling within surrounding sediments. The following research questions and hypotheses were addressed throughout Chapters 2-5. Additional data on the critical erosion threshold of *C. virginica* biodeposits are presented in appendices.

- Does the more rapid deposition of seston in the form of *Crassostrea virginica* biodeposits result in an increase in nitrogen removal through burial of particulate organic nitrogen and enhancement of denitrification in shallow water sediments?

  Hypothesis 1 Particulate organic nitrogen from *C. virginica* biodeposits enhances rates of denitrification through increased availability of NH_4^+ (from mineralization) for coupled nitrification-denitrification (Figure 1.2).

- How do regeneration, burial, and loss of particulate organic nitrogen from *C. virginica* biodeposits vary with changes in benthic photosynthesis?

Hypothesis 2 Mineralization of particulate organic nitrogen from *C. virginica* biodeposits increases effluxes of NH_4^+ from sediments to the water column (Figure 1.3).

Hypothesis 3 Benthic microalgal assimilation reduces the exchange of regenerated nitrogen from biodeposits, and the scale of reduction varies with light availability.

- How is the exchange of phosphorus between shallow water sediments and the overlying water column altered by particulate organic matter and benthic photosynthesis? Is phosphorus exchange driven by mineralization of organic phosphorus from *C. virginica* biodeposits or adsorption of phosphate to iron oxy(hydr)oxides in shallow water sediments with benthic photosynthesis?

Hypothesis 4 Dissolved oxygen from benthic photosynthesis inhibits soluble reactive phosphorus (SRP) exchange when sufficient light is available for photosynthesis and subsequent oxidation of reduced iron (II) to iron oxy(hydr)oxides (Figure 1.4).

Synopsis

Chapter 2

Although the initial intent of this dissertation was to address the influence of *C. virginica* biodeposits on nitrogen removal (i.e., burial, denitrification), establishment of

C. virginica aquaculture in shallow waters of Chesapeake Bay identified the relative influence of benthic microalgae on nutrient exchange at the sediment-water interface (Lowry 2002, Chapter 3). Reductions in NH_4^+ effluxes to near zero or minimal uptake with light and shifts toward greater rates of denitrification with reduced photosynthesis illustrated the potential for benthic microalgae to modulate nitrogen fluxes and, perhaps, lead to variability in shallow water nutrient exchange. Continued research on the influence of *C. virginica* aquaculture incorporated benthic photosynthesis into the experimental design, and sampling of shallow water sediments initially and in reference locations permitted the characterization of spatial and temporal variability in sediment biogeochemistry within a tidal creek (La Trappe Creek) of Chesapeake Bay.

Sediment cores were collected intermittently from late-spring through fall 2002-2005, and shifts in nutrient fluxes (O_2, N_2, NH_4^+, NO_2^- + NO_3^-, SRP), pore water (NH_4^+, SRP, Fe) profiles, and bioirrigation identified factors influencing variability in sediment biogeochemistry. Factors influencing variability within La Trappe Creek sediments were related to shifts in freshwater inputs, macroalgal blooms, nutrient concentrations in overlying waters, and bioirrigation from the clam, *Macoma balthica*. The influence of *C. virginica* biodeposits on biogeochemical processes in shallow water sediments was confounded by this variability, as *C. virginica* aquaculture in tidal creeks had varying effects on sediment biogeochemistry (Chapter 3).

Chapter 3

Off-bottom aquaculture of *C. virginica* was established within shallow waters of Chesapeake Bay in 2002 to assess the influence of *C. virginica* biodeposits on nitrogen

regeneration (NH_4^+, $NO_2^- + NO_3^-$), burial, and denitrification (N_2-N). Recognition of the influence of benthic microalgae on nitrogen fluxes in Lowry Cove led to the placement of *C. virginica* held in aquaculture floats in two different locations in 2003. Aquaculture floats were positioned within greater water depths and beneath stationary piers, so as to reduce the influence of benthic microalgae on nitrogen exchange.

C. virginica biodeposits generally led to gradual increases in surface sediment nitrogen and pore water NH_4^+ through enhanced deposition and concentrations of organic nitrogen. Increased deposition of particulate organic nitrogen did not result in greater rates of denitrification, as increased effluxes of N_2-N were only observed when gross photosynthesis was reduced relative to reference sediments (Figure 1.5). Reductions in benthic photosynthesis likely led to increased availability of NH_4^+ and NO_3^- for nitrifying and denitrifying bacteria and, thus, enhancement of coupled nitrification-dentrification (e.g., Sundback and Miles 2000, Risgaard-Petersen et al. 2004). Water column concentrations of $NO_2^- + NO_3^-$ were minimal.

All sediments exhibited a tendency to release NH_4^+ into the water column, but effluxes of NH_4^+ varied with sampling location and duration of *C. virginica* aquaculture. Benthic microalgae muted the influence of *C. virginica* biodeposits on sediment nitrogen exchange, such that greater effluxes of NH_4^+ from sediments receiving biodeposits only occurred in the dark (Figure 1.6). Discrepancies in the magnitude of nitrogen responses for sediments receiving *C. virginica* biodeposits were due to differences in the quantity and quality of biodeposits deposited. Organic carbon from *C. virginica* biodeposits did not increase aerobic respiration (i.e., dark O_2 fluxes), but increases in sulfate reduction were apparent through changes in total dissolved sulfide, acid-volatile sulfide, and sulfate

to chloride ratios. These field studies illustrated that the varying influence of *C. virginica* aquaculture on sedimentary nitrogen exchange is associated with benthic microalgal production and availability of particulate organic nitrogen. Shifts from aerobic to anaerobic respiration further suggested that *C. virginica* biodeposits may have additional consequences for sediment phosphorus exchange.

Chapter 4

Variability in the response of tidal creek sediments to *C. virginica* aquaculture and observed increases in sulfate reduction prompted the development of a laboratory experiment aimed at addressing how benthic photosynthesis and *C. virginica* biodeposits mediate nitrogen (NH_4^+, $NO_2^- + NO_3^-$, N_2) and soluble reactive phosphorus (SRP) exchange. Potential interactions were investigated through the development of four treatments based on two surface sediment irradiances (~ 10 and 100 μmol photons m^{-2} s^{-1}) and two loadings of *C. virginica* biodeposits (~ 1.5 and 7.5 g C m^{-2} d^{-1}). Given the extent of field studies on nitrogen cycling, research presented in this chapter focused primarily on the influence of benthic photosynthesis and organic loading on SRP exchange and its relationship to fluxes of NH_4^+ and dissolved O_2. Patterns in nitrogen fluxes followed those observed in the field, with greatest effluxes of NH_4^+ occurring in the dark for highly loaded sediments (Figure 1.7). Additions of *C. virginica* biodeposits did not promote, once again, an increase in coupling of nitrification-denitrification, as N_2-N exchange was regulated by water column concentrations of $NO_2^- + NO_3^-$. All sediments, regardless of trophic status, had a net release of nitrogen (mostly as NH_4^+) to

overlying waters; whereas consistent net effluxes of SRP were only observed from highly loaded sediments.

All treatments responded to organic matter deposition with an initial increase in dark effluxes of SRP. Minimal (i.e., near zero) fluxes and uptake, however, eventually occurred in the dark for sediments receiving smaller additions of *C. virginica* biodeposits and in the light for high light, high loading sediments. Uptake of SRP commenced in high light, high loading sediments within the first 10 d of treatment. Although uptake of SRP coincided with sharp increases in benthic O_2 production, gross sediment uptake was not proportional to stoichiometric estimates from gross photosynthesis. SRP fluxes in the light for low loading sediments were consistently near zero, maintaining minimal exchange and incorporating additional phosphorus within sediments. Shifts in net phosphorus exchange were not a result of imbalances in heterotrophic metabolism and benthic photosynthesis in any treatment. Rather, the source of particulate organic matter additions, *C. virginica* biodeposits, proved relevant to SRP exchange (Chapter 5).

Chapter 5

Additions of *C. virginica* biodeposits supplied organic and inorganic particulates of carbon, nitrogen, phosphorus, and iron and manganese oxy(hydr)oxides to the sediment surface of incubated cores, and thereby, enhanced oxidation-reduction cycling within sediments through increases in chemical oxidants and benthic photosynthesis. Observed increases in benthic photosynthesis were influenced by the intensity of surface sediment irradiance and, secondarily, by the availability of inorganic nutrients from bacterial remineralization of organic matter (Chapter 4).

Reoxidation, as identified with profiles of pH and SO_4^{2-} to Cl^- ratios, extended below the penetration depths of dissolved O_2 and, thereby, suggest that additional oxidants, such as iron oxy(hydr)oxides, were responsible for observed oxidation at greater depths. Added manganese oxy(hydr)oxides from *C. virginica* biodeposits did not serve to directly increase phosphorus retention in surface sediments. Rather, manganese oxy(hydr)oxides enhanced the adsorptive capacity of sediments through oxidation of reduced iron and sulfur. Added manganese from biodeposits was not typically incorporated within sediments (Figure 1.8), and peaks in oxidation coincided with increasing concentrations of dissolved iron (II, III). Concentration increases in iron oxy(hydr)oxides in low loading sediments exceeded additions from *C. virginica* biodeposits, and maximum retention of iron coincided with increases in total phosphorus.

Decreased retention of solid-phase phosphorus within the 10 cm core relative to surface (0-1 cm) sediments illustrated the upward migration of phosphorus concurrent with iron oxy(hydr)oxide reduction in highly loaded sediments. Differences in NH_4^+ and SRP concentrations relative to SO_4^{2-} suggest that reduction of iron oxy(hydr)oxides occurs through iron-sulfide mineral formation, and transitions in iron-sulfide profiles were observed. Pulsed additions of *C. virginica* biodeposits identified the importance of iron oxy(hydr)oxides and associated reduction on phosphorus mobility and exchange across the sediment-water interface in shallow, illuminated sediments.

Conclusions

Biodeposits (feces and pseudofeces) from *Crassostrea virginica* aquaculture had varying influences on biogeochemical processes in tidal creek sediments of Chesapeake

Bay but, in general, shallow water sediments were impacted by focused sedimentation from *C. virginica*. The response of tidal creek sediments to *C. virginica* biodeposits was confounded by the natural variability within these systems and associated shifts in the quantity and quality of seston available for oyster feeding (Figure 1.9). The more rapid deposition of seston in the form of *C. virginica* biodeposits led to increases in surface sediment organic nitrogen and pore water NH_4^+, without subsequent increases in nitrogen removal through denitrification. Benthic microalgae typically modulated the influence of *C. virginica* biodeposits on nitrogen fluxes, but sediments often remained a source of NH_4^+ to overlying waters.

The influence of benthic microalgae on phosphorus fluxes were confounded by the availability and retention of iron oxy(hydr)oxides, as dissolved O_2 served to oxidize reduced iron (II) and promote additional adsorption of phosphates. Availability of iron oxy(hydr)oxides for phosphorus retention is dependent on a balance between the organics and inorganics filtered by *C. virginica*. Increases in organic carbon (and phosphorus) relative to manganese and iron oxy(hydr)oxides likely promotes additional effluxes of phosphorus through iron oxy(hydr)oxide reduction and iron-sulfide mineral formation. Given the inherent variability in tidal creek sediments and their tendency to already be net heterotrophic, establishment of *C. virginica* aquaculture should occur in areas less sensitive to sudden bursts in particulate organic matter. Placement of aquaculture in areas with greater flow would likely result in greater dispersal of biodeposits and decreases in the magnitude of sedimentary responses.

Figure Legends

Fig. 1.1 Annual landings (wet meat weight, kg x 10^6) of *Crassostrea virginica* in Maryland (filled circles) and Virginia (open circles) from 1950 through 2006 and the number of market *C. virginica* sold by Virginia aquaculturists (filled bars) in 2005, 2006, and predicted for 2007 (Murray et al. 2007). Numbers of *C. virginica* sold to market were converted to annual landings (open bars, kg x 10^6) assuming that one market oyster is equivalent to 5 g wet meat weight. Percentages (above open bars) indicate the proportion of Virginia landings that were from aquaculture in 2005 and 2006 and that were predicted for 2007. Percentages were determined with the mean (± standard deviation) of 2000 to 2004 and 2006 Virginia landings (gray bar), as no annual landing data were available for 2005 and 2007. The annual landing data for 2006 (0.0070 kg x 10^6) suggested that an even greater percentage of Virginia landings (69.2%) came from *C. virginica* aquaculture. Annual landing data were provided by the National Marine Fisheries Service (personal communication, http://www.st.nmfs.gov/st1/commercial/landings/annual-landings.html).

Fig. 1.2 Conceptual diagram of the potential influence of *Crassostrea virginica* biodeposits (feces and pseudofeces) on nitrogen removal through burial of particulate organic nitrogen and enhancement of coupled nitrification-denitrification (Hypothesis 1). Scenarios illustrate anticipated differences in surface sediment concentrations of particulate organic nitrogen and effluxes of

N_2-N for shallow water sediments receiving *C. virginica* biodeposits (right) and similar reference sediments (left). Benthic microalgal communities are present within both scenarios.

Fig. 1.3 Conceptual diagram of the potential influence of benthic photosynthesis and microalgal assimilation on regeneration and exchange of nitrogen from added *Crassostrea virginica* biodeposits (Hypothesis 2-3). Scenarios illustrate anticipated increases in effluxes of NH_4^+ from sediments receiving *C. virginica* biodeposits (right) relative to similar reference sediments (left). Reductions in nitrogen exchange are expected to occur during the photoperiod and to vary with intensity of surface sediment irradiance.

Fig. 1.4 Conceptual diagram of the potential influence of benthic microalgae and *Crassostrea virginica* biodeposits on phosphorus exchange across the sediment-water interface (Hypothesis 4). Scenarios illustrate how soluble reactive phosphorus (SRP) fluxes are expected to differ under various surface sediment irradiances (high, low) and particulate organic matter loadings (high, low). Minimal SRP effluxes are expected for sediments receiving sufficient light for benthic photosynthesis and subsequent oxidation of reduced iron. Treatment identifications below each scenario correspond to the light and then loading level. HL: high light, low loading. HH: high light, high loading. LL: low light, low loading. LH: low light, high loading.

Fig. 1.5 Conceptual diagram of the influence of *Crassostrea virginica* biodeposits on surface sediment concentrations of particulate organic nitrogen and N_2-N fluxes. Increased deposition of particulate organic nitrogen at Oyster sites (right) did not promote enhanced effluxes of N_2-N from shallow water sediments. *C. virginica* biodeposits only increased sediment exchange of N_2-N with the water column when benthic photosynthesis was reduced relative to Reference sediments. Rates of benthic photosynthesis, and not added particulate organic nitrogen, controlled the magnitude of N_2-N release. All sediments receiving *C. virginica* biodeposits (right) became enriched with organic nitrogen.

Fig. 1.6 Conceptual diagram of the influence of *Crassostrea virginica* biodeposits on nitrogen regeneration and exchange. All sediments exhibited a tendency to release NH_4^+ into overlying waters, and reductions in sediment effluxes were generally observed during light incubations. Differences in the magnitude of NH_4^+ fluxes between Oyster (right) and Reference (left) sites occurred ~ 3-8 wks after establishment of *C. virginica* aquaculture.

Fig. 1.7 Conceptual diagram of the combined influence of benthic microalgae and particulate organic matter from *Crassostrea virginica* biodeposits on nitrogen (NH_4^+, N_2-N, $NO_3^- + NO_2^-$) and soluble reactive phosphorus (SRP) fluxes. Fluxes of nitrogen were predominately influenced by sediment exchanges of NH_4^+. N_2-N exchange at the sediment-water interface was regulated by water column concentrations of $NO_3^- + NO_2^-$. Effluxes of NH_4^+ from high loading treatments

(right) exceeded those with lower organic deposition (left). Although all sediments responded to *C. virginica* biodeposits with an initial increase in SRP effluxes, minimal exchange and uptake of SRP was later observed in sediments receiving less organic deposition (left).

Fig. 1.8 Conceptual diagram of the influence of benthic microalgae and particulate organic matter from *Crassostrea virginica* biodeposits on soluble reactive phosphorus (SRP) exchange and associated oxidation-reduction processes. Scenarios illustrate the relevance of benthic photosynthesis (i.e., O_2) and the addition of iron and manganese oxy(hydr)oxides from biodeposits to oxidation of iron (II) and subsequent retention of phosphates (left). Sediments receiving higher rates of organic deposition (right) released SRP to the water column, as enhanced rates of sulfate reduction led to the reduction of iron oxy(hydr)oxides and subsequent release of adsorbed phosphates.

Fig. 1.9 Conceptual diagram of the influence of *Crassostrea virginica* aquaculture on shallow water sediments supporting benthic microalgal communities. Scenarios illustrate that the influence *C. virginica* aquaculture on shallow water sediments depends on the quantity and quality of seston available for oyster feeding, levels of surface sediment irradiance for benthic photosynthesis, and availability of oxy(hydr)oxides for retention of added phosphorus.

Fig. 1.1

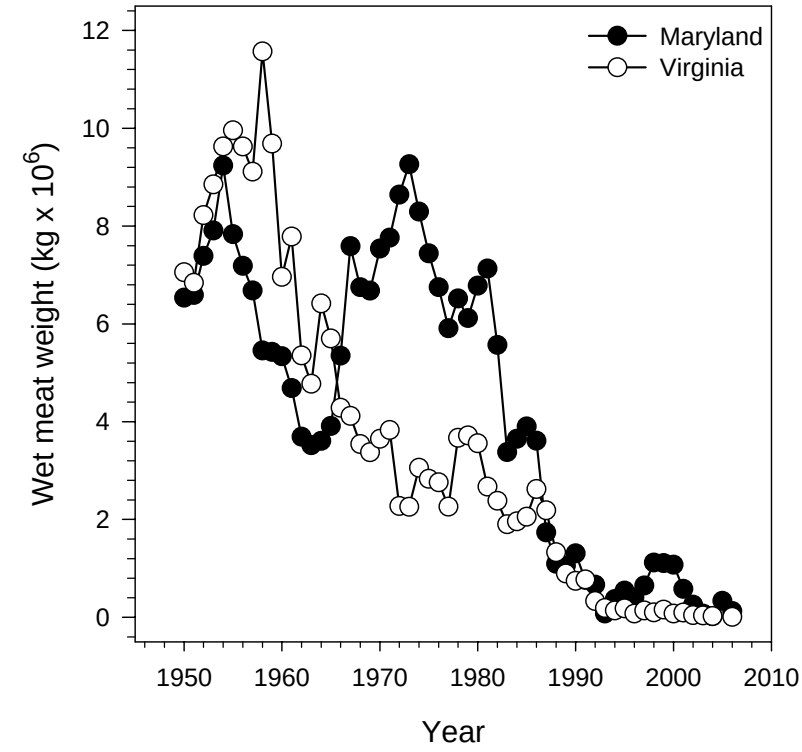
Maryland
Virginia
Wet meat weight (kg x 10^6)
Year
0
2
4
6
8
10
12
1950
1960
1970
1980
1990
2000
2010

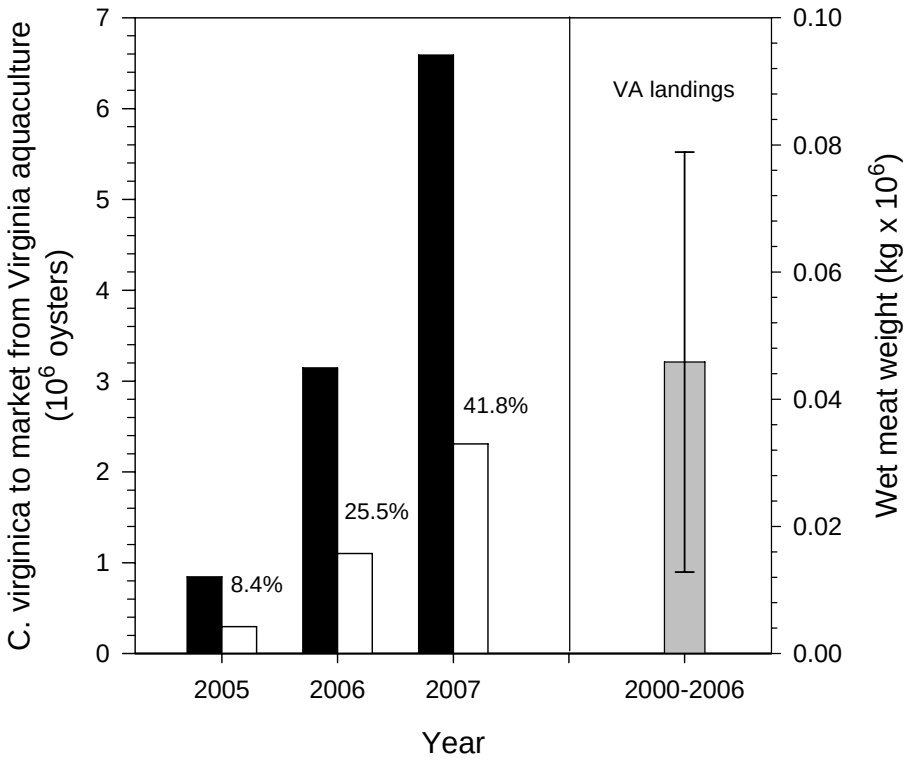
C. virginica to market from Virginia aquaculture (10^6 oysters)
Wet meat weight (kg x 10^6)
VA landings
8.4%
25.5%
41.8%
2005
2006
2007
2000-2006
Year
0
1
2
3
4
5
6
7
0.00
0.02
0.04
0.06
0.08
0.10

Fig. 1.2

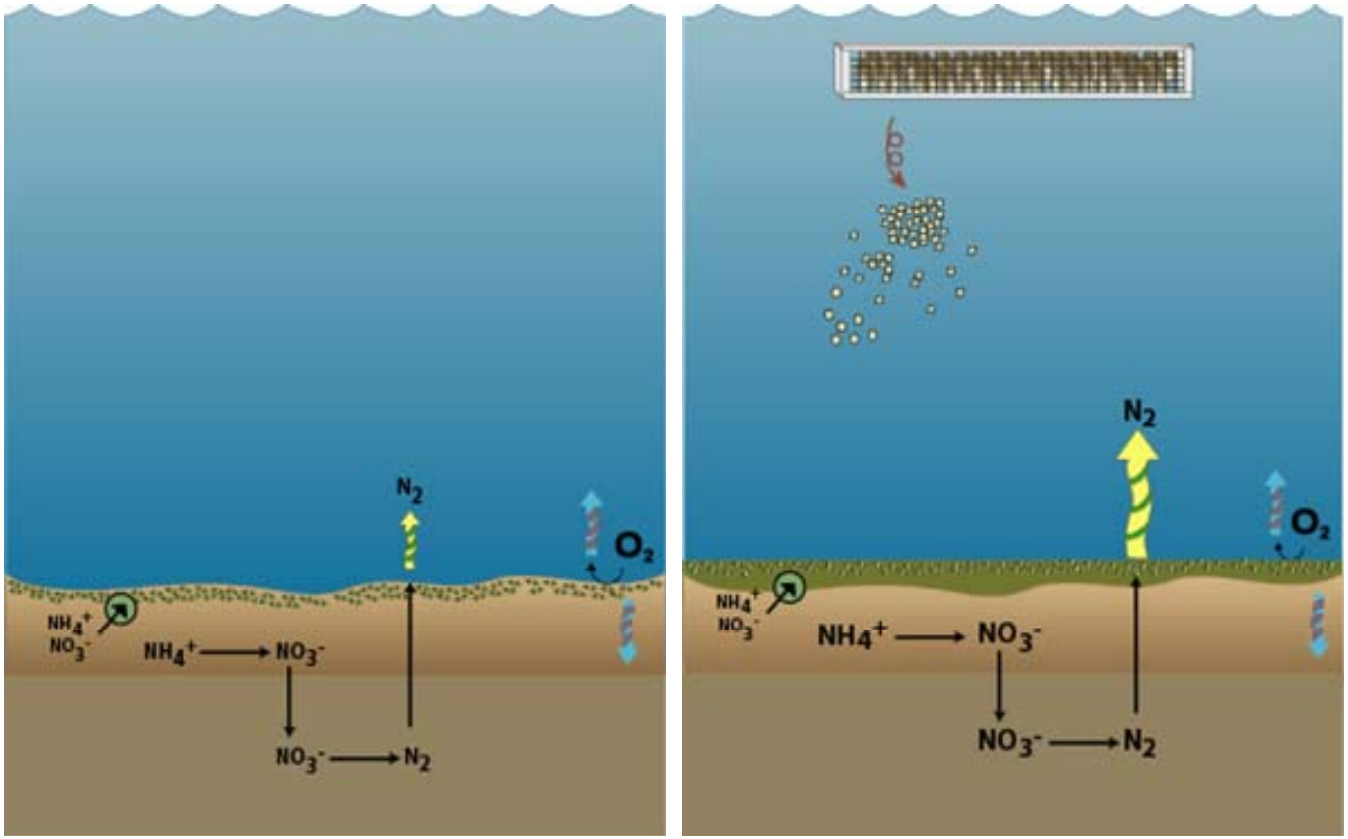

Without biodeposits **With biodeposits**

Fig. 1.3

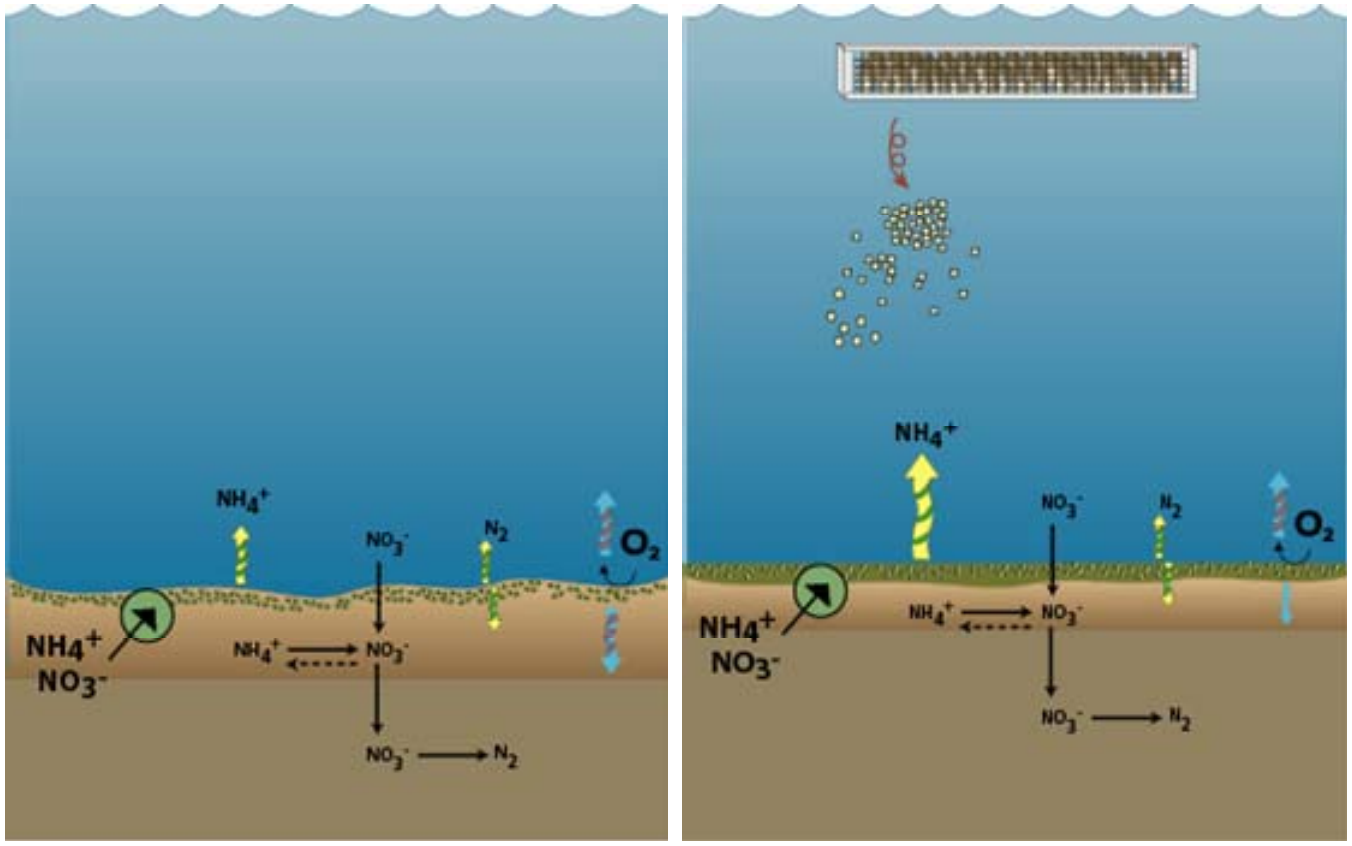

Without biodeposits **With biodeposits**

Fig. 1.4

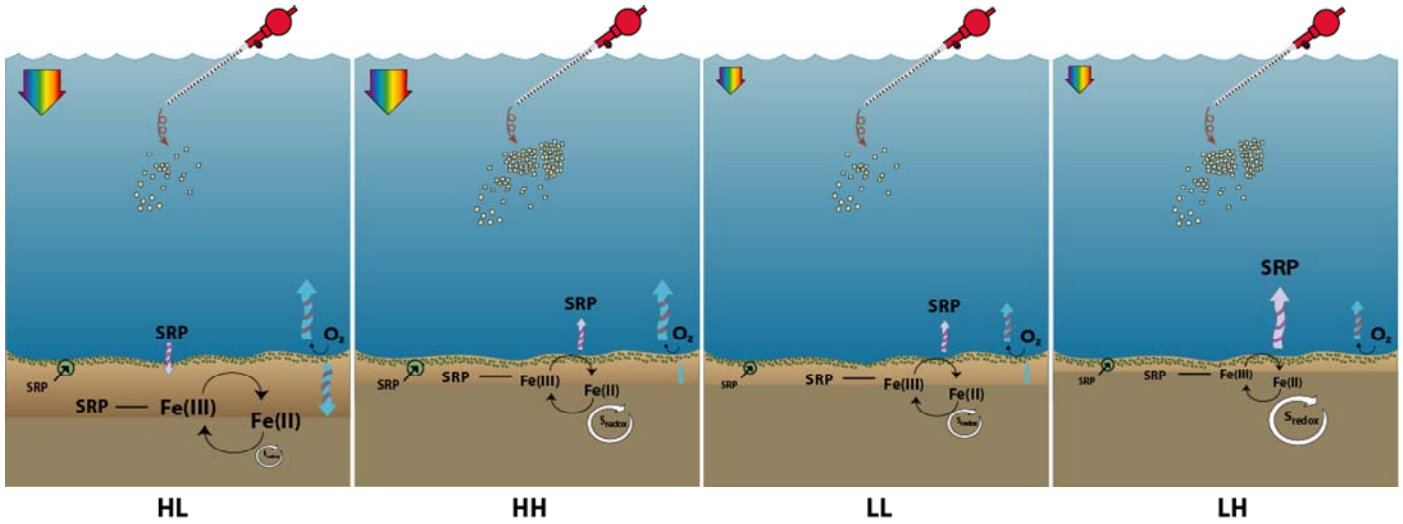

Fig. 1.5

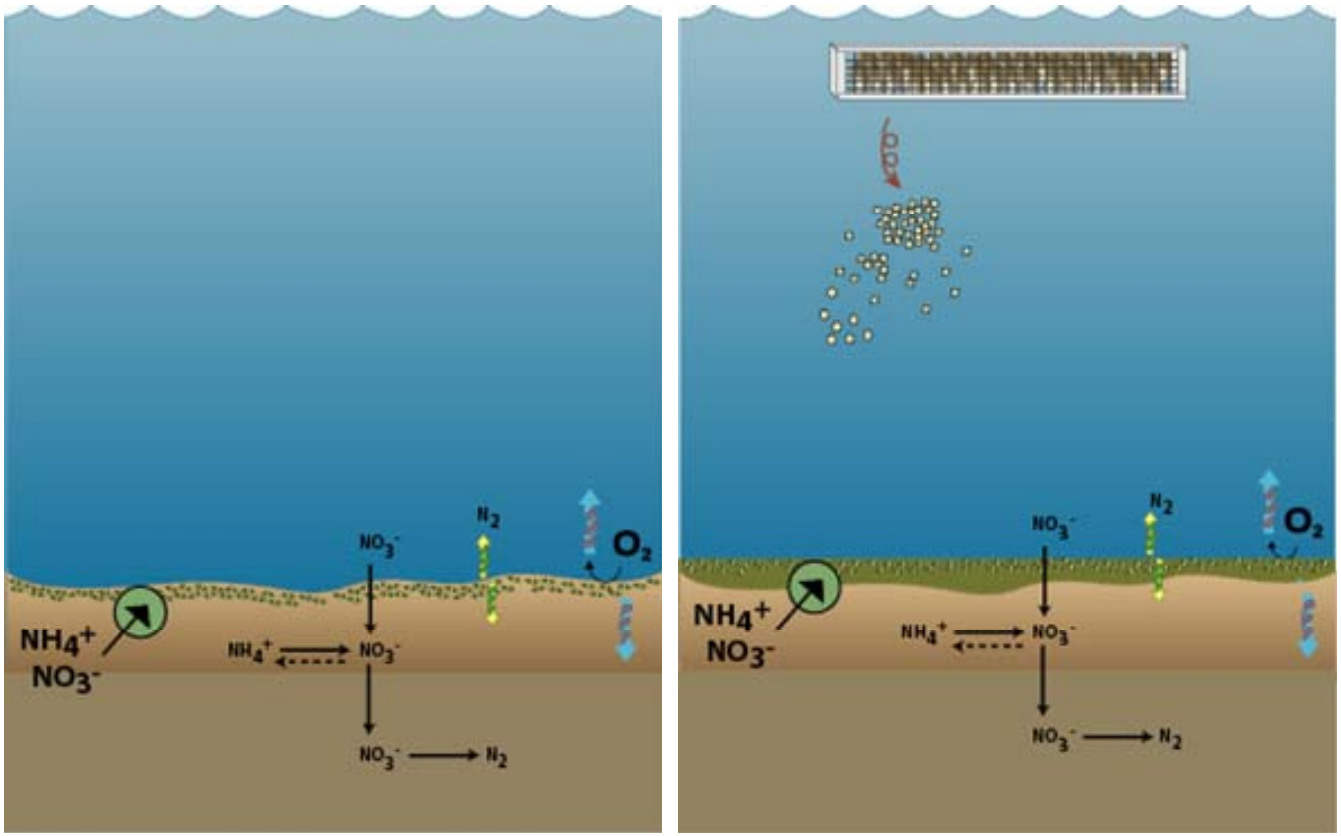

Without biodeposits **With biodeposits**

Fig. 1.6

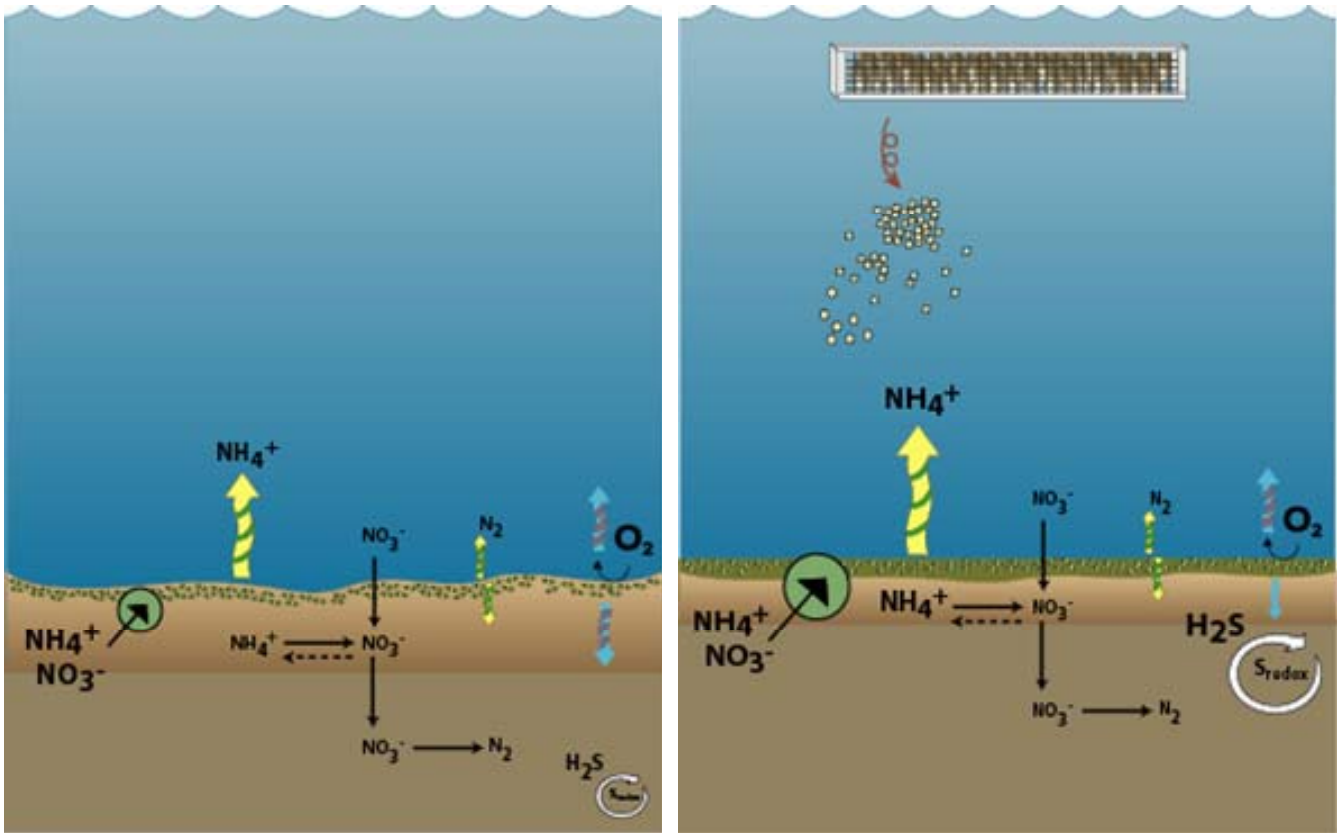

Without biodeposits **With biodeposits**

Fig. 1.7

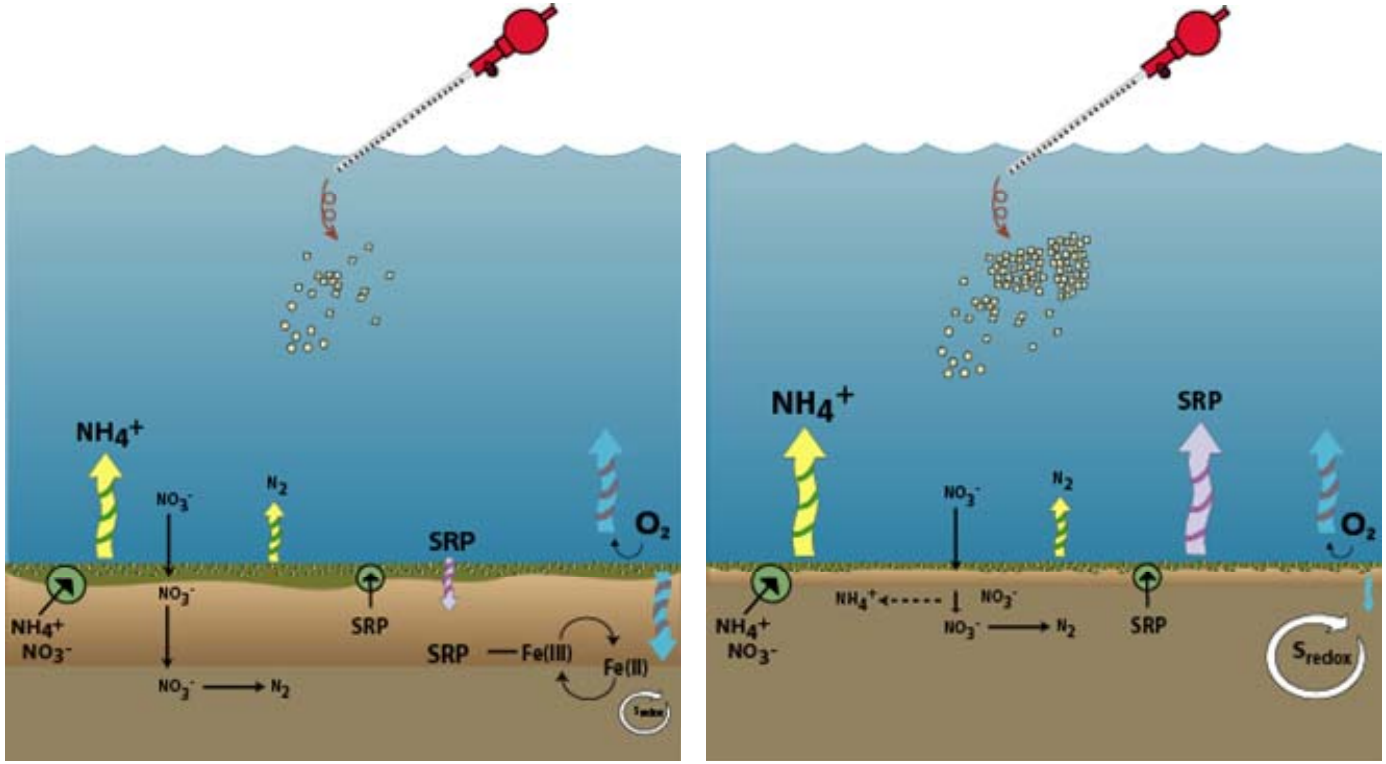

Low **High**

Fig. 1.8

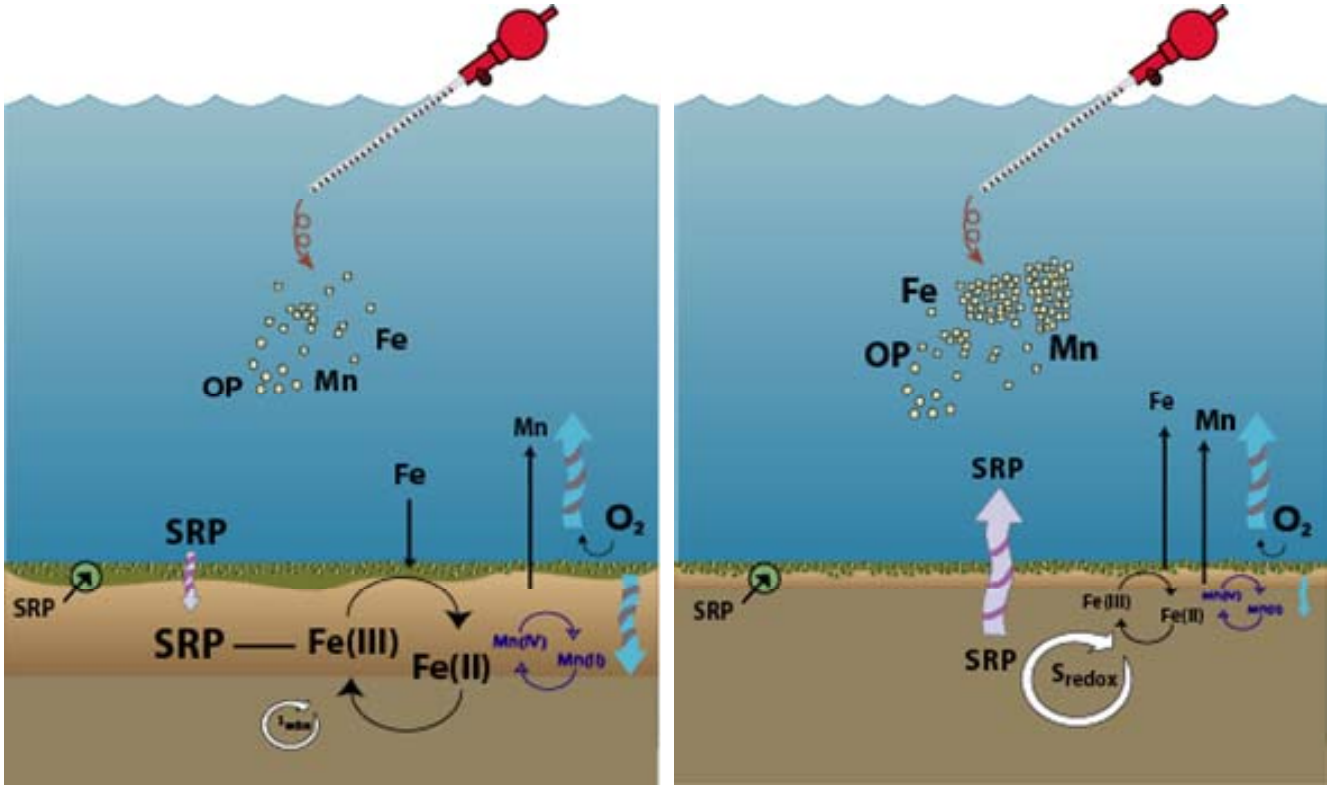

Low **High**

Fig. 1.9

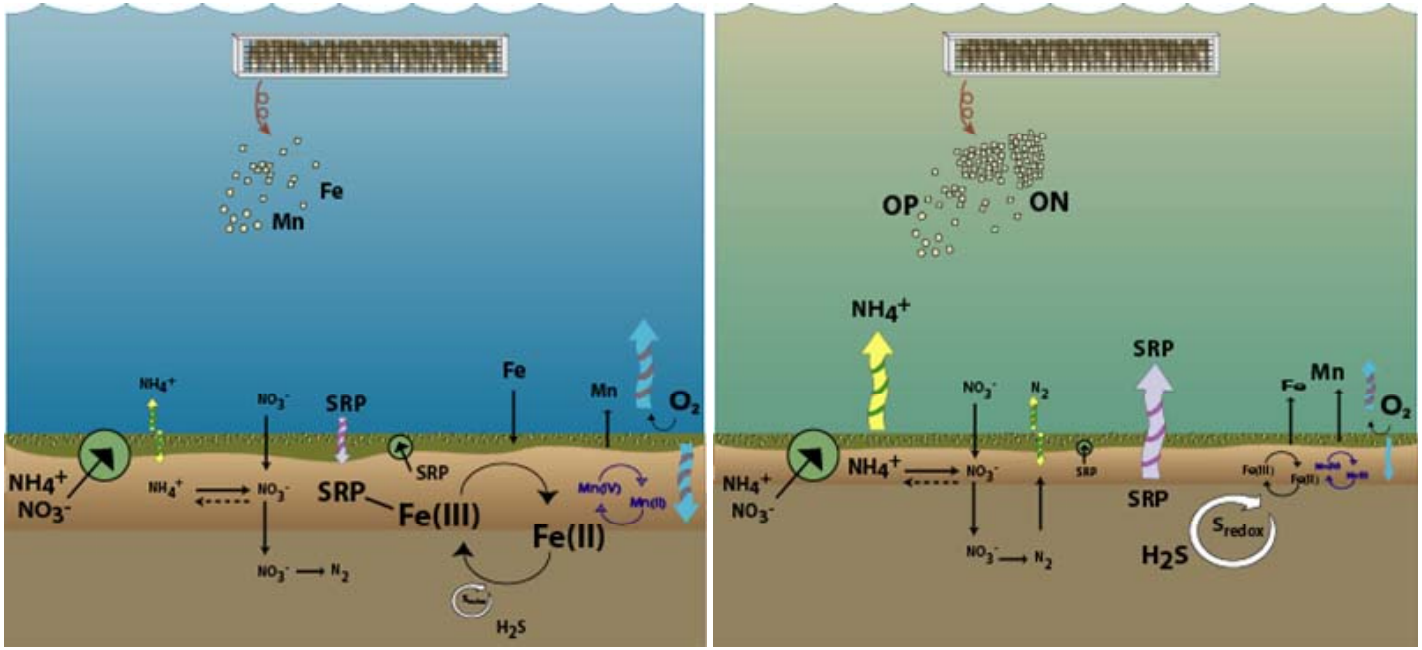

Chapter 2: Variability in Sediment Biogeochemistry and Nutrient Exchange within Tidal Creeks of Mesohaline Chesapeake Bay, USA

Abstract

Shallow water sediments constitute a large proportion of bottom within Chesapeake Bay and yet, relatively few studies on sediment biogeochemistry have been conducted in subtidal sediments supporting benthic microalgal communities. Previous research focuses primarily on sandy sediment and is often limited to single sites or individual sampling dates within seasons. To investigate variability in sediment biogeochemistry and nutrient (O_2, N_2, NH_4^+, $NO_2^- + NO_3^-$, SRP) exchange in shallow (<2 m) subtidal sediments, sediment cores were collected from a mesohaline, tidal creek (La Trappe Creek) intermittently between late-spring and fall 2002-2005. Shifts in pore water (NH_4^+, SRP, Fe) profiles and qualitative estimates of bioirrigation, determined with a conservative tracer (Br^-), identified the transitory influence of benthic fauna in these sediments. Spatial and temporal variability in dark O_2 fluxes was partially attributed to shifts in stream flow and proximity to macroalgal blooms. All sediments were net heterotrophic and, therefore, had a tendency to release NH_4^+ into the water column. SRP fluxes were minimal, except in July 2003. Pore water profiles of NH_4^+ and SRP transitioned from late-spring through summer, with increases in concentrations coinciding with decreases in bioirrigation. Sediments from La Trappe Creek illustrated the potential for sediment biogeochemistry and nutrient exchange from tidal creek sediments to vary spatially and temporally on relatively small scales. Observed variability suggests that temporal and spatial under-sampling can mischaracterize sediment nutrient exchange in tidal creeks and that sudden shifts in *in situ* irradiance and overlying nutrient concentrations have a greater influence on sediment metabolism and nitrogen cycling in marginally illuminated sediments than sediments at water depths <1

m. Collection of sediment cores along transects spanning from euphotic to semi-euphotic zones under differing water column conditions would prove beneficial to better understanding the mechanisms driving the dynamics of mesohaline, tidal creeks.

Introduction

Shallow, subtidal sediments constitute a large proportion of the bottom within Chesapeake Bay. Approximately 1,365 km^2 of bottom within the main-stem (11,500 km^2) has been estimated to have sufficient photosynthetically active radiation (PAR) to support benthic microalgal communities, contributing approximately < 10% of the Bay's total primary productivity (Kemp et al. 1999; Kemp et al. 2005). Inclusion of bottom sediments within shallow (< 2-5 m) sub-estuaries and tidal creeks would increase the surface area capable of supporting benthic photosynthesis 2- to 7-fold, and additional increases in surface area may stem from on-going restoration efforts. Restoration in Chesapeake Bay has targeted dissolved oxygen, algal biomass, and improved water clarity for recovery of submerged aquatic vegetation. Although research has often focused on increases in light attenuation (e.g., Kemp et al. 2005), better nutrient and sediment management will likely result in increased surface area for benthic microalgal production. Nutrient assimilation and production of dissolved O_2 by benthic microalgae have been shown to be important mediators of nitrogen and phosphorus fluxes across the sediment-water interface in other shallow water environments (e.g., Sundback et al. 1991; Sundback and Graneli 1988; Rysgaard et al. 1995; Cerco and Seitzinger 1997; Ferguson et al. 2004), but for Chesapeake Bay, the focus has primarily been on deep sediments (e.g., Cowan and Boynton 1996).

In Chesapeake Bay, relatively few studies on sediment biogeochemistry have been conducted in the large expanse of subtidal sediments supporting benthic microalgal communities (Rizzo and Wetzel 1985; Murray and Wetzel 1987; Simon 1988; Rizzo 1990; Reay et al. 1995). Of the research conducted, the focus has primarily been on sandy sediments located within tributaries (Potomac River, York River) or along the southeastern shore of Chesapeake Bay (Rizzo and Wetzel 1985; Murray and Wetzel 1987; Simon 1988; Rizzo 1990). Studies, including measurements of dissolved O_2 and nutrient fluxes, have been limited to either a single site or individual sampling dates within seasons (Rizzo 1990; Reay et al. 1995), and neither included any measurements on denitrification or N_2 fixation. A comprehensive study of the variability and factors influencing this variability within subtidal sediments, especially in finer-grained silts and clays, has not been conducted. This lack of repeated sampling spatially and temporally has the potential to inaccurately characterize the nature of benthic microalgal sediments, as shifts in water column and sediment properties may alter the influence of benthic microalgae on sediment nutrient dynamics.

To characterize the spatial and temporal variability of biogeochemical processes in shallow waters, I repeatedly measured dissolved O_2, nitrogen (N_2, NH_4^+, $NO_2^- + NO_3^-$), and soluble reactive phosphorus (SRP) fluxes, and their concentrations in pore water profiles (NH_4^+, SRP, Fe(II,III)), from sediment cores collected in a shallow, tidal creek of Chesapeake Bay. Sediment cores were collected at 2-3 week intervals from late-spring through early-fall in 2002 and 2003, with additional sampling occurring in fall 2004 and summer 2005. Observed variability within and among sampling locations was presumably not due to the reproducibility of methodologies, as reproducible results have

been observed for sediment cores maintained under controlled conditions (Chapter 4-5). Factors influencing variability within tidal creek sediments were related to shifts in riverine freshwater inputs, macroalgal blooms, nutrient concentrations in overlying waters, and bioirrigation from the clam, *Macoma balthica*.

Materials and Methods

Study sites

Research was conducted in La Trappe Creek, a shallow, tidal creek located within the Chesapeake Bay drainage (Fig. 2.1). The La Trappe Creek sub-basin lies within the Choptank basin, an agriculturally-dominated (62%) drainage basin located on the eastern shore of Chesapeake Bay, and drains directly into the mesohaline portion of the 300-km^2 Choptank River (Fisher et al. 2006). The La Trappe Creek drainage is comprised predominately of agricultural and forested lands, with urban land uses comprising only a small percent (Lee et al. 2001). Although population densities have remained low within the Choptank relative to other Chesapeake Bay basins, high rates of nutrient inputs, especially from fertilizer application, have led to degradation of these waters (Fisher et al. 2006). Known nutrient inputs within the La Trappe Creek sub-basin include those from a wastewater treatment plant, septic systems, fertilizer application, and sediment transport from shoreline and agricultural erosion (T. R. Fisher personal communication). Shifts in light attenuation coefficients (k_d), measured during my sampling periods, offered insight into the influence of these inputs on water quality (Table 2.1).

Sediment cores were collected from a total of eleven study sites within four locations (i.e., Oyster bar, Lowry Cove, Pier, and Mainstem) in La Trappe Creek

intermittently from mid-May through September in 2002 and 2003, with additional sampling occurring in November 2004 and August 2005 (Table 2.1). Replicate sediment cores (n = 2 – 6) were collected at all 11 sites, with repeated sampling occurring at two sites in Lowry Cove and one site designated as Pier and in Mainstem (*see* Fig. 2.1). Study sites designated as Pier were shaded by existing wooden platforms, which decreased surface water irradiance more than 90% (< 5 – 25 μmol photons m^{-2} s^{-1}). All study sites in the upper reaches of La Trappe Creek were predominately fine-grained sediments; sandy-silts dominated the lower, mesohaline portion of the creek near an existing oyster bar (Table 2.1). Water depths from sampling periods ranged from 0.7 to 2 m. Study sites were located in waters with a tidal range of 0.49 m and a mean tide of 0.34 m (38° 34' N, 76° 04' W).

Inconsistencies in sampling frequency for study sites occurred since the original intent of core collection was designed as a means for monitoring shallow water sediments adjacent to sediments receiving biodeposition from the eastern oyster, *Crassostrea virginica* (Chapter 3). Study sites presented here served as either an initial condition or as a reference for natural temporal variability in shallow, fine-grained sediments in locations without oysters. Biogeochemical conditions in coarser-grained sediments near an existing oyster bar have also been included.

Sediment core collection and aerobic incubations

All sediment cores were collected by pressing a Rumohr-type pole corer fitted with a transparent acrylic tube (6.35 cm I.D.) ~ 10 cm into sediments. Before withdrawing the core from the sediment, a valve was closed to maintain suction on the

core, thereby allowing the core to be removed intact. Upon retrieval, the bottoms and tops of cores were sealed with machined plastic lids fitted with O-rings and stoppers to maintain cores without airspace. Cores remained covered in insulated containers during transportation (< 1 h) to the laboratory. Photosynthetically active radiation (PAR) at the sediment surface was measured with LiCor (2π) sensors.

At the laboratory, sediment cores were transferred to a temperature-controlled chamber set at ambient temperatures (20-32°C). Sediment cores for flux incubations were submerged in incubation tanks (~ 30 – 60 L) filled with ambient (typically filtered, 0.22 – 1 μm) water collected from La Trappe Creek. Empty core tubes, each with an acrylic base positioned at the approximate height of sediment, were used to incubate ambient water (without sediment) as a measure of water column activity (i.e., blanks). PVC-aeration tubes (2.5 cm inner diameter) were inserted into the tops of open cores such that they reached within ~ 1 cm of the sediment surface (Newell et al. 2002). Cores were bubbled (with air) for a minimum of ~ 1 h to > 12 h (i.e., overnight) prior to flux incubations; duration of bubbling depended on the redox conditions of surface sediments. Active bubbling in the open cores and surrounding water was maintained, except during flux incubations.

Nutrient flux incubations

During flux incubations, cores were sealed with machined plastic lids with O-rings, and the overlying water mixed with a Teflon-coated magnetic stirrer (4.5 V) driven by an external magnetic turntable. Baseline solute (NH_4^+, NO_2^- + NO_3^-, SRP) and gas concentrations (O_2, N_2, Ar) were determined in the dark immediately upon sealing the

cores and then in the light for total durations between ~ 4 h and 9 h. Aliquots for NH_4^+, $NO_2^- + NO_3^-$, and soluble reactive phosphorus (SRP) were not collected for sediment cores collected on 20-22 May 2003, and sampling of $NO_2^- + NO_3^-$ concentrations from the August 2005 Mainstem cores was minimal (see Chapter 4; Table 4.4). No flux measurements were conducted on 11 November 2004. Small volumes of water (21-32 ml) were withdrawn for sampling at intervals between ~ 25 and 60 min, depending on rates of sediment oxygen consumption and number of sampling points. Sampling typically occurred four to five times in the dark and light, but fewer sampling points (2-3) were used occasionally. Uniform illumination was provided to surface sediments through broad spectrum, high intensity fluorescent lamps, and height adjustments and mesh, shade cloth were used to modify surface sediment irradiance. Sediment cores were incubated under a diel cycle including 12-14 h of daylight at specified surface sediment irradiances, ranging from ~ 5 to 100 μmol photons m^{-2} s^{-1}. PAR measurements (LiCor 2π) within tanks indicated no differential irradiance for core positions.

Water withdrawn for sampling was replaced by ambient water from sampling locations (i.e., La Trappe Creek) introduced through Tygon tubing to ensure that no air bubbles were introduced to the system. Samples to measure N_2 and O_2 concentrations were taken in gas tubes with ground glass stoppers and preserved with 10 μl 50% saturation $HgCl_2$. Core tubes were stored submerged in water at ambient temperature for no more than 1 week. NH_4^+, $NO_2^- + NO_3^-$, and SRP water column samples were collected in 20 ml syringes and filtered with 0.45 μm filters into 6 ml plastic vials. Samples were immediately stored in freezers (-20°C) until nutrient analyses were performed.

Bioirrigation by benthic infauna

Qualitative estimates of bioirrigation (i.e., solute-transport) by benthic infauna were conducted for representative sediment cores from revisited study sites in Lowry Cove (2002), Pier, and Mainstem (2003). Benthic infaunal activity was identified from discrepancies in modeled and measured profiles of bromide, a known conservative tracer in pore waters (Mackin et al. 1988; Green et al. 2002). Sodium bromide was added to incubation tanks upon completion of nutrient flux incubations or cores collected separately for pore water extraction (*see next section*) at final concentrations near 8-10 mmol $Br^- L^{-1}$. Upon mixing of tank waters, cores were sealed with the same lids and mixed with stirrers, as for nutrient incubations. Waters within the headspace of cores was exchanged with tank water using a peristaltic pump (flow rate: > 3-4 ml m^{-1}). Bromide incubations typically occurred for ~ 16 to 24 h, but longer durations (< 41 h) were often maintained in cores collected from Lowry Cove. Aeration of tank water was continuous with PVC-aeration tubes (2.5 cm inner diameter) or aquaria air stones. Modeled pore water concentrations of Br^- were calculated from Fick's first law of diffusion. Diffusion coefficients within sediments were estimated from diffusion coefficients in free solution at ambient temperature and conversions of porosity to tortuosity squared using Boudreau's law ($\theta^2 = 1 - \ln(\varphi^2)$, Boudreau 1997 *in* Schulz 2000).

Surface sediment, pore water, and solid-phase collection

Pore water and solid-phase samples were collected from sediment cores used for nutrient flux incubations and from cores collected separately within ~ 1 d of incubations.

Sediment cores collected separately were dissected upon return to the laboratory or maintained under aerobic incubations for ~ 16 to 24 h for estimates of benthic infaunal activity. All sediment cores held in the laboratory were maintained aerobically in temperature-controlled chambers set at ambient temperature and under a diel illumination cycle until surface sediment collection or pore water and solid-phase extraction occurred. Sediment cores were held in the laboratory for a maximum of ~ 4 d.

Surface (0-1 cm) sediment collection occurred under aerobic conditions unless cores were sectioned for pore water and solid-phase analyses. The overlying water column was siphoned off prior to sediment collection. Surface sediments were collected with a syringe mini-corer (1.4 cm inner diameter) pressed ~ 1 cm into sediments. Sediment subsamples for chlorophyll *a* were placed in 15 ml centrifuge tubes wrapped in aluminum foil and stored at -20°C until analysis. Sediment subsamples collected for nutrient content were extruded into aluminum pans and dried at 80 °C. Ground sediment was stored in glass scintillation vials until analysis.

Sediment cores for pore water and solid-phase analyses were extruded under N_2 and divided into 8 sections (0-0.5, 0.5-1, 1-1.5, 1.5-2, 2-3, 3-4, 4-7, and 7-10 cm) that were individually placed in 50 ml plastic centrifuge tubes and capped. Sections were centrifuged (822-1,096 xg for 10 min; 3500 rpm; International Equipment Company Centra MP4 and CL2), and the supernatant was filtered with 0.45 μm filters into 6 ml plastic vials for analysis of NH_4^+, SRP, SO_4^{2-}, Br^-, Cl^-, dissolved Fe (II, III), and dissolved sulfide (ΣH_2S: H_2S, HS^-, S^{2-}). Sediment sections were frozen (-20°C) until solid phase analyses could be conducted. Dilutions were done prior to freezing of NH_4^+ and SRP samples. SO_4^{2-}, Br^-, and Cl^- samples were immediately frozen, and dilutions

were performed at the time of analysis. Dissolved Fe samples were acidified and stored in capped vials at room temperature until analysis. Dissolved sulfide samples (1 ml) were fixed with 10 μl of a mixed diamine reagent (250 – 1000 μmol L^{-1}, Cline 1969) and stored at room temperature until analysis.

Analyses

Analysis of NH_4^+ concentrations followed Soloranzo's phenol hypochlorite method (Solaranzo 1969, as presented in Parsons et al. (1984)), modified for a 5 ml sample volume. A composite reagent of molybdic acid, ascorbic acid, and trivalent antimony was used to determine SRP concentrations (Murphy and Riley 1962). NO_2^- + NO_3^- concentrations were determined by automated colorimetry (United States Environmental Protection Agency, 1983a). Total dissolved Fe (II, III) and total dissolved sulfide were also determined from colorimetric analyses, following Gibb's ferrozine reduction technique (Gibb 1979) and methylene blue colorimetry (Cline 1969). SO_4^{2-}, Br^-, and Cl^- concentrations were determined by ion chromatography (United States Environmental Protection Agency 1983b).

Membrane inlet mass spectrometry was used to determine N_2 and O_2 concentrations in water samples collected during flux core incubations (Kana et al., 1994; Kana et al., 1998). N_2 : Ar and O_2 : Ar gas ratios were used to provide a precision of < 0.02% for N_2 and O_2 concentrations. Corrections to N_2 : Ar ratios associated with O_2 effects in the mass spectrometer were applied to all samples (Kana and Weiss, 2004). Nutrient fluxes for each core were calculated from linear regressions performed on nutrient concentrations plotted versus time ($r^2 > \sim 0.8$; $F \leq 0.10$). The difference in

nutrient concentrations between water from cores and blanks was expressed relative to the surface area of the core. Calculations were performed separately for simulated dark and light events, and positive and negative fluxes coincided with sediment release and uptake of nutrients, respectively. Fluxes of N_2-N represented the net exchange of N_2-N at the sediment-water interface since the reactions (e.g., denitrification, annamox, N_2 fixation) mediating these fluxes cannot be separately identified (Kana et al., 1998; Kana and Weiss, 2004). Estimates of gross primary productivity were calculated as 14 h * (O_2 flux measured during light incubations – O_2 flux measured during dark incubations). Net ecosystem metabolism estimates were determined as 14 h * O_2 flux measured during light incubations + 24 h * O_2 flux measured during dark incubations.

Surface sediments (0-1 cm) were analyzed for total and inorganic phosphorus, HCl-extractable Fe, total carbon, total nitrogen, and sediment chlorophyll *a*. Total and inorganic phosphorus concentrations were determined using HCl-extraction and combustion at 550°C for ~ 2 h (Aspila et al. 1976); loss upon combustion (550°C) was used to determine percent organic content. The remaining HCl-extracts from inorganic phosphorus analyses were analyzed using flame atomic absorption to determine HCl-extractable Fe concentrations (Leventhal and Taylor 1990). Percentages of total carbon and nitrogen were determined with a control equipment elemental autoanalyzer (Cornwell et al. 1996) and expressed relative to the dry weight (DW) of sediment (μmol g^{-1} DW). Total chlorophyll *a* content for frozen surface sediments was determined by high-performance liquid chromatography (HPLC; Van Heukelem et al. 1994).

Frozen sediments from core sectioning were analyzed for acid-volatile sulfide (AVS) and chromium-reducible sulfide (CRS). Sediments were analyzed initially for

AVS using a 6 N HCl-extraction and $PbClO_4$ titration (Cornwell and Morse 1987). After analyses for AVS were complete, sediments were processed for CRS concentrations following Canfield et al. (1986). All solid-phase digestions were performed on thawed, well-homogenized sediments. Separate, equivalent amounts of homogenized sediments were dried to a constant weight at 80°C.

Results and Discussion

Characterization of surface sediments

Surface sediments in La Trappe Creek were characteristic of sediment-types found within the main-stem and tributaries of Chesapeake Bay (Table 2.1; Kerhin et al. 1988). Fine-grained silts and clays were present in the upper reaches of the creek, including Lowry Cove, whereas coarser mixtures of sand and silt were identified at Oyster bar near the creek mouth. Surface sediment (0-1 cm) concentrations of total carbon and nitrogen in silt-clays ranged from 2,056 to 4,279 μmol C g^{-1} DW and from 178.5 to 292.7 μmol N g^{-1} DW, respectively (Fig. 2.2), and were comparable to those measured in upper and middle Chesapeake Bay (Marvin-DiPasquale and Capone 1998). A slight decrease in total concentrations was observed for sediments collected from Mainstem in August 2005. Concentrations of total carbon (214 ± 102 μmol C g^{-1} DW) and nitrogen (25.0 ± 9.2 μmol N g^{-1} DW) and percent organic content were lowest in sediments collected from sands adjacent to Oyster bar (Table 2.2). Percent organic content for all study sites ranged from 0 to 13%.

Ratios of total carbon to nitrogen (10.35 ± 1.04) were characteristic of freshly deposited marine organic matter, but inter- and intra-site variability (range: 5.83 – 14.62)

was observed. Total carbon to nitrogen ratios at Oyster bar (8.69 ± 1.19) were between those characteristic of phytoplankton (6.625) and freshly deposited marine organic matter. Closer resemblance to algal composition was not unexpected as maximum concentrations of surface sediment (0-1 cm) chlorophyll *a* occurred at this site (Oyster bar; Table 2.2). A similar difference in microalgal biomass from sandy and silt-clay sediments has been observed at other Chesapeake Bay shallow water sites (Reay et al. 1995). Subsamples of Lowry Cove sediment (n = 2) possessed carbon isotopic ratios (δ PDB) of -23.87 ± 0.03, which are consistent with those for marine algae and C_3 land plants (Peterson and Fry 1987, Meyers 1994 *in* Rullkötter 2000). Isotopic ratios for nitrogen (δ Air) were 5.28 ± 0.12; analyses were performed by University of California Davis (http://stableisotopefacility.ucdavis.edu).

Sediments collected from Lowry Cove and Oyster bar in 2002 possessed greater capacities for surface adsorption of PO_4^{3-}, as determined from ratios of HCl-extractable iron and inorganic phosphorus, than those from Pier and Mainstem (2003-2005; Fig. 2.2; Jensen et al. 1992; Jensen et al. 1995). HCl-extractable iron to inorganic phosphorus ratios in Lowry Cove and Oyster bar sediments ranged between 7.5 and 20.8, with a mean of 14.1 ± 3.1; ratios in Pier and Mainstem sediments were 10.4 ± 1.8. Concentrations of HCl-extractable iron varied from 7.4 to 187.5 μmol Fe g^{-1} DW, with the least and greatest occurring in Oyster bar (39.9 ± 32.4 μmol Fe g^{-1} DW) and Lowry Cove (168.3 ± 16.1 μmol Fe g^{-1} DW) sediments, respectively. Acid-volatile sulfides (AVS) typically accounted for ~ 9% of HCl-extractable iron, but near zero concentrations were not uncommon for sediments collected in Lowry Cove. Similar differences were also observed for concentrations of chromium-reducible sulfides (CRS); surface

sediments from Pier and Mainstem (273.7 ± 51.4 μmol S g^{-1} DW) contained approximately twice as much CRS as those from Lowry Cove (136.2 ± 19.5 μmol S g^{-1} DW). No AVS or CRS data were collected for Oyster bar. Surface sediment concentrations of organic and inorganic phosphorus were 8.5 ± 2.7 μmol P g^{-1} DW and 10.0 ± 3.2 μmol P g^{-1} DW, respectively, for all sampling locations.

Factors influencing sediment oxygen consumption

Sediment exchange of dissolved O_2 with overlying waters during dark incubations exhibited temporal and spatial variability within and among sampling locations. Rates of sediment O_2 consumption varied between -100.8 and -9,553.6 μmol O_2 m^{-2} h^{-1} (Fig. 2.3), with the greatest fluctuations occurring in cores collected from Pier in 2003 (Fig. 2.4). Sediment cores collected on 20-22 May and 07 July 2003 from Mainstem and Pier consumed O_2 in the dark at the greatest rates (-5,189.4 ± 1,812.8 μmol O_2 m^{-2} h^{-1}; -6,204 ± 609.8 μmol O_2 m^{-2} h^{-1}); lowest rates were typically observed in August (-841.2 ± 528.7 μmol O_2 m^{-2} h^{-1}). Mean rates of sediment O_2 consumption for Oyster bar, Lowry Cove, Pier, and Mainstem were -735.6 ± 374.9 μmol O_2 m^{-2} h^{-1}; -1,335.4 ± 676.8 μmol O_2 m^{-2} h^{-1}; -4,695.3 ± 1,741.3 μmol O_2 m^{-2} h^{-1}; and -1,580.1 ± 1,143.3 μmol O_2 m^{-2} h^{-1}, respectively, and were within the range of those observed for other silt-clay sediments of Chesapeake Bay (-5,323 to 7 μmol O_2 m^{-2} h^{-1}, Reay et al. 1995). Sediment O_2 consumption within cores sampled at Oyster bar was not unlike other study sites in August (2002-2005). Similarity in mean rates for Lowry Cove and Mainstem was likely due to analogous sampling dates (late-July through September). Sudden increases in dark O_2 consumption in Mainstem sediments occurred ~ 7 d after Hurricane Isabel (18

September 2003) flushed the creek, increasing surface sediment irradiance (k_d = 1.95). Increases in benthic microalgal biomass, observed as an increase in surface sediment (0-1 cm) chlorophyll *a* (from 9.27 ± 2.76 mg chl *a* m^{-2} to 18.91 ± 7.74 mg chl *a* m^{-2}), may have driven enhanced rates of respiration.

Spatial heterogeneity in dark O_2 fluxes occurred within and among sampling locations, such that study sites within a particular location and locations sampled simultaneously exhibited differences in the magnitude of O_2 consumption. Sediments from an existing oyster bar (i.e., Bar at Oyster bar) consumed O_2 at an hourly rate of -646.2 ± 158.7 μmol O_2 m^{-2} h^{-1}, whereas sandy sediments ~ 10 m away (i.e., Adjacent) consumed nearly twice as much (1,272.2 ± 604.3 μmol O_2 m^{-2} h^{-1}). Similar high variability in sediment O_2 consumption was observed from 20-22 May 2003 at Pier 1, Pier 2, and Mainstem (Upper 3). Mean dark O_2 fluxes in sediment cores from Pier 1, Pier 2, and Mainstem on 20 May 2003 were -6,315.6 ± 699.7 μmol O_2 m^{-2} h^{-1}, -9,125.3 ± 417.9 μmol O_2 m^{-2} h^{-1}, and -3,306.1 ± 1,695.0 μmol O_2 m^{-2} h^{-1}, respectively. Rates of sediment O_2 consumption at Pier sites decreased (i.e., became less negative) in the following ~ 2 d but continued to exceed those at Upper 3. Spatial heterogeneity in mid-May was likely associated with proximity to cove and shoreline blooms of macroalgae that were present during sampling; similar increases in sediment O_2 consumption have been observed elsewhere (Sundback et al. 2003). No blooms were visually observed on 26 May 2003. Collapse of macroalgal blooms may have been linked to increased microalgal abundance and activity, grazing, or nitrate toxicity (Valiela et al. 1997).

A proportion of the temporal variability in sediment O_2 consumption can be attributed to shifts in freshwater inputs (Fig. 2.5). Daily stream flow data from the

Greensboro gauge station (gauge number: 01491000), located below the Choptank fall line, was summed monthly and normalized to the maximum flow recorded within my sampling periods (United States Geological Survey, http://waterdata.usgs.gov/). Correlations of stream flow data from gauge stations in upper Delmarva indicate good agreement for monthly sums ($r^2 \approx 0.8$; Sutton et al. submitted). Relationships between sediment O_2 consumption and monthly stream flow are likely associated more with increased nutrient and sediment inputs than with freshwater supply directly. Additional variability in dark O_2 fluxes (i.e., observed as an increase in r^2) may be accounted for if fluxes collected during the May 2003 macroalgal blooms are removed. Enhanced rates of O_2 consumption during the observed blooms were likely associated with increased supply of labile organic matter. Continual O_2 measurements on 01-03 July 2003 suggested that low water column dissolved oxygen concentrations may have contributed to the divergence of Pier data on 07 July 2003. Dissolved oxygen near the sediment surface decreased, with no indication of rebounding, to concentrations < 63 μmol O_2 L^{-1}; upon moving the oxygen electrodes to surface waters, measured dissolved oxygen concentrations were near saturation. Lowest concentrations typically occurred mid-day, with minima typically occurring within ~ 1 h of low tide. Similar correlations of dark O_2 fluxes and incubation temperature were not rational ($r^2 = 0.25$; $P < 0.0001$), as maximum rates of respiration occurred at 20°C. Removal of macroalgal blooms did not improve this relationship ($r^2 = 0.03$; $P = 0.11$).

Deviations in benthic oxygenic photosynthesis

Variability in dissolved O_2 fluxes during light incubations was derived partially from differences in specified surface sediment irradiances within and among sampling locations. Production of dissolved O_2 in the light typically lessened net oxygen consumption or led to net O_2 evolution in sediment cores (e.g., Oyster bar, Lowry Cove, Mainstem) incubated at ~ 70-100 μmol photons m^{-2} s^{-1} (Fig. 2.4). Smaller reductions in O_2 consumption were observed for Mainstem sediments (August 2005) incubated at ~ 10 μmol photons m^{-2} s^{-1}. Increased (i.e., more negative than dark O_2 fluxes) or comparable rates of sediment oxygen consumption typically occurred in Mainstem (Upper 3) and Pier sediments collected on 20-22 May 2003 when surface sediment irradiances of ~ 8, 25-30, and 45-50 μmol photons m^{-2} s^{-1} were used. Sediment cores from Pier 2 and Pier 1 on 20 and 22 May 2003, respectively, were somewhat uncharacteristic for the macroalgal bloom period, as benthic oxygenic photosynthesis (~ 8 μmol photons m^{-2} s^{-1}; 25-30 μmol photons m^{-2} s^{-1}) decreased rates of net O_2 consumption. Similar decreases were observed in Pier cores incubated under ~ 5 and 25 μmol photons m^{-2} s^{-1} on 26 May and 07 July 2003; fairly analogous O_2 fluxes occurred in the dark and light on 16 June and 28 July 2003.

Mean estimates of gross photosynthetic O_2 production for Pier excluding mid-May (18.9 ± 33.9 mmol O_2 m^{-2} d^{-1}) were comparable to, although more variable than, sediments from Oyster bar (19.2 ± 7.2 mmol O_2 m^{-2} d^{-1}) and Lowry Cove (16.5 ± 10.2 mmol O_2 m^{-2} d^{-1}). Lesser rates of gross photosynthesis were observed for Mainstem (7.3 ± 8.2 mmol O_2 m^{-2} d^{-1}), especially in early-September and under ~ 10 μmol photons m^{-2} s^{-1} (< 1 mmol O_2 m^{-2} d^{-1}). Although rates were highly variable (from -96.4 to 50.9 mmol

O_2 m^{-2} d^{-1}) in sediments collected in mid-May, gross photosynthetic O_2 production was frequently zero (-12.4 ± 35.2 mmol O_2 m^{-2} d^{-1}). Similar benthic microalgal biomass among sites suggest that chlorophyll-specific responses (i.e., photoacclimation, photoinhibition) to irradiance were likely responsible for observed differences in gross photosynthesis (Table 2.2; MacIntyre et al., 1996). Similarity of gross photosynthesis at Oyster bar with other sample locations suggests that a proportion of sediment chlorophyll *a* was deposited in *C. virginica* feces and pseudofeces (Chapter 3).

Benthic oxygenic photosynthesis at all sampling locations was lower than total consumption of dissolved O_2 from sediment metabolism and, as such, all sediments were net heterotrophic (e.g., Fig. 2.3). Rates of net ecosystem metabolisms for all sediment cores ranged from -330.6 to 11.2 mmol O_2 m^{-2} d^{-1}, with a single core from Oyster bar exhibiting dominance by autotrophic processes (Fig. 2.3). Temporal fluctuations in net ecosystem metabolism in Lowry Cove, Mainstem, and Pier were associated with increases in benthic photosynthesis, decreases in O_2 production and consumption, and shifts between periods with and without benthic photosynthetic O_2 production (Fig. 2.4). Mean rates of net ecosystem metabolism, including those from 20-22 May 2003, were -10.0 ± 20.1 mmol O_2 m^{-2} d^{-1}; -22.0 ± 11.9 mmol O_2 m^{-2} d^{-1}; -183.2 ± 72.7 mmol O_2 m^{-2} d^{-1}; and -54.4 ± 55.8 mmol O_2 m^{-2} d^{-1} for Oyster bar, Lowry Cove, Pier, and Mainstem.

Shifts in nutrient exchange at the sediment-water interface

Exchange of N_2-N across the sediment-water interface fluctuated between states of apparent net N_2 fixation and denitrification among sampling locations and, occasionally, also between dark and light incubations (Fig. 2.6; Fig. 2.7). Fluxes of N_2-N

should be considered with caution; rates within the water column (i.e., blank) were often responsible for the magnitude of N_2-N uptake and release. Uptake of N_2-N occurred in Lowry Cove sediment cores during dark incubations on 23 July (-157.1 ± 40.0 μmol N_2-N m^{-2} h^{-1}) and 09 September 2002 (-54.5 ± 9.1 μmol N_2-N m^{-2} h^{-1}). Overlying water column concentrations of NH_4^+ and NO_2^- + NO_3^- were generally less than 1.7 μmol N L^{-1}, but similar water column concentrations typically supported minimal denitrification (17.9 ± 63.7 μmol N_2-N m^{-2} h^{-1}) in sediments from other sampling dates. Rates of apparent net N_2 fixation in July and September were reduced ~ 15 to 30% for irradiance incubations of ~ 70-80 μmol photons m^{-2} s^{-1}. Reduction in uptake of N_2-N was countered by consumption of NH_4^+, which was observed as a decrease or net uptake of NH_4^+ (-24.6 ± 88.9 μmol N m^{-2} h^{-1}) in the light from dark effluxes (148.8 ± 49.3 μmol N m^{-2} h^{-1}). Sediments from Bar at Oyster bar in 2002 consumed N_2-N at ~ 30 μmol N_2-N m^{-2} h^{-1} during incubations, whereas dark effluxes (66.8 ± 120.2 μmol N_2-N m^{-2} h^{-1}) typically occurred from sediments ~ 10 m away. Although cores from Mainstem exhibited the greatest temporal variability in N_2-N fluxes, ranging from -96.6 to 176.0 μmol N_2-N m^{-2} h^{-1}, sediments typically released N_2-N into overlying waters. NO_2^- + NO_3^- uptake (-16.3 ± 20.8 μmol N m^{-2} h^{-1}) occurred on all sampling dates, except for 08 September 2003 when effluxes often exceeded ~ 40 μmol N m^{-2} h^{-1} (Fig. 2.8; Fig. 2.9). Inconsistent rates of N_2-N exchange at Mainstem likely stemmed from greater and more variable concentrations of NH_4^+ and NO_2^- + NO_3^- in overlying waters (2-15 μmol N L^{-1}).

Sediment cores from Pier exhibited diel changes in N_2-N fluxes, such that rates of net denitrification measured in the dark were reduced or increased upon exposing cores to light (~ 5 μmol photons m^{-2} s^{-1}). Sediment exchange of N_2-N in the dark decreased from

178.1 ± 70.0 μmol N_2-N m^{-2} h^{-1} to 55.8 ± 26.1 μmol N_2-N m^{-2} h^{-1} on 26 May 2003. Reduction in net denitrification corresponded with shifts from consumption of NO_2^- + NO_3^- (-381.7 ± 71.9 μmol N m^{-2} h^{-1}) in the dark to sediment release in the light (48.1-304.0 μmol N L^{-1}), suggesting that direct denitrification was responsible for the observed efflux of N_2-N (Rysgaard et al. 1995). Uptake from nitrate-rich waters (59.1 ± 5.2 μmol N L^{-1}) exceeded net denitrification by ~ 53%, and dissimilatory reduction of this nitrate likely accounted for the 1.5-fold increase in NH_4^+ effluxes (682.0 ± 157.7 μmol N m^{-2} h^{-1}) over aerobic mineralization (425.3 ± 69.8 μmol N m^{-2} h^{-1}). Opposing responses occurred in June-July 2003 when water column NO_2^- + NO_3^- and NH_4^+ concentrations were < 3 and ~ 12 μmol N L^{-1}, respectively. Dark N_2-N fluxes (27.5 ± 105.7 μmol N_2-N m^{-2} h^{-1}) were likely enhanced during light incubations (89.6 ± 82.5 μmol N_2-N m^{-2} h^{-1}) through increases in oxygen penetration and available pools of NH_4^+ for nitrification (Fig. 2.11; Risgaard-Petersen et al., 1994; An and Joye, 2001; Dalsgaard, 2003). Changes in N_2-N effluxes also occurred, provided gross photosynthesis was observed, during macroalgal blooms (e.g., Pier 1 on 22 May, Pier 2 on 20 May 2003).

All sampling locations had a tendency to release NH_4^+ from sediments into overlying waters, especially during dark incubations, and thus, were not unlike other sediments of the Delmarva peninsula (-30 to 615 μmol N m^{-2} h^{-1}, Reay et al. 1995). Highest and lowest effluxes of NH_4^+ occurred in cores collected in 2002 during dark and light incubations (99.0 ± 80.9 μmol N m^{-2} h^{-1}; -9.0 ± 69.0 μmol N m^{-2} h^{-1}) and, in the dark, at Pier from late-May through July 2003 (576.2 ± 306.4 μmol N m^{-2} h^{-1}). Although rates of sediment release from Pier were usually reduced in the light (154.8 ± 568.2 μmol N m^{-2} h^{-1}), rates varied greatly (-865.3 to 961.6 μmol N m^{-2} h^{-1}). Mean effluxes from

Mainstem sediments were 182.6 ± 89.1 μmol N m^{-2} h^{-1} during dark incubations, excluding cores from 25 September 2003, and 130.8 ± 190.1 μmol N m^{-2} h^{-1} under ~ 70-80 μmol photons m^{-2} s^{-1}. Substantial reductions in sediment releases (38.9 ± 33.01 μmol N m^{-2} h^{-1}) were observed after Hurricane Isabel led to an increase in benthic microalgal biomass. Rates of NH_4^+ exchange typically followed stoichiometric predictions from dissolved O_2 fluxes (Fig. 2.10), and deviations could usually be accounted for through incorporation of N_2-N and NO_2^- + NO_3^- fluxes. Conversions of dark O_2 fluxes from macroalgal periods suggest that NH_4^+ effluxes could have surpassed those at Pier by as much as ~ 2-fold (234.8 - 1,105.4 μmol N m^{-2} h^{-1}).

Similar tendencies for soluble reactive phosphorus (SRP) were likely (14.7 – 69.1 μmol P m^{-2} h^{-1}), but rates may have been even greater given the potential for iron oxy(hydr)oxide reduction (Chapter 4-5). Maximal effluxes of SRP (29.8 ± 21.1 μmol P m^{-2} h^{-1}) occurred during dark incubations of sediments collected in July 2003. Sediment SRP fluxes for all remaining sediments, including incubations in light, exhibited near-zero or minimal exchange. Deviations from Redfield stoichiometry were likely due to adsorption of PO_4^{3-} onto iron oxy(hydr)oxides, assimilation by benthic microorganisms, and occurrence of near-detection-limit SRP concentrations in the water column (< ~ 1 μmol P L^{-1}).

Temporal variability in pore water profiles and bioirrigation

Pore water concentrations of NH_4^+ ranged from 4.9 to 984.7 μmol N L^{-1} at Lowry Cove, Pier, and Mainstem. Concentrations of NH_4^+ usually increased with depth, such that the least and greatest concentrations occurred in the 0-0.5 and 7-10 cm depth

intervals, respectively. Profiles of NH_4^+ transitioned from late-spring through summer, closely following stepped increases in water temperature until late-September (Fig. 2.11). Minima in profiles, during my study, were observed at temperatures less than 20 °C (i.e., May and November). The 1.5-fold increase in NH_4^+ concentrations in August 2005 compared to 2003 further implied a potential for inter-annual variability in the scale of this seasonal increase.

Variations in pore water profiles of NH_4^+ in 2003 also coincided with shifts in bioirrigation by benthic infauna. Nearly vertical concentration profiles and lower concentrations occurred in the surface ~ 2-4 cm of sediments when sodium bromide additions implied pore water mixing by infauna (Fig. 2.11). Rates of bioirrigation declined between 26 May and 16 June 2003 in Pier sediments, and corresponding surface (0-0.5 cm) sediment concentrations of NH_4^+ increased ~ 1.7-fold. Sediment cores collected from Pier on 26 May released NH_4^+ at rates up to 10 (8.1 ± 2.6) times greater than maximum gradients between surface (0-0.5 cm) sediment pore water and overlying water concentrations. Lesser differences (2.4 ± 2.1) in measured and diffusive fluxes occurred for remaining sampling dates. Similar shifts in bioirrigation activity were observed in Mainstem sediments from 23 July through 25 September 2003. Pore water profiles of Br^- followed modeled predictions for diffusive transport after the initial (23 July 2003) sampling date. Maximum gradients (103.4 ± 33.2 nmol cm^{-4}) in pore water NH_4^+ concentrations were reached in September, at the convergence of measured and diffusive (0-2 cm) fluxes. Qualitative estimates of bioirrigation in Lowry Cove on 6 occasions between 23 July and 30 September 2002 were indicative of diffusive transport.

Macoma balthica, an estuarine endemic clam, was found within sieved (500 μm) sediment cores from Pier and Mainstem during 2003 sampling. Lack of visual observations of *Macoma balthica* during pore water sectioning of Lowry Cove sediments (2002) may have stemmed from differences in salinity between years, as adults have been shown to be negatively correlated with salinity in mesohaline waters (Table 2.1; Holland et al. 1987). Loss of bioirrigation in summer 2003 was likely associated with clam mortality due to low dissolved O_2 concentrations in overlying waters (e.g., Schlutter et al. 2000; Borsuk et al. 2002). Increases in sediment oxygen consumption and surface concentrations of total dissolved sulfide were not observed during transitions to loss or decrease of bioirrigation. Field and laboratory methods were insufficient for determining how temperature directly affects *Macoma balthica* bioirrigation.

Pore water concentrations of SRP were not unlike NH_4^+, as concentrations increased with depth and throughout summer; concentrations varied between 0 and 279.7 μmol P L^{-1}. Ratios of NH_4^+ to SRP declined as pore water NH_4^+ concentrations increased, indicating that release of PO_4^{3-} through iron oxy(hydr)oxide reduction likely contributed to pore water concentrations. Smallest ratios of NH_4^+ to SRP (usually < 8.9) and total dissolved iron (II, III) to SRP (< 5.8) were observed in surface (0-0.5 cm) sediments from Mainstem – followed by Pier – in summer. Summed concentrations of AVS increased with decreasing total dissolved iron (II, II) to SRP ratios; maximum CRS concentrations occurred at depth (7-10 cm) in Pier (511.1 μmol S g^{-1} DW) and Mainstem (453.6 μmol S g^{-1} DW) sediments. Concentrations of AVS and CRS in Lowry Cove sediments were comparable to those recorded for other shallow water sites (Morse and Cornwell 1987; Chambers et al. 1994).

Sediment cores from Lowry Cove exhibited the greatest temporal variability in total dissolved iron (II, III) concentrations, with concentrations ranging from 0 to 218.6 μmol Fe L^{-1} and peaks varying between 0.5 and 4 cm during sampling. Build-up of dissolved iron (II, III) in Lowry Cove sediments illustrated the potential importance of iron (III) reduction in organic matter oxidation in shallow water sediments. Lower concentrations of dissolved iron (II, III) at Pier (24.4 ± 31.8 μmol Fe L^{-1}) and Mainstem (18.3 ± 25.3 μmol Fe L^{-1}) were likely associated with greater rates of SO_4^{2-} reduction and subsequent increases in iron-sulfides (e.g., FeS, FeS_2). Occurrence of greater pore water concentrations of iron (II, III) in Lowry Cove was not due to SO_4^{2-} limitation, as surface (0-0.5 cm) sediment concentrations did not fall below ~ 7 mmol SO_4^{2-} L^{-1}. Slightly lower concentrations of SO_4^{2-} (~ 2-6 mmol SO_4^{2-} L^{-1}) were observed during wetter sampling years. No dissolved sulfide was identified within the surface ~ 2 cm of sediments. Spatial variability in total dissolved iron (II, III) concentrations in pore waters and iron-sulfide mineral formation has also been observed spatially and seasonally in the main-stem of Chesapeake Bay (e.g., Roden and Tuttle 1993; Cornwell and Sampou 1995).

Summary and Conclusions

Shallow water (< 2 m) sediments within La Trappe Creek illustrated the potential for tidal creek sediments to exhibit spatial and temporal variability in sediment biogeochemistry and nutrient exchange across the sediment-water interface. Rates of sediment O_2 consumption were partially (~ 30%) attributed to shifts in stream flow and increased nearly 2- to 5-fold when sediments were within the proximity of macroalgal blooms or low water column concentrations of dissolved O_2. Variations in sediment O_2

consumption were comparable, at times, to other shallow water sediments as well as higher depositional environments, including deep sediments of Chesapeake Bay (e.g., Boynton and Kemp 1985; Rizzo and Wetzel 1985; Rizzo 1990; Reay et al. 1995; Cowan and Boynton 1996; Sundback et al. 2004). Sediment fluxes of NH_4^+ and SRP were, in general, in proportion with stoichiometric conversions (138 O_2 : 16 N : 1 P) of dissolved O_2 fluxes, but benthic microalgae (e.g., nutrient assimilation, benthic oxygenic photosynthesis) and bioirrigation from *Macoma balthica* also had consequences on exchange. Processes mediating N_2-N exchange, not unlike other sediments, varied with water column concentrations of $NO_2^- + NO_3^-$ and NH_4^+, benthic oxygenic photosynthesis, and pore water NH_4^+ concentrations (e.g., Kemp et al. 1990; Sundback et al. 2000; Tobias et al. 2003; Ferguson et al. 2004). Deviations from stoichiometry for SRP were less clear but were likely associated with typically low water column concentrations and interactions of iron and sulfur cycling.

Observed variability from late-spring through early-fall in La Trappe Creek suggests that we must be cautious when we use minimal sampling dates and study sites to characterize sediment nutrient exchange in tidal creeks. Individual sampling dates or study sites may not fully characterize the nature of these transient sediments and may, therefore, only explain a single occurrence or set of biogeochemical processes. Use of this study for extrapolation to other tidal creeks, even within Chesapeake Bay, is limited by its focus on an individual, mesohaline creek in summer and my unfamiliarity for the similarity of this tidal creek (and surrounding watershed) to other shallow water systems. I suspect that a proportion of the variability observed in La Trappe Creek was due to the collection of sediments located within the semi-euphotic zone. Sudden shifts in *in situ*

irradiance and overlying nutrient concentrations seemed to have a greater influence on sediment metabolism and nutrient cycling in sediments from greater depths (e.g., Pier, Mainstem) than sediments at water depths < 1m. Given the nature of sediment core collection, I suggest that a more comprehensive study of the conditions influencing variability within tidal creeks be conducted. Collection of sediment cores along transects spanning from euphotic to semi-euphotic zones under differing water column conditions would prove beneficial to better understanding the mechanisms driving the dynamics of these tidal creeks. Additional measurements within other tidal creeks would improve our understanding of the influence of these shallow water systems on larger, downstream estuaries and may be imperative to forecasting how management strategies may improve water quality.

Acknowledgements

Financial support for this research was provided by the Maryland Sea Grant program (R/P-49) as part of a study quantifying the magnitude of nitrogen and phosphorus removal from the restoration of *Crassostrea virginica* (eastern oysters) in Chesapeake Bay, USA. I thank E. Kiss and J. Burton-Evans for their assistance in the Cornwell laboratory with nutrient flux incubations and pore water sampling, and L. Van Heukelem, C. Thomas, L. Lane, and S. Rhoades for analyzing samples for carbon, nitrogen, chlorophyll *a*, and $NO_2^- + NO_3^-$ content. I thank T. Kana for the use of his membrane-inlet mass spectrometer for dissolved gas analyses, and V. Kennedy and S. Hurder for identifying and determining biomass of benthic macrofauna (i.e., *Macoma balthica*). I also thank J. Seabrease, E. Markin, and A. Lazur for construction and

assistance with laboratory incubations, and especially W. Boicourt, P. Boicourt, and D. Kerstetter for granting me access to La Trappe Creek via their properties. I greatly appreciate the assistance of D. Kimmel in locating daily stream flow data for the Greensboro water gauge station. I would finally like to thank J. Cornwell, M. Owens, and R. Newell for their assistance with core collection, data analysis, and interpretation, and the Dr. Nancy Foster Scholarship Program for providing financial support (Award No. NA04NOS4290250) during preparation of this manuscript.

Table 2.1 Water column and surface sediment (0-1 cm) characteristics for locations within the tidal reaches of La Trappe Creek (Choptank River, Chesapeake Bay, Maryland). Water column and surface sediment characteristics were determined from measurements collected during the specified timeframes, with collections typically occurring at near weekly intervals. The range of measurements for salinity, water depth, and light attenuation coefficients (k_d) are provided unless the location was not revisited; all study sites were located in waters with a tidal range of 0.49 m and a mean tide of 0.34 m. Porosities (mean ± standard deviation) were estimated from percent water for representative cores, assuming a sediment density of 2.5 g cm^{-3} (Cornwell et al. 1996). Standard deviations were determined for mean porosities estimated for the 0-0.5 cm and 0.5-1.0 cm depth intervals and replicate cores (n = 1-6). nd: no data available.

Location	Sampling timeframe	Salinity	Water depth (m)	k_d (m^{-1})	Porosity Sediment-type
Oyster Bar	13 Aug 2002	13.4	0.99	1.63	nd Sand, Silty-sand
Lowry Cove	23 July – 30 Sept 2002	12 – 16	0.73 – 1.15	2.02 – 3.87	0.87 ± 0.02 Silt-clay

Pier	20 May – 28 July 2003	4 – 9	1.08 – 1.70	1.35 – 3.85	0.90 ± 0.02 Silt-clay
Mainstem	20-21 May	8 – 9	1.08 – 1.31	1.35 – 1.96	nd Silt-clay
	23 July – 25 Sept 2003	5 – 8	1.10 – 2.00	1.95 – 5.88	0.90 ± 0.01 Silt-clay
	10 Nov 2004	11.5	1.18	1.24	nd Silt-clay
	31 Aug 2005	10.6 – 10.7	1.70	2.85	0.83 ± 0.03 Silt-clay

Table 2.2 Percent organic content (%; mean ± standard deviation), determined from loss on ignition at 550 °C, and concentrations of sediment chlorophyll *a* (mg chl *a* m^{-2}; mean ± standard deviation) for the 0-1 cm depth interval of sediment. Sediments for chlorophyll *a* analyses were collected with a syringe mini-corer (1.4 cm I.D.) and frozen in centrifuge tubes wrapped in aluminum foil until analysis via high performance liquid chromatography (Van Heukelem et al. 1994; centrifuged at 1,643 xg in International Equipment Company Centra MP4 and CL2; 3500 rpm). Number of observations (n) are provided in parentheses.

Site	Percent organic content (%)	Sediment chlorophyll *a* (mg chl *a* m^{-2})
Location		
Oyster Bar		
Bar[a]	2.42 ± 2.36 (6)	22.41 ± 14.40 (6)
Adjacent[a]	0.40 ± 0.56 (2)	39.52 ± 20.60 (4)
Lowry Cove		
Cove 1	11.68 ± 0.71 (10)	11.14 ± 2.27 (12)
Cove 2	12.25 ± 0.95 (3)	11.98 ± 4.50 (6)
Cove 3[a]	12.00 ± 0.51 (5)	12.65 ± 2.44 (6)
Pier		

Pier 1	11.21 ± 0.51 (20)	18.96 ± 5.47 (20)
Pier 2[a]	11.82 ± 0.33 (5)	21.24 ± 6.06 (5)
Mainstem		
Upper 1	10.61 ± 0.57 (20)	11.68 ± 6.04 (20)
Upper 2[a]	10.29 ± 0.80 (5)	7.16 ± 2.40 (5)
Upper 3	nd	nd
Upper 4[a]	9.08 ± 1.93 (6)	8.05 ± 3.10 (6)

[a] Surface sediments for percent organic content and sediment chlorophyll *a* were only collected once. Oyster Bar: 13 August 2002; Lowry Cove (Cove 3): 23 July 2002; Pier (Pier 2): 26 May 2003; Mainstem (Upper 2): 23 July 2003; Mainstem (Upper 4): 31 August 2005.

Figure Legends

Fig. 2.1 Location of study sites within La Trappe Creek, a tributary of the Choptank River, Chesapeake Bay, Maryland, USA. Study sites occurred within four locations: Oyster bar (filled circles); Lowry Cove (open circles); Pier (filled triangles); and Mainstem (open triangles).

Fig. 2.2 Surface sediment (0-1 cm) concentrations of total nitrogen (μmol N g^{-1} DW) versus total carbon (μmol C g^{-1} DW) and HCl-extractable iron (μmol Fe g^{-1} DW) versus inorganic phosphorus (μmol P g^{-1} DW) for cores collected at study sites located within Oyster bar (filled circles), Lowry Cove (open circles), Pier (filled triangles), and Mainstem (open triangles). Dashed lines indicate significant trends ($P < 0.0001$), with r^2 values as shown. Linear regressions: C/N: $y = 10.66 x – 35.16$; Fe/P: $9.44 x + 18.39$.

Fig. 2.3 Medians, first and third quartiles, and ranges for dark O_2 fluxes (μmol O_2 m^{-2} h^{-1}; n = 132), light O_2 fluxes (μmol O_2 m^{-2} h^{-1}; n = 104), gross primary productivity (GPP; mmol O_2 m^{-2} d^{-1}; n = 99), and net ecosystem metabolism (NEM; mmol O_2 m^{-2} d^{-1}; n = 99) for cores collected at study sites located within Oyster bar, Lowry Cove, Pier, and Mainstem. Estimates of gross primary productivity were determined as 14 h * (O_2 flux measured during light incubations – O_2 flux measured during dark incubations). Net ecosystem metabolism estimates were determined as 14 h * O_2 flux measured during light incubations + 24 h * O_2 flux

measured during dark incubations. Surface sediment irradiances maintained during light incubations varied with sampling date and location. **Oyster bar:** ~ 100 μmol photons m^{-2} s^{-1}; **Lowry Cove:** ~ 70-80 μmol photons m^{-2} s^{-1}; **Pier:** ~ 5 μmol photons m^{-2} s^{-1}, except on 21-22 May 2003 (~ 25-30 μmol photons m^{-2} s^{-1}); **Mainstem:** ~ 70-80 μmol photons m^{-2} s^{-1}, except on 21-22 May 2003 (~25-30 μmol photons m^{-2} s^{-1}) and 31 August 2005 (~ 10 and 100 μmol photons m^{-2} s^{-1}).

Fig. 2.4 Mean (± standard deviation; n = 3-5) dark O_2 fluxes (μmol O_2 m^{-2} h^{-1}) and rates of net ecosystem metabolism (mmol O_2 m^{-2} d^{-1}) for study sites revisited in Lowry Cove, Pier, and Mainstem in 2002 and 2003. Estimates of net ecosystem metabolism (gray squares) were determined as 14 h * O_2 flux measured during light incubations + 24 h * O_2 flux measured during dark incubations. Surface sediment irradiances of approximately 70-80 μmol photons m^{-2} s^{-1} were maintained during light incubations for sediment cores collected in Lowry Cove and Mainstem. Sediment cores from Pier were incubated at approximately 5 μmol photons m^{-2} s^{-1}, except on 21-22 May 2003 when surface sediment irradiances approaches ~ 25 – 30 and 45 – 50 μmol photons m^{-2} s^{-1}. Note differences in scale for net ecosystem metabolism.

Fig. 2.5 Monthly and daily stream flow for the Greensboro water gauge station, Choptank River, Chesapeake Bay, Maryland versus dark O_2 fluxes (μmol O_2 m^{-2} h^{-1}) for sediment cores collected within Oyster bar (filled circles), Lowry Cove (open circles), Pier (filled triangles), and Mainstem (open triangles). Monthly and

daily stream flows were normalized to the maximum monthly and daily stream flow, respectively, recorded during the sampling periods (July – September 2002; May – September 2003; November 2004; August 2005). Gray triangles represent sediment cores collected during a macroalgal bloom within the vicinity of Pier and Mainstem in May 2003. Solid and dashed lines indicate significant trends ($P < 0.0001$), with r^2 values as shown, for data including and excluding the macroalgal bloom, respectively.

Fig. 2.6 Mean (± standard deviation) dark N_2-N fluxes (μmol N m^{-2} h^{-1}) for cores collected at study sites located within Oyster bar (squares; n = 3-6), Lowry Cove (circles; n = 2-3), Pier (triangles; n = 2-5), and Mainstem (diamonds; n = 2-7).

Fig. 2.7 Mean (± standard deviation) light N_2-N fluxes (μmol N m^{-2} h^{-1}) for cores collected at study sites located within Oyster bar (squares; n = 4-6), Lowry Cove (circles; n = 1-3), Pier (triangles; n = 1-5), and Mainstem (diamonds; n = 2-8). Surface sediment irradiances maintained during light incubations varied with sampling date and location. **Oyster bar:** ~ 100 μmol photons m^{-2} s^{-1}; **Lowry Cove:** ~ 70-80 μmol photons m^{-2} s^{-1}; **Pier:** ~ 5 μmol photons m^{-2} s^{-1}, except on 21-22 May 2003 (~ 25-30 μmol photons m^{-2} s^{-1}); **Mainstem:** ~ 70-80 μmol photons m^{-2} s^{-1}, except on 21-22 May 2003 (~25-30 μmol photons m^{-2} s^{-1}) and 31 August 2005 (~ 10 and 100 μmol photons m^{-2} s^{-1}).

Fig. 2.8 Mean (± standard deviation) dark NO_3^- + NO_2^- fluxes (μmol N m^{-2} h^{-1}) for cores collected at study sites located within Oyster bar (squares; n = 1), Lowry Cove (circles; n = 1-2), Pier (triangles; n = 1-5), and Mainstem (diamonds; n = 3-5). No significant dark NO_3^- + NO_2^- fluxes were determined for Adjacent or Cove 3, and no NO_3^- + NO_2^- samples were collected on 20-22 May 2003 (Pier 1-2, Upper 3). See Chapter 4 (Table 4.4) for a description of NO_3^- + NO_2^- fluxes for Upper 4.

Fig. 2.9 Mean (± standard deviation) light NO_3^- + NO_2^- fluxes (μmol N m^{-2} h^{-1}) for cores collected at study sites located within Oyster bar (squares; n = 1-2), Lowry Cove (circles; n = 1), Pier (triangles; n = 1-4), and Mainstem (diamonds; n = 1-5). No significant light NO_3^- + NO_2^- fluxes were determined for Cove 1, and no NO_3^- + NO_2^- samples were collected on 20-22 May 2003 (Pier 1-2, Upper 3). See Chapter 4 (Table 4.4) for a description of NO_3^- + NO_2^- fluxes for Upper 4. Surface sediment irradiances maintained during light incubations varied with sampling date and location. **Oyster bar:** ~ 100 μmol photons m^{-2} s^{-1}; **Lowry Cove:** ~ 70-80 μmol photons m^{-2} s^{-1}; **Pier:** ~ 5 μmol photons m^{-2} s^{-1}, except on 21-22 May 2003 (~ 25-30 μmol photons m^{-2} s^{-1}); **Mainstem:** ~ 70-80 μmol photons m^{-2} s^{-1}, except on 21-22 May 2003 (~25-30 μmol photons m^{-2} s^{-1}) and 31 August 2005 (~ 10 and 100 μmol photons m^{-2} s^{-1}).

Fig. 2.10 Mean (± standard deviation; n = 1-6) fluxes of O_2 (μmol O_2 m^{-2} h^{-1}) versus NH_4^+ (μmol N m^{-2} h^{-1}) and soluble reactive phosphorus (μmol P m^{-2} h^{-1}) for dark (a, b) and light (c, d) incubations of sediment cores collected within Oyster bar

(filled circles), Lowry Cove (open circles), Pier (filled triangles), and Mainstem (open triangles). Solid lines indicate stoichiometric ratios of O_2 : N and O_2 : P as predicted from Redfield ratios (138 O2 : 16 N : 1 P).

Fig. 2.11 Mean (± standard deviation; n = 2-6) pore water concentrations of NH_4^+ (μmol N L^{-1}) and Br^- (mmol L^{-1}) measured or modeled within sediment cores from sites revisited in Pier (a, c) and Mainstem (b, d). Sampling dates for measured profiles are provided within each panel for NH_4^+ and Br^-. Modeled concentrations of Br^- were determined using Fick's first law of diffusion, assuming steady-state conditions and molecular diffusion. Diffusion coefficients within sediments were estimated from diffusion coefficients in free solution at ambient temperatures and Boudreau's law ($\theta^2 = 1 - \ln(\varphi^2)$, Boudreau 1997 *in* Schultz 2000).

Fig. 2.1

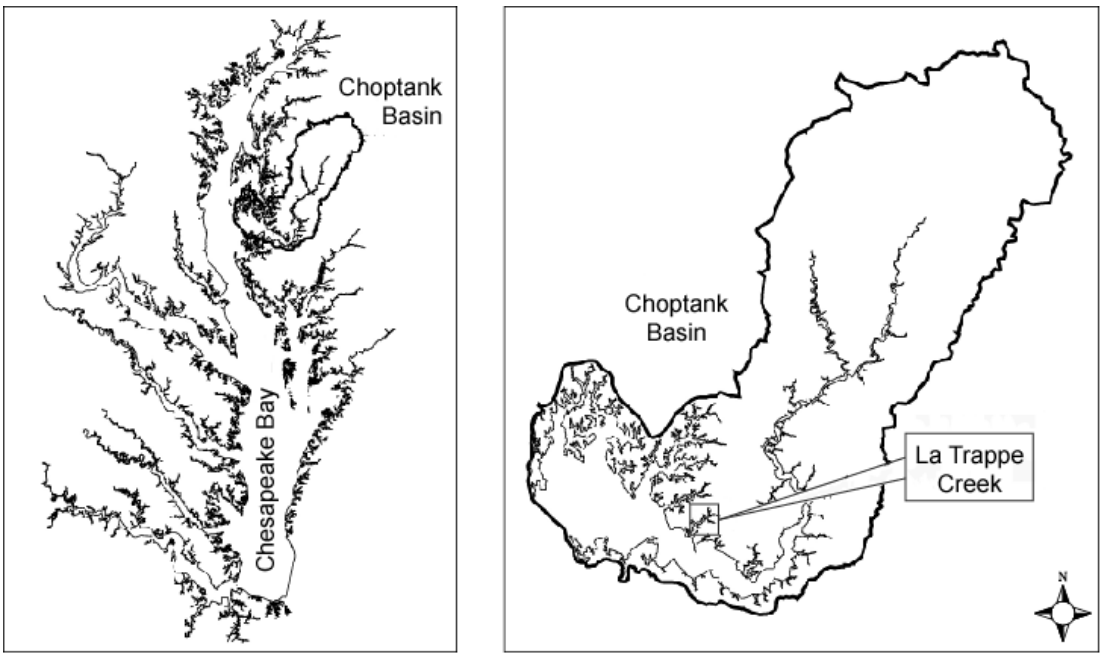

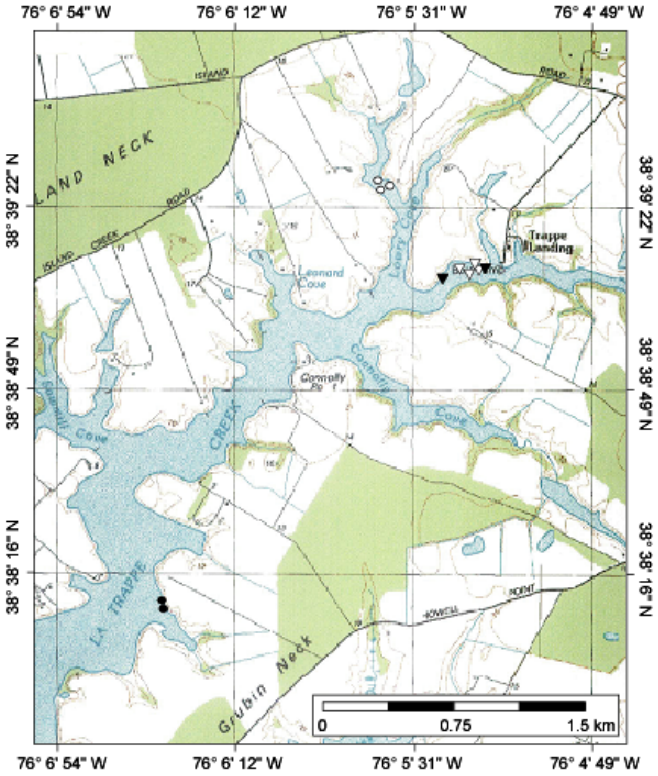

Figure 1
R. R. Holyoke

Fig. 2.2

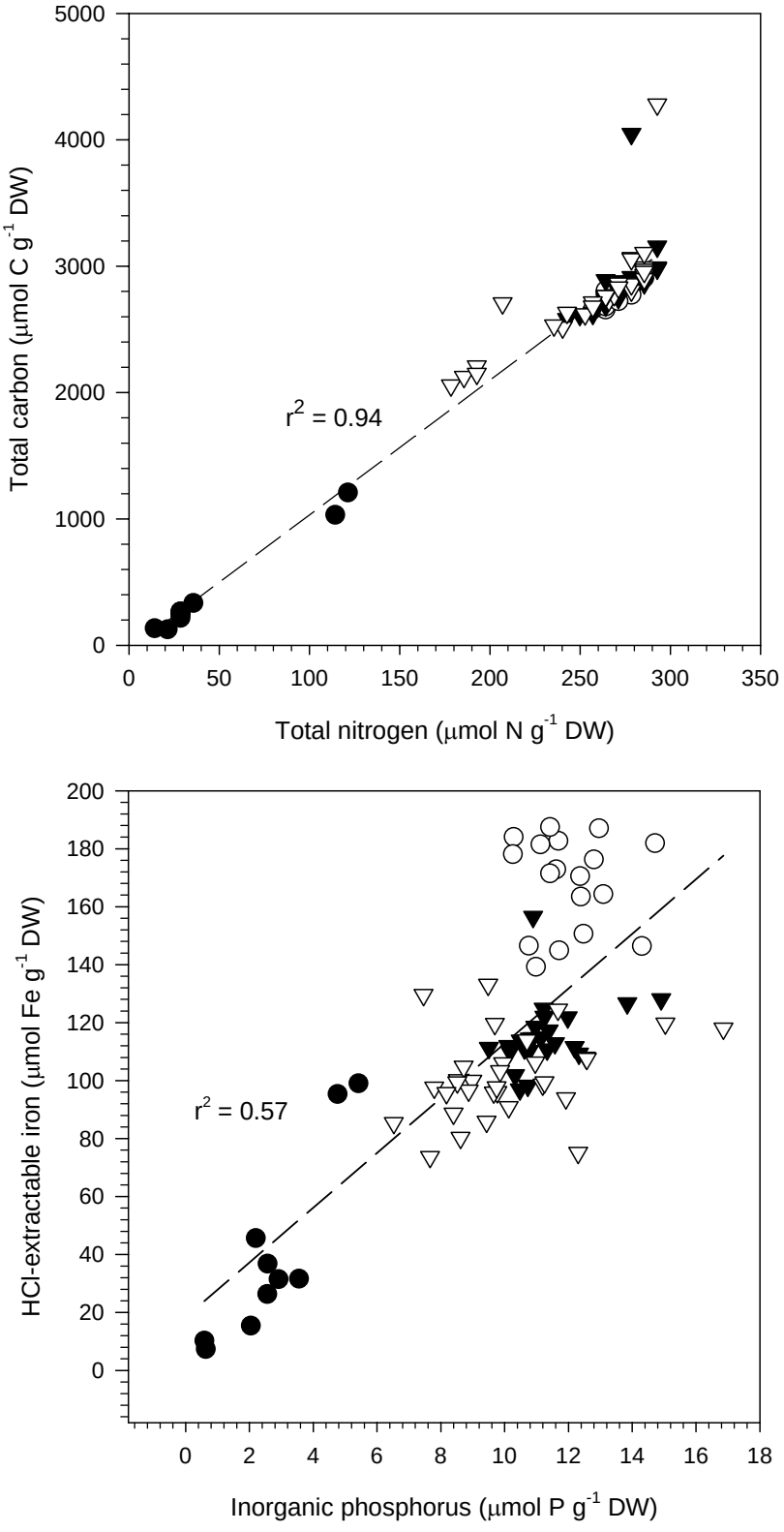
Total carbon (μmol C g-1 DW)
Total nitrogen (μmol N g-1 DW)
r2 = 0.94
HCl-extractable iron (μmol Fe g-1 DW)
Inorganic phosphorus (μmol P g-1 DW)
r2 = 0.57

Fig. 2.3

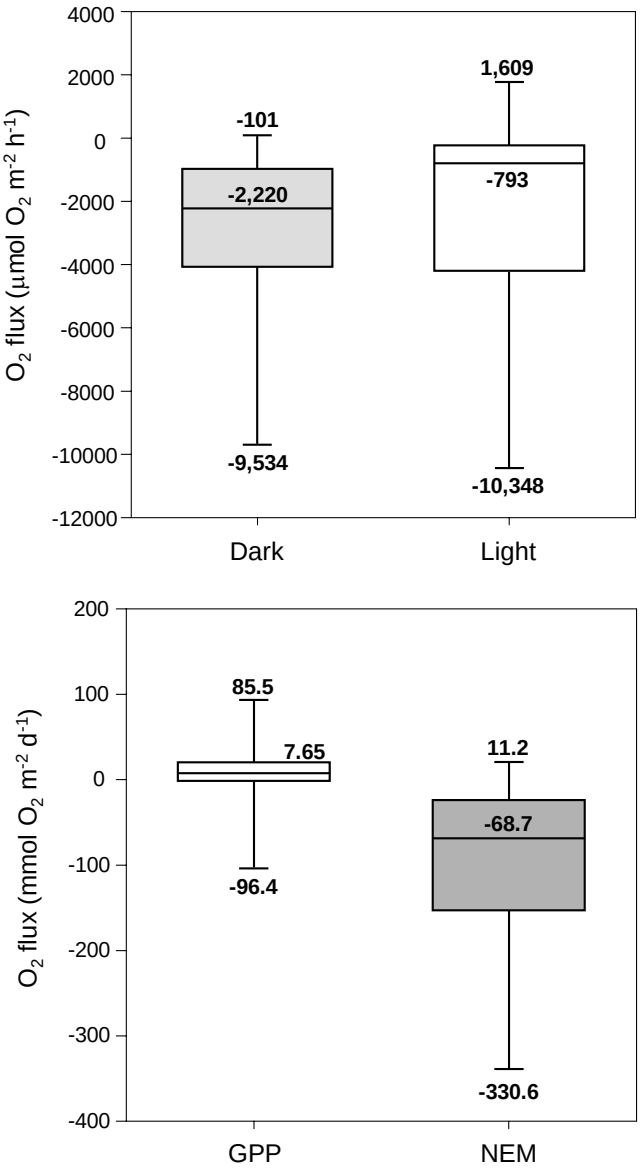
4000
2000
0
-2000
-4000
-6000
-8000
-10000
-12000
O2 flux (µmol O2 m-2 h-1)
-101
-2,220
-9,534
1,609
-793
-10,348
Dark
Light
200
100
0
-100
-200
-300
-400
O2 flux (mmol O2 m-2 d-1)
85.5
7.65
-96.4
11.2
-68.7
-330.6
GPP
NEM

Fig. 2.4

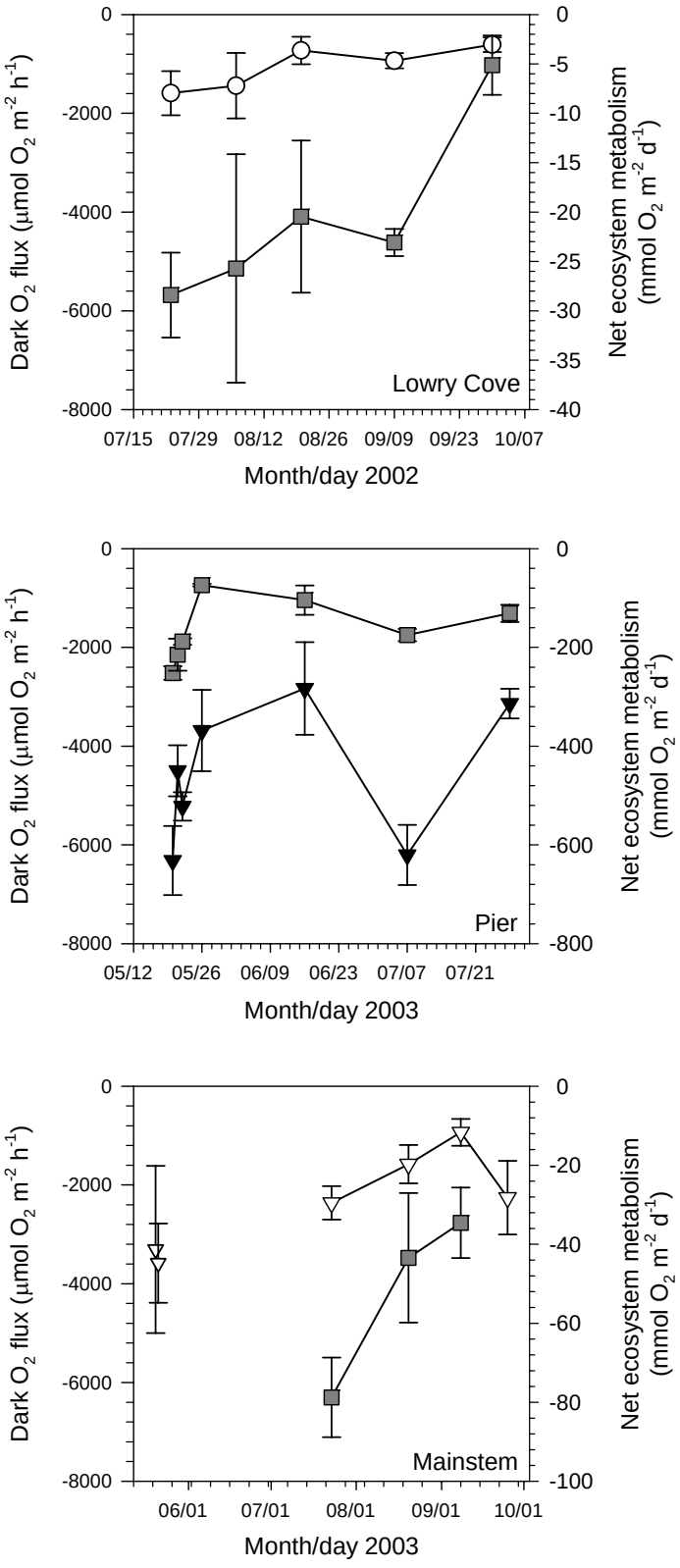
Dark O_2 flux (µmol O_2 m^{-2} h^{-1})
Net ecosystem metabolism (mmol O_2 m^{-2} d^{-1})
0
-2000
-4000
-6000
-8000
0
-5
-10
-15
-20
-25
-30
-35
-40
Lowry Cove
07/15 07/29 08/12 08/26 09/09 09/23 10/07
Month/day 2002
0
-2000
-4000
-6000
-8000
0
-200
-400
-600
-800
Pier
05/12 05/26 06/09 06/23 07/07 07/21
Month/day 2003
0
-2000
-4000
-6000
-8000
0
-20
-40
-60
-80
-100
Mainstem
06/01 07/01 08/01 09/01 10/01
Month/day 2003

Fig. 2.5

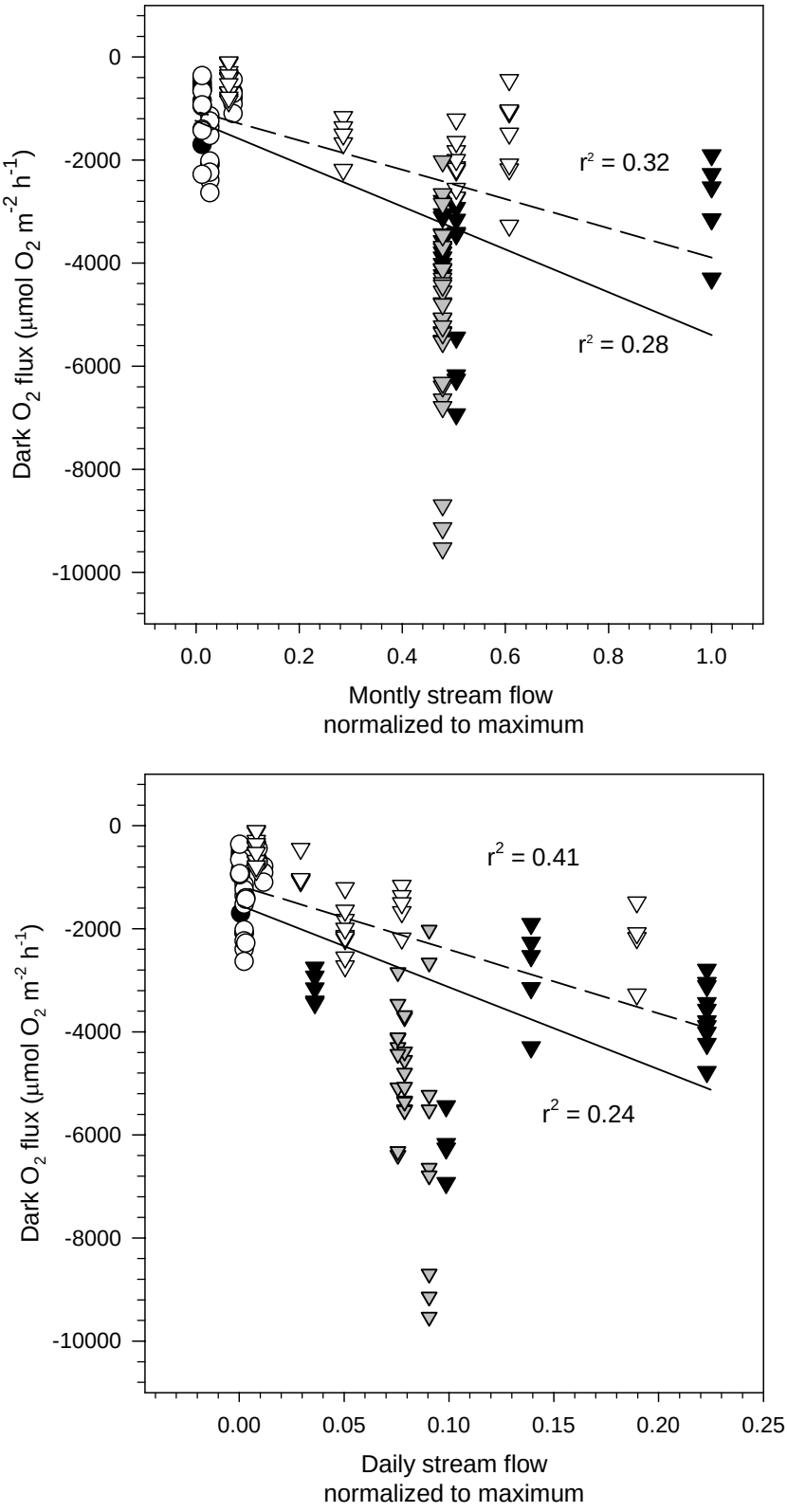
0
-2000
-4000
-6000
-8000
-10000
Dark O_2 flux (µmol O_2 m^{-2} h^{-1})
r^2 = 0.32
r^2 = 0.28
0.0
0.2
0.4
0.6
0.8
1.0
Montly stream flow
normalized to maximum
0
-2000
-4000
-6000
-8000
-10000
Dark O_2 flux (µmol O_2 m^{-2} h^{-1})
r^2 = 0.41
r^2 = 0.24
0.00
0.05
0.10
0.15
0.20
0.25
Daily stream flow
normalized to maximum

Fig. 2.6

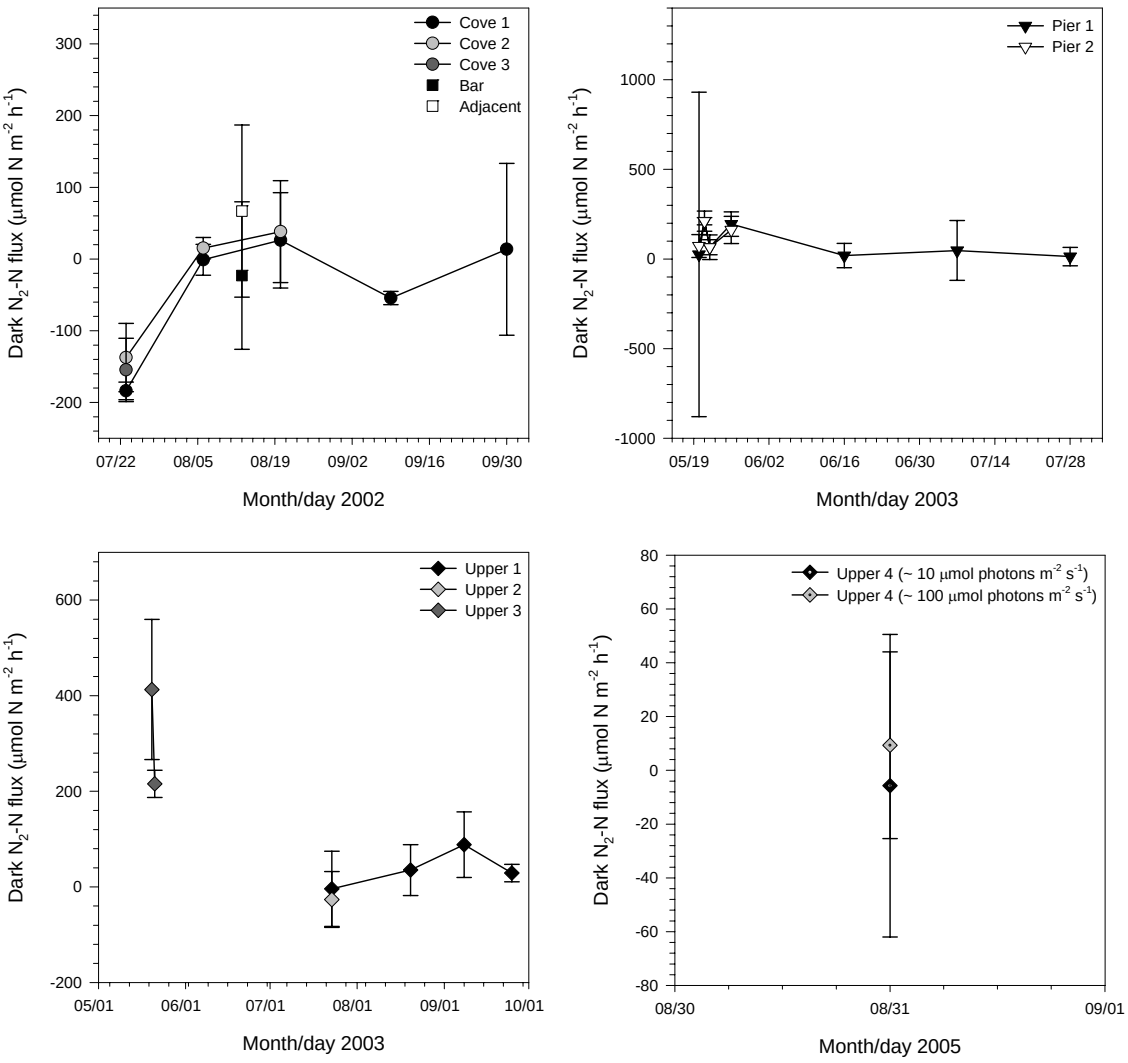
Cove 1
Cove 2
Cove 3
Bar
Adjacent
Dark N2-N flux (μmol N m-2 h-1)
300
200
100
0
-100
-200
07/22
08/05
08/19
09/02
09/16
09/30
Month/day 2002
Pier 1
Pier 2
Dark N2-N flux (μmol N m-2 h-1)
1000
500
0
-500
-1000
05/19
06/02
06/16
06/30
07/14
07/28
Month/day 2003
Upper 1
Upper 2
Upper 3
Dark N2-N flux (μmol N m-2 h-1)
600
400
200
0
-200
05/01
06/01
07/01
08/01
09/01
10/01
Month/day 2003
Upper 4 (~ 10 μmol photons m-2 s-1)
Upper 4 (~ 100 μmol photons m-2 s-1)
Dark N2-N flux (μmol N m-2 h-1)
80
60
40
20
0
-20
-40
-60
-80
08/30
08/31
09/01
Month/day 2005

Fig. 2.7

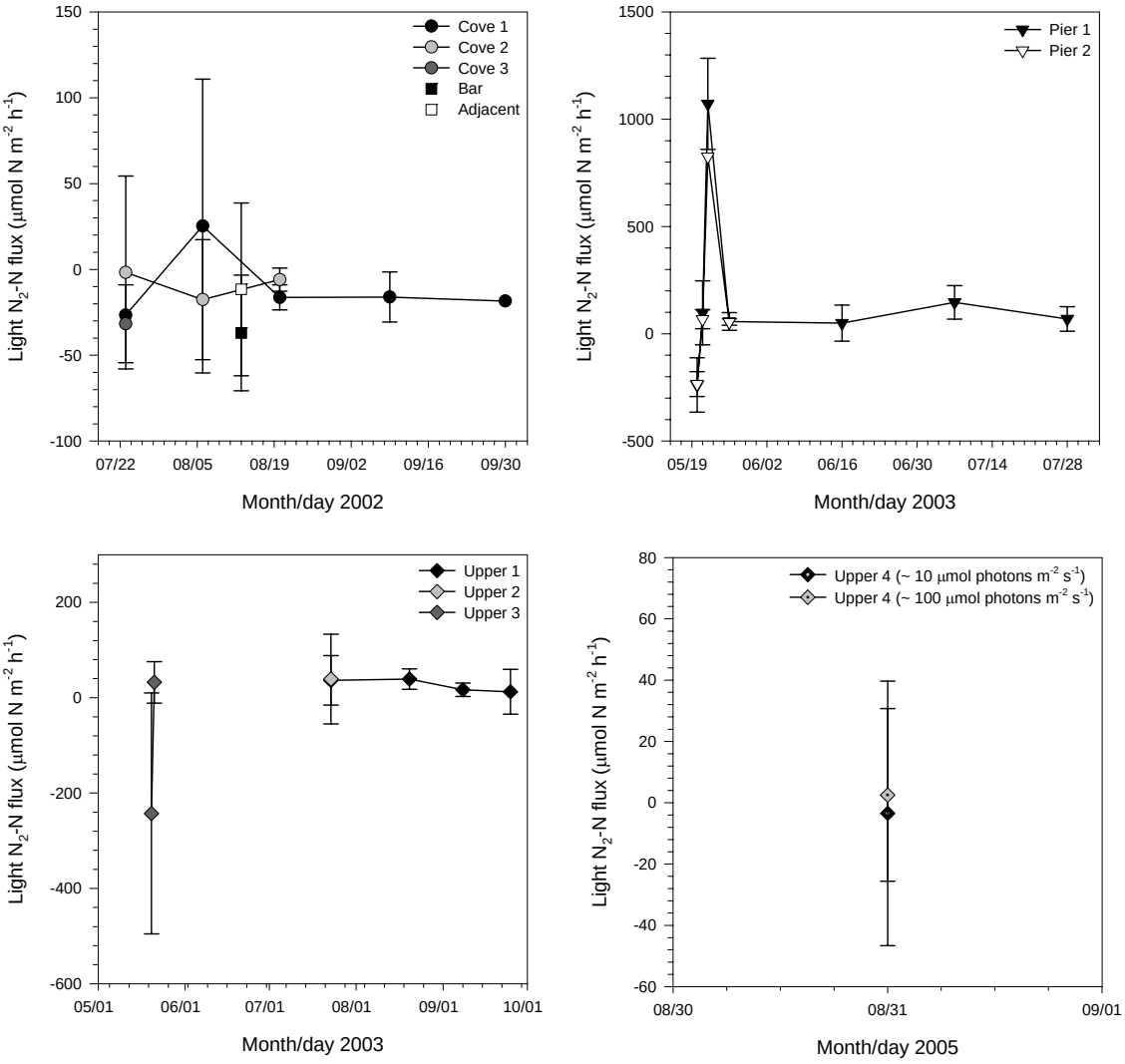
Cove 1
Cove 2
Cove 3
Bar
Adjacent
Light N_2-N flux (μmol N m^{-2} h^{-1})
Month/day 2002
Pier 1
Pier 2
Month/day 2003
Upper 1
Upper 2
Upper 3
Month/day 2003
Upper 4 (~ 10 μmol photons m^{-2} s^{-1})
Upper 4 (~ 100 μmol photons m^{-2} s^{-1})
Month/day 2005

Fig. 2.8

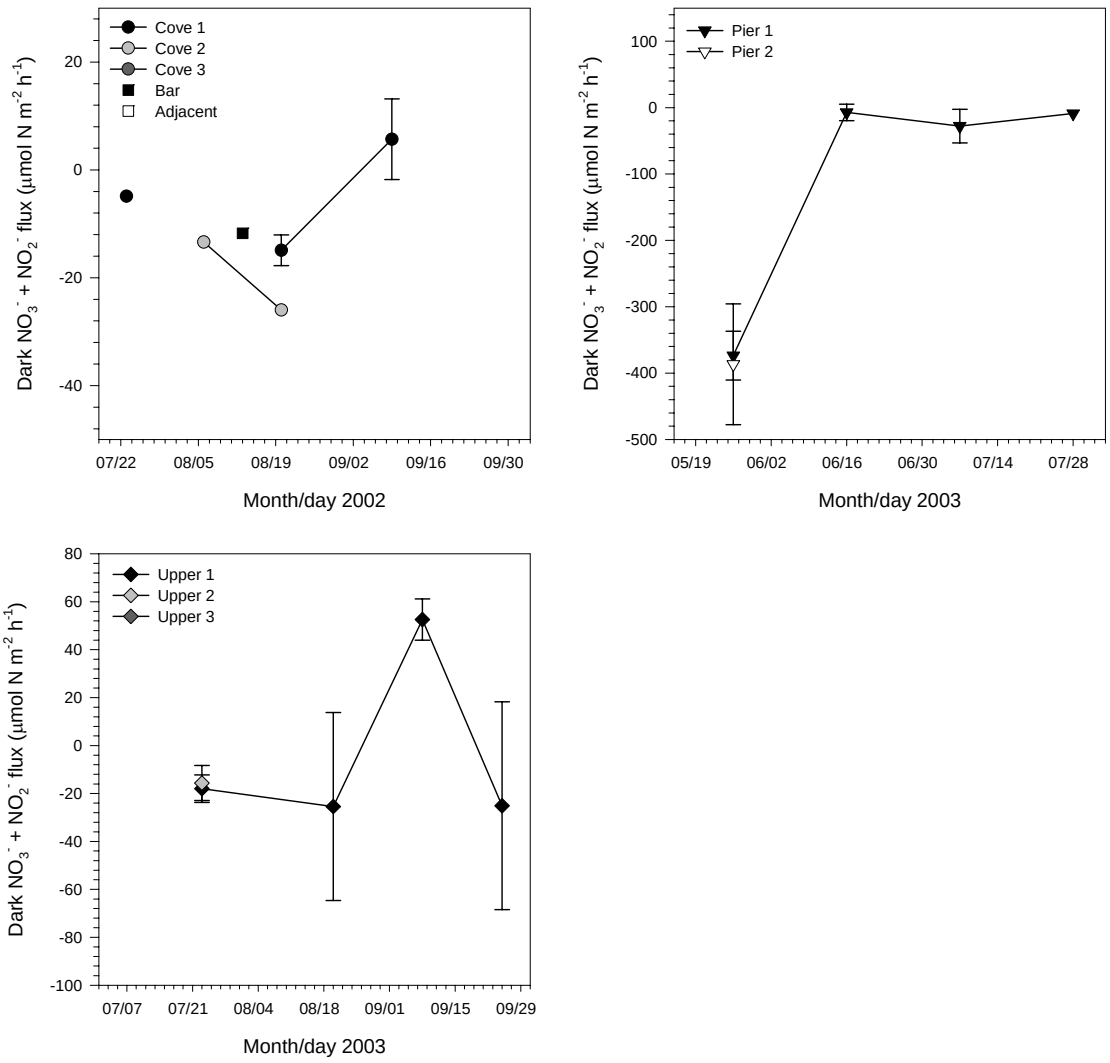
Cove 1
Cove 2
Cove 3
Bar
Adjacent
Dark NO3- + NO2- flux (µmol N m-2 h-1)
20
0
-20
-40
07/22
08/05
08/19
09/02
09/16
09/30
Month/day 2002
Pier 1
Pier 2
100
0
-100
-200
-300
-400
-500
05/19
06/02
06/16
06/30
07/14
07/28
Month/day 2003
Upper 1
Upper 2
Upper 3
80
60
40
20
0
-20
-40
-60
-80
-100
07/07
07/21
08/04
08/18
09/01
09/15
09/29
Month/day 2003

Fig. 2.9

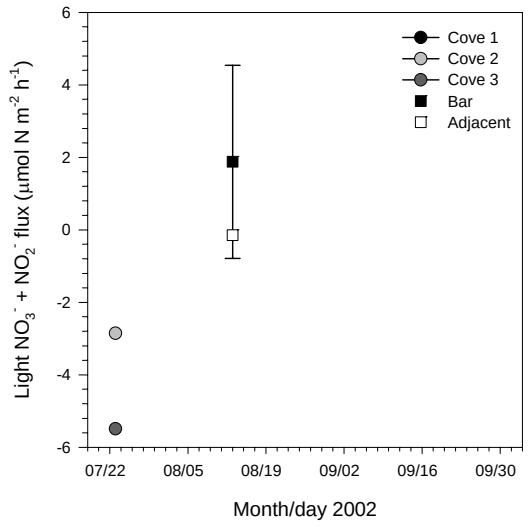
Cove 1
Cove 2
Cove 3
Bar
Adjacent
Light NO_3^- + NO_2^- flux (µmol N m^{-2} h^{-1})
6
4
2
0
-2
-4
-6
07/22
08/05
08/19
09/02
09/16
09/30
Month/day 2002

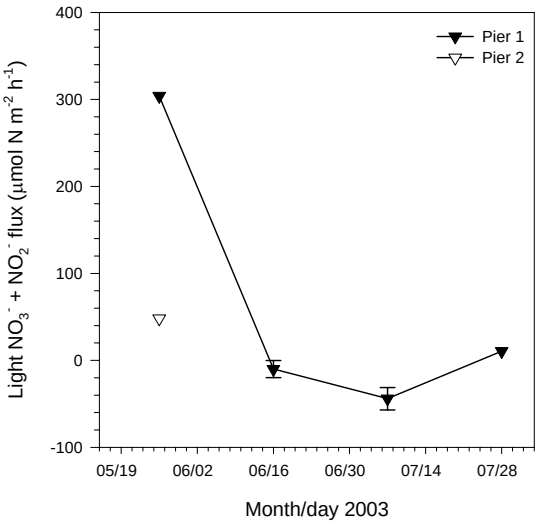
Pier 1
Pier 2
Light NO_3^- + NO_2^- flux (µmol N m^{-2} h^{-1})
400
300
200
100
0
-100
05/19
06/02
06/16
06/30
07/14
07/28
Month/day 2003

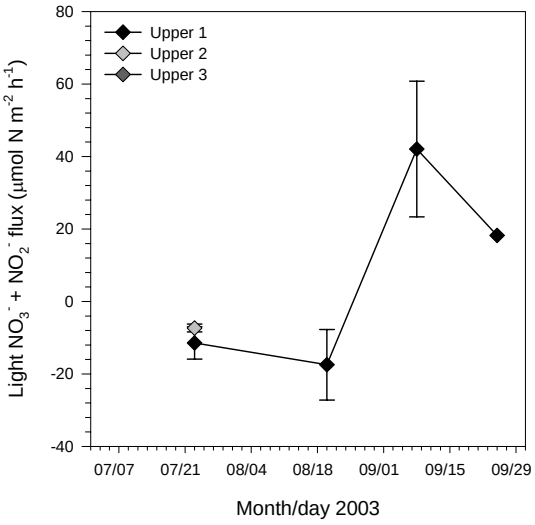
Upper 1
Upper 2
Upper 3
Light NO_3^- + NO_2^- flux (µmol N m^{-2} h^{-1})
80
60
40
20
0
-20
-40
07/07
07/21
08/04
08/18
09/01
09/15
09/29
Month/day 2003

Fig. 2.10

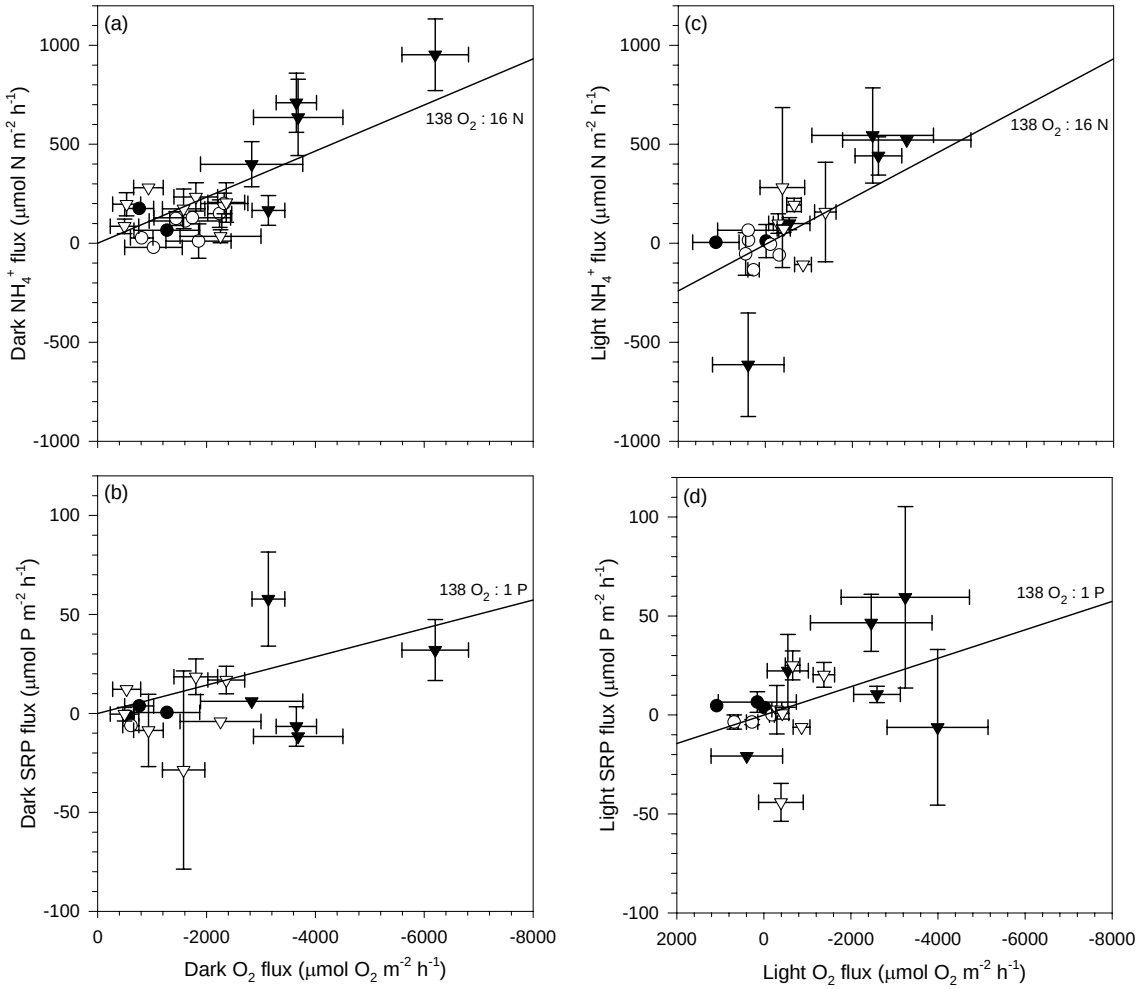
(a)
138 O2 : 16 N
Dark NH4+ flux (µmol N m-2 h-1)
1000
500
0
-500
-1000
(c)
138 O2 : 16 N
Light NH4+ flux (µmol N m-2 h-1)
(b)
138 O2 : 1 P
Dark SRP flux (µmol P m-2 h-1)
100
50
0
-50
-100
0
-2000
-4000
-6000
-8000
Dark O2 flux (µmol O2 m-2 h-1)
(d)
138 O2 : 1 P
Light SRP flux (µmol P m-2 h-1)
2000
Light O2 flux (µmol O2 m-2 h-1)

Fig. 2.11

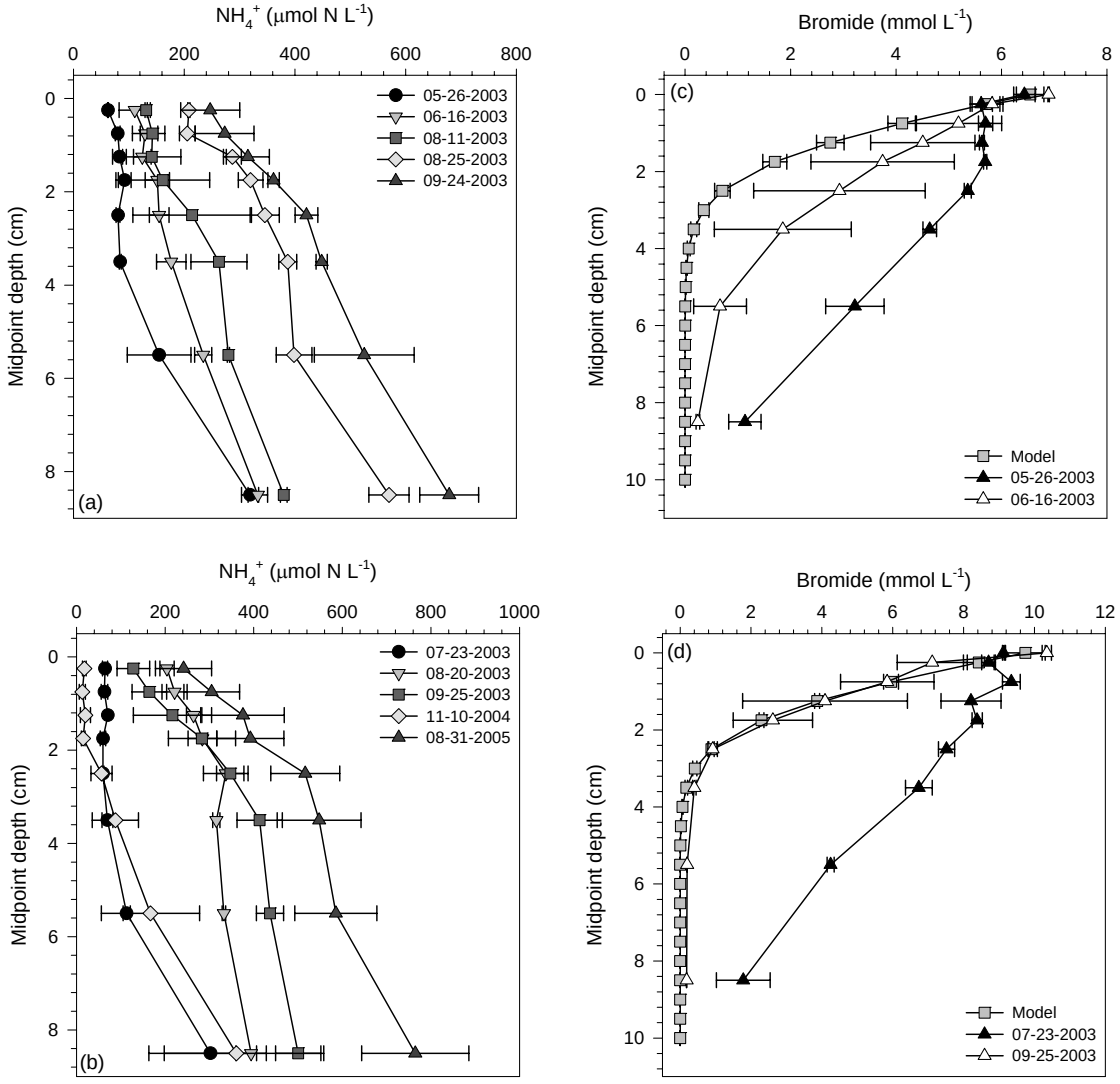
NH4+ (μmol N L-1)
Midpoint depth (cm)
05-26-2003
06-16-2003
08-11-2003
08-25-2003
09-24-2003
(a)
Bromide (mmol L-1)
(c)
Model
05-26-2003
06-16-2003
NH4+ (μmol N L-1)
Midpoint depth (cm)
07-23-2003
08-20-2003
09-25-2003
11-10-2004
08-31-2005
(b)
Bromide (mmol L-1)
(d)
Model
07-23-2003
09-25-2003

Chapter 3: Biogeochemical Responses of Shallow Water Sediments to Small-scale Aquaculture of the Eastern Oyster, *Crassostrea virginica*

Abstract

Stocks of the eastern oyster, *Crassostrea virginica*, have been declining in Chesapeake Bay since the late 19th century, and current efforts to restore *C. virginica* include increasing subtidal suspension (i.e., off-bottom) culture of *C. virginica*. The influence of *C. virginica* biodeposits on sediment nitrogen cycling, particularly nitrogen burial and denitrification, is unclear. To assess the influence of *C. virginica* biodeposits on nitrogen regeneration (NH_4^+, $NO_2^- + NO_3^-$), burial, and denitrification (N_2-N), off-bottom aquaculture of *C. virginica* was established at a total of three sites within shallow waters of Chesapeake Bay in summer 2002 and 2003. *C. virginica* biodeposits led to gradual increases in surface sediment nitrogen and pore water NH_4^+ through enhanced deposition and organic nitrogen concentrations. Rates of benthic microalgal production, and not added particulate organic nitrogen from biodeposits, influenced sediment exchanges of N_2-N with the water column. Benthic microalgae modulated NH_4^+ release from sediments during light and some dark incubations. Organic carbon from *C. virginica* biodeposits did not increase aerobic respiration (i.e., dark O_2 fluxes), but increases in sulfate reduction were apparent through concentration changes in total dissolved sulfide and acid-volatile sulfide. Discrepancies in the magnitude of sedimentary responses were due to differences in the quantity and quality of *C. virginica* biodeposits being deposited to the sediment surface. These field studies illustrated that *C. virginica* aquaculture in tidal creeks of Chesapeake Bay may have varying effects on sediment biogeochemistry, and these effects may be influenced by benthic microalgae and availability of particulate organic nitrogen.

Key words: Aquaculture, biodeposits, Chesapeake Bay, eastern oyster, nitrogen fluxes, pore water, tidal creek

Introduction

Standing stocks of the eastern oyster, *Crassostrea virginica* (Gmelin 1791), have been continuously declining in Chesapeake Bay since the late 19th century (Kennedy & Breisch 1981). These declines in *C. virginica* abundance have stemmed primarily from oyster harvesting and the resulting loss of oyster reef habitats (Rothschild et al. 1994, Smith et al. 2003), but they have also been exacerbated by mortalities from the protozoan parasites, *Perkinsus marinus* (Dermo) and *Haplosporidium nelsoni* (MSX, Ford & Tripp 1996). Loss of *C. virginica* has weakened the commercial fishery in Chesapeake Bay and reduced the potential for these suspension feeders to exert partial top-down control on phytoplankton and to enhance coupling of benthic and pelagic processes (Newell 1988, Newell et al. 2005).

Ecological and economic benefits of *C. virginica* prompted restoration efforts, such that, at minimum, a 10-fold increase in standing stocks from a 1994 baseline be achieved by 2010 (http://www.chesapeakebay.net/agreement.htm, 19 June 2007). Efforts to restore *C. virginica* have been met with difficulty, as harvesting techniques and siltation have left little shell suitable for larval settlement (Rothschild et al. 1994, Smith et al. 2005). Restoration activities in Chesapeake Bay have typically been through production of hatchery-reared *C. virginica* spat that are placed on existing oyster bars (National Research Council 2004). Subtidal suspension (i.e., off-bottom) culture of *C. virginica* has been limited, thus far, to on-growing of hatchery brood-stock and seed

nurseries (including oyster gardening) and a relatively limited number of aquaculture operations in sheltered tidal creeks. Current strategies involve increasing off-bottom operations for growth of *C. virginica* and possibly the non-native Suminoe oyster, *Crassostrea ariakensis* (National Research Council 2004). Increases in aquaculture of *C. virginica* have already been observed in Virginia, USA, with 16.1 and 3.1 million oysters planted on-bottom and sold by aquaculturists in 2006 (Murray et al. 2007). Studies on the influence of subtidal *C. virginica* aquaculture on Chesapeake Bay sediments will advance our understanding of this activity while offering insight into the influence of oyster biodeposits (feces and pseudofeces) on sediment biogeochemistry. It is difficult to perform such studies on native oyster bars due to the technical difficulty of working on sediment processes in the presence of oyster shell.

The ecological function of *C. virginica* has been studied largely from the perspective of the influence of these suspension feeders on water column nutrient concentrations and reductions or increases in phytoplankton biomass (e.g., Dame et al. 1989, Dame et al. 1992, Dame & Libes 1993, Nelson et al. 2004). Increased water column concentrations and excretion of NH_4^+ (urine) have been used to suggest that *C. virginica* recycle nitrogen rapidly and, thereby, enhance water column production (Dame et al. 1984, Pietros & Rice 2003). However, reductions in biomass of phytoplankton have the potential to redirect photosynthesis in shallow waters to seagrasses and benthic microalgae through increased light penetration (Newell & Koch 2004, Porter et al. 2004). Additionally, *C. virginica* biodeposits transfer particulate organic nitrogen (PON) to sediments, and the influence of these biodeposits on sediment nitrogen cycling, particularly nitrogen burial and denitrification, remain unclear (Newell et al. 2004,

Newell et al. 2005). Sediment increases in PON have been observed in sediments beneath long-line aquaculture of the Pacific oyster, *Crassostrea gigas*, in spring and summer (Mazouni 2004).

There are no published measurements of denitrification, or N_2-N loss, for sediments receiving *C. virginica* biodeposits. Indirect measurements using the acetylene block technique, however, have identified greater denitrification potentials in sediments beneath long-lines of *Crassostrea gigas* (Gilbert et al. 1997) and on culture ropes in New Zealand mussel farms (Kaspar et al. 1985). In laboratory studies, approximately 20% of nitrogen added to Chesapeake Bay sediments, in the form of a phytoplankton analog for biodeposits, was denitrified in the absence of benthic microalgae (Newell et al. 2002). The influence of benthic microalgae on denitrification depends on the availability of and competition for inorganic nitrogen and sediment penetration of dissolved O_2 (e.g., Tiedje et al. 1989, Rysgaard et al. 1995, Sundback & Miles 2000, An & Joye 2001, Risgaard-Petersen et al. 2004). Accumulation of biodeposits on surface sediments may alter the influence of microalgae on nitrogen retention and transformations through burial of the photoautotrophs or increased nutrient availability for growth (Gibbs et al. 2005).

Off-bottom aquaculture of *C. virginica* was established within shallow waters (<2 m) of Chesapeake Bay to assess the influence of biodeposits on nitrogen regeneration (NH_4^+, $NO_2^- + NO_3^-$) and removal (N_2-N, TN). Surface (0-1 cm) sediment chlorophyll *a* and fluxes of dissolved O_2 were used to assess the presence and activity of benthic microalgae, and dark O_2 fluxes and sedimentary sulfur (ΣH_2S, AVS, CRS) identified shifts in organic matter degradation. Rates of total nitrogen deposition and percent organic content were used to illustrate the ability of benthic microalgae to incorporate

added nitrogen from biodeposits and lessen nitrogen exchange across the sediment-water interface. I found that shallow water sediments responded to small-scale (<9 m^2) aquaculture of *C. virginica* through increased concentrations of pore water NH_4^+, total dissolved sulfide, and iron-sulfides; differences in NH_4^+ fluxes for sediments at Oyster and Reference sites were minimal.

Materials and Methods

Study sites

Study sites were located in La Trappe Creek, a shallow, tidal tributary located on the northern bank (38° 37' 36"N, 76° 07' 13"W) of the Choptank River in the Maryland portion of Chesapeake Bay. Off-bottom aquaculture of the eastern oyster, *Crassostrea virginica*, was established at a total of three sites in the upper, mesohaline portions of La Trappe Creek in 2002 and 2003 (Oyster, Table 3.1). Additional sites, identified as Reference, were selected ~ 70 to 300 m from aquaculture sites and served as a means to monitor temporal variability in nearby sediments not overlain by small-scale aquaculture operations. Sampling occurred at one Oyster and one Reference site from July through September in Lowry Cove (Lowry) in 2002 and an upper, mesohaline reach of La Trappe Creek (Mainstem) in 2003. A third run was conducted from 26 May to 28 July 2003 at sites artificially shaded by stationary piers (Pier); maximum surface sediment irradiances observed at Pier sites were 5-25 μmol photons m^{-2} s^{-1}. Light attenuation coefficients (k_d), measured during sediment core collections, were comparable (1.37-4.73) among sites. All Oyster and Reference sites consisted of fine-grained sediments with porosities, as determined from percent water, of ~ 0.9 (0-0.5 cm, Cornwell et al. 1996). Water depths

ranged from 0.73 to 2.0 m, with shallower sites occurring in Lowry Cove. Increased stream flow in 2003 (287.1 x 10^6 m^3 d^{-1}) compared to 2002 (91.1 x 10^6 m^3 d^{-1}) led to decreased salinities (4-8) during sampling at Mainstem and Pier (http://waterdata.usgs.gov, 07 June 2007).

Off-bottom aquaculture of *Crassostrea virginica* was established at Oyster sites on 24 July 2002, 26 May 2003, and 29 July 2003 and maintained for ~ 7-9 wks. *C. virginica* were distributed in wire-mesh Taylor floats (Luckenbach et al. 1999), positioned 0.30-0.41 m below the water's surface (Table 3.2). Taylor floats, initially containing 184-216 oysters m^{-2}, were tethered together and anchored within areas <9 m^2. Oysters (shell height: 7-12 cm) were scrubbed of surface epibiota before their deployment and at one to two week intervals thereafter; fouled aquaculture floats were moved from mooring location and cleaned by power-washing and scrubbing. Oyster mortality decreased densities 2-32% during sampling.

Sedimentation traps

Sedimentation traps (0.002, 0.005, and 0.046 m^2) were suspended beneath aquaculture floats and at Reference sites once every 1-2 wks for ~ 24 h during oyster deployment. Square (aspect ratio: 1:1) sedimentation traps were deployed weekly from 30 July through 04 September 2002 in Lowry Cove (Table 3.2). One sedimentation trap was deployed under each of the 3 aquaculture floats deployed at Lowry Oyster, and three additional traps were deployed within the vicinity of the Reference site. Sedimentation traps (i.e., opening) were positioned ~ 0.3 m above the sediment surface at both sites. In 2003, cylindrical sedimentation traps with an aspect ratio (length : width) of 4:1 were

positioned ~ 0.5 m above the sediment surface. Sedimentation traps were deployed a total of 7 times at one and 1-2-week intervals between 03 June and 13 July 2003 and between 29 July and 25 September 2003. Nine and 6 sedimentation traps with inner diameters of 5.08 and 7.62 cm were deployed at Oyster and Reference sites, respectively. Contents of the cylindrical sedimentation traps were combined randomly to provide three samples with sufficient material for nutrient analyses. Collected material was transferred into 4 L carboys for transport back to the laboratory.

At the laboratory, the carboys were stored in a -1°C temperature-controlled chamber for ~ 24 h during the settling phase. I siphoned the supernatant off and rinsed the particulate material into tared beakers with deionized (DI) water. The sediments were allowed to settle again for ~ 12 h and the supernatant again removed prior to drying at 80°C. Dried material was weighed, powdered with a mortar and pestle, and stored in scintillation vials until analysis of carbon and nitrogen. Percentages of total carbon and nitrogen were determined with a Control Equipment elemental analyzer (Cornwell et al. 1996). Rates of deposition were determined by expressing measured nutrient concentrations (or percent compositions) relative to the surface area of sedimentation traps and the time of deployment (mmol m^{-2} h^{-1}). Ratios of total carbon to nitrogen (C/N) were based on molar depositions. Percent organic content was determined from weight loss upon combustion (550°C).

Sediment core collection and incubations

Sediment cores were collected ~ 0.5-6 d before deployment of *Crassostrea virginica* in aquaculture floats and 3 times at 2-3 wk intervals thereafter. Additional

cores were collected on 09 and 30 July 2003 from Pier Oyster and Reference for determination of pore water and solid-phase profiles. Collections at Pier sites occurred within ~ 2 h of low tide to facilitate sampling. All sediment cores were collected with a pole corer fitted with a transparent acrylic tube (6.35 cm ID) that was pressed ~ 10 cm into sediments. A valve was closed to maintain suction on the core before withdrawing cores from sediments, and bottoms and tops of cores were sealed with machined plastic lids fitted with O-rings and stoppers, respectively, upon retrieval. Cores remained covered in coolers while in route (<1 h) to the laboratory.

At the laboratory, sediment cores were submerged in an incubation tank (~ 60 L) filled with ambient (typically filtered, 0.22-1 μm) water collected during core collection. Incubation tanks were held in constant temperature-controlled chambers set at ambient water temperatures (20-32 °C). PVC-aeration tubes (2.5 cm ID) were inserted into the tops of open cores such that they reached within ~ 1 cm of the sediment surface (Newell et al. 2002). Aeration was typically maintained in open cores and surrounding waters on the night (~ 12 h) preceding flux incubations, but duration of bubbling was reduced to ~ 15 min of every 1 h for Pier sites on 07 and 28 July 2003. Aeration was reduced on these dates to minimize reoxidation of surface sediments; prolonged exposure to bubbling resulted in visual changes (i.e., light brown) in surface sediments.

On the following morning, cores were sealed with machined plastic lids with O-rings, and the overlying water mixed with a Teflon-coated magnetic stirrer (4.5 V) driven by an external magnetic turntable. Baseline solute (NH_4^+, NO_2^- + NO_3^-) and gas concentrations (O_2, N_2, Ar) were determined in the dark immediately upon sealing the cores and then in the light. Ambient water without sediment was incubated in duplicate

(2002) or triplicate (2003) as a measure of water column activity (i.e., blanks). Samples were taken at intervals of ~ 40-60 min for 4 to 5 time points in the dark and light. Surface sediment irradiances of 70-80 μmol photons m^{-2} s^{-1} were maintained during light incubations of Lowry and Mainstem sediments; sediments from Pier were incubated at a lower level (5 μmol photons m^{-2} s^{-1}). Active bubbling in open cores and surrounding water was maintained at all times upon completion of flux incubations.

The small amounts of water (21-32 ml) withdrawn for sampling were replaced by ambient La Trappe Creek water introduced through Tygon tubing to ensure no air bubbles were introduced to the system. Samples to measure O_2 and N_2 concentrations were taken in gas tubes with ground glass stoppers and preserved with 10 μl 50% saturated $HgCl_2$. Tubes were stored submerged in water at ambient temperatures (20-32°C) until determination (<1 wk) of O_2 : Ar and N_2 : Ar via membrane inlet mass spectrometry (Kana et al. 1994, Kana et al. 1998, Kana & Weiss 2004). NH_4^+ and NO_2^- + NO_3^- water column samples were collected in 20 ml syringes and filtered with 0.45 μm filters into 6 ml plastic vials. Samples were stored frozen until colorimetric analyses were conducted (Solaranzo 1969, as presented in Parsons et al. 1984, United States Environmental Protection Agency 1983a).

Nutrient fluxes for each core were calculated from linear regressions performed on nutrient concentrations plotted versus time ($r^2 > \sim 0.8$; $F \leq 0.10$). The difference in nutrient concentrations between water from cores and blanks was expressed relative to the surface area of the core. Calculations were performed separately for simulated dark and light events, and positive and negative fluxes coincided with sediment release and uptake of nutrients, respectively. Fluxes of N_2-N represented the net exchange of N_2-N at

the sediment-water interface since the reactions (e.g., denitrification, annamox, N_2 fixation) mediating these fluxes cannot be identified (Kana et al., 1998; Kana and Weiss, 2004). Estimates of net ecosystem metabolism (NEM) were calculated as 14 h * O_2 flux measured during light incubations + 24 h * O_2 flux measured during dark incubations. Gross primary productivity (GPP) estimates were determined as 14 h * (O_2 flux measured during light incubations – O_2 flux measured during dark incubation).

Surface sediment, pore water, and solid-phase collection

Pore water and solid-phase samples were collected from sediment cores used for nutrient flux incubations and from cores collected separately within ~ 1 d of incubations. Sediment cores collected separately were sectioned upon return to the laboratory or maintained under aerobic incubations for ~ 16 to 24 h. All sediment cores held in the laboratory were maintained aerobically in temperature-controlled chambers set at ambient temperature and under a 14 h light : 10 h dark cycle until surface sediment collection or pore water and solid-phase extraction occurred. Sediment cores were held in the laboratory for a maximum of ~ 4 d. Overlying water columns were siphoned so not to disturb the sediment surface prior to sediment collection.

Surface (0-1 cm) sediment collection occurred under aerobic conditions unless cores were sectioned for pore water and solid-phase analyses. Surface sediments were collected with a syringe mini-corer (1.4 cm inner diameter) pressed ~ 1 cm into sediments. Sediments collected for total carbon and nitrogen content were extruded into aluminum pans and dried at 80°C. Ground sediment was stored in glass scintillation vials until analysis. Percentages of total carbon and nitrogen were determined with a Control

Equipment elemental analyzer and expressed relative to the dry weight (DW) of sediment (μmol g^{-1} DW). Weight loss upon combustion (550°C) was used to determine percent organic content. Sediments for chlorophyll *a* were placed in 15 ml centrifuge tubes wrapped in aluminum foil and stored frozen (-80 to -20°C) until analysis by high-performance liquid chromatography (HPLC, Van Heukelem et al. 1994; centrifuged at 1,643 xg in International Equipment Company Centra MP4 or CL2; 3500 rpm).

Sediment cores for pore water and solid-phase analyses were extruded under N_2 and divided into 8 sections (0-0.5, 0.5-1, 1-1.5, 1.5-2, 2-3, 3-4, 4-7, and 7-10 cm) that were individually placed in 50 ml plastic centrifuge tubes and capped. Sections were centrifuged (822-1,096 xg for 10 min; 3500 rpm; International Equipment Company Centra MP4 or CL2), and the supernatant was filtered with 0.45 μm filters into 6 ml plastic vials for analysis of NH_4^+ and total dissolved sulfide (ΣH_2S: H_2S, HS^-, S^{2-}). Dilutions were done prior to freezing of NH_4^+ samples. Determination of NH_4^+ concentrations followed Soloranzo's (Solaranzo 1969, as presented in Parsons et al. (1984)) phenol hypochlorite method, modified for a 5 ml sample volume. Total dissolved sulfide samples (1 ml) were fixed with 10 μl of a mixed diamine reagent (250 – 1000 μmol L^{-1}, Cline 1969) and stored at room temperature until analysis by methylene blue colorimetry no more than 1 week later.

Pore water sediments were frozen (-20°C) until solid phase analyses could be conducted. Frozen sediments from core dissections were analyzed for acid-volatile sulfides (AVS) and chromium-reducible sulfides (CRS). Sediments were analyzed initially for AVS using a 6 N HCl-extraction and $PbClO_4$ titration (Cornwell and Morse 1987). After analyses for AVS were complete, sediments were processed for CRS

concentrations following Canfield et al. (1986). All solid-phase digestions were performed on thawed, well-homogenized sediments. Separate, equivalent amounts of homogenized sediments were dried to a constant weight at 80°C.

Results

Deposition

Total nitrogen deposition (mmol N m^{-2} h^{-1}), determined from material collected in sedimentation traps, was variable throughout the sampling periods (Fig. 3.1-3.3), but was typically greater at Oyster sites than corresponding Reference sites (Table 3.3). Deposition of total nitrogen at Lowry and Mainstem Oyster declined in mid-August, with rates decreasing to and holding at ~ 2 mmol N m^{-2} h^{-1}, respectively. These declines coincided with increasing oyster mortality. Similar declines were not observed at Pier Oyster, as rates of total nitrogen deposition remained constant (8.67 ± 1.44 mmol N m^{-2} h^{-1}) after peaking on 10 June 2003. Total nitrogen deposition on 10 June 2003 at Pier Oyster (17.58 ± 1.96 mmol N m^{-2} h^{-1}) exceeded those at the Reference site nearly 2,400%. Deposition of total nitrogen on remaining sampling dates were ~ 3.5- to 10-fold greater at Pier Oyster than Pier Reference; lesser differences in total nitrogen deposition were determined for Lowry (1.5-6) and Mainstem (1.8-4.6) sites.

Increased deposition of total nitrogen at Oyster sites was associated both with elevated percent total nitrogen contents and rates of deposition (g DW m^{-2} h^{-1}) from *Crassostrea virginica* aquaculture. Percent composition of total nitrogen in deposition from Oyster sites was typically ~ 60% greater than those at corresponding Reference sites; percentages of total nitrogen (mean ± SD) at Lowry, Mainstem, and Pier Oyster

were 0.67 ± 0.18%, 1.13 ± 0.33%, and 1.37 ± 0.34%, respectively. Fluctuations in rates of deposition (g DW m^{-2} h^{-1}) did not coincide with variability in percentages of total nitrogen, as increases in one were not met with increases in the other. Rates of deposition (g DW m^{-2} h^{-1}) at Lowry and Mainstem Oyster exceeded those at corresponding Reference sites by as much as ~ 320%; rates at Pier Oyster were ~ 250 to 1,200% greater than those at Pier Reference. Variation in percent organic content often, although not always, coincided with observed patterns in percentages of total nitrogen. All Oyster sites exhibited greater percentages of organic matter in material collected in sedimentation traps than corresponding Reference sites on the same sampling date (Fig. 3.4). Mean (± SD) percent organic contents for Lowry, Mainstem, and Pier Oyster and Reference sites were as follows: 17.04 ± 6.04%, 13.08 ± 1.43%, 20.41 ± 5.73%, 17.06 ± 2.58%, 24.19 ± 5.65%, and 19.57 ± 6.62%. Smaller (~ 43%) increases in percentages of total carbon relative to nitrogen led to an enrichment of total nitrogen at Oyster sites, such that total carbon to nitrogen ratios in deposition at Lowry, Mainstem, and Pier Oyster were reduced by ~ 0.5-1 to 8.8 ± 0.6, 8.1 ± 0.6, and 7.6 ± 0.6, respectively (Fig. 3.5).

Surface sediments

Surface sediment (0-1 cm) concentrations of total nitrogen and carbon at Oyster sites increased with deployment of *Crassostrea virginica* aquaculture floats (Fig. 3.1-3.3). Total nitrogen concentrations at Reference sites ranged from 242.7 to 292.7 μmol N g^{-1} DW, with mean concentrations near ~ 270 μmol N g^{-1} DW (Table 3.3). Final surface sediment (0-1 cm) concentrations at Oyster sites in 2002 and 2003 were ~ 6 and 29% greater than means from Reference sediments. Lesser increases in surface sediment (0-1

cm) concentrations of total carbon were observed at Lowry Oyster (2,814 ± 59 μmol C g^{-1} DW) and Mainstem Oyster (3,414 ± 88 μmol C g^{-1} DW); surface sediments (0-1 cm) at Reference sites maintained concentrations of 2,763 ± 84 μmol C g^{-1} DW and 2,950 ± 331 μmol C g^{-1} DW. The scale of increase in total carbon concentrations at Pier Oyster (~ 22%, 28 July 2003) was more comparable to observed increases in total nitrogen. Surface sediment (0-1 cm) total carbon to nitrogen ratios for Reference sites in 2002 and 2003 were 10.3 ± 0.2 and 10.6 ± 0.9 (Fig. 3.5). Total carbon to nitrogen ratios during deployment of *C. virginica* at Lowry, Mainstem, and Pier Oyster were 10.0 ± 0.3, 9.9 ± 0.3 and 10.1 ± 1.02. Percentages of organic matter in 2003 Reference sediments (Mainstem: 10.61 ± 0.57%, Pier: 11.21 ± 0.51%) were consistent during sampling (Fig. 3.4), and increases at Oyster sites after ~ 8-9 wks of deployment were comparable (15-22%) to observed increases in total carbon. Modifications at Lowry Oyster were unclear, as percent organic contents fluctuated (10.92-12.39%) at Oyster and decreased at Reference sites; means for Lowry Oyster (11.78 ± 0.62%) and Reference (11.79 ± 0.84%) were equivalent.

Surface sediment (0-1 cm) chlorophyll *a* concentrations at Oyster sites exceeded those at Reference sites after establishment of *C. virginica* aquaculture (Table 3.3). Concentrations of benthic chlorophyll *a* remained fairly constant at all Reference sites, but varied greatly within and among Oyster sites during sampling (Fig. 3.1-3.3). At Mainstem Oyster, surface sediment (0-1 cm) chlorophyll *a* concentrations increased continually from 23 July (7.16 ± 2.40 mg chl *a* m^{-2}) through 25 September 2003 (50.13 ± 32.02 mg chl *a* m^{-2}); maximum concentrations also occurred on the final sampling date at Mainstem Reference (18.91 ± 7.74 mg chl *a* m^{-2}). Increasing concentrations of

chlorophyll *a* at Mainstem sites after 20 August 2003 was likely associated with continual decreases in light attenuation (k_d: 4.02 – 2.61). Greatest chlorophyll *a* concentrations (26.50 ± 5.04 mg chl *a* m^{-2}) at Lowry Oyster were concurrent with maximum rates of total nitrogen deposition (06-07 August 2002, 12.00 ± 2.40 mmol N m^{-2} h^{-1}); similar chlorophyll *a* concentrations occurred on 09 September 2003. Surface sediment chlorophyll *a* concentrations at Pier Oyster and Reference exceeded those measured at other Oyster and Reference sites, respectively. Peak concentrations of chlorophyll *a* were observed on 16 June and 07 July 2003 at Pier Oyster, with concentrations ranging from 26.56 to 550.91 mg chl *a* m^{-2}. Sediment chlorophyll *a* concentrations declined with sampling at Pier Reference (25 – 14 mg chl *a* m^{-2}).

Net ecosystem metabolism

Rates of net ecosystem metabolism were typically comparable for corresponding Oyster and Reference sites, but discrepancies among sites were apparent on a few sampling dates (Fig. 3.6). Differences in net ecosystem metabolism in Lowry Cove occurred on 06 and 20 August 2002 when gross photosynthesis at Lowry Oyster was <10% of production at the Reference site (11.4 ± 11.3 mmol O_2 m^{-2} d^{-1}); more similar rates of gross photosynthesis (Oyster: 10.8 ± 3.2 mmol O_2 m^{-2} d^{-1}, Reference: 9.3 ± 2.01 mmol O_2 m^{-2} d^{-1}) occurred on 09 September 2002. Sediment oxygen consumption, determined as dark O_2 fluxes, at Lowry Oyster (-1,278,0 ± 500.6 μmol O_2 m^{-2} h^{-1}) and Reference (-1,189.8 ± 544.1 μmol O_2 m^{-2} h^{-1}) were comparable throughout the ~ 7 wk sampling period. Light O_2 fluxes at Lowry Oyster (-1,008.9 ± 1,121.4 μmol O_2 m^{-2} h^{-1})

were consistently less than those at Lowry Reference (4.4 ± 421.0 μmol O_2 m^{-2} h^{-1}) during deployment of oysters in Taylor floats.

Comparable O_2 fluxes were observed for Mainstem sites during dark and light sediment core incubations. Mean (± SD) rates of sediment oxygen consumption and light O_2 fluxes were -1,709.0 ± 898.4 μmol O_2 m^{-2} h^{-1} and -836.8 ± 478.1 μmol O_2 m^{-2} h^{-1}. No estimates for net ecosystem metabolism were determined for 25 September 2003, as no light O_2 fluxes were significant ($r^2 > \sim 0.8$, $F \leq 0.10$); rates of sediment oxygen consumption were maximal on this sampling date (Oyster: -3,373.5 ± 1,859.2 μmol O_2 m^{-2} h^{-1}, Reference: -2,257.6 ± 743.3 μmol O_2 m^{-2} h^{-1}). Divergence of net ecosystem metabolism on 07 July 2003 was associated with elevated rates of sediment oxygen consumption (-6,204.1 ± 609.8 μmol O_2 m^{-2} h^{-1}) and gross primary productivity (60.65 ± 13.35 mmol O_2 m^{-2} d^{-1}) at Pier Reference. Dark and light O_2 fluxes were comparable overall at Pier Oyster (-2,828.1 ± 888.3 μmol O_2 m^{-2} h^{-1}, -2,860.7 ± 1,466.5 μmol O_2 m^{-2} h^{-1}) and Reference (-3,846.8 ± 1,447.9 μmol O_2 m^{-2} h^{-1}, -2,617.6 ± 1,632.5 μmol O_2 m^{-2} h^{-1}).

Pore water NH_4^+ profiles

Concentrations of pore water NH_4^+ in the upper 4 cm of sediment remained unchanged in 2002 and increased in 2003 during small-scale aquaculture of *Crassostrea virginica*. Pore water concentrations of NH_4^+ from sediments collected in Lowry Cove ranged from 59.0 to 984.7 μmol N L^{-1}, with the greatest concentrations occurring at depth (7-10 cm). Profiles of NH_4^+ concentrations shifted towards slightly greater concentrations (at depth) as sampling progressed, but differences were not identified

between Lowry Oyster and Reference (Fig. 3.7). Concentration gradients of NH_4^+ in the surface 2 cm generally predicted diffusive fluxes (51.4 ± 31.2 μmol N m^{-2} h^{-1}) within a factor of 2 of NH_4^+ fluxes measured from dark incubations (88.2 ± 86.3 μmol N m^{-2} h^{-1}, Fig. 3.8). Discrepancies in pore water NH_4^+ profiles from Oyster and Reference sites were considerable in 2003 sediments from Mainstem and Pier.

Nearly vertical concentration profiles of NH_4^+ and least concentrations (<100 μmol N L^{-1}) occurred in the surface 3 cm of sediments collected on initial sampling dates at Mainstem and Pier. Diffusive fluxes predicted from initial, vertical concentration gradients (0-2 cm) of pore water NH_4^+ were <15 μmol N m^{-2} h^{-1}, but measured fluxes during dark incubations typically exceeded ~ 200 μmol N m^{-2} h^{-1}. Greater concentration gradients of pore water NH_4^+ (>51 nmol cm^{-4}) were observed on sampling dates during *C. virginica* deployment at Mainstem sites; increases at Mainstem Oyster (254.7 ± 90.0 nmol cm^{-4}) were ~ 3.5-fold greater than those at Reference (69.1 ± 31.6 nmol cm^{-4}). Pore water concentration of NH_4^+ in sediments from Mainstem Oyster after ~ 8 wks of aquaculture ranged from 229.7 to 1,214.6 μmol N L^{-1}; concentrations at Reference were consistently <580.2 μmol N L^{-1}. Similar concentrations of pore water NH_4^+ (32.4 - 593.5 μmol N L^{-1}) were observed at Pier Reference, but the scale of increase at Pier Oyster was substantially greater. Pore water NH_4^+ concentrations approached ~ 3,900 μmol N L^{-1} on 30 July 2003, with maximum concentrations occurring between ~ 3-4 cm. Maximum NH_4^+ concentrations migrated downward during *C. virginica* aquaculture, with peaks occurring between 1.5 and 3 cm after ~ 3 and 6 wks of deployment (<962.0 μmol N L^{-1}, <3,318.5 μmol N L^{-1}). More subtle transitions, coinciding with increases in water

temperature and shifts in bioirrigation, in pore water NH_4^+ profiles at Reference sites have been presented elsewhere (Chapter 2).

Nitrogen fluxes

All sediments exhibited a tendency to release NH_4^+ into overlying waters during dark incubations, but the magnitude of NH_4^+ fluxes were dependent on sampling locations and duration of *Crassostrea virginica* aquaculture (Fig. 3.8). Greatest effluxes of NH_4^+ occurred in cores collected from Pier, with maximal rates occurring after *C. virginica* had been deployed for ~ 6 wks (1,525 – 2,972 μmol N m^{-2} h^{-1}). Effluxes of NH_4^+ from sediments collected at Lowry and Mainstem did not exceed ~ 350 μmol N m^{-2} h^{-1}. Sediment releases of NH_4^+ were comparable at Oyster and Reference sites within the first 3-8 wks of aquaculture operations, but differences eventually developed at all three sampling locations. Dark NH_4^+ effluxes at Lowry Oyster on 20 August 2002 were between ~ 44 and 261 μmol N m^{-2} h^{-1}; whereas rates at Lowry Reference never exceeded ~ 30 μmol N m^{-2} h^{-1}. Similarly, on 25 September 2003, effluxes at Mainstem Oyster were ~ 2- to 5-fold greater (122 – 336 μmol N m^{-2} h^{-1}) than those at Mainstem Reference. Sediment effluxes of NH_4^+ at Pier sites diverged on 16 June and 07 July 2003, as effluxes approached ~ 3,000 μmol N m^{-2} h^{-1} at Pier Oyster. Shifts toward dark uptake of NH_4^+ on 28 July 2003 were not influenced by water column activity (i.e., blanks); water column concentrations were typically ~ 0.2-10 μmol N L^{-1}.

No differences were identified for NH_4^+ fluxes determined during light incubations, as much greater variability (i.e., SD) was exhibited within and among sites (Fig. 3.8). Reductions in sediment effluxes were generally observed in sediments from

all sampling locations during light incubations. Near zero or minimal uptake was typically observed in sediments from Lowry Cove and upon completion of *C. virginica* aquaculture at Pier. Sediment exchanges of NH_4^+ on 16 June 2003 were comparable during dark and light incubations. Although light NH_4^+ fluxes were similar on 07 July 2003 at Pier sites, gross rates of NH_4^+ uptake at Pier Oyster (-23.9 ± 8.3 mmol N m^{-2} d^{-1}) exceeded those at Reference nearly 3-fold. Net effluxes of NH_4^+ from Pier Oyster and Reference sediments on 07 July were 59.6 ± 14.3 mmol N m^{-2} d^{-1} and 29.0 ± 4.7 mmol N m^{-2} d^{-1}, respectively.

Differences between sediment fluxes of N_2-N with overlying waters were difficult to discern, as rates within the water column (i.e., blanks) often determined the direction and magnitude of exchange (Fig. 3.9). Rates of net denitrification and apparent net N_2 fixation were similar in sediment cores from Oyster and Reference sites at Mainstem (-98 to 176 μmol N m^{-2} h^{-1}) and Pier (-273 to 340 μmol N m^{-2} h^{-1}). Sediment uptake of NO_2^- + NO_3^- at Mainstem and Pier sites were typically 10-40 μmol N m^{-2} h^{-1}, but greater rates (-381.7 ± 71.9 μmol N m^{-2} h^{-1}) were measured in the dark on 26 May 2003. Uptake of NO_2^- + NO_3^- in mid-May coincided with maximum effluxes of N_2-N at Pier Oyster (161.8 ± 75.6 μmol N m^{-2} h^{-1}) and Reference (194.5 ± 68.2 μmol N m^{-2} h^{-1}). Rates of net denitrification were reduced (55.8 ± 26.1 μmol N m^{-2} h^{-1}) and NO_2^- + NO_3^- fluxes reversed upon exposure to surface sediment irradiance. Effluxes of N_2-N from sediments collected at Lowry Oyster (70.8 ± 5.4 μmol N m^{-2} h^{-1}) on 06 August 2002 were approximately 10 times greater than effluxes from its corresponding Reference site. Rates of net denitrification at Lowry Oyster were reduced two-thirds during light incubations; concentrations of NO_2^- + NO_3^- in overlying waters were typically below

detection. N_2-N fluxes on other sampling dates in Lowry Cove and Pier were modified by water column processes.

Sedimentary sulfur

Pore water concentrations of total dissolved sulfide (ΣH_2S: H_2S, HS^-, S^{2-}) transitioned at depths ≥ 4 cm in Reference sediments and within the surface 4 cm of cores collected from Oyster sites in Mainstem and Pier (Fig. 3.10). Total dissolved sulfide concentrations at depth (4-10 cm) fluctuated in Oyster and Reference sediments from Lowry Cove, with concentrations ranging from near zero to 1,210 μmol S L^{-1}; no total dissolved sulfide was identified above 4 cm. Concentrations of total dissolved sulfide increased (52-698 μmol S L^{-1}) at depths of 7-10 cm as sampling progressed at Mainstem Reference, but greater total dissolved sulfide concentrations occurred in sediments from Mainstem Oyster. Peak concentrations after 3 wks and 6-8 wks of *Crassostrea virginica* aquaculture were at depths between 7 to 10 cm and 2 to 3 cm, respectively. Total dissolved sulfide concentrations in pore waters from Pier Oyster also transitioned during *C. virginica* aquaculture, but concentrations >800 μmol S L^{-1} only occurred on 16 June 2003 (1-10 cm). Pore water concentrations decreased nearly 2-fold by 09 July 2003, and double peaks (0-1.5 cm, 7-10 cm) persisted through July. Concentrations at Pier Reference were <150 μmol S L^{-1}.

Concentrations of SO_4^{2-} were nearly consistent in sediment cores collected from Oyster and Reference sites in Mainstem and Pier initially, ranging from 3.34 to 4.30 mmol SO_4^{2-} L^{-1}. Profiles of SO_4^{2-} concentrations within sediment cores from Pier Reference remained nearly consistent throughout sampling, shifting only with changes in

salinity (i.e., chloride; Fig. 3.11). Peak concentrations in sediments from Pier Reference did not exceed 8.35 mmol SO_4^{2-} L^{-1}. Concentrations decreased with depth in sediments from Pier Oyster after 3 wks of *C. virginica* aquaculture. Minimum SO_4^{2-} concentrations (1.14-1.67 mmol SO_4^{2-} L^{-1}) were observed in the 1.5 to 2 and 3 to 4 cm depth-intervals for replicate (n = 2) sediment cores on 16 June 2003. Concentrations were < 2 mmol SO_4^{2-} L^{-1} in the surface 1 cm of sediments on 07 and 28 July 2003, and concentrations below this depth approached 0.07 mmol SO_4^{2-} L^{-1}. After 3 wks of *C. virginica* aquaculture, concentrations of SO_4^{2-} decreased with depth in sediment cores collected from Mainstem Oyster and Reference, but gradients (0-2 cm) of SO_4^{2-} in Oyster sediments exceeded those determined for Mainstem Reference. Concentrations of SO_4^{2-} in Oyster sediments approached asymptotic concentrations (< 1 mmol SO_4^{2-} L^{-1}) typically within the 2 to 4 cm depth-intervals, whereas concentrations declined linearly in sediments from Mainstem Reference.

Ratios of SO_4^{2-} to Cl^- in all sediments initially ranged from 0.015 to 0.065, with the greatest ratios occurring within surface sediments (Fig. 3.11). Decreased SO_4^{2-} : Cl^- ratios were observed in Oyster profiles after establishment of *C. virginica* aquaculture at Mainstem and Pier, but sediment cores from Pier Oyster exhibited the greatest difference in ratios relative to corresponding Reference sediments. No differences in SO_4^{2-} concentrations profiles or SO_4^{2-} : Cl^- ratios were identified for Lowry Oyster and Reference, as concentrations profiles (n =1) were noisy.

Acid-volatile sulfide (AVS) concentrations increased in sediments collected from Oyster sites upon termination of *C. virginica* aquaculture. Concentrations < 13 μmol S g^{-1} DW were initially identified within sediments from Lowry Cove, and concentrations

increased no more than 50% by 09 September 2002. Peak concentrations occurred within the 3-4 cm depth interval at Lowry Oyster and Reference, but a second, smaller peak (< 12 μmol S g^{-1} DW, 0.5-1.5 cm) was identified at Lowry Oyster after ~ 7 wks of *C. virginica* aquaculture. Profiles of AVS at Mainstem Oyster and Reference also possessed sub-surface peaks in concentrations, but the magnitude of increase at Mainstem Oyster was much greater (Fig. 3.12). AVS concentrations at Mainstem Oyster ranged from 4.8 to 63.1 μmol S g^{-1} DW on 25 September 2003. Intermediate sampling (16 June 2003) for AVS at Pier Oyster illustrated the progression of increase in AVS at Oyster sites, as maximum concentrations increased from 52.8 μmol S g^{-1} DW on 26 May to 77.5 and to 87.9 μmol S g^{-1} DW on 16 June and 30 July 2003. AVS concentrations at Pier Reference were < 20 μmol S g^{-1} DW, and maximum concentrations typically occurred at depth (7-10 cm) rather than above 4 cm. Although concentrations of chromium-reducible sulfide transitioned in sediments, no differences were identified among Oyster and Reference sites. Concentrations of CRS ranged from 96.9 to 419.3 μmol S g^{-1} DW and from 105.9 to 516.2 μmol S g^{-1} DW in 2002 and 2003.

Discussion

Crassostrea virginica held in Taylor aquaculture floats in shallow waters of Chesapeake Bay led to the gradual enrichment of surface (0-1 cm) sediments and pore water through enhanced deposition and heightened concentrations of organic carbon and nitrogen. Modifications to pore water NH_4^+ and surface (0-1 cm) sediment concentrations of nitrogen were not typically expressed at the sediment-water interface, as discrepancies among nitrogen (NH_4^+, NO_2^- + NO_3^-, N_2-N) fluxes were minimal

between Oyster and Reference sites. Nutrient assimilation and photosynthesis by benthic microalgae muted the influence of *C. virginica* biodeposits on sediment nitrogen exchange, such that greater effluxes of NH_4^+ from Oyster sediments only occurred in the dark. Shifts in anaerobic (Fig. 3.11), rather than aerobic (Fig. 3.6), respiration were responsible for increased pore water concentrations of NH_4^+. Minimal differences observed in net ecosystem metabolism (O_2) were driven by loss or reduction of benthic photosynthesis (i.e., at Lowry Oyster) not increased sediment O_2 consumption. Discrepancies in the magnitude of nitrogen responses at Lowry, Mainstem, and Pier were due to differences in the quantity and quality of *C. virginica* feces and pseudofeces being deposited to the sediment surface.

Greater rates of deposition at Oyster (relative to Reference) sites stemmed from the manner in which *C. virginica* filter particulates from the water column and generate mucous-coated biodeposits with increased settling velocities (Haven & Morales-Alamo 1968). *C. virginica* filter seston in the range of 3 to 25 μm, and quantities of feces and pseudofeces produced depend primarily on the availability of seston in this size-fraction (Haven & Morales-Alamo 1966, Haven & Morales-Alamo 1970, Mohlenberg & Riisgard 1978). Rates of deposition at Lowry Reference (6.50 ± 3.63 g DW m^{-2} h^{-1}) exceeded those determined for other Reference sites (2.51 ± 1.865 g DW m^{-2} h^{-1}), suggesting that *C. virginica* in 2002 experienced a greater supply of seston for filtration. Heightened seston concentrations in Lowry Cove coincided with the greatest deposition (12.15 ± 8.56 g DW m^{-2} h^{-1}), but not with the greatest total or organic nitrogen deposition, at an Oyster site. Near comparable rates (10.37 ± 4.37 g DW m^{-2} h^{-1}) were determined for Pier Oyster, as minimal mortality of *C. virginica* maintained high rates of deposition.

Mortality of 32 and 24% of oysters in Lowry and Mainstem, respectively, caused a gradual decline in the production of biodeposits over the course of the study.

Sediments underlying *C. virginica* Taylor floats in 2003 at Mainstem and Pier exhibited greater changes in surface (0-1 cm) sediment concentrations of total nitrogen and pore water NH_4^+ than sediments at Lowry Oyster. Heightened responses at Mainstem and Pier Oyster in 2003 were due to the higher quality of biodeposits, as indicated by greater percent organic content and lesser ratios of total carbon to nitrogen. Somewhat greater rates of total nitrogen deposition at Lowry relative to Mainstem Oyster were not sustained for organic nitrogen, as percent organic content at Lowry Oyster was reduced approximately 20%. In Lowry Cove, percentages of total nitrogen and organic matter in Reference deposition more closely resembled percentages identified in surface (0-1 cm) sediments, suggesting that resuspension contributed largely to material filtered by *C. virginica*. Current speeds sufficient for erosion and transport of surface sediments would enhance dispersal of biodeposits, further reducing the supply of organics to sediments underlying Lowry aquaculture floats. The minimal response of Lowry sediments to *C. virginica* biodeposits was also likely due to reduced deposition of organic matter associated with preferential retention and ingestion of organic particles by *C. virginica* (Newell & Jordan 1983). Scaled increases in pore water concentrations of NH_4^+ at Pier Oyster corresponded with greatest organic nitrogen deposition, inferred from deposition of total nitrogen and percent organic content.

Particulates collected in sedimentation traps beneath *C. virginica* aquaculture floats were enriched in total nitrogen compared to material from corresponding Reference sites. Ratios of total carbon to nitrogen in material collected at Mainstem and Pier

Reference were less than those of underlying surface (0-1 cm) sediments; much smaller reductions were identified for Lowry Reference. Further decreases in ratios of total carbon to nitrogen at all Oyster sites were generated by the ability of *C. virginica* to select for more nutritious particles, including phytoplankton and microzooplankton, with typical carbon to nitrogen ratios near 6-7 (Newell & Jordan 1983, Meyers 1994, Meyers 1997 *in* Rullkotter 2000, Kreeger & Newell 2001). Least ratios observed in 2003 were associated with greater phytoplankton blooms supported by high inorganic nutrient availability from unusually high stream flows (Chapter 2). Dilutions of total carbon to nitrogen ratios were likely due to enhanced consumption and sedimentation of phytoplankton, as increases in surface (0-1 cm) sediment chlorophyll *a* were observed at all aquaculture locations.

Microbial degradation of organic matter and mucus in biodeposits may have provided additional inorganic nutrients for benthic microalgal growth (Cognie & Barille 1999, Chapter 4), but lack of an increase in gross primary productivity at Oyster sites suggests that deposition was responsible for observed increases in sediment chlorophyll *a* (Barranguet 1997). Deposition of intact chlorophyll *a* was not surprising as photosynthetic viability of phytoplankton has been shown even after being egested in bivalve biodeposits (Miura & Yamashiro 1990), and chlorophyll *a* under aerobic conditions generally persists for 7-10 d (Sun et al. 1993). Lack of a difference in estimates of gross primary productivity does not preclude enhanced microalgal growth, as greater mat thicknesses and siltation may have simply shaded microalgae. Shifts in benthic photosynthesis in sediments receiving simulated biodeposition in the laboratory were dependent on the magnitude of organic loadings, with lesser and greater levels

exhibiting reduced and enhanced gross primary productivity, respectively (Newell et al. 2002). Physiological adaptations to minimal *in situ* irradiance, such as greater chlorophyll *a* per cell, and increased nitrogen concentrations in overlying water at Pier sites promoted greatest concentrations of sediment chlorophyll *a* for Oyster and Reference sites. Similar chlorophyll *a* concentrations at Lowry and Mainstem Oyster were likely the result of differences in surface sediment irradiance, as waters in Lowry Cove are shallower than in Mainstem, and the occurrence of the tellinid clam, *Macoma balthica*, in 2003 (Chapter 2). Grazing by these *M. balthica* in 2003 likely reduced and prevented *in situ* growth of microalgae at sampling locations (Olafsson et al. 2005). Similar reductions in microalgal biomass were not observed for additions of simulated biodeposits as laboratory sediments underwent defaunation (Newell et al. 2002).

Organic carbon in *C. virginica* biodeposits did not prompt increases in aerobic respiration (i.e., dark O_2 fluxes) at Oyster sites, but increases in sulfate reduction were apparent through concentration changes in total dissolved sulfide and acid-volatile sulfide (AVS) and sulfate to chloride ratios. All sediments underlying *C. virginica* aquaculture floats demonstrated increased concentrations of AVS after ~ 7-9 wks of deployment, and the greatest increase in AVS (Pier Oyster) coincided with the greatest percent organic content. Increases in total dissolved sulfide concentrations occurred initially in surface (0-4 cm) sediments from Mainstem and Pier Oyster; fluctuations thereafter were likely associated with changes in rates of organic deposition and production of iron-sulfides (Canfield 1989, Canfield et al. 1992, Leon et al. 2004). Greater concentrations of iron oxy(hydr)oxides in Lowry Cove compared to 2003 sediments helped to impede the build-up of total dissolved sulfide through iron (III) reduction and iron sulfide formation

(Chapter 2), but minimal increases in sedimentary sulfur were also coupled with limited availability and distribution of organic deposition.

Greater rates of sulfate reduction and sediment O_2 consumption often occur in sediments overlain by bivalve aquaculture operations (e.g., Tenore et al. 1982, Tuttle & Jonas 1992, Mazouni et al. 1996, Barranguet 1997), with scaled increases depending on dispersal of enhanced deposition (Kaspar et al. 1985). Increased consumption of dissolved O_2 by these sediments has typically been ascribed to reoxidation of reduced sulfur species (e.g., Richard et al. 2007), but the occurrence of reoxidation does not always coincide with increases in anaerobic metabolism. Greater rates of sediment O_2 consumption at Oyster (relative to Reference) sites likely occurred after termination of *C. virginica* aquaculture. Brief deployments of *C. virginica* aquaculture floats may have been insufficient for conversion of AVS to CRS; minimal reoxidation of reduced sulfur likely precluded the formation of FeS_2 through lack of intermediate oxidative states (Fig. 3.10-3.11). Differences in chromium-reducible sulfide (CRS) concentrations were not discernable due to spatial heterogeneities (e.g., depth, site) and elevated background concentrations of CRS present in La Trappe Creek sediments.

Increased deposition of particulate organic nitrogen at Oyster sites did not promote enhanced effluxes of N_2-N from shallow water sediments. *C. virginica* biodeposits only increased sediment exchanges of N_2-N with the water column when benthic photosynthesis was reduced relative to Reference sediments. This suggests that rates of benthic microalgal photosynthesis, and not added particulate organic nitrogen, controlled the magnitude of N_2-N release. Greater rates of net denitrification at Lowry Oyster occurred after ~ 2 wks of *C. virginica* deployment, when gross primary

productivity was <10% of Reference production. Reduction of benthic photosynthesis likely led to increased availability of NH_4^+ and NO_3^- for nitrifying and denitrifying bacteria (e.g., Sundback & Miles 2000, Risgaard-Petersen et al. 2004); competition between benthic microalgae and bacteria was apparent as N_2-N effluxes were reduced during light incubations. Coupled nitrification-denitrification likely supported observed rates of net denitrification, as water column $NO_2^- + NO_3^-$ concentrations in Lowry Cove were minimal. Enhanced rates of net denitrification were not observed after ~ 4 wks of deployment, when loss of gross primary productivity at Lowry Oyster likely led to a decrease in the thickness of the aerobic layer for nitrification (Henriksen & Kemp 1988). Inhibition or reduction of net denitrification through competition for nitrogen between bacteria and benthic microalgae was not unexpected; benthic microalgae elsewhere have been shown to limit denitrification through nutrient assimilation and O_2 production (e.g., Rysgaard et al. 1995). Direct denitrification was reduced during light incubations of sediments collected in late-May from Pier Oyster and Reference. Persistence of some N_2-N loss was likely due to sediment irrigation by benthic infauna (Chapter 2) and a saturating supply of nitrogen from water column NO_3^- and pore water NH_4^+ for benthic microalgae. Lack of an increase in net denitrification (N_2-N loss) in this study does not preclude the potential for *C. virginica* biodeposits to enhance denitrification through burial of particulate organic nitrogen in aerobic sediments (Newell et al. 2002), as increases may have been observed provided measurements extended beyond summer (Kaspar et al. 1985, Gilbert et al. 1997).

Anaerobic degradation of particulate organic nitrogen in *C. virginica* biodeposits influenced effluxes of NH_4^+ during dark incubations through increases in pore water

concentrations of NH_4^+. Greater concentration gradients (0-2 cm) of pore water NH_4^+ led to enhanced effluxes in Pier sediments after approximately 3 and 6 wks of *C. virginica* deployment. Increases in pore water concentrations of NH_4^+ at Mainstem Oyster were not typically expressed at the sediment-water interface; sediments released NH_4^+ to the water column in the dark at comparable rates throughout sampling. Differences in late-September were associated with a reduction in NH_4^+ effluxes from Mainstem Reference; lesser fluxes of NH_4^+ from Reference sediments were likely due to luxury uptake of nitrogen as microalgal biomass increased. Greater sediment release of NH_4^+ (dark) at Lowry Oyster relative to the Reference site transpired when benthic photosynthesis was absent from Oyster sediments.

Benthic microalgae consistently modulated the response of sediments to additional nitrogen from *C. virginica* biodeposits during light incubations. Similarity of light NH_4^+ fluxes measured from Oyster and Reference sediments suggested that at least a proportion of increased benthic microalgae (i.e., sediment chlorophyll *a*) at Oyster sites were photosynthesizing and, therefore, assimilating added nitrogen. Greater rates of gross primary productivity were not observed at Oyster sites, but O_2 produced may have been readily consumed during reoxidation of inorganic compounds (e.g., sulfide). The similarity of rates of sediment O_2 consumption at Oyster and Reference sites may have been coincidental since consumption of O_2 could have occurred through a combination of mineral reoxidation and respiration of benthic fauna. Loss of *M. balthica* from sediments coincided with the greatest effluxes of NH_4^+ at Pier Oyster; similar decreases in *M. balthica* biomass were identified in Oyster sediments from Mainstem (Fig. 3.13). Clam mortality was likely due to the presence of dissolved sulfide in surface sediments (Diaz &

Rosenberg 1995). Sediment O_2 consumption at Lowry Oyster and Reference were comparable since *C. virginica* biodeposits supplied minimal organics.

Field studies with *C. virginica* held in Taylor floats were conducted from late-spring through early-fall for a relatively short timeframe and were designed to encompass the period of maximum oyster feeding. Longer deployments of *C. virginica* floats or establishment of aquaculture sites in cooler months may have resulted in different changes in sediment biogeochemistry and nitrogen exchange across the sediment-water interface. Continuous supply of organic material from oyster biodeposits would have likely increased rates of sulfate reduction, and production of dissolved sulfide would have caused persistent sediment anoxia, with consequent changes in benthic communities. Dissolved sulfide concentrations may have become so great even at these shallow depths to inhibit nitrification and kill benthic fauna and microalgae (Henriksen & Kemp 1988, Joye & Hollibaugh 1995, Sloth et al. 1995). Loss of these species has consequences for sediment nitrogen cycling. Persistence of aquaculture in winter may have led to increases in sediment O_2 consumption from reoxidation of reduced chemical species produced during warmer months. Sediment conditions may have then gradually relaxed when *C. virginica* feeding slowed and eventually ceased due to decreasing water temperatures and seston concentrations (Newell & Langdon 1996). The time required for return of sediments to reference conditions is unclear. Some sediments exposed to aquaculture have responded rapidly to removal of aquaculture operations (O'Connor et al. 1989); others have maintained elevated concentrations of dissolved sulfide and enhanced rates of sulfate reduction for some time (Ito & Imai 1955). For La Trappe Creek, additional sediment cores collected ~ 2 wks after Taylor floats were removed indicated that

dissolved sulfide concentrations decreased rapidly. Retention of similar dissolved sulfide and increasing AVS concentrations ~ 2 mo later suggests that complete reoxidation and restoration of sediments to initial conditions may occur on longer timeframes; slower relaxation at this site may have been associated with consistently elevated temperatures, which promote greater rates of sediment respiration.

These field studies illustrated that *C. virginica* aquaculture in tidal creeks of Chesapeake Bay may have varying effects on sediment biogeochemistry, and these effects may be influenced by benthic microalgae and availability of particulate organic nitrogen. This suggests that continued sediment sampling of aquaculture sites should be conducted to monitor influence of *C. virginica* on shallow water sediments when waters contain high phytoplankton biomass for oyster feeding. Furthermore, it is essential that the biogeochemistry of a proposed aquaculture site be well-studied before establishment of aquaculture operations. In this way, the aquaculture rafts can be relocated when the receiving sediments are starting to show detrimental changes (O'Connor et al. 1989, Newell 2004).

Acknowledgements

My research was supported with funding supplied to R.I.E. Newell and J.C. Cornwell from Maryland Sea Grant (SA07528051-F) through NOAA award NA16RG2207. I thank M. Owens, J. Burton-Evans, E. Kiss, and T. Coley for their assistance in the Cornwell laboratory, and T. Kana for the use of his membrane-inlet mass spectrometer for dissolved gas analyses. I thank L. Lane, C. Thomas, and L. Van Heukelem for analyzing samples for carbon, nitrogen, and chlorophyll *a* content, and S.

Rhoades for analyzing water samples for concentrations of NO_2^- + NO_3^-. I thank S. Hurder, A. Padeletti, and J. Seabrease for their help with experimental maintenance, and W. Boicourt, P. Boicourt, and D. Kerstetter for granting me access to study sites. I especially thank S. Alexander, D. Meritt, B. Parks, and the Oyster Recovery Partnership (and crew) for providing *Crassostrea virginica*, S. Hurder for determining the biomass-length relationship of *M. balthica*, and R.I.E. Newell and J. C. Cornwell for their support with field manipulations and data interpretation.

Table 3.1 Sample logistics and water column and surface sediment (0-0.5 cm) characteristics for three sampling locations in the upper, mesohaline portion of La Trappe Creek, Maryland, USA. Water column and surface sediment characteristics were determined from measurements collected on or near specified sampling dates, and data presented are either ranges (min – max) or means ± one standard deviation. All study sites were located in waters with a tidal range of 0.49 m and a mean tide of 0.34 m (38° 34' N, 76° 04' W). Porosities were estimated from percent water for representative cores (n = 1-3), assuming a sediment density of 2.5 g cm^{-3} (Cornwell et al. 1996).

Field data	Lowry	Mainstem	Pier
Latitude, Longitude			
Oyster	38° 39' 27"N	38° 39' 12"N	38° 39' 13"N
	76° 05' 35"W	76° 05' 14"W	76° 05' 13"W
Reference	38° 39' 26"N	38° 39' 12"N	38° 39' 11"N
	76° 05' 37"W	76° 05' 18"W	76° 05' 21"W
Sampling dates[a]			
Initial	23 July 2002	23 July 2003	26 May 2003
Aquaculture	24 July 2002	29 July 2003	26 May 2003
Final	09 Sept 2002	25 Sept 2003	28 July 2003
Site characteristics			

Salinity	13.25 ± 0.96	6.75 ± 1.50	5.50 ± 1.29
Water depth (m)	0.73 – 1.15	1.10 – 2.0	1.08 – 1.70
k_d [b]	2.75 – 3.87	2.61 – 4.73	1.37 – 3.85
Percent water (%)	75.1	78.7 ± 2.8	80.0 ± 3.0
Porosity	0.88	0.90 ± 0.01	0.91 ± 0.02

[a] Sampling dates correspond with sediment core collections before (i.e., initial) and after ~ 7-9 wks of oyster deployment (i.e., final) and the date at which aquaculture floats were deployed (i.e., aquaculture).

[b] Sediment cores collected from Lowry and Mainstem were incubated under a diel cycle of 12-14 h of daylight and a surface sediment irradiance of ~ 70-80 μmol photons m^{-2} s^{-1}. Surface sediment irradiance during Pier incubations was ~ 5 μmol photons m^{-2} s^{-1}.

Table 3.2 Quantitative description of small-scale aquaculture of *Crassostrea virginica* at three sampling locations in a tidal creek of the Choptank River, Chesapeake Bay, Maryland, USA.

Scale of aquaculture	Lowry Cove	Mainstem	Pier[a]
Oysters (#)[b]	728-1075	1226-1607	1607-1647
Aquaculture floats (#)	3	6	6
Area of rafts (m^2)	4.98	8.93	8.93
Float dimensions (m)			
Length	1.5, 3	2.44	2.44
Width	0.32, 0.75	0.61	0.61
Cage depth	0.30	0.41	0.41
Mesh size	0.25 x 0.25	0.25 x 0.51	0.25 x 0.51
Sediment traps			
Aspect ratio	1:1[c]	4:1	4:1
Shape	Square	Cylindrical	Cylindrical
Inner diameter (cm)	21.53	5.08, 7.62[d]	5.08, 7.62[d]
Depth below cage (m)[e]	0.16	0.2	0.2

[a] Pier dimensions (length, width) for Oyster and Reference sites were 18.3 m by 3.7 m and 6.1 m by 2.9 m, respectively.

[b] *Crassostrea virginica* (7-12 cm) were maintained in aquaculture rafts in Lowry Cove in 2002; rafts in 2003 generally housed the larger oysters.

[c] Sediment traps with aspect ratios <3:1 allow water currents to erode a portion of trapped material (Hargrave & Burns 1979, Bloesch & Burns 1980, Gardner 1980a, Gardner 1980b, Blomqvist & Kofoed 1981).

[d] Sediment traps with an inner diameter of 5.08 cm and 7.62 cm were deployed beneath oyster aquaculture floats and at reference sites, respectively, in 2003. Material from 2 to 3 sediment traps were combined into a single replicate (n = 3) so that sufficient material was available for nutrient analyses.

[e] Depth of the opening of sediment traps positioned beneath oyster aquaculture floats; sediment traps at reference sites were positioned approximately 0.3 to 0.5 m above the sediment surface.

Table 3.3 Deposition of total nitrogen (mmol N m^{-2} h^{-1}) and surface (0-1 cm) sediment concentrations of total nitrogen (μmol N g^{-1} DW) and chlorophyll *a* (mg chl *a* m^{-2}) from Oyster and Reference sites in Lowry Cove, Mainstem, and Pier. All values are means ± one standard deviation; number of observations (n) are provided in parentheses. Mean values for surface sediment concentrations at Oyster sites are for sampling dates after deployment of Taylor floats.

Sampling location Study site	Deposition of total nitrogen[a] (mmol N m^{-2} h^{-1})	Surface sediment total nitrogen (μmol N g^{-1} DW)	Surface sediment chlorophyll *a* (mg chl *a* m^{-2})
Lowry Cove			
Oyster	5.4 ± 3.5 (18)	278.4 ± 11.7 (4)	22.1 ± 10.4 (7)
Reference	2.0 ± 1.1 (17)	268.7 ± 8.6 (11)	11.4 ± 3.2 (15)
Mainstem			
Oyster	3.4 ± 1.8 (21)	321.3 ± 33.5 (14)	29.4 ± 21.0 (14)
Reference	1.3 ± 0.5 (17)	277.4 ± 10.9 (20)	11.7 ± 6.0 (20)
Pier			

Oyster	10.0 ± 3.6	(21)	328.4 ± 29.6	(15)	83.9 ± 132.2	(15)
Reference	1.3 ± 0.8	(21)	271.0 ± 13.3	(20)	19.0 ± 5.5	(20)

[a] Sedimentation traps for the determination of total nitrogen deposition in 2002 and 2003 had aspect ratios (length : width) of 1:1 and 4:1, respectively. Simultaneous deployment of cylindrical (4:1) and square (1:1) sedimentation traps occurred at Mainstem sites on 08 and 25 September 2003. Square traps collected 47% (± 0.09) of material collected in cylindrical traps used in 2003; corrections to Lowry Cove data were not done, as differences in flow regimes (e.g., current velocities) at sites may have affected calibrations.

Figure Legends

Fig. 3.1 (A) Deposition of total nitrogen and surface (0-1 cm) sediment concentrations of (B) total nitrogen and (C) chlorophyll *a* on sampling dates (July – September 2002) for Lowry Oyster (filled) and Reference (open) sites. Replicates for measurements of deposition and surface sediment concentrations were 1-3 and 2-4, respectively; data are means ± SD.

Fig. 3.2 (A) Deposition of total nitrogen and surface (0-1 cm) sediment concentrations of (B) total nitrogen and (C) chlorophyll *a* on sampling dates (July – September 2003) for Mainstem Oyster (filled) and Reference (open) sites. Replicates for measurements of deposition and surface sediment concentrations were 2-3 and 4-5, respectively; data are means ± SD. Rates of total nitrogen deposition at Reference on 25 August 2003 were not presented (*), as resuspension of bottom sediment associated with a nearby boat led to unusually high rates.

Fig. 3.3 (A) Deposition of total nitrogen and surface (0-1 cm) sediment concentrations of (B) total nitrogen and (C) chlorophyll *a* on sampling dates (May – July 2003) for Pier Oyster (filled) and Reference (open) sites. Replicates for measurements of deposition and surface sediment concentrations were 3-5 and 5, respectively; data are means ± SD.

Fig. 3.4 Mean (± SD) percent organic content, determined from weight loss upon ignition (550°C), for material collected in sedimentation traps (deposition) and surface (0-1 cm) sediments retrieved from (A-B) Lowry, (C-D) Mainstem, and (E-F) Pier. Organic content was measured in triplicate for trap material; observations of surface sediments ranged from 1 to 5 depending on sampling location (**Lowry:** 1-3; **Mainstem:** 4-5; and **Pier:** 5).

Fig. 3.5 Mean (± SD) ratios of total carbon to nitrogen for material collected in sedimentation traps (deposition) and surface (0-1 cm) sediments retrieved from (A-B) Lowry, (C-D) Mainstem, and (E-F) Pier. Number of observations of nutrient ratios varied with material (n = 2-3) and sampling location (**Lowry:** 1-3; **Mainstem:** 4-5; and **Pier:** 5).

Fig. 3.6 Mean (± SD) rates of net ecosystem metabolism, determined from dark and light O_2 fluxes, for Oyster (filled) and Reference (open) sites on sampling dates at (A) Lowry, (B) Mainstem, and (C) Pier. Flux measurements for dissolved O_2 were conducted on 2-4 and 5 sediment cores in 2002 (A) and 2003 (B-C), but sample sizes were often reduced (n = 1-5). Linear regressions of dissolved O_2 concentrations versus time were not always significant ($r^2 > \sim 0.8$, $F \leq 0.10$). NS: no significant fluxes. Note difference in scale for (C) Pier.

Fig. 3.7 Mean (± SD) pore water NH_4^+ concentrations in sediment cores collected from Oyster (filled) and Reference (open) sites at (A-D) Mainstem, (E) Lowry, and (F)

Pier. Pore water NH_4^+ profiles (n = 2) are provided for Pier on (F) 30 July 2003 and for each Mainstem sampling date: (A) 23 July, (B) 20 August, (C) 08 September, and (D) 25 September 2003. Profiles for (E) Lowry Oyster and Reference are means (± SD; n = 3-4) of single core dissections from the last 3 and all sampling dates, respectively. Note scale difference for (F) Pier.

Fig. 3.8 Mean (± SD) NH_4^+ flux (μmol N m^{-2} h^{-1}) during (A, C, D) dark and (B) light incubations for Oyster (filled) and Reference (open) sites on sampling dates. NH_4^+ fluxes presented are from (A) dark and (B) light incubations for Mainstem and dark incubations for (C) Lowry and (D) Pier. NH_4^+ fluxes were performed on replicate (n = 5) sediment cores; sample size varied (n = 1-5) with significance of linear regressions of NH_4^+ concentrations versus time ($r^2 > \sim 0.8$, $F \leq 0.10$). NS: no significant fluxes. Note difference in scale for NH_4^+ fluxes.

Fig. 3.9 Mean (±SD) N_2-N flux (μmol N m^{-2} h^{-1}) during (A, C, D) dark and (B, D, F) light incubations for Oyster (filled) and Reference (open) sites sampled at (A-B) Lowry, (C-D) Mainstem, and (E-F) Pier. Rates of N_2-N exchange should be reviewed cautiously, as rates within the water column (i.e., blanks) often determined the direction and magnitude of exchange (*See text*). N_2-N fluxes were performed on replicate (n = 2-5) sediment cores; sample size varied (n = 1-5) with significance of linear regressions of N_2-N concentrations versus time ($r^2 > \sim 0.8$, $F \leq 0.10$) . Note difference in scale for fluxes.

Fig. 3.10 Mean (± SD) pore water concentrations of total dissolved sulfide in sediment cores collected from Oyster (filled) and Reference (open) sites at (A-D) Mainstem, (E) Lowry, and (F) Pier. Profiles of total dissolved sulfide (n = 2) are provided for Pier on (F) 30 July 2003 and for each Mainstem sampling date: (A) 23 July, (B) 20 August, (C) 08 September, and (D) 25 September 2003. Profiles for (E) Lowry Oyster and Reference are means (± SD; n = 3-4) of single core dissections from the last 3 and all sampling dates, respectively.

Fig. 3.11 Pore water concentration (mmol L^{-1}; n = 1-2) ratios of sulfate to chloride in sediment cores collected from Oyster (A, C, E) and Reference (B, D, F) sites at (A-B) Lowry, (C-D) Mainstem, and (E-F) Pier. SO_4^{2-} to Cl^- ratios in seawater are typically 0.0517 (molality).

Fig. 3.12 Solid-phase profiles of (A) acid-volatile sulfide and (B) chromium-reducible sulfide in duplicate (n = 2) sediment cores from Mainstem Oyster (filled) and Reference (open) on 23 July (circles) and 25 September 2003 (triangles).

Fig. 3.13 (A) Relationship of benthic biomass (g DW) for the clam, *Macoma balthica*, to shell length (mm), as determined from a subsample of clams (n = 16) sieved from sediment cores collected at Pier Oyster and Reference. The exponential fit equation ($y = 0.0001e^{0.3757x}$, $R^2 = 0.8967$) provided was used to determine the (B) mean (± SD; n = 3-6) biomass (g DW) of *M. balthica* present in cores collected on sampling dates. No data was collected on 28 July 2003. Although biomasses

were only determined on 20 August 2003 for Mainstem, no *M. balthica* were found in sediment cores from Mainstem Oyster; three clams were found in a single sediment core from Mainstem Reference.

Fig. 3.1

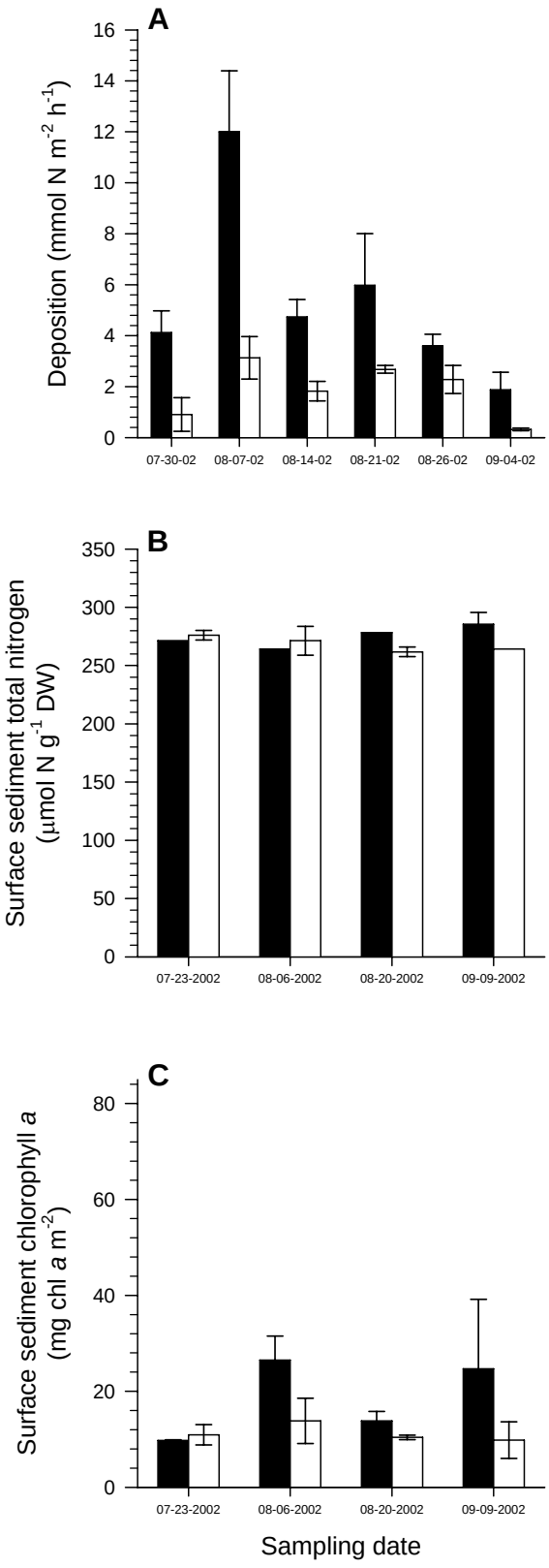
A
Deposition (mmol N m-2 h-1)
0
2
4
6
8
10
12
14
16
07-30-02
08-07-02
08-14-02
08-21-02
08-26-02
09-04-02
B
Surface sediment total nitrogen (µmol N g-1 DW)
0
50
100
150
200
250
300
350
07-23-2002
08-06-2002
08-20-2002
09-09-2002
C
Surface sediment chlorophyll a (mg chl a m-2)
0
20
40
60
80
07-23-2002
08-06-2002
08-20-2002
09-09-2002
Sampling date

Fig. 3.2

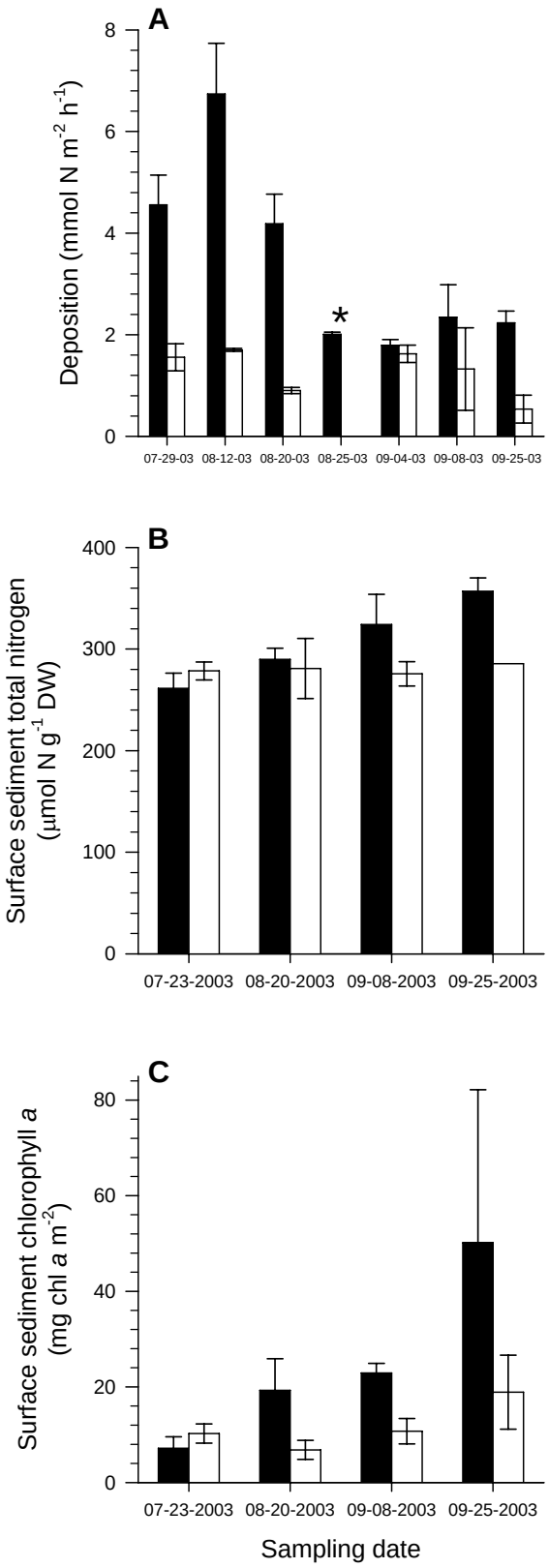
A
Deposition (mmol N m-2 h-1)
0
2
4
6
8
*
07-29-03
08-12-03
08-20-03
08-25-03
09-04-03
09-08-03
09-25-03
B
Surface sediment total nitrogen (μmol N g-1 DW)
0
100
200
300
400
07-23-2003
08-20-2003
09-08-2003
09-25-2003
C
Surface sediment chlorophyll a (mg chl a m-2)
0
20
40
60
80
07-23-2003
08-20-2003
09-08-2003
09-25-2003
Sampling date

Fig. 3.3

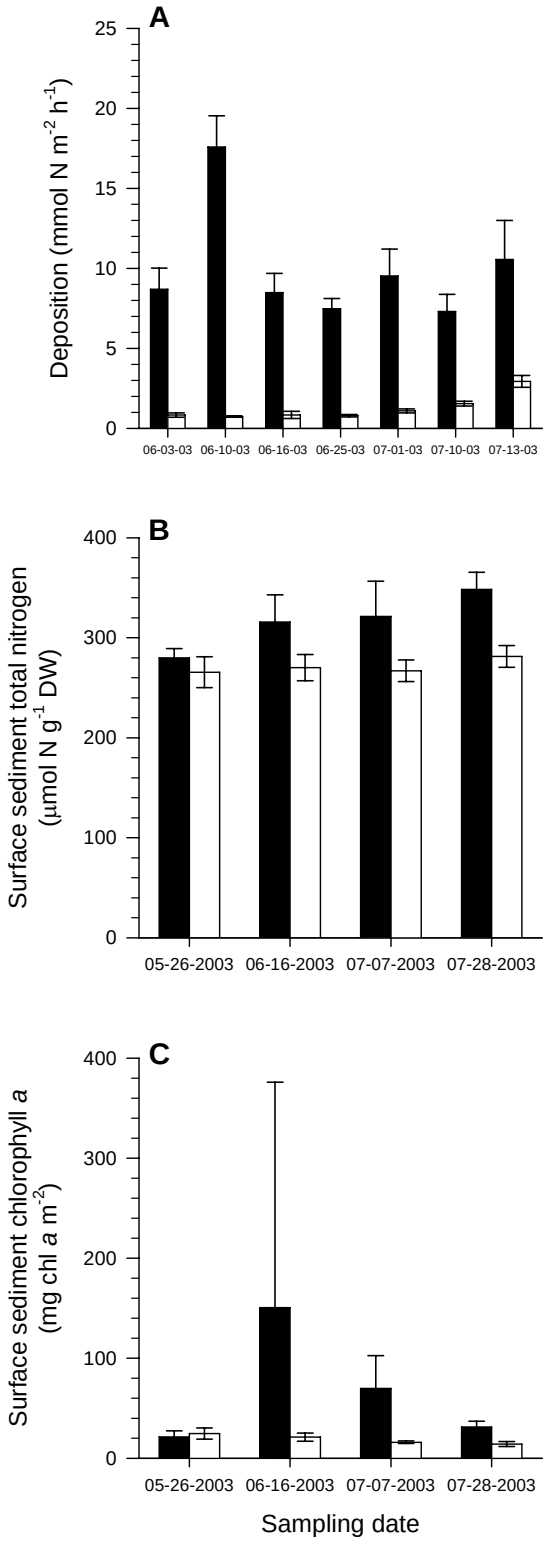
A
Deposition (mmol N m-2 h-1)
25
20
15
10
5
0
06-03-03
06-10-03
06-16-03
06-25-03
07-01-03
07-10-03
07-13-03
B
Surface sediment total nitrogen (µmol N g-1 DW)
400
300
200
100
0
05-26-2003
06-16-2003
07-07-2003
07-28-2003
C
Surface sediment chlorophyll a (mg chl a m-2)
400
300
200
100
0
05-26-2003
06-16-2003
07-07-2003
07-28-2003
Sampling date

Fig. 3.4

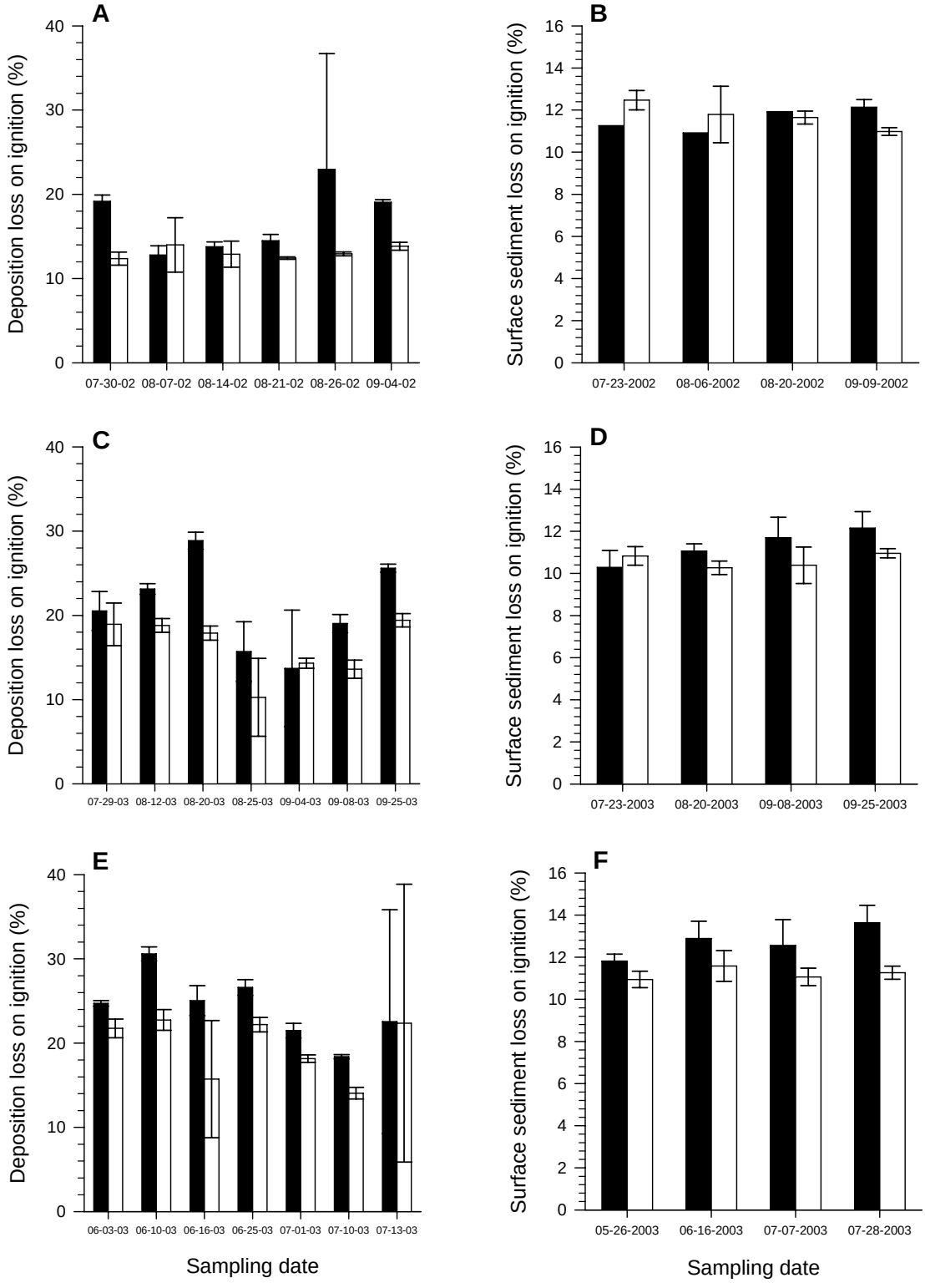
A
B
C
D
E
F
Deposition loss on ignition (%)
Surface sediment loss on ignition (%)
07-30-02
08-07-02
08-14-02
08-21-02
08-26-02
09-04-02
07-23-2002
08-06-2002
08-20-2002
09-09-2002
07-29-03
08-12-03
08-20-03
08-25-03
09-04-03
09-08-03
09-25-03
07-23-2003
08-20-2003
09-08-2003
09-25-2003
06-03-03
06-10-03
06-16-03
06-25-03
07-01-03
07-10-03
07-13-03
05-26-2003
06-16-2003
07-07-2003
07-28-2003
Sampling date
Sampling date

Fig. 3.5

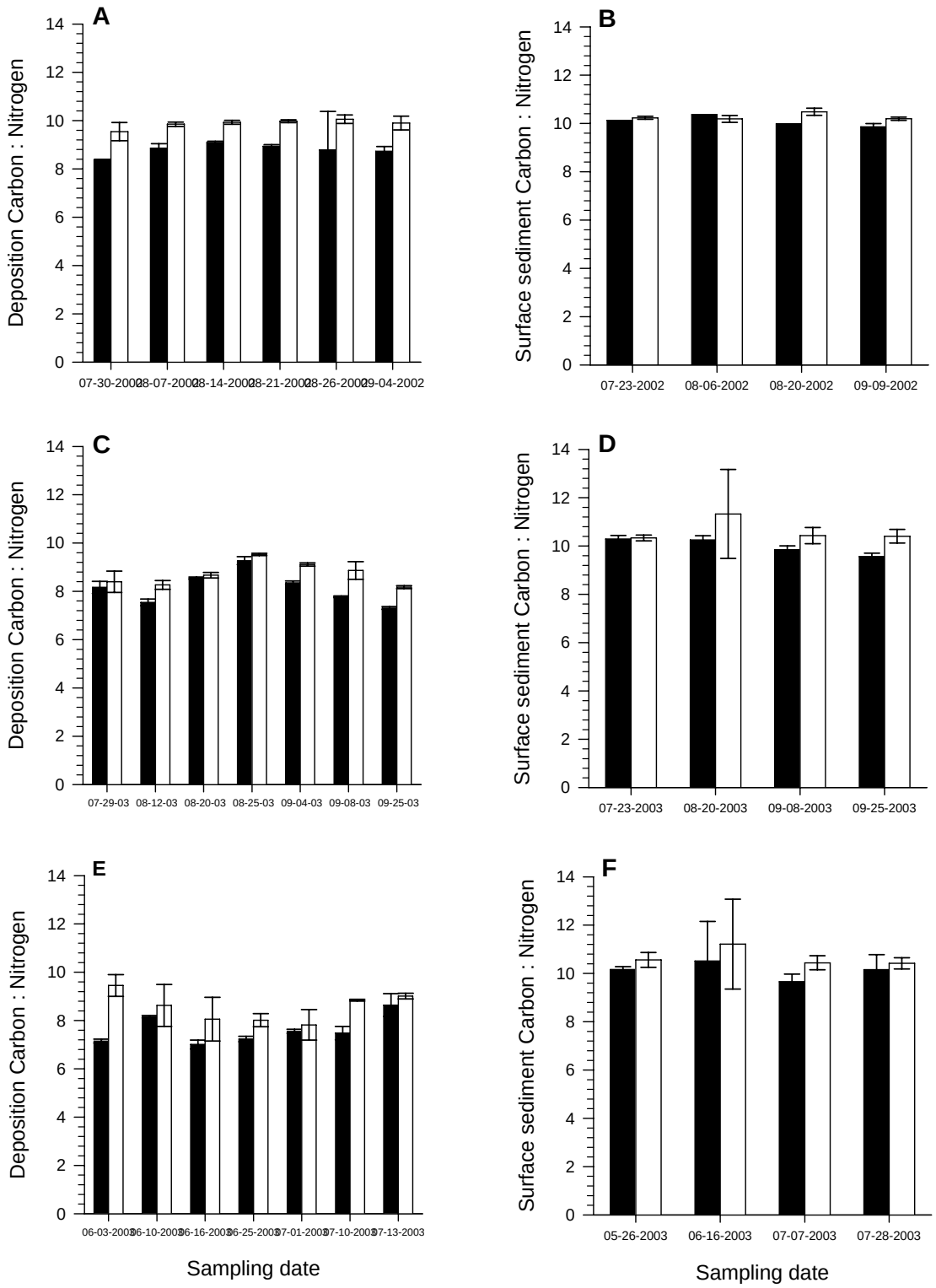
A
B
C
D
E
F
Deposition Carbon : Nitrogen
Surface sediment Carbon : Nitrogen
0
2
4
6
8
10
12
14
07-30-2002
08-07-2002
08-14-2002
08-21-2002
08-26-2002
09-04-2002
07-23-2002
08-06-2002
08-20-2002
09-09-2002
07-29-03
08-12-03
08-20-03
08-25-03
09-04-03
09-08-03
09-25-03
07-23-2003
08-20-2003
09-08-2003
09-25-2003
06-03-2003
06-10-2003
06-16-2003
06-25-2003
07-01-2003
07-10-2003
07-13-2003
05-26-2003
06-16-2003
07-07-2003
07-28-2003
Sampling date
Sampling date

Fig. 3.6

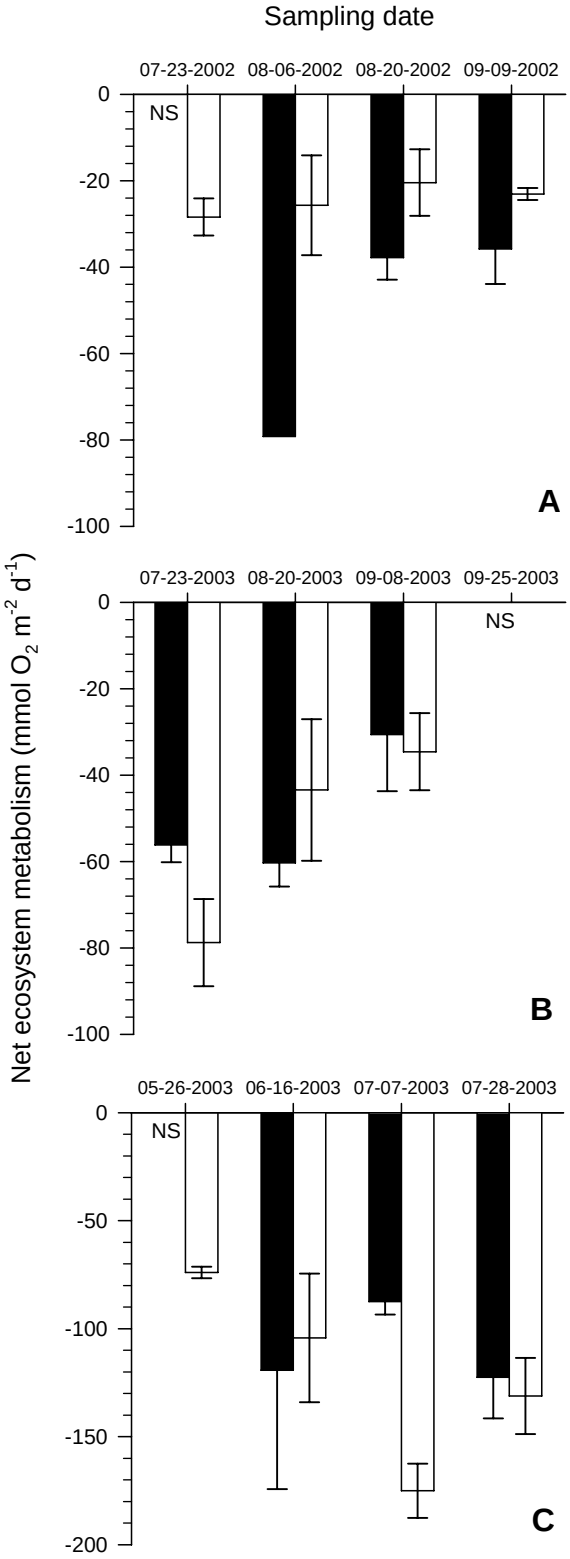
Sampling date
07-23-2002
08-06-2002
08-20-2002
09-09-2002
NS
A
07-23-2003
08-20-2003
09-08-2003
09-25-2003
NS
B
05-26-2003
06-16-2003
07-07-2003
07-28-2003
NS
C
Net ecosystem metabolism (mmol O2 m-2 d-1)
0
-20
-40
-60
-80
-100
-50
-150
-200

Fig. 3.7

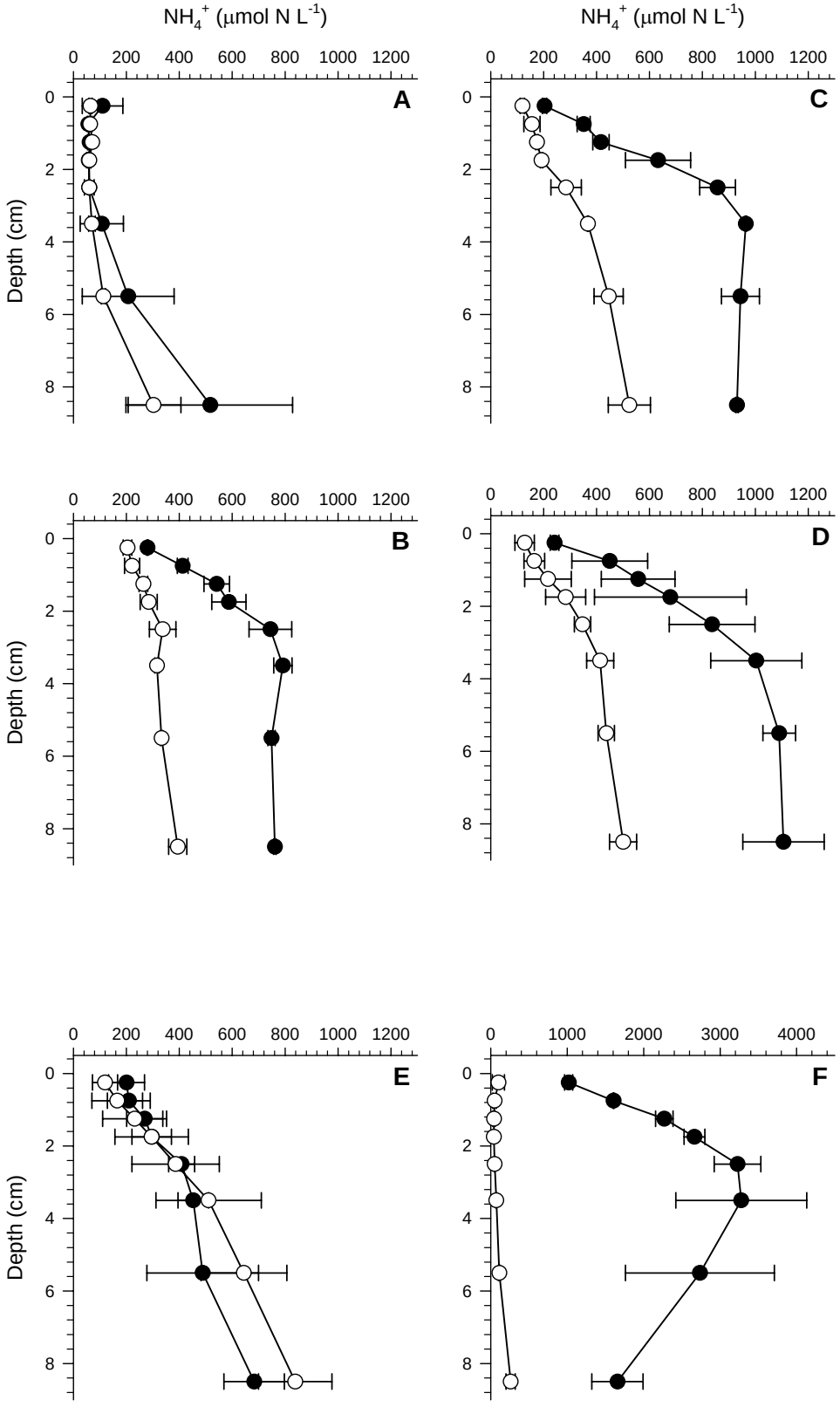
NH4+ (μmol N L-1)
NH4+ (μmol N L-1)
Depth (cm)
Depth (cm)
Depth (cm)
A
B
C
D
E
F
0 200 400 600 800 1000 1200
0 1000 2000 3000 4000
0 2 4 6 8

Fig. 3.8

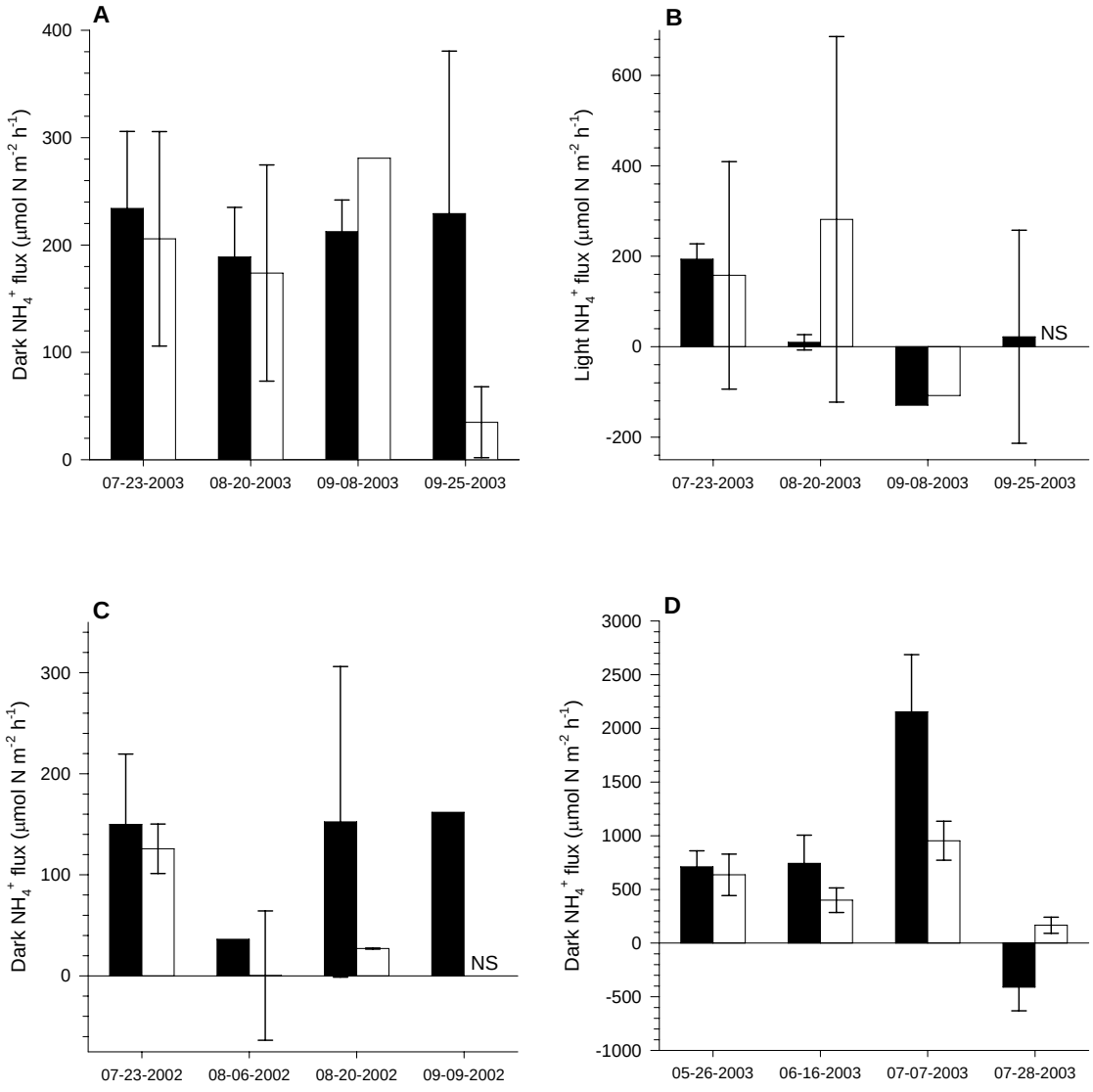
A
Dark NH4+ flux (µmol N m-2 h-1)
400
300
200
100
0
07-23-2003
08-20-2003
09-08-2003
09-25-2003
B
Light NH4+ flux (µmol N m-2 h-1)
600
400
200
0
-200
NS
07-23-2003
08-20-2003
09-08-2003
09-25-2003
C
Dark NH4+ flux (µmol N m-2 h-1)
300
200
100
0
NS
07-23-2002
08-06-2002
08-20-2002
09-09-2002
D
Dark NH4+ flux (µmol N m-2 h-1)
3000
2500
2000
1500
1000
500
0
-500
-1000
05-26-2003
06-16-2003
07-07-2003
07-28-2003

Fig. 3.9

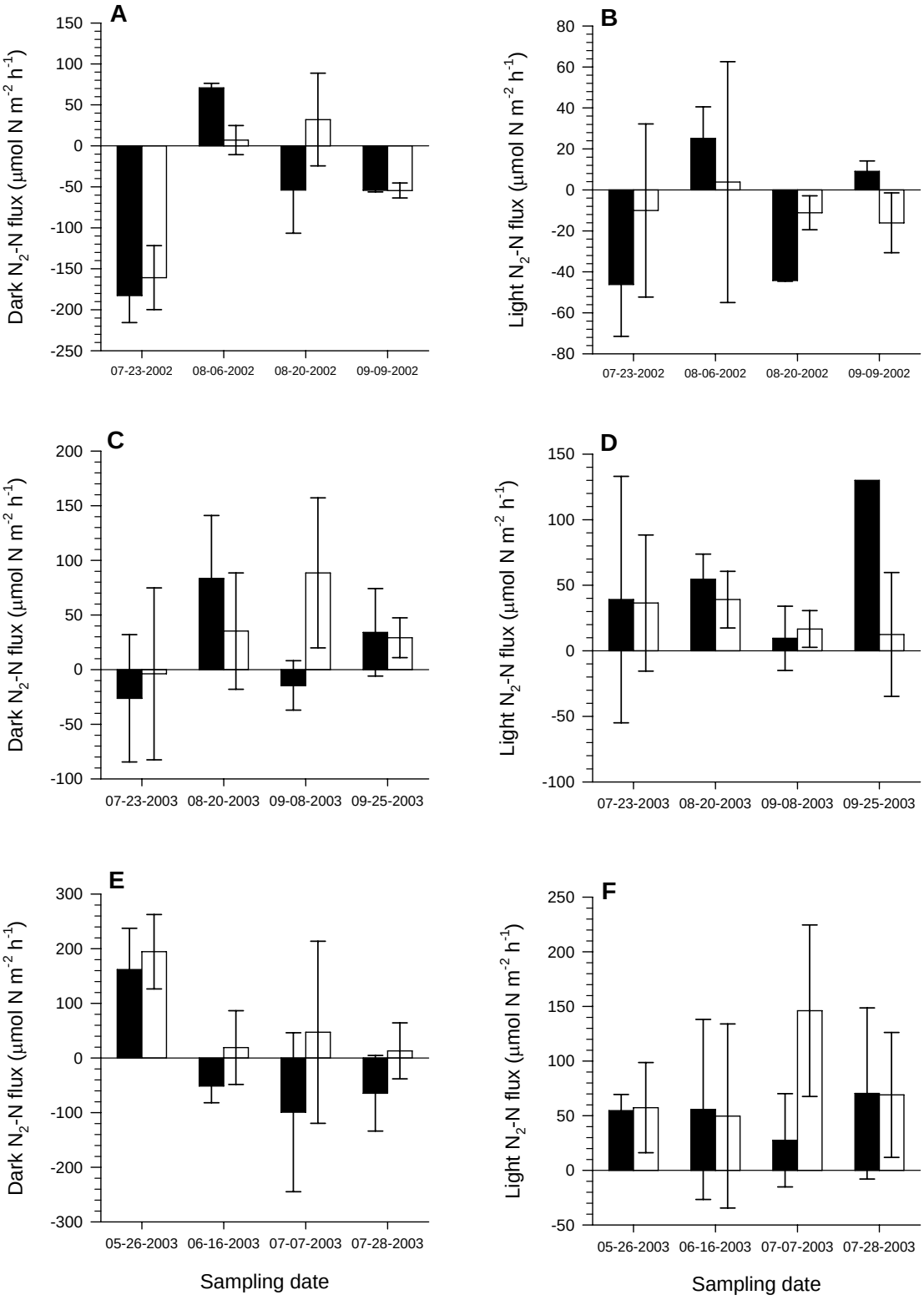
A
B
C
D
E
F
Dark N_2-N flux (μmol N m^{-2} h^{-1})
Light N_2-N flux (μmol N m^{-2} h^{-1})
07-23-2002
08-06-2002
08-20-2002
09-09-2002
07-23-2003
08-20-2003
09-08-2003
09-25-2003
05-26-2003
06-16-2003
07-07-2003
07-28-2003
Sampling date

Fig. 3.10

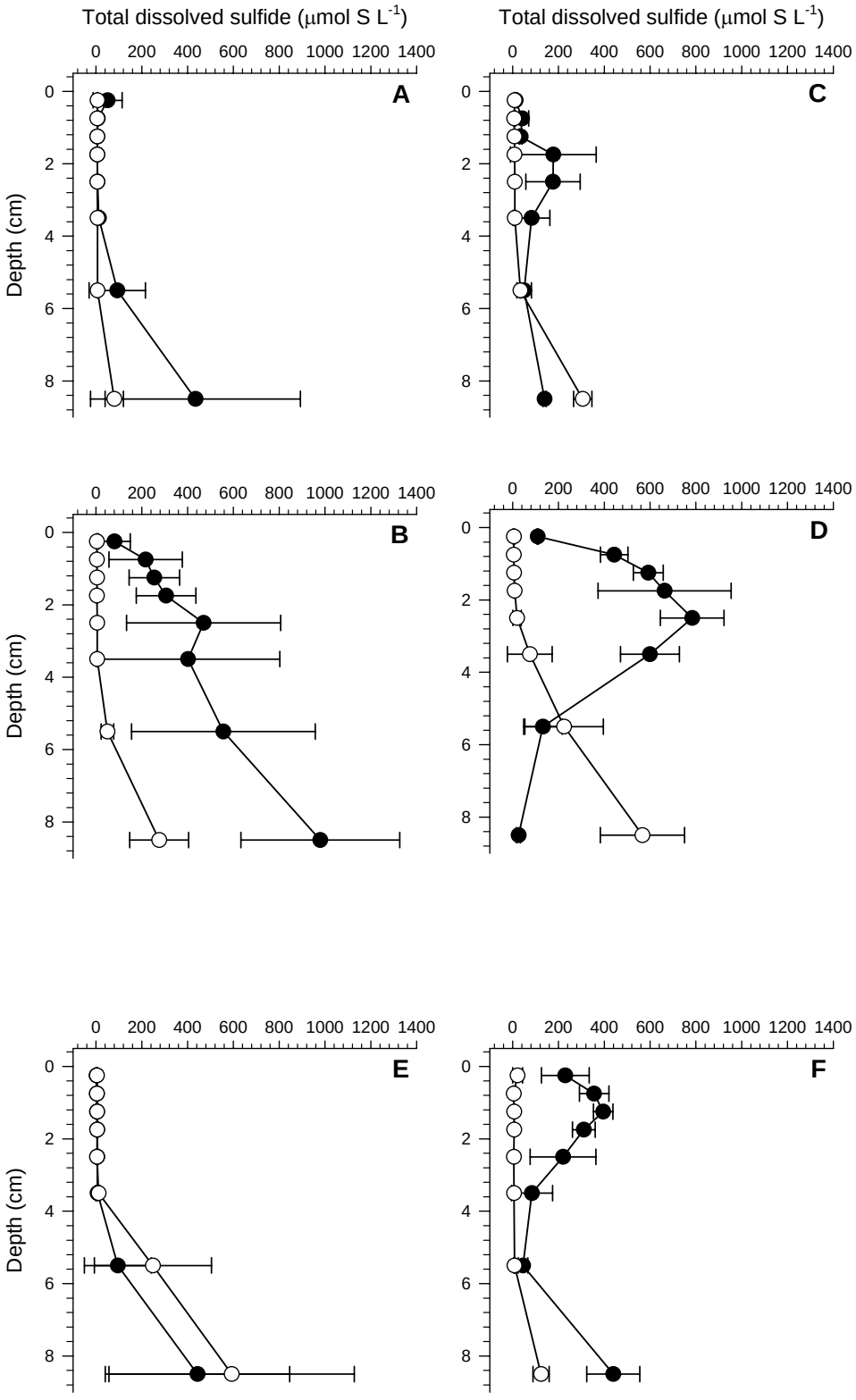
Total dissolved sulfide (μmol S L-1)
Total dissolved sulfide (μmol S L-1)
Depth (cm)
Depth (cm)
Depth (cm)
0 200 400 600 800 1000 1200 1400
0 2 4 6 8
A
B
C
D
E
F

Fig. 3.11

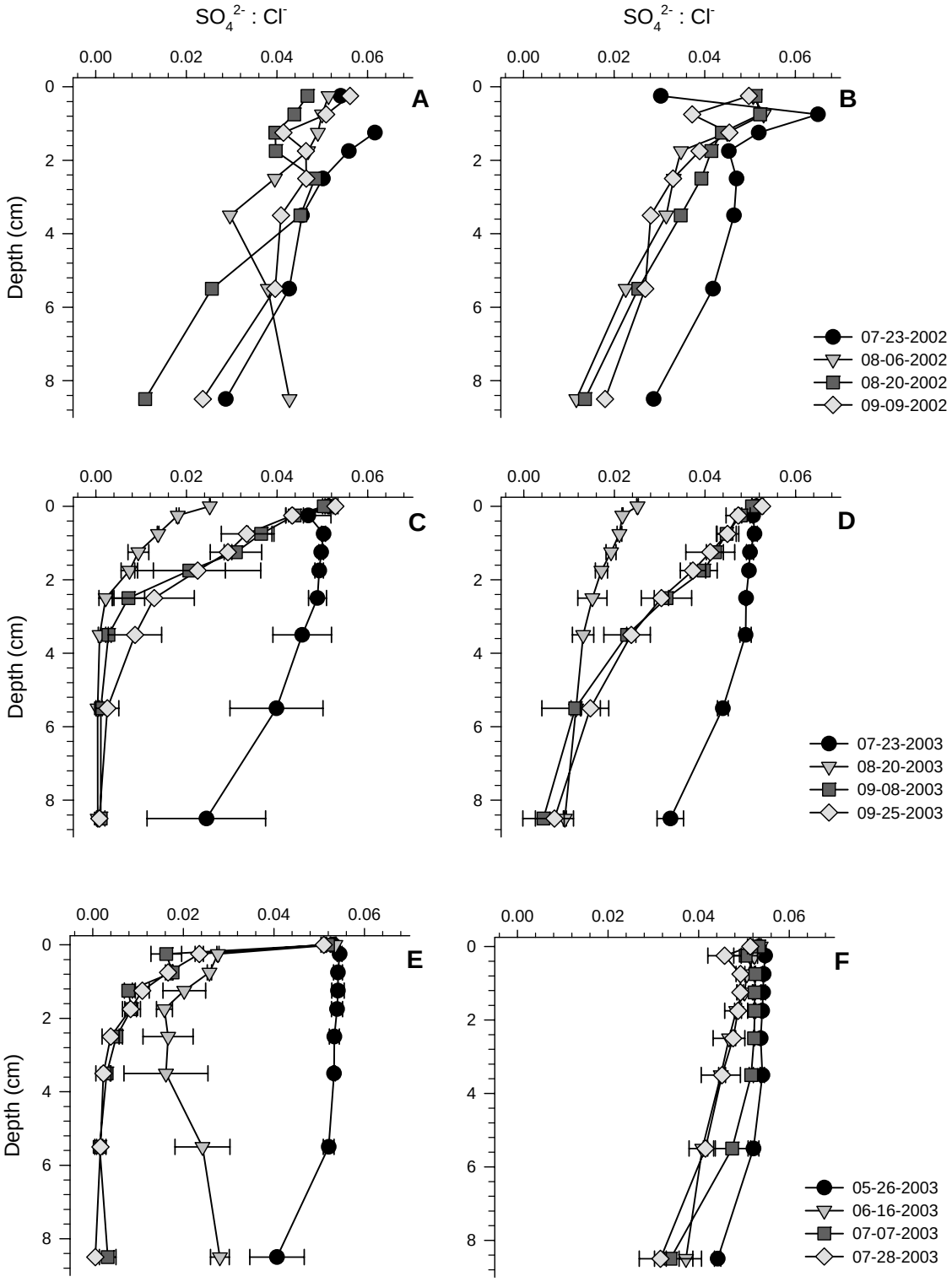
SO_4^{2-} : Cl^-
0.00
0.02
0.04
0.06
Depth (cm)
0
2
4
6
8
A
B
C
D
E
F
07-23-2002
08-06-2002
08-20-2002
09-09-2002
07-23-2003
08-20-2003
09-08-2003
09-25-2003
05-26-2003
06-16-2003
07-07-2003
07-28-2003

Fig. 3.12

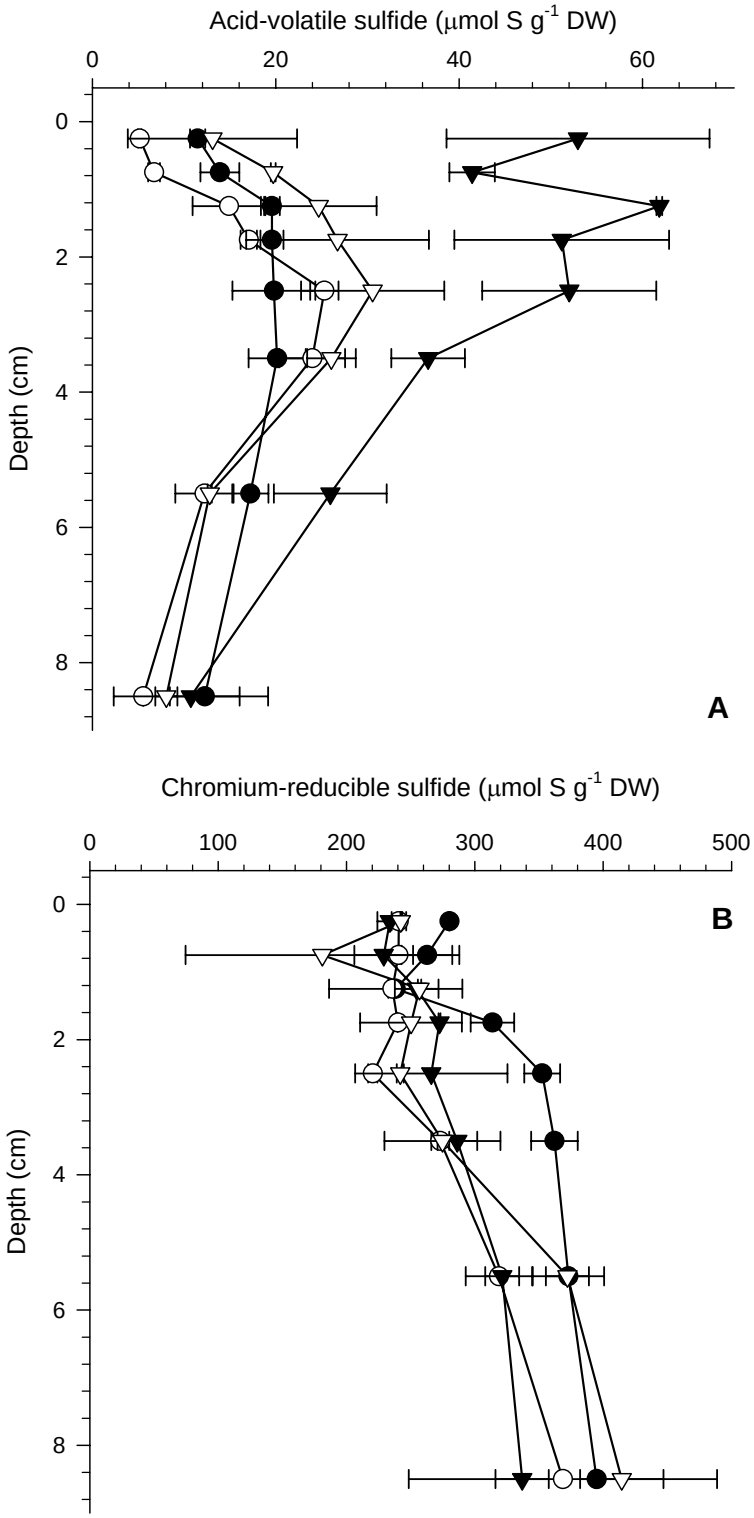
Acid-volatile sulfide (μmol S g-1 DW)
0
20
40
60
Depth (cm)
0
2
4
6
8
A
Chromium-reducible sulfide (μmol S g-1 DW)
0
100
200
300
400
500
Depth (cm)
0
2
4
6
8
B

Fig. 3.13

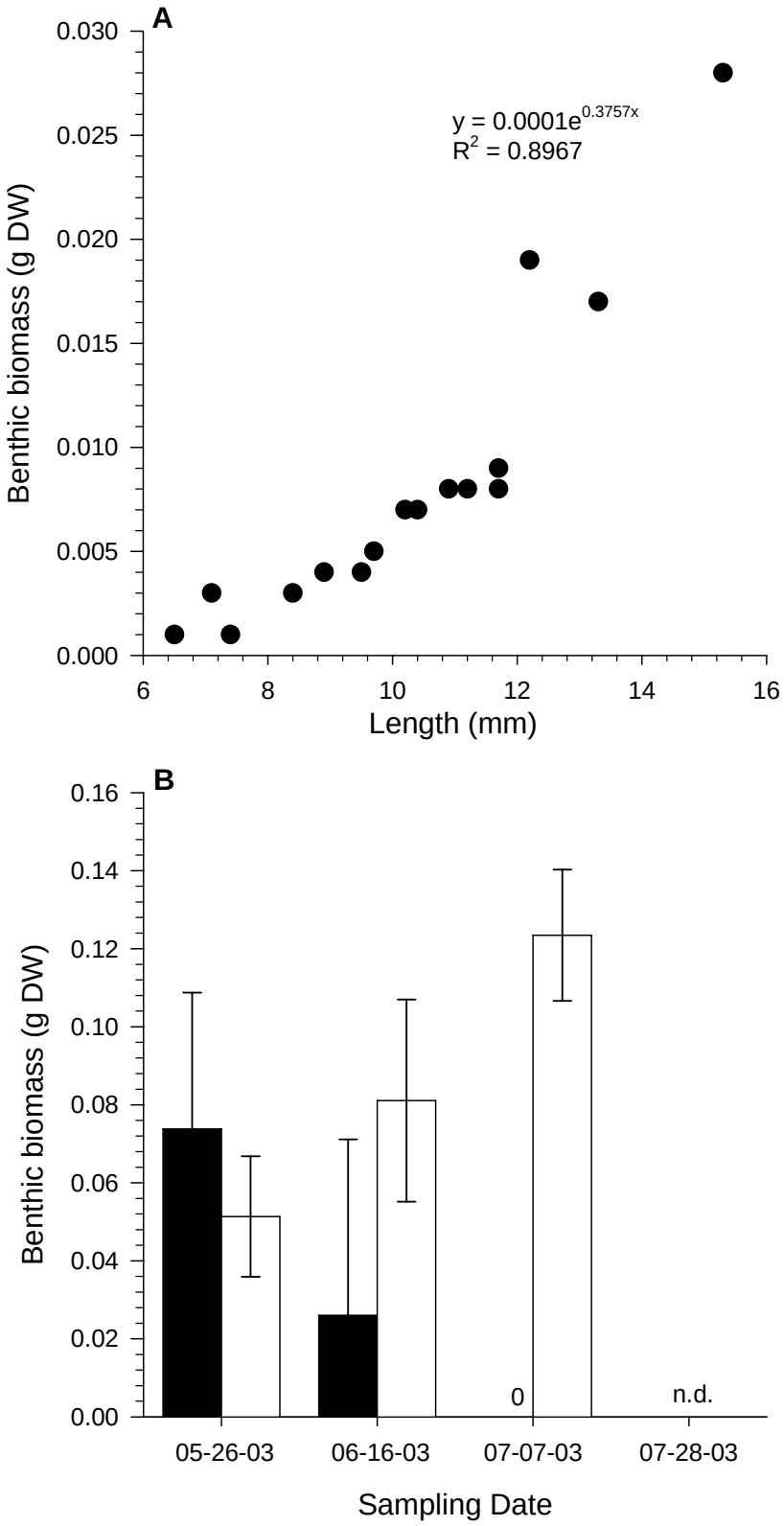
A
y = 0.0001e^0.3757x
R^2 = 0.8967
Benthic biomass (g DW)
Length (mm)
0.000
0.005
0.010
0.015
0.020
0.025
0.030
6
8
10
12
14
16
B
Benthic biomass (g DW)
Sampling Date
0.00
0.02
0.04
0.06
0.08
0.10
0.12
0.14
0.16
0
n.d.
05-26-03
06-16-03
07-07-03
07-28-03

Chapter 4: Temporal Variation in Sediment Nitrogen and Phosphorus Fluxes as Mediated by the Interactions of Benthic Microalgae and Organic Deposition

Abstract

Disparities in estimated rates of benthic photosynthesis and heterotrophic metabolism, determined from O_2 fluxes, have been used to illustrate the dominance of autotrophic and heterotrophic processes within shallow water sediments, and classifications have recently been extended to suggest whether sediments serve as net sinks or sources of nutrients to overlying waters. Given the potential for short-term variations in benthic photosynthesis and heterotrophic metabolism to affect sediment nitrogen and phosphorus dynamics differently, a laboratory experiment was conducted to investigate how and on what timeframe shifts in these processes may influence stoichiometric ratios and directions of nitrogen and phosphorus exchange. Sediment cores from a mesohaline, tidal creek of Chesapeake Bay were divided into four treatments based on two surface sediment irradiances (~10 and 100 μmol photons m^{-2} s^{-1}) and two organic loadings (~1.5 and 7.5 g C m^{-2} d^{-1}) and incubated aerobically for ~ 3 wks to measure shifts in nutrient (O_2, N_2, NH_4^+, NO_2^- + NO_3^-, SRP) fluxes and benthic microalgal biomass (i.e., sediment chlorophyll *a*). Transitions in nitrogen and phosphorus exchange at the sediment-water interface were observed as changes in the speciation, direction, and magnitude of flux, as well as the ratio of nitrogen to phosphorus release or uptake. All sediments responded to organic loading through increases in sediment O_2 consumption. Gross photosynthesis was primarily influenced by the intensity of surface sediment irradiance and, secondarily, by organic matter deposition. Sediments from all treatments released NH_4^+ into the water column, with greatest net effluxes occurring in low light, high loading sediments. Water column concentrations of NO_2^- + NO_3^- regulated N_2-N exchange, so no differences in apparent N_2 fixation or net

denitrification were identified. Shifts in net phosphorus exchange were driven by anaerobic remineralization and concentrations of iron and manganese oxy(hydr)oxides, with transitions in fluxes coinciding with changes in benthic photosynthesis and reoxidation of surface sediments. Trophic states typically were not good indicators of the capacity of sediments to serve as net sinks or sources of nutrients; nor did these classifications provide any insight into the relative exchange of nitrogen and phosphorus (i.e., N:P) across the sediment-water interface. Use of trophic states as a management tool for defining nutrient exchange may be insufficient in shallow, fine-grain sediments receiving high rates of organic deposition.

Introduction

Benthic microalgal communities (BMA) inhabit and concentrate at the sediment-water interface of illuminated sediments in aquatic systems. In sheltered inlets, tidal tributaries, and the upper reaches of estuaries, sediments are often dominated by fine grained silts and clays, high organic content, and high rates of particulate organic matter (POM) deposition. Granulometry and organic content of these sediments limits light penetration to the upper ~ 2 to 3 mm (MacIntyre et al., 1996), thereby, limiting the migration and distribution of these communities below these depths. By "capping" sediments, BMA influence sediment nutrient exchange with overlying waters directly and indirectly through assimilatory uptake of nutrients, photosynthetic O_2 production, and heterotrophic metabolism.

Rates of benthic O_2 production and heterotrophic metabolism within BMA and at depth interact to influence the trophic state (i.e., autotrophic, heterotrophic) of shallow

water sediments, and imbalances in these rates have been used to classify sediments as net sinks or sources of nutrients to overlying waters (Rizzo et al., 1996). Such simple classification of shallow water sediments as simply unidirectional sinks or sources may be insufficient, however, given the potential for variability in rates of photosynthetic O_2 production and heterotrophic metabolism diurnally and seasonally, as well as the differential influences these processes may have on nitrogen and phosphorus dynamics.

Diel and seasonal patterns of benthic primary productivity are often associated with variations in incident irradiance (Rizzo et al., 1992), temperature (Hancke and Glud, 2004), benthic microalgal biomass (MacIntyre et al., 1996), accessibility of inorganic nutrients (Graneli and Sundback, 1985; Simon, 1988; Nilsson et al., 1991), grazing pressure (Nilsson et al., 1991; Sundback et al., 1996), and stochastic events, such as freshwater inflows and sediment resuspension (Miles and Sundback, 2000; Sundback et al., 2000). In general, rates and variations of photosynthetic activity are considered to be primarily driven by the availability of surface sediment irradiance (MacIntyre et al., 1996). Correlations between *in situ* irradiance and benthic primary production have been shown to be site specific (Miles and Sundback, 2000), and are often a function of microalgal biomass and chlorophyll-specific responses (i.e., photoacclimation, photoinhibition) to irradiance (MacIntyre et al., 1996).

Rates of heterotrophic metabolism within shallow water sediments are largely a function of microbial consumption of organic matter and the respiratory demands of benthic photoautotrophs. Rates of aerobic and ananerobic remineralization of POM depends largely on the quantity, sedimentation, burial, and lability of POM (Muller and Suess, 1979); availability of terminal electron acceptors (Capone and Kiene, 1988);

microbial speciation; temperature (Eyre and Ferguson, 2005); and sediment reworking from bioturbators (Aller, 1994). Supply of POM and temperature have a positive influence on rates of heterotrophic metabolism, such that increased metabolic rates occur with enhanced deposition, lability, and temperatures, and vary spatially and temporally with changes in these processes. Similar increases with temperature have been observed for gross photosynthesis; however, optimal temperatures and stimulation of gross O_2 production are less than for bacterial respiration (Hancke and Glud, 2004). Increases in heterotrophic metabolism and sediment oxygen demand may be further supported by benthic autotrophic processes (Ferguson et al., 2004); increased benthic microalgal biomass supports higher rates of autotrophic respiration and bacterially-mediated heterotrophic metabolism. Release of photosynthetic products and labile carbon through cell leakage, resuspension, grazing, and decomposition provides additional sources of organic nutrients to heterotrophic bacteria (Tobias et al., 2003). Additional contributions to sediment metabolism occur through abiological oxidation of POM and reduced chemical species, which may consume a proportion of benthic O_2 flux and sub-oxic metabolites.

Variations in nitrogen and phosphorus exchange at the sediment-water interface within and among shallow, estuarine systems may be associated with temporal variations in benthic photosynthesis and heterotrophic metabolism. Temporal shifts in the trophic state of shallow water sediments have been shown to vary seasonally (Cerco and Seitzinger, 1997; Ferguson et al., 2003; Eyre and Ferguson, 2005), but daily (Miles and Sundback, 2000) and weekly changes in O_2 production (Caffrey et al., 1998) suggest that shallow water sediments may transition within even shorter timeframes. Such short-term

variability may be associated with sudden changes in the source or supply of POM, which may influence both heterotrophic metabolism and BMA through shifts in labile carbon, nutrient availability, and surface sediment irradiance. Transitions in organic matter deposition, especially in areas of fine-grained sediments, are often influenced by terrestrially-derived particulates and dissolved nutrients transported in freshwater flows, overlying water column production, and stochastic wind or tidal events that enhance shoreline erosion and sediment resuspension (reviewed by Rullkötter, 2000).

As sediments transition from highly autotrophic to fully heterotrophic (Benthic Trophic State Index (BTSI), Rizzo et al., 1996) or increase in the intensity of one of these trophic states, I suspect that sediments will not respond like an on/off switch – first serving as a sink and then as a source of nitrogen and phosphorus to overlying waters. Rather, differences in the direction and/or relative magnitude (i.e., Redfield stoichiometry) of nitrogen and phosphorus fluxes may occur, especially since the primary mechanisms influencing nitrogen and phosphorus cycling are different. Sediment nitrogen fluxes in shallow waters are primarily a function of the assimilatory uptake of NH_4^+ and NO_3^- by BMA and associated competition between benthic autotrophs, nitrifiers, and denitrifiers (Sundback and Miles, 2000; Risgaard-Petersen et al., 2004). Additionally, penetration of dissolved O_2 into sediments may have varying effects on nitrogen fluxes at the sediment-water interface since it may contribute to increases or decreases in coupled nitrification-denitrification (Tiedje et al., 1989; Risgaard-Petersen et al., 1994; Rysgaard et al., 1995; An and Joye, 2001; Dalsgaard, 2003) and decreases in direct denitrification (Rysgaard et al., 1995). Assimilatory uptake by BMA is generally considered to have a lesser effect on sediment phosphorus exchange than O_2 production

by these communities (Sundback and Graneli, 1988). Redox conditions within oxic/suboxic sediments and authigenic mineral formation (Ruttenberg and Berner, 1993) determine the extent of phosphorus release at the sediment-water interface. In systems with overlying oxygenated waters, as is common for well-mixed, shallow water sites, effluxes only occur at times when high rates of sulfate reduction lead to the production of FeS and FeS_2 (Rozan et al., 2002).

Given the potential for short-term variations in benthic O_2 production and heterotrophic metabolism to affect sediment nitrogen and phosphorus dynamics differently, I designed a laboratory experiment to investigate how and on what timeframe shifts in these processes may affect stoichiometric ratios and directions of fluxes. Surface sediment irradiance and levels of POM loading were used as proxies for photosynthetic O_2 production and sediment metabolism, respectively, since variability in these two factors are likely the dominant influence on BMA and remineralization in fine-grained sediments. Biodeposits (feces and pseudofeces) from the eastern oyster, *Crassostrea virginica*, served as the source of POM since continued pressure to restore *C. virginica* and oyster fisheries has led to an increase in aquaculture in shallow water systems (Murray et al., 2007; See Chapter 3). Transitions in three measures of trophic status (P/R: Odum and Hoskin, 1958; BTSI: Rizzo et al., 1996; NEM) were assessed to determine the value of these tools in predicting variation in nitrogen and phosphorus exchange in shallow, illuminated sediments.

Materials and Methods

Sediment core collection

On 31 August 2005, twenty-two sediment cores (6.35 cm I.D.) were collected in the upper reaches of La Trappe Creek (38° 39.223' N, 076° 05.267' W), a shallow, tidal tributary of the Choptank River in the Maryland portion of Chesapeake Bay. Sediment core collection occurred within 2 h of the lower high tide (mean tide = 0.3 m) when water depths ranged from 1.3 to 1.7 m and surface sediment irradiances were ~ 10 μmol photons m^{-2} s^{-1} (Table 4.1). Variable water depths (~ 1.1 to 2 m) and turbidities ($1.95 < k_d < 5.16$) within this mesohaline portion of La Trappe Creek influence surface sediment irradiance, such that irradiances have ranged from ~ 0 to 70 μmol photons m^{-2} s^{-1} (Chapter 2). Organic content, as determined from loss on ignition at 550°C, and percentages of total carbon and nitrogen for the surface cm of sediment were 9.1 ± 1.9%, 2.81 ± 0.32%, and 0.29 ± 0.04%, respectively (Control Equipment elemental analyzer, Cornwell et al. 1996).

All sediment cores were collected with a pole corer fitted with a transparent acrylic tube (6.35 cm I.D.) that was pressed ~ 10 cm into the fine-grained mud (Percent water: 66.7 ± 5.5%; Porosity: 0.83 ± 0.03; 0-1 cm; Cornwell et al. 1996). Before withdrawing from the sediment, a valve was closed to maintain suction on the core, thereby allowing the core to be removed intact from the sediment. After retrieval, the bottom of the core was sealed with a machined plastic lid and O-ring that prevented the loss of core material. Cores were capped and maintained without airspace, thereby preventing resuspension from water movement, and stored in coolers to maintain near ambient temperature.

Sediment core incubations

Aerobic incubations. At the laboratory, sediment cores were transferred from the transport cooler into a temperature-controlled chamber set at ambient temperature (28°C). Overlying water for six of the twenty-two sediment cores was aerated with electric aquarium pumps until the collection of surface sediments for chlorophyll *a* analyses. The remaining sixteen sediment cores were equally divided into and submerged in two enamel-coated aluminum tanks (~ 30.2 L) containing filtered 2 μm estuarine water from the Choptank River (Figure 4.1). Empty core tubes, each with an acrylic base positioned at the approximate sediment height, were used to incubate ambient water (without sediment) as a measure of water column activity (i.e., blanks). PVC-aeration tubes (2.5 cm I.D.) were inserted into the tops of the open cores such that they reached within ~ 1 cm of the sediment surface (Newell et al., 2002). Active air bubbling in the open cores and surrounding water was maintained at all times, except during core/tank maintenance or sample collection. Water in the incubation tanks was exchanged every 2 d with ambient, filtered 2 μm estuarine water, and microbial growth on the inside walls of sediment cores was scraped and allowed to settle to the sediment surface (for all cores) at these times. The inside walls of incubation tanks and aeration tubes were scrubbed and rinsed with deionized water as needed. Aerobic core incubations persisted for < ~ 3 wks, with termination occurring once gross primary productivity (GPP) stabilized, to prevent further enhancement of container effects (e.g., exclusion of lateral transport) and degradation of BMA (Cornwell, *personal communication*).

Irradiance. Sediment cores, submerged in filtered 2 μm Choptank estuarine water, were incubated under a diel cycle of 14 h of daylight and 10 h of darkness, using Teklight T5H0 greenhouse lights (www.1000bulbs.com). A full spectrum, uniform illumination (~ 100 μmol photons m^{-2} s^{-1}) was provided to surface sediments by alternating the eight lamps within the light bank with low heat factor cool (6500 K) and warm (3000 K) bulbs. Light measurements (LiCor model 2π) indicated no differential irradiance along the length and width of the incubation tank. Layers of mesh, shade cloth were used to provide a 10-fold decrease (~ 10 μmol photons m^{-2} s^{-1}) in surface sediment irradiance to half of the cores and water column blanks in each incubation tank.

Particulate organic matter additions. Dewatered, homogenized slurries of *Crassostrea virginica* (eastern oyster) biodeposits served as the source of particulate organic matter (POM) for treatment additions. Biodeposits were collected from eastern oysters (>7 cm) feeding in ambient flowing Choptank estuarine water and stored at 4°C in a temperature-controlled chamber until decanting the supernatant. Biodeposits were homogenized and divided into low density polyethylene ether (LDPE) 500 ml Nalgene bottles and sterilized by Cobalt-60 gamma irradiation at 50 kGY (~ 788 min). Bottles were subsequently stored in the dark at 4 °C to eliminate microbial respiration throughout the duration of the experiment. Opened bottles of irradiated biodeposits were discarded after 4 d of use. Percent water content of biodeposits was ~ 91 percent, and the C : N : P ratio indicated a composition predominately of phytoplankton (105 : 13 : 1). Subsamples for loss on ignition (n = 17) indicated an organic content of 22.5 ± 0.8%.

POM was added on a volume basis (Low: ~ 0.8 ml, High: ~ 4 ml) to the overlying water in sediment cores and allowed to settle before aeration was restored. Deposition rates of total carbon for the ~ 0.8 ml and ~ 4 ml aliquots were ~ 1.5 g C m^{-2} d^{-1} and ~ 7.5 g C m^{-2} d^{-1}, respectively. POM loadings began on 02 September 2005 (Day 0) and continued daily until 20 September 2005 (Day 18). No additions of POM occurred on a given day until completion of necessary experimental maintenance or nutrient flux incubation.

Experimental design and treatments. Initial randomization of sediment cores into positions within incubation tanks allowed for the unbiased assignment of treatments. Sediment cores were systematically placed within incubation tanks by alternating treatments based on the two POM loadings (Figure 4.1). Blanks for measuring water column activity were positioned between sets of low and high loading treatments, with one blank per irradiance level per tank. Shadows from mesh, shade cloth prohibited the placement of individual cores receiving low surface sediment irradiance (L: ~ 10 μmol photons m^{-2} s^{-1}) among cores receiving ~ 100 μmol photons m^{-2} s^{-1} (H). Identifications for the four treatments, developed from two surface sediment irradiances and two POM loadings, correspond to the light and then loading level as follows: HL: high light, low loading; HH: high light, high loading; LL: low light, low loading; and LH: low light, high loading.

Nutrient flux incubations. Nutrient flux incubations for dissolved gases (O_2, N_2), NH_4^+, and soluble reactive phosphorus (SRP) were performed for all sediment cores and blanks

initially on 02 September 2005 (Day 0), prior to POM additions on Day 4, 10 and 13, and on the day after final additions (Day 19). During flux incubations, cores were sealed with machined plastic lids with O-rings, and the overlying water mixed with a Teflon-coated magnetic stirrer (4.5 V) driven by an external magnetic turntable. Baseline solute (NH_4^+, SRP) and gas concentrations (O_2, N_2, Ar) were determined in the dark immediately upon sealing the cores and then in the light at ~ 3 h intervals. Small amounts of water were withdrawn for sampling at five points ($T_0 - T_4$) for < 3 h in the dark and at five time points ($T_4 - T_8$) over ~ 3 h in the light. Additional aliquots for $NO_2^- + NO_3^-$ concentrations were collected from a subset of cores at T_0, T_4, and T_8.

Water withdrawn for sampling was replaced by ambient, filtered 2μm water from the Choptank River, introduced through Tygon tubing to ensure that no air bubbles were introduced to the system. Samples to measure N_2 and O_2 concentrations were taken in gas tubes with ground glass stoppers and preserved with 10 μl 50% saturation $HgCl_2$. Tubes were stored submerged in water at ambient temperature (28°C) for no more than 1 week. NH_4^+, $NO_2^- + NO_3^-$, and SRP water column samples were collected in 20 ml syringes and filtered through 0.45 μm filters into 6 ml plastic vials. Nutrient samples were immediately frozen (-20°C) until analysis.

Analyses

Chemical analyses. Membrane inlet mass spectrometry was used to determine N_2 and O_2 concentrations in water samples collected during flux core incubations (Kana et al., 1994; Kana et al., 1998). N_2 : Ar and O_2 : Ar gas ratios were used to provide a precision of < 0.02% for N_2 and O_2 concentrations. Corrections to N_2 : Ar ratios associated with O_2

effects in the mass spectrometer were applied to all samples (Kana and Weiss, 2004); sample points with percent O_2 saturations exceeding 97% were removed from N_2 flux calculations (n = 7). Colorimetric analyses were used to determine concentrations of NH_4^+, SRP, and $NO_2^- + NO_3^-$. NH_4^+ and SRP followed the phenol hypochlorite (Solorzano, 1969) and molybdic acid – trivalent antimony (Murphy and Riley, 1962) procedures, respectively, as outlined in Parsons et al. (1984). $NO_2^- + NO_3^-$ measurements were determined by automated colorimetry (United States Environmental Protection Agency, 1983a).

Nutrient fluxes for each core were calculated from linear regressions performed on nutrient concentrations plotted versus time ($r^2 > \sim 0.8$; $F \leq 0.10$). The difference in nutrient concentrations between water from cores and blanks was expressed relative to the surface area of the core. Calculations were performed separately for simulated dark (T_0-T_4) and light (T_4-T_8) events, and positive and negative fluxes coincided with sediment release and uptake of nutrients, respectively. Fluxes of N_2-N represented the net exchange of N_2-N at the sediment-water interface since the reactions (e.g., denitrification, annamox, N_2 fixation) mediating these fluxes cannot be discerned by membrane inlet mass spectrometry (Kana et al., 1998; Kana and Weiss, 2004).

Estimates of gross primary productivity (GPP) were calculated as 14 h * (O_2 flux measured during light incubations – O_2 flux measured during dark incubations). Net ecosystem metabolism (NEM) estimates were determined as 14 h * O_2 flux measured during light incubations + 24 h * O_2 flux measured during dark incubations. Similar estimates were calculated for gross and net phosphorus (i.e., SRP) and nitrogen (N_2, NH_4^+, $NO_2^- + NO_3^-$).

Benthic microalgal biomass. Surface sediments for chlorophyll *a* analyses were collected with a syringe mini-corer (1.4 cm I.D.) pressed ~ 1 cm into sediments. Sediments were frozen in 15 ml centrifuge tubes wrapped in aluminum foil. HPLC-grade acetone was added to thaw sediment samples, and tubes were sonicated in an ice water bath for ~ 1 h. Samples were refrozen for a minimum of 12 h and then centrifuged for 10 min at 1643 xg (3500 rpm; International Equipment Company Centra MP4 or CL2). I filtered the supernatant with 0.45 μm Titan filters into HPLC vials. Total chl *a* content of surface sediments for each core was measured by HPLC (Van Heukelem et al., 1994). Background chlorophyll *a* concentrations for La Trappe Creek sediments were determined from the six additional sediment cores collected on 31 August 2005. Sediment chlorophyll *a* analyses for eight of the incubated cores occurred upon completion of the final flux incubation (Day 19); the remaining sediments were collected the following morning.

HPLC chlorophyll *a* analyses were also conducted on subsamples (n = 17) of biodeposits, which served as the POM source for this experiment. Approximately 1 cm (~ 0.8 ml) of the barrel of the syringe mini-corer (1.4 cm I.D.) was filled with biodeposits at each addition. Storage and analyses of biodeposits for chlorophyll *a* followed that for surface sediments.

Statistical analyses. Statistical tests were conducted in SAS (Version 9.1 for Windows) using Proc Glm and Proc Mixed for ANOVA and Repeated Measures analyses, respectively. A Model III (one-way) ANOVA was used to test for differences in

measured chlorophyll *a* concentrations for surface sediments. Split-plot repeated measures, nesting cores within treatments, were used to detect differences due to treatment, time, and the treatment by time interaction, where time corresponded to the sampling day (i.e., days of loading), for O_2, N_2, NH_4^+, N, and SRP flux datasets. Main effects (treatment, time) are presented with caution where treatment*time (i.e., simple) interactions were statistically significant ($P \leq 0.05$). I used fit statistics (AIC model) to determine the appropriate covariance model for each repeated measure performed. Statistical tests relied on autoregressive, compound symmetry, Huynh-Feldt, and unstructured covariance models. Non-normally distributed data (dark O_2 fluxes, NEM) were transformed with log-base 10 transformations, and standardization of data (mean = 0, standard deviation = 1) provided homogeneity of variance. Significant differences and effects were determined for $P \leq 0.05$.

Results

Initial conditions

Dark : light nutrient flux incubations for dissolved gases (O_2, N_2), NH_4^+, and SRP were conducted for all sediment cores and blanks initially on 02 September 2005; data from initial flux incubations have been presented as Day 0 within subsequent tables and figures. Sediment cores designated to receive HL and HH treatments were incubated in the light at ~ 100 μmol photons m^{-2} s^{-1}; whereas low light cores (LL, LH) were covered with mesh, shade cloth to reduce this surface sediment irradiance 10-fold. Significant treatment*time effects were identified for O_2 ($P = 0.0005$) and N_2 ($P = 0.0069$) fluxes calculated for dark incubations, and for O_2 ($P < 0.0001$), NH_4^+ ($P = 0.0010$), and SRP in

the light ($P < 0.0001$, Table 4.2). No significant differences in O_2 and N_2 flux rates were identified initially between cores in the dark or under differential surface sediment irradiances ($P > 0.05$). Similarly, no significant differences were identified for time-changing NH_4^+ and SRP concentrations during light incubations ($P > 0.05$). Simple effects for dark NH_4^+ and SRP fluxes were not statistically significant; differences of least squares means suggests no initial difference between sediments ($P > 0.05$).

Initial incubations indicated that all sediments were net heterotrophic, with flux rates of -513 ± 249 μmol O_2 m^{-2} h^{-1} and -362 ± 144 μmol O_2 m^{-2} h^{-1} for dark and light incubations, respectively. Mean net N_2 fluxes were approximately zero but variable, and ranged from -97 to 69 μmol N_2 – N m^{-2} h^{-1}. An efflux of NH_4^+ was observed for all sediments during dark and light incubations, as expected for net heterotrophic systems, but minimal rates of SRP exchange were observed. Mean SRP flux approached ~ 2 μmol P m^{-2} h^{-1}, with a single core releasing 12 μmol P m^{-2} h^{-1}. Duplicate regressions (two-point) indicated a release of $NO_2^- + NO_3^-$ during dark and light incubations, with a 2- to 5-fold reduction in efflux in the light, regardless of surface sediment irradiance.

Benthic microalgal biomass

Surface sediment (top ~ 1 cm) chlorophyll *a* concentrations were significantly different due to treatment ($P = 0.0026$), as determined from a Model III, fixed effect ANOVA. Post hoc analysis, using Tukey-Kramer least squares means, determined that chlorophyll *a* concentrations for HH cores were significantly greater than concentrations measured initially ($n = 6$, $P = 0.0026$) and treatments receiving ~ 10 μmol photons m^{-2} s^{-1} (LL: $P = 0.0095$; LH: $P = 0.0271$). Chlorophyll *a* concentrations for HL cores were not

significantly different from HH (P = 0.3799), LL (P = 0.2992), LH (P = 0.5746) or initial sediments (P = 0.1473). Mean chlorophyll *a* concentrations for HL and HH sediments approached 200 mg chl *a* m^{-2} and 350 mg chl *a* m^{-2}, respectively (Table 4.3). Initial chlorophyll *a* concentrations for La Trappe Creek sediments were ~ 3 to 40 times lower than concentrations after cores underwent treatments for ~ 19 d. I observed mean chlorophyll *a* concentrations for equivalent volumes of biodeposits near 120 mg chl *a* m^{-2}.

Temporal variations in measured fluxes

Dissolved Oxygen. Repeated measures analyses identified a significant difference for dark and light O_2 fluxes associated with treatment*time effects (P = 0.0005; P < 0.001). Post hoc analysis, using differences of least squares means, detected no significant difference in dark O_2 fluxes between HH and LH or between HL and LL treatments after 4 d of POM loading (Figure 4.2). Community respiration (i.e., O_2 consumption) during dark incubations for high loading treatments (HH, LH) exceeded rates for low loading cores (HL, LL). O_2 consumption for all treatments increased until reaching a plateau between 13 d and 19 d of additions (Time: P < 0.001; Comparison: P = 0.2780).

Sediment O_2 exchange during light incubations began as decreased consumption of O_2 in all cores, and cores which received ~ 100 μmol photons m^{-2} s^{-1} progressed to an efflux of O_2. Sediments in cores under decreased irradiance continued to take up O_2, with stepped increases in consumption occurring after 4 and 13 d of POM loading (Time: P < 0.001). Differences in treatment with time varied (P < 0.0001), such that only HL

differed from other treatments on Day 4 and light O_2 fluxes for low and high light treatments were significantly different by Day 10.

Differences in the mechanisms influencing O_2 fluxes in the dark and light resulted in disparity of gross (GPP) and net ecosystem metabolism (NEM) within and among treatments. Significant treatment*time effects were identified for GPP ($P < 0.0001$) and NEM ($P < 0.0001$), and for main effects ($P < 0.0001$). On Day 4, mean (± S.D.) rates of GPP for HL sediments (24.4 ± 11.2 mmol O_2 m^{-2} d^{-1}) were statistically different than those for LL (6.84 ± 4.25 mmol O_2 m^{-2} d^{-1}) and LH (12.4 ± 1.64 mmol O_2 m^{-2} d^{-1}), but not HH (2.64 ± 6.97 mmol O_2 m^{-2} d^{-1}), which were not significantly different from low light treatments (Figure 4.3). After nine additional days of loading, differences of least squares means identified three separate significant groupings: (1) HH; (2) HL and LL; and (3) LH. Six days later a decline in GPP for HL sediment cores resulted in GPP rates comparable to LH ($P = 0.2187$); whereas HH and LL cores were statistically different from HL and LH and each other. Overall treatment effects identified that all four treatments were statistically different ($P < 0.0001$), and mean rates of O_2 evolution during daylight hours for all treatments was only equivalent on Day 10 and Day 13 ($P = 0.4733$).

Net ecosystem metabolism for the four treatments diverged after 4 d of POM loading, with high loading treatments (HH, LH) becoming more net heterotrophic than low loading cores (HL, LL; Figure 4.3). Repeated measures analysis, using differences of least squares means, identified a significant difference between the NEM of sediments undergoing the LH treatment on Day 10 than rates of NEM for other treatments. Net daily O_2 fluxes for HL and HH did not differ significantly on Day 10, but unlike HH ($P = 0.0978$), HL cores were significantly different than LL sediment cores ($P = 0.0158$).

Only NEM for LH sediments differed from other treatments after 13 d and 19 d of loading. No significant difference in NEM due to treatment ($P < 0.0001$) was identified for HH and LL sediments, but HL and LH treatments were significantly different from HH, LL and each other. Mean (± S.D.) rates of NEM for sediment cores receiving HL and LH treatments were the least (-8.82 ± 28.2 mmol O_2 m^{-2} d^{-1}) and most negative (-85.4 ± 19.3 mmol O_2 m^{-2} d^{-1}), respectively, upon receiving additions of POM.

Nitrogen cycling. Sediment exchanges of NH_4^+ with overlying waters during dark incubations were influenced by POM loading (Treatment: $P = 0.003$; Day: $P < 0.0001$), such that the NH_4^+ efflux from sediments receiving ~ 1.5 g C m^{-2} d^{-1} was less than that of cores receiving ~ 5 times more organic deposition (Figure 4.4). Mean (± S.D.) NH_4^+ efflux for low (HL, LL) and high loading (HH, LH) treatments during periods of POM loading were 261 ± 185 μmol NH_4^+ - N m^{-2} h^{-1} and 609 ± 165 μmol NH_4^+ - N m^{-2} h^{-1}, respectively. Maximum concentrations of NH_4^+ in overlying waters, upon sealing cores for incubations, were ~ 35 μmol N L^{-1}, except during initial incubations when concentrations were < 5 μmol N L^{-1}. Uptake of NH_4^+ by overlying waters (i.e., blanks) exceeded that of sediment cores at all times in the dark.

A significant treatment*time effect was identified for NH_4^+ fluxes calculated for light incubations ($P = 0.0010$). After 4 d of loading, LH cores released NH_4^+ into overlying waters at an hourly rate ~ 4 to 5 times greater than the initial mean (± S.D.) flux of all sediment cores (86 ± 38 μmol NH_4^+ - N m^{-2} h^{-1}); whereas NH_4^+ efflux from HL, HH, and LL sediments decreased and often resulted in an uptake of NH_4^+. No significant difference in NH_4^+ flux was identified for HH and HL after 10 d of additions

(P = 0.1009). LL and LH are significantly different from one another (P = 0.0030) and from cores receiving ~ 100 μmol photons m^{-2} s^{-1} (P ≤ 0.05). Light NH_4^+ fluxes after 13 d and 19 d of loading are not significantly different for treatments receiving low levels of POM (P = ~ 0.8). Increased NH_4^+ uptake by HH sediments and continued release of NH_4^+ by LH sediments were, however, statistically different from the mean fluxes of HL and LL. Statistical differences among treatments on Day 13 and Day 19 are consistent with the overall treatment effect (P < 0.0001).

Linear changes in concentrations were generally observed for N_2 measurements, except when O_2 saturation increased to 97% or more (n = 7). Significant differences in N_2 fluxes during dark incubations were associated with a treatment*time interaction (P = 0.0069), whereby only HL sediments differed in N_2 flux after 13 d and 19 d of POM loading. Dark N_2 fluxes increased in all treatments from an initial mean of zero to concentrations leveling off between ~ 11 and 130 μmol N_2 – N m^{-2} h^{-1} (Table 4.4). Initial dark N_2 fluxes for HL (34 ± 29 μmol N_2 – N m^{-2} h^{-1}) sediment cores, although not statistically different than other sediment cores, indicated net denitrification, in contrast to minimal denitrification (Mean: 4.4 μmol N_2 – N m^{-2} h^{-2}) or net N_2 uptake (Mean: -14 μmol N_2 – N m^{-2} h^{-2}) observed for other cores. Dark N_2 fluxes (mean ± S.D.) after 19 d of POM loading for HL, HH, LL, and LH were as follows: 12 ± 33 μmol N_2 – N m^{-2} h^{-1}; 79 ± 30 μmol N_2 – N m^{-2} h^{-1}; 67 ± 67 μmol N_2 – N m^{-2} h^{-1}; and 41 ± 12 μmol N_2 – N m^{-2} h^{-1}.

I determined a significant difference for light N_2 fluxes due to time (P = 0.003) but not due to the addition of POM (P = 0.6716). N_2 fluxes during light incubations fell within the range of those measured in the dark, with again minimal or no net

denitrification prior to POM additions. Measured rates of N_2 exchange for initial sediment conditions (Day 0) were significantly different than those calculated for all other days ($P < 0.0005$).

The limited dataset available for $NO_2^- + NO_3^-$ concentrations indicated that sediment cores were initially releasing $NO_2^- + NO_3^-$ from the sediment in the dark at rates between ~ 60 and 120 μmol N m^{-2} h^{-1}. By the fourth day of POM additions, sediments were consuming as much $NO_2^- + NO_3^-$ as initially released, and after 19 d of loading, rates of $NO_2^- + NO_3^-$ consumption were approximately the same or greater than corresponding rates of net denitrification. Light $NO_2^- + NO_3^-$ fluxes followed the same pattern as mentioned for dark fluxes, with approximately half as much $NO_2^- + NO_3^-$ initially fluxing out of and then into sediments. Initial water column concentrations of $NO_2^- + NO_3^-$ (3.5 ± 1.0 μmol N L^{-1}) were two to three times less than those measured throughout the laboratory experiment (10.0 ± 1.9 μmol N L^{-1}).

Phosphorus cycling. Repeated measures analysis determined a significant difference for dark and light SRP fluxes due to treatment ($P < 0.0001$) and treatment*time effects ($P < 0.0001$), respectively. After 4 d of POM loading, mean (± S.D.) SRP fluxes for HH and LH and HL and LL in the dark were 136 ± 40 μmol P m^{-2} h^{-1} and 9.3 ± 5.5 μmol P m^{-2} h^{-1} (Figure 4.5). Sediments receiving ~ 7.5 g C m^{-2} d^{-1} continually released SRP to overlying waters throughout the course of the experiment. Dark uptake of SRP occurred in HL and LL cores after a total of 28 g C m^{-2} had been added to surface sediments. SRP fluxes during light incubations were initially controlled by loading (Day 4), with no significance difference identified among POM treatments (L: $P = 0.8607$; H: $P = 0.0545$). After the

tenth POM addition, sediment uptake of SRP occurred within HH cores during light incubations; mean (± S.D.) uptake rates of SRP were ~ 40 μmol P m^{-2} h^{-1}. Minimal uptake and continued release of SRP was observed for low loading and LH cores, respectively.

Discussion

Sediment metabolism and benthic photosynthesis

Sediment exchange of dissolved O_2 with overlying waters during dark incubations was dictated by the level of POM loading. All treatments responded to organic matter deposition by increasing sediment O_2 consumption, with rates leveling off between the tenth and nineteenth day of additions (Figure 4.2). Similar rates of O_2 consumption for HH and LH treatments after 13 d of POM loading may have been an artifact of the length of sediment core incubations, as water column oxygen concentrations often approached or decreased below ~ 78 μmol O_2 L^{-1} (Cowan and Boynton, 1996). Sediments receiving high levels of POM loading (HH, LH) consumed one-third to two times more dissolved O_2 in the dark than corresponding low loading treatments (HL, LL), and were comparable to dark O_2 fluxes measured in August for other silt-clay sediments in Chesapeake Bay (Reay et al., 1995). Rates of sediment O_2 consumption for HL and LL treatments were more within the range of those for lower Chesapeake Bay (- 2,514 ± 489 μmol O_2 m^{-2} h^{-1}; Reay et al., 1995), the Neuse River (Fear et al., 2005), and sub-tropical, organic sediments (Ferguson et al., 2003) in autumn and spring. Initial sediment metabolism did not exceed ~ 1,000 μmol O_2 m^{-2} h^{-1}. High rates of organic deposition for all sediments receiving treatments resulted in dark O_2 fluxes comparable to high depositional

environments, like the mid-Bay sediments of Chesapeake Bay (Boynton and Kemp, 1985; Cowan and Boynton, 1996).

Dissolved O_2 fluxes measured during light incubations and estimates of gross primary production (GPP) support the notion that photoautotrophic growth within BMA may be limited separately or simultaneously by availability of inorganic nutrients (Graneli and Sundback, 1985; Nilsson et al., 1991; Sundback et al., 2000; Welker et al., 2002) and/or surface sediment irradiance. After just 4 d of elevated surface sediment irradiance (~ 100 mmol photons m^{-2} s^{-1}), photosynthetic O_2 production in sediments receiving the HL treatment surpassed hourly rates of sediment O_2 consumption and evolved O_2 (Figure 4.3). Similar patterns in light O_2 fluxes occurred for HH cores once photosynthetic O_2 production overcame greater rates of heterotrophic metabolism (Day 10), and with time, all high light sediments fluxed dissolved O_2 at rates comparable to some marine sands (Ferguson et al., 2003). Delayed responses in O_2 evolution for HH may have been associated with disparities in increasing rates of heterotrophic metabolism and gross photosynthesis with temperature (Hancke and Glud, 2004). Although hourly rates of photosynthetic O_2 production for LL and LH cores did not follow those for sediments receiving greater surface sediment irradiance, all treatments evolved O_2 during the 14 h photoperiod (GPP).

Estimates of GPP suggest that photosynthetic O_2 production within BMA is primarily influenced by the intensity of surface sediment irradiance and, secondarily, by organic matter deposition. Sediments receiving ambient irradiance (~ 10 μmol photons m^{-2} s^{-1}) produced two to five times less O_2 during the photoperiod than those which received a 10-fold increase in surface sediment irradiance. Additional disparities in GPP

occurred with time, such that benthic O_2 production in HH and LH cores surpassed HL and LL cores, respectively, after 19 d of treatment. I suggest that the delayed response in high loading treatments resulted from bacterial remineralization of the added POM and subsequent regeneration of dissolved inorganic nutrients into surrounding pore waters and the overlying water column. Increased concentrations of and accessibility to these dissolved nutrients promoted enhanced O_2 production by benthic photoautotrophs. Competition between autotrophic and heterotrophic species was likely reduced since an inexhaustible supply of labile carbon was made available through daily POM additions.

Similar stepwise increases in benthic microalgal biomass were not significant between all treatments; however, statistical similarities in biomass for HH and HL treatments, as well as the overlap between HL and sediments receiving ambient irradiance (LL, LH), further supported the sequential importance of light intensity and nutrients on benthic photosynthesis. Lack of statistical significance for all treatments was likely associated with the inherent spatial variability that may exist within these communities and not the addition of chlorophyll *a* incorporated in POM loadings. Concentrations of chlorophyll *a* in single aliquots (0.8 ml) of POM were as much as 25 times greater than initial chlorophyll *a* concentrations in sediments, and therefore, would have increased final concentrations in treated cores between ~ 10- and 150-fold more than measured values. Aerobic degradation of chlorophyll *a* generally occurs within a week to 10 d (Sun et al., 1993). Although it is unclear to me how gamma irradiation (of biodeposits) may have affected chlorophyll *a* degradation, faster rates may have been encouraged by breaking of chemical bonds and the subsequent availability of smaller, more easily metabolized compounds.

Greater chlorophyll-normalized estimates of gross photosynthesis were observed for low light cores compared to high light treatments (determined from Figure 4.3 and Table 4.3), suggesting fine-grained sediments may reach a maximum capacity for benthic microalgal biomass. As biomass increased in HL and HH cores, accumulated microalgae and sedimentary characteristics (e.g., granulometry, organic content) may have restricted light availability to photoautotrophic species positioned at greater depths. Surface (0-1 cm) sediment concentrations of chlorophyll *a* in the field (La Trappe Creek) have never approached these values, as resuspension and grazing are more likely to occur (Chapter 2, 5.1-70.0 mg chl *a* m^{-2}).

Net ecosystem metabolism and the trophic classification of sediments

The trophic state of shallow, illuminated sediments has been used to classify the relative importance of these sediments on nutrient fluxes at the sediment-water interface. The three most commonly used measures of trophic status are: ratios of gross primary productivity to respiration (P/R; Odum and Hoskin, 1958); net ecosystem metabolism (NEM); and the benthic trophic state index (BTSI; Rizzo et al., 1996). All three methodologies have limitations when applied to the sediment core incubations presented here, and therefore, a combination of all three will be offered to assist in understanding the transition of sediments with varying levels of organic deposition and benthic O_2 production. The ability of P/R ratios, NEM, and the BTSI to provide accurate reflections of the transitory trophic states within treatments may be limited by the extrapolation of short-term, dissolved O_2 fluxes (Odum and Wilson, 1962; Rizzo and Wetzel, 1986) and the 14 h photoperiod, where surface sediment irradiances < 300 μmol photons m^{-2} s^{-1}

were maintained (Rizzo et al., 1996). Estimates of respiration for P/R were calculated by extrapolating dark O_2 fluxes over 24 h; sediments with ratios ≥ 1.4 (14 h light : 10 h dark), rather than ≥ 1 (12 h light : 12 h dark), were identified as being dominated by autotrophic processes. Hourly rates of net community production and community respiration for the BTSI were defined as light and dark O_2 flux, respectively (Risgaard-Petersen, 2003), and positive and negative estimates of NEM correspond directly to net autotrophy and net heterotrophy.

Initial fluxes of dissolved O_2 indicated that all sediments, except a single LL core (P/R = 2.67), were originally dominated by heterotrophic processes (Table 4.5). Sediments ranged from fully to net heterotrophic (BTSI: 0-1), with estimated rates (net) of O_2 consumption between -7.0 mmol O_2 m^{-2} d^{-1} and -27.5 mmol O_2 m^{-2} d^{-1}. After just 4 d of POM additions, HH and LH sediments had already progressed to a greater degree of net heterotrophy (NEM: -57.1 ± 27.5 mmol O_2 m^{-2} d^{-1}), and consumed as much O_2 on a daily basis as other mid-Atlantic shallow estuaries with surface sediment irradiances < 100 μmol photons m^{-2} s^{-1} (Cerco and Seitzinger, 1997). NEM in low loading treatments exhibited either less of an increase in the degree of heterotrophy (LL) or greater variability in the magnitude and/or direction of net production (HL). BTSI determined an increase in autotrophic processes for high light treatments, with indices ranging from net heterotrophic (BTSI: 1) to highly autotrophic (BTSI: 3) for HL and from net heterotrophic to net autotrophic (BTSI: 2) for HH sediments. P/R ratios and NEM only identified one HL replicate as net autotrophic.

Six days later (Day 10), benthic O_2 production within two additional HL and two HH cores exceeded daily sediment O_2 consumption (NEM, P/R). Calculated means of

NEM for high light treatments identified the transition of HL sediments from a net heterotrophic to a more autotrophic state but not the transition of HH cores. Increases in the autotrophic nature of high light treatments were identified by the BTSI; whereby HL and HH replicates no longer illustrated net autotrophy or heterotrophy, respectively.

On the 13th and 19th day of treatments, estimates of NEM and P/R ratios suggested that all sediments were once again dominated by heterotrophic processes. Only a single HL replicate displayed net autotrophic tendencies (P/R = 2.27) on Day 13, but other high light sediments still possessed P/R ratios ≥ 1. BTSI indices suggested a slower transition for the net to highly autotrophic high light treatments, such that HH and HL sediments did not become solely net autotrophic or vary between these two states, respectively, until Day 19. All treatments, according to NEM, resulted in net heterotrophic O_2 consumption after 19 d, and rates often exceeded daily metabolism for other shallow water systems (Sundback et al., 1991; Sundback and Miles, 2000; Sundback et al., 2000; Tyler and McGlathery, 2003). Elevated biological and abiological respiratory demands by sediments and BMA and decreased gross photosynthesis with increasing benthic microalgal biomass may likely be responsible for discrepancies in rates. Sediments may have responded differently if temperatures or POM loads were lower, as has been seen for subtidal communities in cooler months (Schreiber and Pennock, 1995).

Influence of sediment metabolism and benthic photosynthesis on nutrient cycling

Nitrogen cycling. Fluxes of nitrogen at the sediment-water interface were predominately influenced by sediment exchanges of NH_4^+ with overlying waters (Figure 4.4, Table 4.4).

Sediments from all treatments released NH_4^+ into the water column during dark incubations, with stepped increases in NH_4^+ effluxes after 4 d and 13 d of POM additions. Dark effluxes of NH_4^+ from high loading treatments exceeded those with lower organic deposition, but factored differences (2.7 ± 1.2) were less than the five-fold increase in total nitrogen added (1,467 mmol TN m^{-2}; Table 5.1). HL sediments released NH_4^+ in the dark on Day 13 at rates (528 ± 230 μmol N m^{-2} h^{-1}) comparable to those if all the added nitrogen was remineralized by heterotrophic metabolism (~ 643 μmol TN m^{-2} h^{-1}; determined from data in Table 5.1); measured NH_4^+ effluxes for all other days and LL sediments were below this threshold. All treatments released NH_4^+ in the dark at greater rates than those measured for sediments with similar sediment O_2 consumption (Reay et al., 1995).

In the light, fluxes of NH_4^+ reversed directions for sediments receiving ~ 100 μmol photons m^{-2} s^{-1} after 4 d of treatment, and similar directional shifts in NH_4^+ were observed after 13 d in LL sediments. Fluxes from LH sediments, although still directed toward the water column, were reduced. Although sediment uptake of NH_4^+ in the light did not balance net effluxes of nitrogen, all treated sediments acted like a sink to nitrogen during the 14 h photoperiod, consuming nitrogen in proportion to benthic O_2 production (i.e., gross; Figure 4.6). Uptake of NH_4^+ in all treatments corresponded to an increase in surface (0-1 cm) sediment chlorophyll *a* after 19 d, with the greatest rates of NH_4^+ uptake in HH treatments paralleling maximum increases in benthic microalgal biomass.

N_2-N exchange at the sediment-water interface was regulated by water column concentrations of $NO_2^- + NO_3^-$ (Table 4.4), as has been observed in other systems with persistently high (Risgaard-Petersen et al., 2005) or seasonally elevated concentrations of

NO_2^- + NO_3^- in overlying waters (Owens and Cornwell, *unpublished data*). Initially, sediment cores exhibited minimal rates of N_2-N exchange, with most cores fluctuating near zero, and an efflux of NO_2^- + NO_3^- during dark and light incubations. Once NO_2^- + NO_3^- concentrations doubled in overlying waters, sediment uptake of NO_2^- + NO_3^- commenced, and net denitrification occurred at similar rates in all cores. Similarity of dark and light N_2-N fluxes indicated that O_2 penetration from benthic photosynthesis did not limit the availability of NO_3^- to denitrifying bacteria in most cores. Reduced rates of net denitrification from HL sediments occurred during dark incubations and, therefore, were more likely a consequence of variability in measurements than an enlarged aerobic zone. No significant difference in rates of net denitrification during light incubations were determined for HL sediments when the distance water column NO_3^- would have to diffuse would be the greatest (Revsbech et al., 1988; Rysgaard et al., 1995). Decreased uptake of NO_2^- + NO_3^- during light incubations further suggested that denitrifying bacteria and not benthic photoautotrophs were taking up NO_2^- + NO_3^- (Bartoli et al., 2003).

Although a limited dataset was available to evaluate sediment exchanges of NO_2^- + NO_3^- within treatments, fluxes of NO_2^- + NO_3^- offered some insights into the potential variability in the mechanisms influencing net denitrification in treatments. NO_2^- + NO_3^- fluxes in LH cores suggest that nitrogen transformations and reactions occurring in these more reduced sediments (Chapter 5) might differ from other treatments. After 13 d and 19 d of treatment, sediment uptake of NO_2^- + NO_3^- in LH cores exceeded rates of net denitrification. Additional NO_2^- + NO_3^- consumed by sediments might have undergone dissimilatory NO_3^- reduction to NH_4^+ or been used to oxidize Fe^{2+} to Fe^{3+} (abiotic),

thereby, serving as an additional source for effluxes of NH_4^+ at the sediment-water interface. Discrepancies in sediment uptake of $NO_2^- + NO_3^-$ and net denitrification during light incubations for high light and LL treatments were likely associated with greater uptake rates in the dark or the enhancement of coupled nitrification-denitrification. Stimulation of coupled nitrification-denitrification rather than exclusion of nitrification likely occurred in these shallow, temperate sediments since high NH_4^+ concentrations persisted (Risgaard-Petersen et al., 1994; An and Joye, 2001; Dalsgaard, 2003).

A proportion of the nitrogen contained within added POM that was not exchanged at the sediment-water interface was likely assimilated to support increases in benthic microalgal and bacterial biomass or remained stored in sediments. Surface (0-1 cm) sediments from HL, HH, LL, and LH treatments incorporated ~ 49%, 89%, 91% and 69% of the total nitrogen added with POM additions (Table 5.1). Conversions of total nitrogen to chlorophyll *a* (1 mg chl *a* m^{-2} = 1 mmol N m^{-2}; Gowen et al., 1992) suggested that the remaining fractions not stored in sediments could have supported the observed increases in benthic microalgal biomass. Although observed increases in benthic microalgal biomass were analogous to estimated increases from non-stored nitrogen for HL (~ 150 mg chl a m^{-2}), HH (~ 163 mg chl a m^{-2}), and LL (27 mg chl a m^{-2}) treatments, measured effluxes of NH_4^+ suggest that other nitrogen sources (i.e., water column, pore water) may have also played a role.

Assimilatory uptake and subsequent increases in benthic microalgal biomass were not sufficient to account for the fraction of total added nitrogen not stored within the surface of LH sediments. The remaining ~ 380 mmol N m^{-2} would have required a net efflux of ~ 20 mmol N m^{-2} d^{-1}, and roughly 14.9 mmol N m^{-2} were released from these

sediments daily (net). A proportion of this nitrogen may have been incorporated in intermediary biomass of microalgae, as mat thickness visually resembled HH treatments after ~ 1 week and then declined rapidly with the appearance of white filamentous bacteria on surface sediments (Figure 4.7). Additional fractions may have been lost through sediment exchange of dissolved organic nitrogen or assimilated to support growth of heterotrophic bacteria (e.g., sulfur bacteria, dissimilatory NO_3^- reducers).

Phosphorus cycling. All treatments responded to organic matter deposition with an initial increase in dark effluxes of SRP (Figure 4.5). Maximal rates of SRP exchange from HL and LL sediments to overlying waters occurred after 10 d of POM additions, whereas effluxes of SRP from high loading sediments remained constant between the 4th and 19th addition. SRP fluxes from HH and LH sediments exceeded those of corresponding low loading treatments by as much and as little as 2,600% and 150%, respectively. Rates of sediment SRP release from high loading treatments were comparable to those necessary to account for the added phosphorus not stored in sediments (~ 180 μmol P m^{-2} h^{-1}; determined from data in Table 5.1) and, thereby, suggested the potential for non-refractory phosphorus contained within added POM to influence SRP exchange (Ingall and Jahnke, 1997). Minimal fluxes (i.e., near zero) and dark uptake of SRP in HL and LL sediments corresponded with an observed increase in sedimentary storage of phosphorus, whereby these sediments incorporated all the phosphorus added from POM additions (23 mmol P m^{-2}) and some from additional sources (~ 8-37 mmol P m^{-2}; Table 5.1). Bursts in community respiration and associated nutrient regeneration may have been responsible for the initial inability of low loading

sediments to bind phosphorus (Rizzo, 1990). Initial and continual releases of SRP from low and high loading sediments, respectively, may have also been dictated by the extent and duration of Fe-S mineral formation and associated release of phosphorus from Fe oxy(hydr)oxides (Rozan et al., 2002).

SRP fluxes during light incubations were initially (Day 4) separated according to levels of POM loading, with HH and LH sediments releasing SRP to overlying waters at equivalent rates (136 ± 40 μmol P m^{-2} h^{-1}). Sediment uptake of SRP commenced in HH cores after 10 d of treatment, and coincided with sharp increases in benthic O_2 production (i.e., light O_2 fluxes, GPP). Gross sediment uptake of SRP for HH sediments was not proportional to benthic O_2 production (i.e., gross; Figure 4.6). Removal of excess SRP in HH sediments was likely associated with the adsorption of PO_4^{3-} onto Fe and Mn oxides and potentially the formation of phosphorus minerals if pore water concentrations were high (Slomp et al., 1996). Reoxidation of reduced Fe and Mn species could account for discrepancies in gross SRP fluxes and, thereby, suggest that GPP may poorly represent benthic O_2 production when sediments have elevated rates of chemical oxygen demand.

Minimal decreases in SRP effluxes were observed for LH sediments between the 10^{th} and 19^{th} additions (Figure 4.5), as sediments sustained similar rates of gross photosynthesis (Figures 4.3). Gross estimates of SRP flux for LH sediments were typically comparable to rates predicted from GPP (Figure 4.6). SRP fluxes in the light for HL and LL sediments were consistently near zero, maintaining minimal exchange with overlying waters and retaining incorporated phosphorus within sediments. Lower rates of heterotrophic metabolism (i.e., O_2 flux) for HL and LL sediments likely corresponded to lower rates of Fe/Mn oxy(hydr)oxides reduction and subsequently the

availability of more adsorption sites and an increased barrier to diffusive SRP flux (Rozan et al., 2002). Analytical uncertainties for nominal fluxes (< 5 μmol P m^{-2} h^{-1}) may have contributed to discrepancies and scatter among gross estimates of SRP flux for HL cores.

Transitions in nitrogen and phosphorus exchange: Disconnect with trophic status

All sediments exhibited transitions in sediment O_2 consumption and benthic photosynthesis and, thereby, experienced fluctuations in sediment release and uptake of nitrogen and phosphorus (Table 4.6). Shifts in these biogeochemical processes occurred within 4 d of the onset of treatment and fluctuated (HH), often rebounding to near initial conditions (HL, LL), or progressed to a greater degree of nutrient release (LH) within the 19 d experiment. Transitions in nitrogen and phosphorus exchange at the sediment-water interface were observed as changes in the speciation, direction, and magnitude of flux, as well as the ratio of nitrogen to phosphorus release or uptake. Fluctuations in nitrogen and phosphorus exchange were likely associated with the perturbation of surface sediments through daily additions of *C. virginica* biodeposits, and introductions of organic and inorganic particulates of carbon, nitrogen, phosphorus, and iron and manganese oxy(hydr)oxides (Chapter 5) likely prevented the establishment of steady-state conditions. Absence of a new equilibrium, however, does not lessen the importance of the observed variation in nutrient fluxes, as pulsed additions to sediment cores are consistent with continued deposition of POM by cultured bivalves.

The trophic status of sediments, whether static or transient, typically was not a good indication of the capacity of sediments to serve as a net sink or source of nutrients;

nor did these classifications provide any insight into the relative exchange of nitrogen and phosphorus (i.e., N:P ratios) at the sediment-water interface. P/R ratios, NEM, and the BTSI each identified shifts in the trophic status of sediments receiving high surface sediment irradiance (~ 100 μmol photons m^{-2} s^{-1}) and consistently categorized LL and LH sediments as being dominated by heterotrophic processes. Discrepancies among classification schemes were immaterial, as none accurately classified all treatments with regard to net exchange of nitrogen and phosphorus. Only the classification of initial sediments (Day 0) and LH sediments continually as net heterotrophic coincided with measured, net exchanges of nutrients. Ineffectiveness of trophic states as a means for predicting variation in nitrogen and phosphorus exchange was likely associated with the absence of steady-state conditions and the relative role of iron and manganese oxy(hydr)oxides in phosphorus exchange.

All sediments, regardless of trophic status, had a net release of nitrogen (mostly as NH_4^+) to overlying waters; whereas consistent net effluxes of phosphorus were only observed in high loading treatments. Minimal phosphorus effluxes for HL and LL sediments transitioned into net uptakes after ~ 2 weeks, and the greatest, measured releases of phosphorus for high light treatments coincided with when these sediments were classified as the most autotrophic (Day 10). Net sediment fluxes of nitrogen (NH_4^+ + N_2-N) and phosphorus (SRP) measured from sediment core incubations often exceeded fluxes predicted from stoichiometric conversions of NEM (138 O_2 : 16 N : 1 P; Figure 4.6). Measured exchanges of net nitrogen generally did not exceed stoichiometric predictions by more than ~ 300%. Inclusion of the net uptake of NO_2^- + NO_3^- (Mean: -2,700 μmol N m^{-2} d^{-1}) suggested that effluxes of nitrogen from HL, HH and LL

sediments likely resembled predicted fluxes more closely; however, reductions in net exchanges through inclusion of NO_2^- + NO_3^- did not result in the net uptake of nitrogen for any treatment. Similarity in net fluxes of nitrogen for HL, HH and LL sediments was not surprising, as estimates of NEM were not statistically different after 10 d of treatment. Greater effluxes of nitrogen for LH sediments corresponded with estimates of NEM approximately twice as great as those for other treatments. Nitrogen availability from high rates of POM deposition may have exceeded the demand of BMA and, therefore, constituted the net release of nitrogen even during transient autotrophic states.

Greater variability and divergence between measured and predicted rates were observed for net sediment phosphorus than for net nitrogen exchange. Measured rates for HL and LL treatments generally coincided with stoichiometric predictions from NEM; whereas net sediment effluxes of phosphorus from high loading sediments always exceeded predicted fluxes once treatment began. Maximum deviations between measured and predicted fluxes occurred after 4 d and 10 d of POM loading for high and low loading treatments, respectively, when dark O_2 fluxes approached ~ 1,800 μmol O_2 m^{-2} h^{-1}. Unlike rates of sediment O_2 consumption, trophic states and quantitative estimates of NEM (HL: ~ 13 mmol O_2 m^{-2} d^{-1}; LL, HH, LH: < -50 mmol O_2 m^{-2} d^{-1}) were not similar among treatments. This indicated that the extent of sediment respiratory demands and subsequent reducing conditions were more of a driving force for net phosphorus fluxes than measured imbalances in O_2 consumption and production. Enhanced effluxes of phosphorus relative to nitrogen (~ 5 N : 1 P) for all treatments further suggested that the reduction of Fe/Mn oxy(hydr)oxides was more crucial in determining net phosphorus fluxes than aerobic remineralization of POM (Chapter 5).

Decreases in the divergence of measurements with time likely occurred as benthic O_2 production increased and sediments were capable of oxidizing a proportion of reduced species (e.g., Fe^{2+}, Mn^{2+}, FeS; Chapter 5). Additional reductions in net phosphorus release for HH and LH treatments may have resulted as the available phosphorus became limiting within sediments; a proportion of continued effluxes was likely supported from continual POM additions.

Daily fluctuations in net sediment fluxes led to shifts in the relative exchange of nitrogen and phosphorus at the sediment-water interface. All sediments released a greater amount of nitrogen than phosphorus to overlying waters, but ratios of N:P varied with time in each treatment. Low loading treatments typically released nitrogen and phosphorus in proportions greatly exceeding the expected Redfield ratio (21-680:1), with increased phosphorus fluxes only reducing N:P ratios for HL and LL (17:1, 7:1) after 10 d of treatment. Variability in N:P ratios for low loading treatments stemmed from the minimal release and then net uptake of phosphorus after 13 d. Ratios of N:P for HH and LH sediments typically fell within the range of 3:1 and 6:1 until transitioning to greater ratios with the stabilization of sediment O_2 consumption (Day 10). As less Fe/Mn oxy(hydr)oxides were available to release phosphorus, remineralization of POM became a more important source for determining phosphorus exchange (~ 10:1). Resolution of N:P ratios was limited to the use of means (± standard deviation) presented in Fig. 4.4-4.5 and Table 4.4, as linear regressions of N, NH_4^+, SRP, N:P, and NH_4^+ : P versus time identified no significant trends and only 11-16% of incubations consisted of significant N, NH_4^+, and P fluxes (all) for the determination of N:P or NH_4^+ : P.

Conclusions

This study illustrated that the use of trophic states as a management tool for defining shallow, illuminated sediments as net sinks or sources of nutrients may be insufficient for fine-grained sediments receiving high rates of organic deposition. The trophic status of sediments, whether determined by P/R ratios, NEM, or the BTSI, may inaccurately describe nutrient exchange at the sediment-water interface for two reasons: (1) it assumes that the direction of net sediment nitrogen and phosphorus fluxes are the same; and (2) that autotrophic sediments have the capacity to continually incorporate added nutrients. This laboratory experiment demonstrated that for sediments with sufficient Fe/Mn oxy(hydr)oxides neither may be accurate, and as such, classification of sediments as net sinks or sources of nutrients should be reserved for those less influenced by oxidation-reduction processes. Since repetition of analyses presented here are costly in time and funding, further studies should be conducted to verify observed discrepancies in nature and for the development of additional indices.

Fluxes of nitrogen and phosphorus did not respond the same to shifts in heterotrophic metabolism and/or benthic photosynthesis. Sediment exchange of nitrogen was driven largely by the remineralization of POM and assimilatory uptake of NH_4^+ and NO_3^- by benthic microalgae and, to a lesser degree, by nitrifying and denitrifying bacteria. Net fluxes of nitrogen were comparable for sediments with similar rates of NEM, which suggests that the trophic status of sediments may accurately represent the direction of nitrogen exchange provided the supply of nitrogen from POM does not exceed the demand of BMA. Shifts in net phosphorus exchange, however, were not a result of imbalances in heterotrophic metabolism and benthic photosynthesis. Rather,

anaerobic remineralization, including sediment O_2 demands, and presence of Fe/Mn oxy(hydr)oxides were most crucial to determining effluxes and retention of added phosphorus. Mechanistic differences in nitrogen and phosphorus cycling were observed as temporal variations in the direction and ratio of fluxes.

Acknowledgements

Financial support was provided by the Maryland Sea Grant Program, as part of a study quantifying the water quality value of benthic microalgae in shallow water sediments, and through the Dr. Nancy Foster Scholarship Program (Award No. NA04NOS4290250). I thank V. Adams and the Radiation Facility at the University of Maryland College Park for irradiating my samples of biodeposits, and D. Kimmel for advice on statistics. I would also like to thank E. Kiss, J. O'Keefe, and S. Rhoades for their assistance in the laboratory with nutrient flux incubations and experimental maintenance, and T. Kana for the use of his membrane-inlet mass spectrometer for dissolved gas analyses. I thank L. Lane, C. Thomas, and L. Van Heukelem for analyzing subsamples of eastern oyster (*Crassostrea virginica*) biodeposits for carbon and nitrogen content and surface sediments for chlorophyll *a*. I also thank J. Seabrease for construction of aluminum incubation tanks and magnetic turntables, D. Meritt and C. Rounsaville for assistance with collection of *C. virginica* biodeposits, and E. Markin and A. Lazur for the use of their Teklight light bank. I would finally like to thank M. Owens and J. Cornwell for their insight into experimental manipulations, incubation techniques, and data interpretation.

Table 4.1 Physical and chemical properties of the location of sediment core collection within the main-stem of La Trappe Creek (38° 39.223' N, 076° 05.267' W), a tributary of the Choptank River sub-estuary (Chesapeake Bay, USA), on 31 August 2005 between approximately 12 pm and 3 pm. Data is provided for subsurface and sediment surface (~ 1.6 m) conditions where available.

Property (units)	Initial conditions
Temperature (°C)	28.1 – 28.3
Salinity	10.6 – 10.7
NH_4^+ (μmol N L^{-1})	0.35
Soluble reactive phosphorus (μmol P L^{-1})	0.10
Sulfate (mmol SO_4^{2-} L^{-1})	7.6
Depth of water column (m)	1.3 – 1.7
Irradiance (μmol photons m^{-2} s^{-1})	
Subsurface	978
At a water depth of 1.61 m	10
Light attenuation coefficient (k_d)	2.85

Table 4.2 Summary statistics for nutrient (O_2, N_2, NH_4^+, SRP) flux incubations and sediment (0-1 cm) chlorophyll *a*. Statistical tests were conducted in SAS (Version 9.1 for Windows) using Proc Glm and Proc Mixed for ANOVA (chlorophyll *a*) and Repeated Measures (O_2, N_2, NH_4^+, SRP) analyses, respectively. Probabilities of significant differences from post-hoc analyses, using difference of least squares means, were converted to lower-case letters and presented for significant main (i.e., treatment, day) and simple (i.e., treatment*day) effects ($P \leq 0.05$). Classifications with the same letter were not significantly different from one another ($P \geq 0.05$), and question marks identify where differences were unable to be determined. Main effects should be considered with caution when simple effects are statistically significant (i.e., presented).

Nutrient	Treatment	Day	Treatment*Day
O_2 dark	a b a c HH HL LH LL	a b c d d 0 4 10 13 19	(Day 0) a a a a HH HL LH LL (Day 4-19) a b a b HH HL LH LL
O_2 light	a a b b HH HL LH LL	a a b b c 0 4 10 13 19	(Day 0) a a a a HH HL LH LL (Day 4) b b a a a HH HL LH LL

(Day 10-19)
a a b b
HH HL LH LL

GPP

a b c d
HH HL LH LL

a b c c d
0 4 10 13 19

(Day 0)
b b b
a a a
HH HL LH LL

(Day 4)
b b
a a a
HH HL LH LL

(Day 10)
c c
a a b b
HH HL LH LL

(Day 13)
a b c b
HH HL LH LL

(Day 19)
a b b c
HH HL LH LL

NEM

a b c a
HH HL LH LL

c c
a b b d
0 4 10 13 19

(Day 0)
a a a a
HH HL LH LL

(Day 4)
a b a b
HH HL LH LL

(Day 10)
c d
a a b a
HH HL LH LL

(Day 13-19)
a a b a
HH HL LH LL

N_2 dark

c c
a b b b b
0 4 10 13 19

(Day 0-10)
a a a a
HH HL LH LL

(Day 13-19)
a b a a
HH HL LH LL

N_2 light

a b b b b
0 4 10 13 19

NH_4^+ dark

a b a b
HH HL LH LL

a b b c b
0 4 10 13 19

NH_4^+ light

a b c b
HH HL LH LL

c c
a a b b a
0 4 10 13 19

(Day 0)
a a a a
HH HL LH LL

(Day 4)
a a b a
HH HL LH LL

(Day 10)
a a b c
HH HL LH LL

(Day 13-19)
a b c b
HH HL LH LL

SRP dark

? a b a
HH HL LH LL

SRP light

? ? a b
HH HL LH LL

d d
a b c a ?
0 4 10 13 19

(Day 0)
a a a a
HH HL LH LL

(Day 4)
a b a b
HH HL LH LL

(Day 10)
a b c b
HH HL LH LL

(Day 13)
c c
a a b
HH HL LH LL

(Day 19)
? ? a b
HH HL LH LL

Chl *a*

b b b b
a a
HH HL LH LL I

Table 4.3 Sediment chlorophyll *a* (mg chl a m^{-2}), as a proxy for benthic microalgal biomass, for the initial state of La Trappe Creek sediments (Initial, n = 6) and four treatments (n = 4) developed from two surface sediment irradiances (L: ~ 10 μmol photons m^{-2} s^{-1}, H: ~ 100 μmol photons m^{-2} s^{-1}) and two biodepositional loadings (L: ~ 1.5 g C m^{-2} d^{-1}, H: ~ 7.5 g C m^{-2} d^{-1}). Treatment identifications correspond to the light and then loading level. HL: high light, low loading. HH: high light, high loading. LL: low light, low loading. LH: low light, high loading. Surface sediments (~ 1 cm) for sediment chlorophyll *a* analyses were collected with a syringe mini-corer (1.4 cm I.D.), frozen in aluminum foil wrapped centrifuge tubes, and later analyzed via high performance liquid chromatography.

Treatment	Mean	Standard deviation
Initial	8.1	3.1
HL	199.7	99.3
HH	357.6	266.5
LL	27.4	17.0
LH	71.4	38.2
Biodeposits*	121.0	20.1

[*] Although biodeposits were added to sediment cores daily on a per volume basis, subsamples (n = 17) of biodeposits for sediment chlorophyll *a* analyses were collected by filling approximately 1 cm of the barrel of the plastic syringe (1.4 cm ID).

Table 4.4 Sediment exchange of N_2 and $NO_3^- + NO_2^-$ (μmol N m^{-2} h^{-1}) from HL, HH, LL, and LH sediment cores initially (Day 0) and after 4, 10, 13, and 19 days of treatment. Fluxes of $NO_3^- + NO_2^-$ were estimated for one randomly selected sediment core per treatment, using two-point linear regressions for dark (T0, T4) and light incubations (T4, T8). N_2 fluxes were calculated from linear regressions of all available time points (T0-T8). Standard deviations for mean N_2 fluxes are within parentheses.

	N_2 flux			
	HL	HH	LL	LH
Day 0				
Dark	33.9 (29.9)	-15.3 (17.5)	4.4 (46.2)	-13.3 (68.8)
Light‡	3.8 (37.6)	1.6 (25.3)	-14.7 (10.0)	7.8 (62.5)
Day 4				
Dark	38.4 (25.5)	89.7 (40.6)	85.5 (33.7)	90.2 (25.6)
Light	39.5 (28.9)	75.4 (38.2)	73.6 (40.4)	58.5 (41.8)
Day 10				
Dark	95.8 (33.1)	61.5 (32.9)	72.6 (27.2)	89.8 (28.2)
Light	58.7 (57.9)	57.2 (62.7)	68.5 (15.5)	99.6 (39.5)
Day 13				
Dark	11.9 (59.3)‡	68.8 (37.5)	94.9 (38.2)	129.6 (23.3)
Light	36.4 (31.2)	106.8 (98.9)	72.0 (49.2)	68.2 (22.8)
Day 19				
Dark	12.2 (32.9) ‡	79.2 (29.7)	66.7 (67.3)	40.6 (12.3)

Light	66.6 (27.0)	66.0 (31.2)	49.8 (40.1)	68.2 (66.7)

	$NO_3^- + NO_2^-$ flux			
	HL	HH	LL	LH
Day 0				
Dark	80.0	68.0	58.7	116.8
Light	37.7	11.7	19.3	24.7
Day 4				
Dark	- 57.3	- 74.7	- 70.1	- 95.5
Light	- 19.9	-108.3	- 46.4	- 91.5
Day 10				
Dark	- 37.1	- 95.8	6.27	- 61.9
Light	- 79.0	- 61.8	- 17.6	- 82.9
Day 13				
Dark	- 58.5	-110.5	- 32.3	-114.6
Light	-136.1	- 13.4	- 89.4	- 73.6
Day 19				
Dark	- 60.3	- 94.7	- 72.3	-182.2
Light	- 17.7	- 28.1	- 35.4	- 92.5

‡ Repeated measures analyses identified that dark N_2 fluxes for HL sediment cores were significantly different than those for other treatments after 13 d and 19 d of treatment.

Additionally, initial N_2 fluxes determined from light incubations were significantly different than those calculated for all other days.

Table 4.5 Trophic status of HL, HH, LL, and LH sediments initially (Day 0) and after 4, 10, 13, and 19 days of treatment, as determined from ratios of gross primary productivity to respiration (P/R; Odum and Hoskin, 1958), the benthic trophic state index (BTSI; Rizzo et al. 1996), and net ecosystem metabolism (NEM). Methods of calculating trophic states for each classification scheme have been presented in the Discussion (i.e., *Net ecosystem metabolism and the trophic classification of sediments*).

Days of loading	P/R	BTSI[†]		NEM
Treatment	*(Autotrophic)*	Range	Mean	(Status)
Day 0				
HL		0-1	1	Heterotrophic
HH		1	1	Heterotrophic
LL	LL-4	0-1	1	Heterotrophic
LH		0-1	1	Heterotrophic
Day 4				
HL	HL-4	1-3	2	Both (Hetero)
HH		1-2	1	Heterotrophic
LL		1	1	Heterotrophic
LH		1	1	Heterotrophic

Day 10				
HL	HL-1,3,4	3	3	Both (Auto)
HH	HH-1,3	2-3	3	Both (Hetero)
LL		1	1	Heterotrophic
LH		1	1	Heterotrophic
Day 13				
HL	HL-2	2-3	3	Both (Hetero)
HH		2-3	2	Heterotrophic
LL		1	1	Heterotrophic
LH		1	1	Heterotrophic
Day 19				
HL		2-3	2	Heterotrophic
HH		2	2	Heterotrophic
LL		1	1	Heterotrophic
LH		1	1	Heterotrophic

† **0:** Fully heterotrophic, light O_2 flux ≤ dark O_2 flux; **1:** Net heterotrophic, light O_2 flux > dark O_2 flux > 0; **2:** Net autotrophic, 0 < light O_2 flux < |dark O_2 flux|; and **3:** Highly autotrophic, 0 < |dark O_2 flux| < light O_2 flux

Table 4.6 Fluctuations in the direction of nitrogen and phosphorus exchange at the sediment-water interface during dark (0 μmol photons m^{-2} s^{-1}) and light (~ 10 or 100 μmol photons m^{-2} s^{-1}) sediment core incubations prior and after 4, 10, 13 and 19 days of particulate organic matter loading. Arrows indicate the dominate direction of nitrogen and/or phosphorus exchange, with footnotes denoting when minimal fluxes (†,*) are possible in the opposite direction. Treatment identifications are as described in the legend of Table 4.3.

			Days of loading			
		0	4	10	13	19
Dark	N P					
	▲▲	HL	HL	HL	LL	HH
		LL	LL	LL	HH	LH
			HH	HH	LH	
			LH	LH		
	▲▼	LH†	---	---	HL*	HL
						LL
Light	N P					
	▲▲	HL*	HH†	LL*	LH	LH
		LL	LH	LH		

▲▼	HH*	HL†*	---	---	?
	LH*	LL*			
▼▲	---	---	HL*		?
▼▼	---	---	HH	HL*	LL
				HH	
				LL*	

† Minimal nitrogen exchange in the opposing direction.

* Minimal phosphorus exchange in the opposing direction.

Figure Legends

Fig. 4.1 Schematic of the systematic arrangement of sediment cores and incubation tanks held in a temperature-controlled chamber at 28 °C under a diel cycle of 14 h of light and 10 h of darkness. Full spectrum irradiance was provided from eight alternating lamps (40,000 lumens) of 6500 K and 3000 K. Two incubation tanks, with the same air and water supply, were positioned under this full spectrum light bank to achieve a uniform surface sediment irradiance of approximately 100 μmol photons m^{-2} s^{-1}. Layered shade cloth reduced the uniform irradiance 10-fold in half of each incubation tank so that two surface sediment irradiances (~ 10 and ~ 100 μmol photons m^{-2} s^{-1}) were achieved. No differential irradiance was noted along the length or width of the light bank. Sediment cores were systematically placed within tanks by alternating treatments based on loading (low, high). One water column blank for each treatment of surface sediment irradiance (a total of two) were positioned between sets of low and high loading cores.

Fig. 4.2 Mean (± S.D.) O_2 flux (μmol O_2 m^{-2} h^{-1}) during dark (A) and light (B) incubations for four treatments (HL, HH, LL, LH) developed from two surface sediment irradiances and two biodepositional loadings as described in the legend of Table 4.3. Shading within bars corresponds to the number of days sediments have been receiving treatment, and the numbers positioned above bars indicate the number of significant flux cores.

Fig. 4.3 Mean (± S.D.) estimates of gross primary productivity (A) and net ecosystem metabolism (B) for four treatments (HL, HH, LL, LH) developed from two surface sediment irradiances and two biodepositional loadings as described in the legend of Table 4.3. Shading within bars corresponds to the number of days sediments have been receiving treatment, and the numbers positioned above bars indicate the number of significant flux cores. Estimates of gross primary productivity were calculated as 14 h * (O_2 flux measured during light incubations – O_2 flux measured during dark incubations). Net ecosystem metabolism estimates were determined as 14 h * O_2 flux measured during light incubations + 24 * O_2 flux measured during dark incubations.

Fig. 4.4 Mean (± S.D.) NH_4^+ flux (μmol NH_4^+ - N m^{-2} h^{-1}) during dark (A) and light (B) incubations for four treatments (HL, HH, LL, LH) developed from two surface sediment irradiances and two biodepositional loadings as described in the legend of Table 4.3. Shading within bars corresponds to the number of days sediments have been receiving treatment, and the numbers positioned above bars indicate the number of significant flux cores.

Fig. 4.5 Mean (± S.D.) soluble reactive phosphorus flux (μmol P m^{-2} h^{-1}) during dark (A) and light (B) incubations for four treatments (HL, HH, LL, LH) developed from two surface sediment irradiances and two biodepositional loadings as described in the legend of Table 4.3. Shading within bars corresponds to the number of days

sediments have been receiving treatment, and the numbers positioned above bars indicate the number of significant flux cores.

Fig. 4.6 Measured gross (A, C) and net (B, D) daily N_2-N + NH_4^+ and soluble reactive phosphorus (SRP) fluxes (μmol m^{-2} d^{-1}) versus predicted fluxes determined from stoichiometric conversions (138 O_2 : 16 N : 1 P) of gross (GPP) and net ecosystem metabolism (NEM). Treatment identifications are as described in the legend for Table 4.3. GPP was estimated as 14 h * (O_2 flux measured during light incubations – O_2 flux measured during dark incubations). NEM is estimated as 14 h * O_2 flux measured during light incubations + 24 h * O_2 flux measured during dark incubations. Solid lines indicate the 1:1 ratio of measured flux versus stoichiometric predicted fluxes; dashed lines correspond to the 3:1 and 10:1 ratio for N_2-N + NH_4^+ and SRP, respectively. Note the difference in scales between the panels.

Fig. 4.7 Photographs illustrating the progression of benthic microalgal mat thickness in a representative high light, high loading (HH, A-C) and low light, high loading (LH, D-F) sediment core initially (A, D) and after six (B, E) and twelve (C, F) days of treatment. Initially (01 September 2005), no benthic microalgal communities were visible at the surface of sediment cores collected from La Trappe Creek. Within the first ~ 1 wk (Day 6), benthic microalgal mats were observed within all sediment cores, with the thinnest mats occurring in low light, low loading (LL) cores and comparable thicknesses observed in highly loaded

treatments (HH, LH). Although mat thicknesses continued to increase within HH cores, a proportion of the benthic microalgal mats in LH cores were beginning to be replaced by white, filamentous bacteria by Day 12.

Fig. 4.1

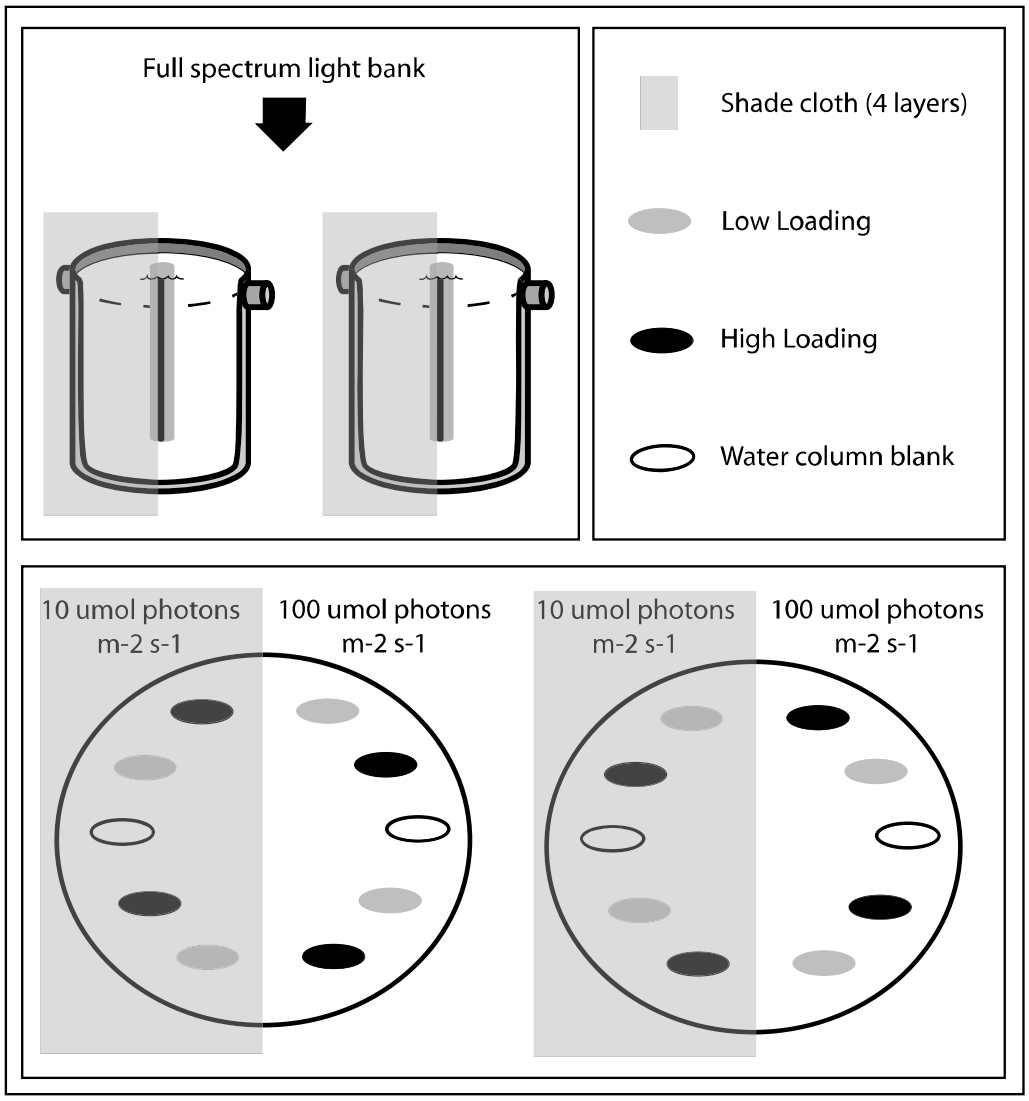

R. R. Holyoke
Figure 1

Fig. 4.2

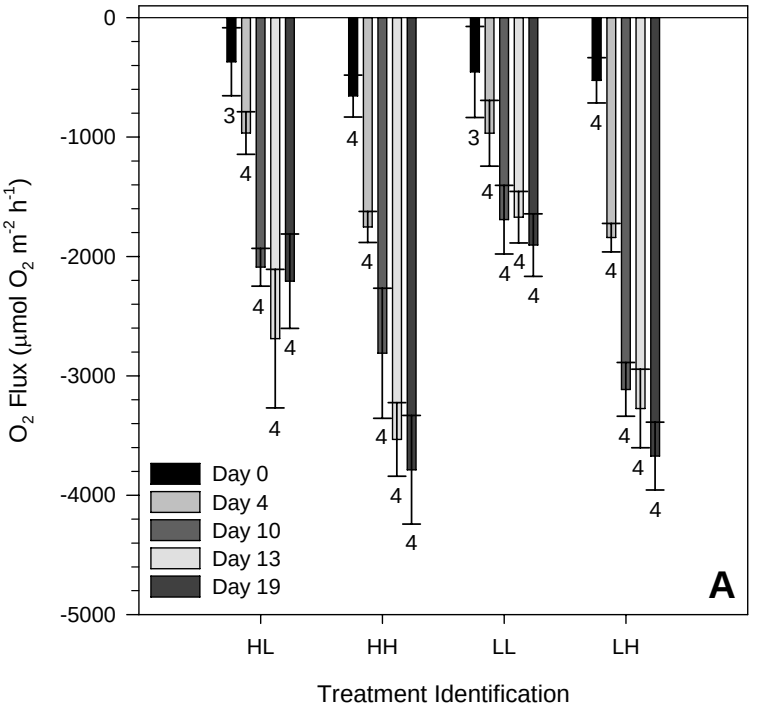
0
-1000
-2000
-3000
-4000
-5000
O2 Flux (µmol O2 m-2 h-1)
Day 0
Day 4
Day 10
Day 13
Day 19
A
HL
HH
LL
LH
Treatment Identification

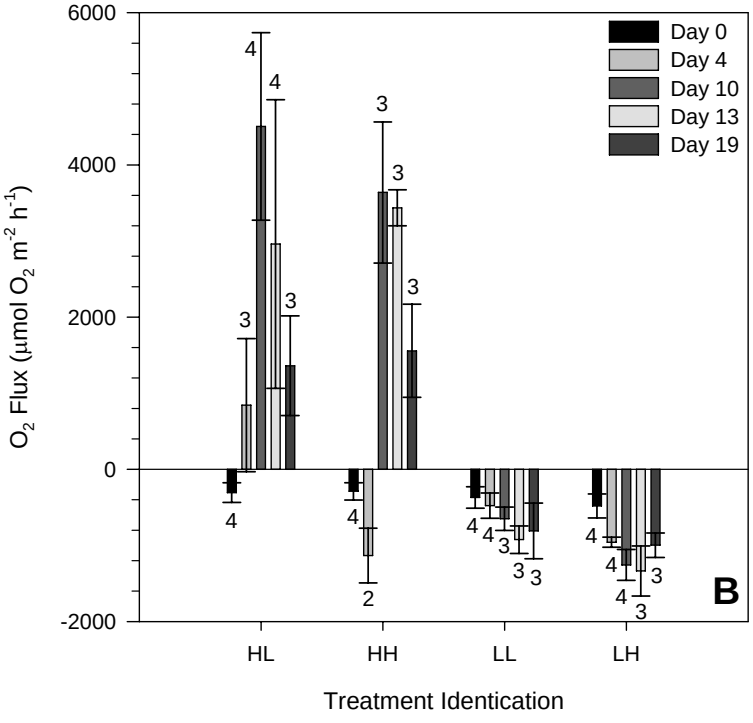
6000
4000
2000
0
-2000
O2 Flux (µmol O2 m-2 h-1)
Day 0
Day 4
Day 10
Day 13
Day 19
B
HL
HH
LL
LH
Treatment Identication

Fig. 4.3

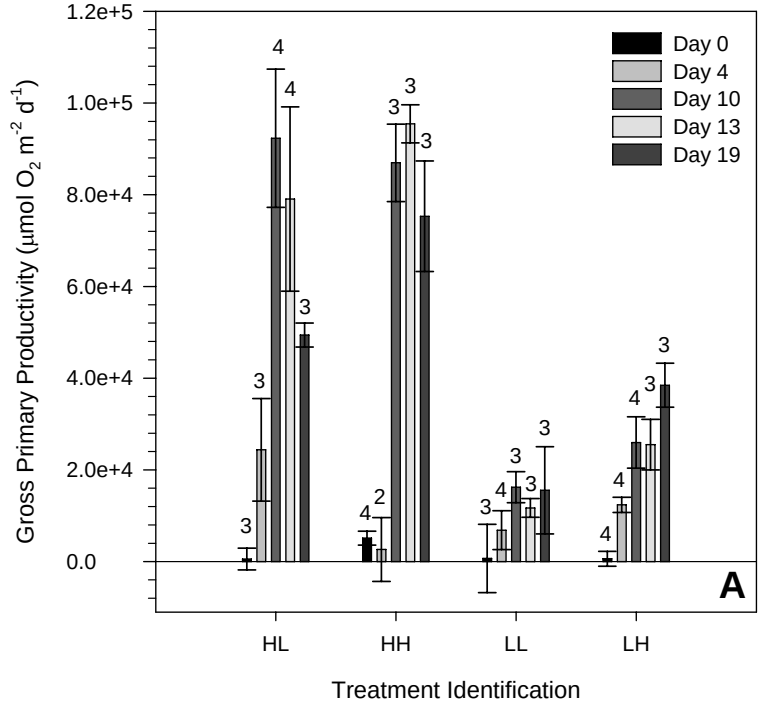
Gross Primary Productivity (µmol O_2 m^{-2} d^{-1})
1.2e+5
1.0e+5
8.0e+4
6.0e+4
4.0e+4
2.0e+4
0.0
Day 0
Day 4
Day 10
Day 13
Day 19
A
HL
HH
LL
LH
Treatment Identification

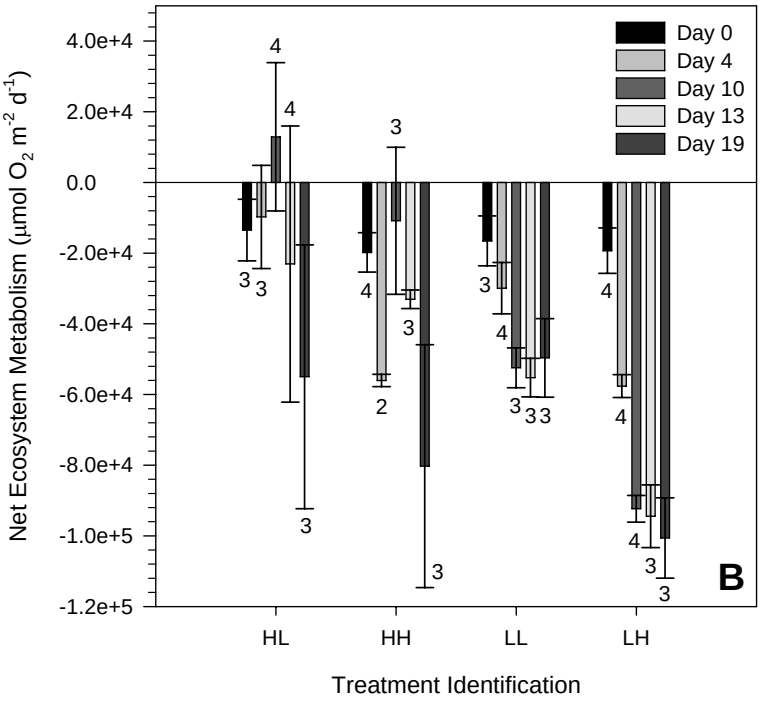
Net Ecosystem Metabolism (µmol O_2 m^{-2} d^{-1})
4.0e+4
2.0e+4
0.0
-2.0e+4
-4.0e+4
-6.0e+4
-8.0e+4
-1.0e+5
-1.2e+5
Day 0
Day 4
Day 10
Day 13
Day 19
B
HL
HH
LL
LH
Treatment Identification

Fig. 4.4

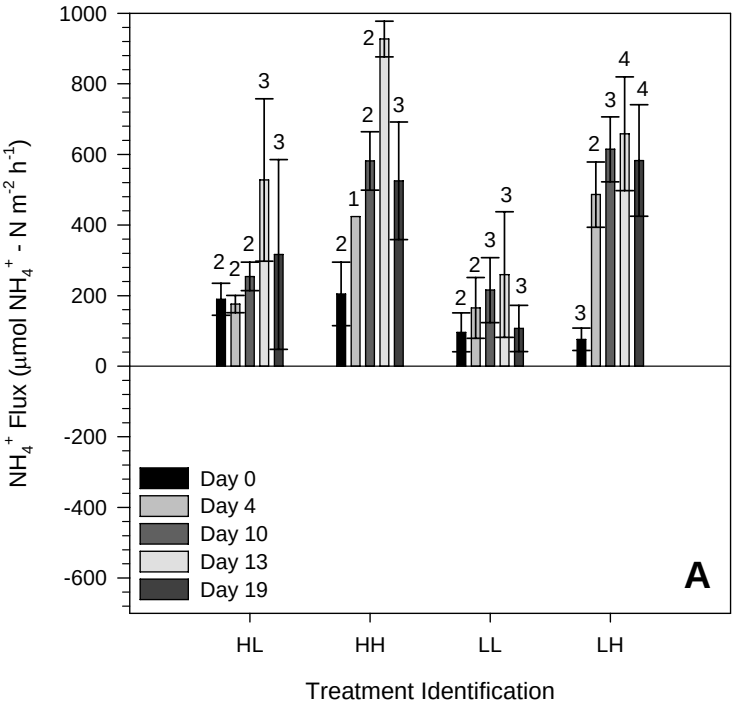
1000
800
600
400
200
0
-200
-400
-600
NH4+ Flux (µmol NH4+ - N m-2 h-1)
Day 0
Day 4
Day 10
Day 13
Day 19
A
HL
HH
LL
LH
Treatment Identification

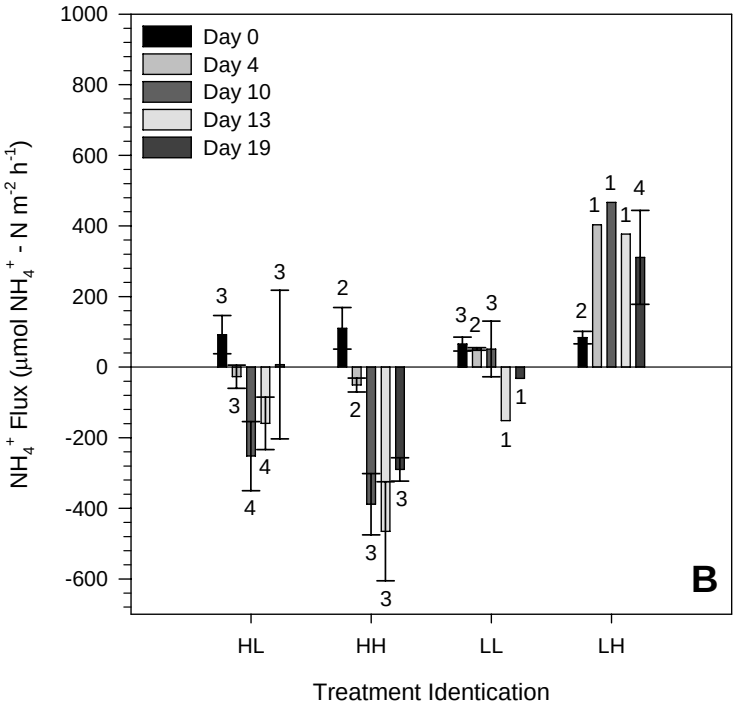
1000
800
600
400
200
0
-200
-400
-600
NH4+ Flux (µmol NH4+ - N m-2 h-1)
Day 0
Day 4
Day 10
Day 13
Day 19
B
HL
HH
LL
LH
Treatment Identication

Fig. 4.5

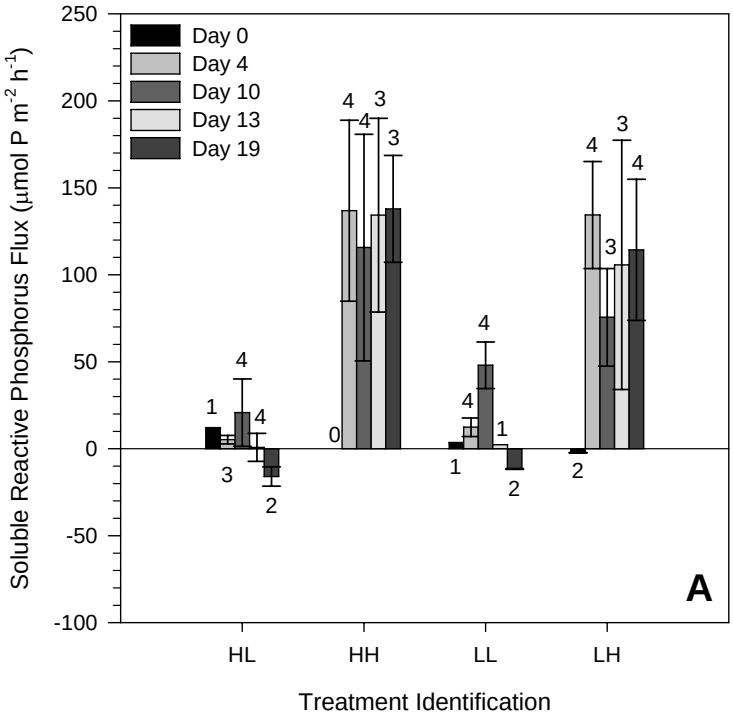
Day 0
Day 4
Day 10
Day 13
Day 19
Soluble Reactive Phosphorus Flux (µmol P m-2 h-1)
250
200
150
100
50
0
-50
-100
HL
HH
LL
LH
Treatment Identification
A

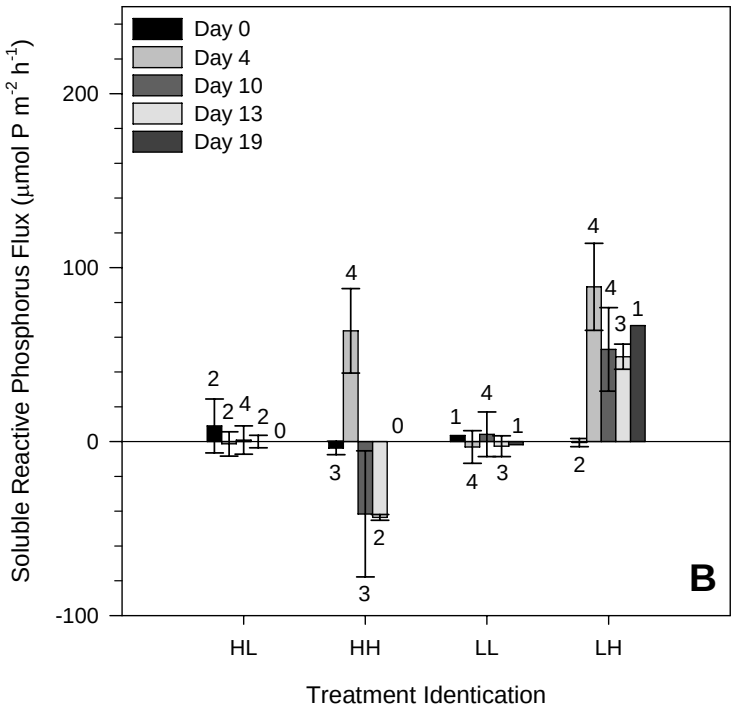
Day 0
Day 4
Day 10
Day 13
Day 19
Soluble Reactive Phosphorus Flux (µmol P m-2 h-1)
200
100
0
-100
HL
HH
LL
LH
Treatment Identication
B

Fig. 4.6

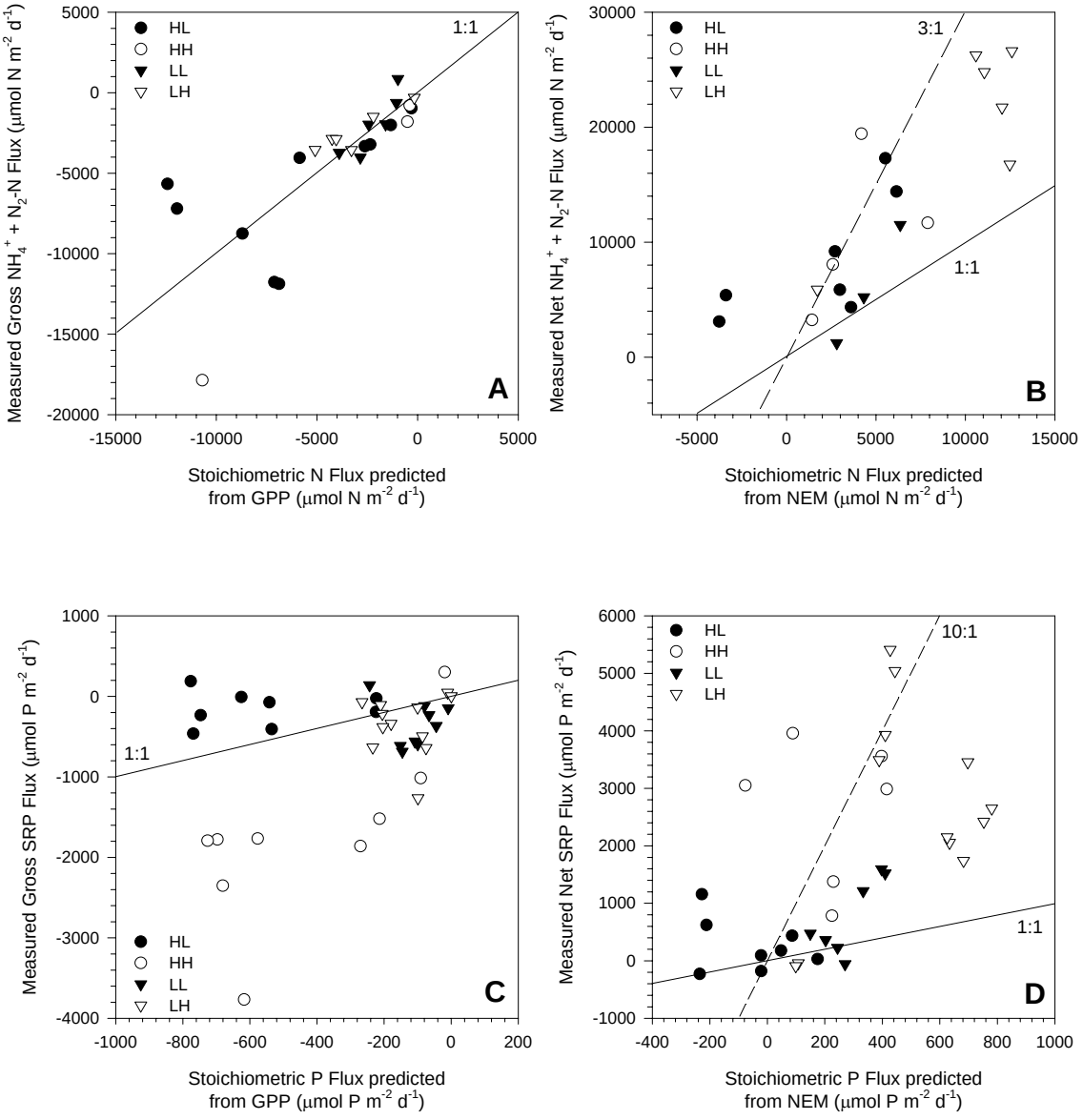
A
Measured Gross NH_4^+ + N_2-N Flux (μmol N m^{-2} d^{-1})
Stoichiometric N Flux predicted from GPP (μmol N m^{-2} d^{-1})
HL
HH
LL
LH
1:1
B
Measured Net NH_4^+ + N_2-N Flux (μmol N m^{-2} d^{-1})
Stoichiometric N Flux predicted from NEM (μmol N m^{-2} d^{-1})
3:1
1:1
C
Measured Gross SRP Flux (μmol P m^{-2} d^{-1})
Stoichiometric P Flux predicted from GPP (μmol P m^{-2} d^{-1})
D
Measured Net SRP Flux (μmol P m^{-2} d^{-1})
Stoichiometric P Flux predicted from NEM (μmol P m^{-2} d^{-1})
10:1

Fig. 4.7

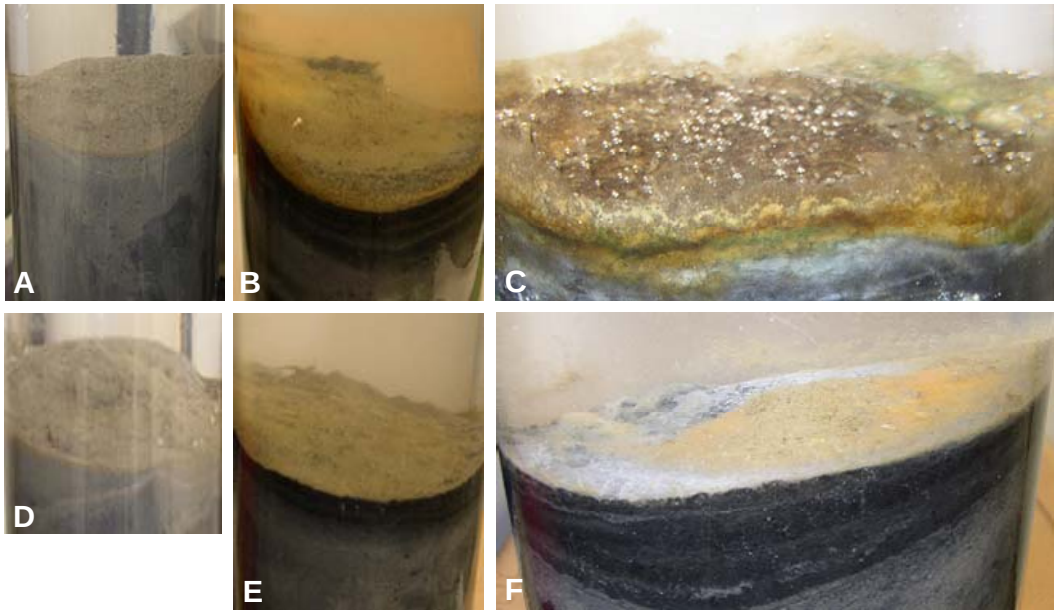

Chapter 5: Dynamic Response of Pore Water and Solid-phase Constituents to Perturbations in Benthic Photosynthesis and Organic Matter Deposition

Abstract

Studies in shallow, illuminated sediments have included only a portion of the potential interactions involved with regulating sediment phosphorus fluxes and, as such, it remains unclear if remineralization of organic phosphorus or oxidation-reduction is responsible for exchange. The combined influence of benthic oxygenic photosynthesis and organic matter deposition on phosphorus mobility and retention was investigated in sediment cores from a Chesapeake Bay tidal creek after ~ 3 wks of aerobic incubations. Cores had been divided into four treatments based on two surface sediment irradiances (~10 and 100 μmol photons m^{-2} s^{-1}) and two loadings (~1.5 and 7.5 g C m^{-2} d^{-1}) of *Crassostrea virginica* biodeposits. Additions of biodeposits enhanced oxidation-reduction cycling within sediments through enhanced benthic oxygenic photosynthesis and increased availability of manganese and iron oxy(hydr)oxides. Pulsed additions of manganese and iron oxy(hydr)oxides supported incorporation of added phosphorus and prevented exchange at the sediment-water interface in the absence of iron-sulfide mineral formation. Low loading treatments incorporated phosphorus supplied from biodeposits and a proportion of pore water SRP within the solid-phase fraction. Differences in relationships for NH_4^+ and SRP concentrations with SO_4^{2-} and decreased retention of solid-phase phosphorus within the 10 cm core relative to surface (0-1 cm) sediments illustrated the upward migration of phosphorus released from the reduction of iron oxy(hydr)oxides at depth in high loading treatments. Comparisons of pore water (NH_4^+, SRP, total dissolved Fe, SO_4^{2-}, Cl^-, ΣH_2S), solid-phase (TP/IP, HCl-Fe, HCl-Mn, AVS, CHN), and microelectrode (O_2, ΣH_2S) profiles verified the presumed importance of iron

oxy(hydr)oxide reduction in sediment phosphorus mobility and availability for exchange at the sediment-water interface in shallow, illuminated sediments.

Keywords Dissolved O_2 · Iron and sulfur speciation · Pore water profiles · Redox cycling · Shallow water sediments · Solid-phase profiles

Introduction

Benthic microalgal communities (BMA) have the potential to regulate nutrient cycling in shallow, illuminated sediments through nutrient assimilation, heterotrophic metabolism, and oxygenic photosynthesis. Assimilation by BMA reduces the availability of nitrogen and phosphorus (e.g., NH_4^+, NO_3^-, PO_4^{3-}) within pore waters and the overlying water column when diffusion across the benthic boundary layer is not rate-limiting (Simon 1988). Modifications to nutrient concentrations and pore water gradients may alter diffusive fluxes across the sediment-water interface and the availability of nutrients for bacterially-mediated processes. Studies have focused on the competition for NH_4^+ and NO_3^- among benthic photoautotrophs, nitrifiers, and denitrifiers in shallow, coastal sediments (Tiedje et al. 1989; Rysgaard et al. 1995; Sundback and Miles 2000; Bartoli et al. 2003; Risgaard-Petersen et al. 2004); less emphasis has been placed on the assimilatory uptake of PO_4^{3-} by BMA. There have been fewer studies on phosphorus assimilation by BMA, perhaps, because of the perception that assimilatory uptake by BMA has a lesser effect on sediment phosphorus exchange than benthic oxygenic photosynthesis (Sundback and Graneli 1988).

Benthic oxygenic photosynthesis increases dissolved oxygen concentrations and pH in surface sediments (Revsbech and Jorgensen 1983; Revsbech et al. 1983) and, thereby, alters the thickness of the oxidized sediment layer (i.e., positive oxidation-reduction potential; Revsbech et al. 1980a). Increased penetration of dissolved oxygen into sediments contributes to variations in sediment nitrogen exchange as coupled nitrification-denitrification and direct denitrification are stimulated or reduced (Risgaard-Petersen et al. 1994; Rysgaard et al. 1995; An and Joye 2001; Dalsgaard 2003). Concurrent measurements of dissolved oxygen profiles and phosphorus exchange across the sediment-water interface, unlike for nitrogen, have not been conducted (Risgaard-Petersen et al. 1994). Influences of benthic oxygenic photosynthesis on phosphorus cycling have been inferred from flux measurements of dissolved oxygen, nitrogen, and phosphorus (Graneli and Sundback 1985; Sundback and Graneli 1988; Rizzo 1990; Reay et al. 1995) and deviations in nutrient stoichiometry. Additional inferences have been derived from the current understanding of phosphorus retention in near shore, continental margin, and freshwater sediments, including the role of manganese and iron oxy(hydr)oxide (e.g., MnO_2, MnOOH, FeOOH, Fe_2O_3) reduction and non-refractory organic matter in phosphorus mobility (e.g., Williams et al. 1971; Carignan and Flett 1981; Krom and Berner 1981; Jensen et al. 1992; Sundby et al. 1992; Thamdrup et al. 1994; Slomp et al. 1996; Christensen et al. 1997; Ingall and Jahnke 1997; McManus et al. 1997; Anschutz et al. 1998). Studies in shallow, illuminated sediments have been compartmentalized to include only a portion of the interactions among dissolved oxygen, phosphorus, manganese, iron and sulfur species (e.g., Kostka and Luther 1995; Epping et al. 1998; Rozan et al. 2002; Ma et al. 2006).

Reoxidation of reduced manganese (II, III) and iron (II) during benthic oxygenic photosynthesis and subsequent chemical precipitation of oxy(hydr)oxides is the mechanism expected to be responsible for the retention of phosphorus in shallow water sediments. Removal of phosphorus from pore waters occurs through the adsorption of PO_4^{3-} onto oxy(hydr)oxides, as well as phosphorus mineral precipitation when pore water concentrations are high (Slomp et al. 1996). The adsorptive capacity of oxidized sediments decreases with the age and crystallinity of oxides, such that newly-formed, less crystalline oxy(hydr)oxides include more adsorption sites for PO_4^{3-} than older, more crystalline oxides (Lijklema 1980). Fluctuations in dissolved oxygen production, penetration, and reoxidation will likely lead to the availability of more less-crystalline iron and manganese oxy(hydr)oxides and an associated increase in phosphorus retention.

Although effluxes of phosphorus from sediments are generally considered to be the result of the release of inorganic phosphorus bound to oxy(hydr)oxides (McManus et al. 1997), non-refractory organic phosphorus released from mineralization may also play a role in sediment phosphorus exchange in sediments receiving high rates of organic deposition (Ingall and Jahnke 1997). Remineralized phosphorus may be released from sediments if insufficient oxides (surface sites) exist to bind regenerated inorganic phosphorus or sudden bursts in remineralization exceed the uptake capacity or demand of BMA (Rizzo 1990). Additionally, rates of decomposition and supply of labile organic matter are relevant to the reduction of solid-phase oxy(hydr)oxides and the release of bound inorganic phosphorus. High rates of deposition result in the consumption of dissolved oxygen and, thereby, limit both aerobic respiration to the upper few mm of sediment and the reoxidation of reduced chemical species. Production of dissolved

sulfide from anaerobic degradation may increase phosphorus release from and the production of iron sulfide minerals in sediments overlain by oxygenated waters (Rozan et al. 2002).

In shallow water sediments, it is unclear if the remineralization of organic phosphorus or the reduction of iron and manganese oxy(hydr)oxides is responsible for the availability of phosphorus for exchange at the sediment-water interface. To address this uncertainty I developed a laboratory experiment to address the combined influence of benthic oxygenic photosynthesis and organic matter deposition on phosphorus fluxes, mobility, and retention within sediments. *Crassostrea virginica* (eastern oyster) feces and pseudofeces served as the source of POM additions, supplying undigested phytoplankton and inorganic particulates (and associated minerals) to surface sediments (Langdon and Newell 1996; Cognie and Barille 1999; Newell 2004). Such biodeposits from suspension-feeding mollusks can be a major source of particulate deposition, especially in areas of high natural population abundances or aquaculture farms. Variable light intensities were used to generate variable levels of benthic oxygenic photosynthesis. Comparisons of pore water (NH_4^+, SRP, dissolved Fe (II, III), SO_4^{2-}, Cl^-, ΣH_2S), solid-phase (TP/IP, HCl-Fe, HCl-Mn, AVS, CHN), and microelectrode (O_2, ΣH_2S) profiles among treatments are presented here to explain the dual role of organic and iron-bound phosphorus in sediment fluxes. Interactions (i.e., oxidation-reduction reactions) among organic matter oxidants are inferred from shifts in sedimentary and pore water profiles and proximity of constituents. Referenced phosphorus fluxes across the sediment-water interface have been presented elsewhere (Chapter 4).

Materials and Methods

Sediment core collection and incubation

On 31 August 2005, twenty-two sediment cores were collected at a depth of ~ 1.5 m in an upper, mesohaline portion of La Trappe Creek, Chesapeake Bay, MD (38° 39.223' N, 076° 05.267' W). All cores were collected by pressing a Rumohr-type pole corer fitted with a transparent acrylic tube (6.35 cm inner diameter) ~ 10 cm into the fine-grained sediments. Upon retrieval, the bottoms and tops of cores were sealed with machined plastic lids fitted with O-rings and stoppers, respectively, to maintain cores without airspace. Cores remained covered in coolers until transport to the laboratory.

Upon returning to the laboratory, sediment cores were placed within a temperature-controlled chamber set at 28°C. Six of the twenty-two sediment cores were set aside, and the overlying water was aerated until cores were sampled for initial pore water (NH_4^+, SRP, dissolved Fe (II, III), SO_4^{2-}, Cl^-, ΣH2S) and solid-phase (TP/IP, HCl-Fe, HCl-Mn, AVS, CHN) constituents. The sixteen remaining cores were equally divided into two incubation tanks and randomly separated into four treatments based on two surface sediment irradiances (~ 10 μmol photons m^{-2} s^{-1}, ~ 100 μmol photons m^{-2} s^{-1}) and two depositional loadings (~ 1.5 g C m^{-2} d^{-1}, ~ 7.5 g C m^{-2} d^{-1}). Labels for the four treatments correspond to the light and then loading level as follows: HL: high light, low loading; HH: high light, high loading; LL: low light, low loading; and LH: low light, high loading.

Sediment cores were incubated in filtered 2 μm estuarine water from the Choptank River (salinity: 10.4 – 13.4), exchanged every other day, under a diel cycle of 14 h of daylight and 10 h of darkness beginning on 31 August 2005. Teklight T5H0

(www.1000bulbs.com) greenhouse lights provided a uniform illumination (~ 100 μmol photons m^{-2} s^{-1}) to surface sediments; mesh, shade cloth was used to provide a 10-fold decrease (~10 μmol photons m^{-2} s^{-1}) in surface sediment irradiance to eight of the sediment cores. Aeration was maintained in the open cores and surrounding water, using an air compressor, and tanks and bubblers were scrubbed and rinsed with deionized water as needed. Microbial growth on the inside walls of cores was scraped and allowed to settle to the sediment surface once every two days. A more detailed description of sediment core incubations is presented in Chapter 4.

Additions of dewatered, irradiated slurries of *Crassostrea virginica* (eastern oyster) biodeposits, which served as the source of particulate organic matter (POM), began on 02 September 2005 and continued for 19 d. Biodeposits, stored in low density polyethylene ether (LDPE) 500 ml bottles, were sterilized by gamma irradiation at 50 kGy (~ 788 min) and refrigerated (4°C) in the dark throughout the duration of the experiment. POM loadings were added daily on a volume basis (~ 0.8 ml, ~ 4 ml); aliquots were collected from LDPE bottles with a 10 ml syringe and slowly released into the overlying water of cores. Biodeposits were allowed to settle before aeration was restored. A subsample of biodeposits (~ 4 ml) was collected at each addition, dried to a constant weight at ~ 80 °C, and ground for percent water, total carbon, total nitrogen, total and inorganic phosphorus, HCl-extractable Mn and HCl-extractable Fe analyses. A second subsample (~ 4 ml daily) was frozen in a 15 ml centrifuge tube until later analysis of acid-volatile sulfides (AVS). An experimental duration < ~ 3 wks was selected so I could observe the immediate and prolonged influence of benthic oxygenic photosynthesis and organic deposition on sediment phosphorus cycling. Termination occurred once

gross primary production (GPP) stabilized within treatments; prolonged exposure of microcosms to experimental treatments results in enhancement of container effects (e.g., exclusion of particle advective losses) and eventual degradation of the BMA (Cornwell, *personal communication*).

Pore water and solid-phase sectioning

Pore water and solid-phase sectioning for the six initial and sixteen incubated sediment cores were performed on 31 August 2005 and on 21 – 22 September 2005, respectively. The overlying water column was siphoned to minimize disturbance of the sediment surface, and collection of surface sediments (top ~ 1 cm) occurred prior to sediment sectioning. A syringe mini-corer (1.4 cm inner diameter) was pressed ~ 1 cm into sediments, and collected sediment was extruded into an aluminum pan and dried at 80°C. Ground sediment was stored in glass scintillation vials until analysis.

All pore water cores were extruded under N_2 and divided into 8 sections (0-0.5, 0.5-1, 1-1.5, 1.5-2, 2-3, 3-4, 4-7, and 7-10 cm) that were individually placed in 50 ml plastic centrifuge tubes and capped. Sections were centrifuged (1,096 xg for 10 min; 3500 rpm; International Equipment Company Centra MP4), and the supernatant was filtered with 0.45 μm filters into 6 ml plastic vials for analysis of NH_4^+, soluble reactive phosphorus (SRP), SO_4^{2-}, Cl^-, dissolved Fe (II, III), and dissolved sulfide (ΣH_2S: H_2S, HS^-, S^{2-}). Pore water sediments were frozen until solid phase analyses could be conducted. Dilutions were done prior to freezing of NH_4^+ and SRP samples. SO_4^{2-} and Cl^- samples were immediately frozen, and dilutions were performed at the time of analysis. Dissolved Fe samples were acidified and stored in capped vials at room

temperature until analysis. Dissolved sulfide samples (1 ml) were fixed with 10 μl of a mixed diamine reagent (250 – 1000 μmol L^{-1}, Cline 1969) and stored at room temperature until analysis.

Analyses

Pore water analyses. Standard colorimetric and ion chromatographic seawater methods were used to determine concentrations of dissolved inorganic pore water nutrients. Determination of NH_4^+ concentrations followed Soloranzo's (Solaranzo 1969, as presented in Parsons et al. (1984)) phenol hypochlorite method, modified for a 5 ml sample volume. A composite reagent of molybdic acid, ascorbic acid, and trivalent antimony was used to determine SRP concentrations (Murphy and Riley 1962). Total dissolved Fe (II, III) and total dissolved sulfide were also determined from colorimetric analyses, following Gibb's ferrozine reduction technique (Gibb 1979) and methylene blue colorimetry (Cline 1969). SO_4^{2-} and Cl^- concentrations were determined by ion chromatography (United States Environmental Protection Agency 1983b).

Solid-phase analyses. Frozen sediments from core dissections and sub-sampling of biodeposits were analyzed for acid-volatile sulfides (AVS) using a 6 N HCl-extraction and $PbClO_4$ titration (Cornwell and Morse 1987). All solid phase digestions were performed on thawed, well-homogenized sediments. Separate, equivalent amounts of homogenized sediments were dried to a constant weight at 80°C. pH was measured by direct insertion of a combination electrode calibrated with NIST-traceable standards.

Dried subsamples of biodeposits, surface sediments (top ~ 1 cm), and frozen sediment sections were analyzed for percent water, total and inorganic phosphorus, HCl-extractable Mn and HCl-extractable Fe. Inorganic and total phosphorus concentrations were determined using HCl-extraction of dried (~ 80°C) and ashed (550°C) sediments following Aspila et al. (1976); loss upon combustion was used to determine the percent organic content. The remaining HCl-extracts from inorganic phosphorus analyses were analyzed using flame atomic absorption to determine HCl-extractable Mn and Fe (Leventhal and Taylor 1990) concentrations. Iron oxy(hydr)oxides (i.e., Fe oxides) concentrations were calculated as the difference in HCl-extractable Fe and AVS concentrations. Percentages of total carbon and nitrogen were determined for subsamples of biodeposits and surface sediments (top ~ 1 cm) with a Control Equipment elemental autoanalyzer (Cornwell et al. 1996) and expressed relative to the dry weight (DW) of biodeposits or sediment (μmol g^{-1} DW) and the surface area of a core (mmol m^{-2}). Percent water was determined gravimetrically for surface sediments (0-1 cm) and sediment porosity was estimated using a sediment density of 2.5 g cm^{-3} (Cornwell et al. 1996).

Microsensors. Dissolved O_2 and ΣH_2S profiles in the upper millimeters of surface sediments were determined using Clark-type Ox50 and H2S50 microsensors (50 μm tip), constructed by Unisense (www.unisense.com). Ox50 microsensors generate a linear relationship of the partial pressure of O_2 within a pA range; two-point linear regressions of recorded pA at 0 and 100% saturation are sufficient for calibration. Ox50 construction and functioning follows Revsbech (1989). I measured dissolved O_2 concentrations in

incubated cores every 100 μm beginning ~ 0.2 mm above the sediment surface (i.e., water column) and extending 1.5 mm into sediments prior to and on the morning after the 3rd, 6th, 9th, 12th and 17th depositional loading.

Amperometric microsensors for sulfide measure the H_2S that diffuses across a membrane; the H_2S is deprotonated and the oxidation of HS- by Fe(III) on platinum anodes is measured (Jeroschewski et al. 1996). H2S50 microsensors are linear in the range of 0 to 300 μmol H_2S L^{-1} and curvilinear at concentrations exceeding 300 μmol H_2S L^{-1}. I calibrated the H2S50 microsensors within the lower, linear range using sequential additions of Na_2S to Ar-purged pH 4 buffer. ΣH_2S concentrations were calculated as follows

$$[\Sigma H_2S] = [H_2S] / (1 + K_1 / [H_3O^+])$$

where $K_1 = 10^{-pK1}$, and calculations of the pK_1 for the dissociation of H_2S followed Millero et al. (1988).

$$pK_1^* = - 98.080 + 5{,}765.4 / T + 15.0455 \ln T + (-0.1570)(S^{1/2}) + (0.0135)(S)$$

Concentrations of H_3O^+ were determined for the upper 2 cm of sediment from pH of thawed, well-homogenized sediments (0.5 cm intervals) used for AVS analyses. Profiles of H_2S for the determination of ΣH_2S were performed prior to the first and 19th addition of POM. H_2S concentrations were measured at 1 mm intervals.

All microsensor profiles were conducted during daylight hours inside the 28°C environmental chamber. Sediment cores were removed individually from incubation tanks and positioned below a micromanipulator, capable of controlling discrete step intervals, located opposite incubation lamps. Cores remained aerated with an air-stone

connected to an electric aquarium pump. Two to three replicate profiles were conducted per core.

Statistical analyses. All statistical analyses were conducted in SAS (version 9.1 for Windows) using Proc GLM, Npar1way, and Proc Mixed for parametric and non-parametric analysis of variance (ANOVA) and Repeated Measures analyses, respectively. Non-normally distributed data were transformed with a log-base 10 transformation, and in the case where data could not be transformed to meet the conditions of normality, non-parametric (one-way) ANOVAs were conducted. All data were centered (mean = 0) and standardized within one standard deviation of zero. Significant differences and effects were determined for $P \leq 0.05$.

Multivariate analysis of variance (MANOVA) was used to test for overall treatment and tank effects. The Wilks' Lamba test statistic concluded that there was an overall treatment effect for surface sediment ($P < 0.0001$) and pore water and solid-phase concentrations ($P = 0.0095$). No significant tank effects were identified for surface sediments ($P = 0.8854$), pore water ($P = 0.4158$), or solid-phase ($P = 0.6914$) constituents.

Model III, single-factor ANOVAs were conducted for surface sediment (top ~ 1 cm) concentrations and pore water and solid-phase concentrations integrated over the surface 2 cm and the 10 cm core. Depth-integrated concentrations were calculated as the sum of pore water or solid-phase concentrations, corrected for the total volume of water or mass of dry sediment, respectively, and the surface area of the core, over the specified depth (2 cm or 10 cm). I used Tukey-Kramer least squares means (adjustment for

multiple comparisons) to identify groupings and statistical significance if the null hypothesis of no treatment effect was rejected. A Kruskal-Wallis non-parametric (one-way) ANOVA was used to test for differences in the depth at which ΣH_2S exceeded 50 μmol L^{-1}, as determined from H_2S microelectrode profiles and pH. Split-plot repeated measures analysis, nesting sediment cores within treatments, was used to detect differences in the penetration depth of dissolved O_2 ($O_2 \geq 20$ μmol L^{-1}), and fit statistics (AIC model) were used to determine that compound symmetry was the appropriate covariance model to use.

Results

Initial conditions

Immediate sampling of six sediment cores (i.e., identified as ***Initials*** in Tables and Figures) on 31 August 2005 served as a means to determine the initial state of La Trappe Creek sediments prior to exposure to treatments. Collected surface sediments (0-1 cm) had a percent water content of 66.7 ± 5.5% (porosity, $\varphi = 0.83 \pm 0.03$) and a percent organic content of 9.1 ± 1.9%. Percent organic contents remained fairly constant between 0.5 cm and 3 cm (9.4 ± 1.3%) before decreasing to 7.6 ± 0.9% (7 – 10 cm). Mean (± standard deviation) surface sediment (0-1 cm) carbon was initially ~ 2,343 ± 270 μmol C g^{-1} DW, and mean nitrogen equaled ~ 205 ± 25.0 μmol N g^{-1} DW. Gradients of pore water NH_4^+ in the surface 3 cm of sediment suggested a diffusive flux out of the sediment, consistent with the direction of measured NH_4^+ fluxes presented in Chapter 4. Pore water NH_4^+ concentrations ranged from 134 to 939 μmol N L^{-1}, with the greatest concentrations occurring in deeper (7 to 10 cm) sediments.

Initial SRP pore water concentration profiles were shaped similarly to profiles of NH_4^+, whereby maximum concentrations (~ 200 μmol P L^{-1}) occurred at depth. Minimum concentrations and relatively vertical gradients of SRP in the upper 3 cm were consistent with an initial, measured flux of ~ 2 μmol P m^{-2} h^{-1} (Chapter 4). Surface sediment (0-1 cm) concentrations of organic and inorganic phosphorus were 6.8 ± 2.6 μmol P g^{-1} DW and 9.0 ± 2.1 μmol P g^{-1} DW, respectively. Total phosphorus concentrations decreased steadily with depth to a mean of ~ 11.8 μmol P g^{-1} DW in five of the Initials; a sixth core possessed a subsurface peak in total (77.5 μmol P g^{-1} DW) and inorganic (33.3 μmol P g^{-1} DW) phosphorus at a midpoint depth of 1.75 cm. Percent organic phosphorus varied from 8.5 to 65.6% but typically remained constant (42.0 ± 10.0) within the surface 10 cm of all initial cores.

Vertical profiles of HCl-extractable Mn consisted of concentrations between 0.41 and 1.12 μmol Mn g^{-1} DW. Surface sediments (0-1 cm) possessed a mean (± standard deviation) of 0.69 ± 0.26 μmol Mn g^{-1} DW, and concentrations minimally decreased with depth. HCl-extractable Fe concentrations decreased two-fold from a mean (± standard deviation) surface concentration of 107.6 ± 20.8 μmol Fe g^{-1} DW to 47.6 ± 4.4 μmol Fe g^{-1} DW in bottom sediments. Variability within measurements (i.e., standard deviation) also declined with depth. AVS fractions never exceeded 25% of HCl-extractable Fe, with minimum and maximum AVS-Fe concentrations of ~ 4 and 25 μmol Fe g^{-1} DW.

Dissolved Fe (II, III) concentrations initially peaked at the sediment surface, with concentrations in the top 0.5 cm ranging from 1.1 to 86 μmol Fe L^{-1} (33 ± 32 μmol Fe L^{-1}). Minimal dissolved Fe was detected below 4 cm. Concentrations of ΣH_2S (Range: 4 – 20 μmol L^{-1}), as determined with methylene blue colorimetry (Cline 1969), suggested the

presence of sulfide in the surface 2 cm of initial sediment cores. Sulfide concentrations below ~ 20 μmol L^{-1} were below the limit of detection because of the mixed diamine reagent (250 – 1000 μmol L^{-1}) selected. Microsensor profiles (H2S50) detected no ΣH_2S within the top 2 cm of cores initially, except for duplicate cores designated to receive high light and high loading (HH) treatments (depth ≥ 14.8 mm). Below 2 cm, ΣH_2S concentrations increased, approaching ~ 1,100 μmol L^{-1}. Significant treatment*time effects for dissolved O_2 penetrations (P = 0.0135) identified no significant difference in initial O_2 penetrations (P > 0.69). Initially, dissolved O_2 often penetrated ≥ 1.5 mm, and pH profiles were essentially constant, with values ranging from 7.4 to 7.6.

Biodeposits

Dewatered, homogenized slurries of *C. virginica* biodeposits had a percent water content of 91.0 ± 0.5% (n = 8, 0.074 g DW ml^{-1}) and a percent organic content, determined from loss on ignition, of 22.5 ± 0.8%. Total C : N : P ratios (105 : 13 : 1) were similar to the Redfield Ratio (106 : 16 : 1), as expected for eastern oysters feeding on ambient, estuarine suspended material during summer (Table 5.1). Percentages of total carbon and nitrogen were determined to be 8.06 ± 0.10% C and 1.17 ± 0.02% N; less than ~ 25% of total phosphorus was organic. HCl-extractable Mn concentrations (57.9 ± 3.1 μmol Mn g^{-1} DW) exceeded initial surface sediment concentrations (0.69 ± 0.26 μmol Mn g^{-1} DW) 50-fold. Concentrations of HCl-extractable Fe (174.1 ± 9.3 μmol Fe g^{-1} DW) were more similar to initial surface conditions. No measurable AVS was detected in 4 ml subsamples (n = 9) of biodeposits, collected upon opening and

discarding sample bottles, but small changes in initial and final mV readings for $PbClO_4$ titrations suggested a small increase in AVS over these 4 d windows.

Surface sediments

Surface sediment (top ~ 1 cm) concentrations of carbon and nitrogen were significantly different due to treatment ($P < 0.0001$; $P < 0.0001$), as determined from Model III, fixed effect ANOVAs. Post hoc analysis, using Tukey-Kramer least squares means, determined that treatments receiving ~ 7.5 g C m^{-2} d^{-1} (HH, LH) were significantly different from HL, LL and initial means ($P < 0.05$). Mean (± standard deviation) surface sediment concentrations of total carbon for HH and LH and HL and LL were as follows: 4,526 ± 871 μmol C g^{-1} DW and 2,671 ± 296 μmol C g^{-1} DW. Surface nitrogen concentrations were approximately 10% and 8% of total carbon concentration for high and low loading treatments, respectively. Percent organic content for HL, HH, LL, and LH treatments were as follows: 11.2 ± 1.6%, 16.5 ± 1.6%, 10.8 ± 1.3%, and 14.6 ± 1.4%.

Significant differences due to treatment were also identified for concentrations of total ($P = 0.0277$) and organic phosphorus ($P = 0.0016$). Total phosphorus concentrations for HH (28.9 ± 6.6 μmol P g^{-1} DW) were significantly different from initial concentrations ($P = 0.0206$); neither differed from HL, LL, or LH. No significant difference in organic phosphorus concentrations were identified when comparing HH and LH sediments ($P = 0.6186$), but mean concentrations for HH (15.9 ± 3.6 μmol P g^{-1} DW; $P < 0.03$), unlike LH (12.8 ± 0.4 μmol P g^{-1} DW), were statistically different than those for HL, LL, and Initials (7.5 ± 3.1 μmol P g^{-1} DW).

No significant differences due to treatment were identified for inorganic phosphorus ($P = 0.1437$) or HCl-extractable Fe and Mn ($P = 0.1463$; $P = 0.1789$). Mean inorganic phosphorus concentrations for all treatments, excluding initial conditions, were 13.0 ± 3.1 μmol P g^{-1} DW. HCl-extractable Fe concentrations were 132 ± 33 μmol Fe g^{-1} DW, with a non-significant separation between HL (106 ± 34 μmol Fe g^{-1} DW) and high loading treatments (143 ± 37 μmol Fe g^{-1} DW; 148 ± 24 μmol Fe g^{-1} DW). Mean HCl-extractable Mn (1.9 ± 1.0 μmol Mn g^{-1} DW) for all treatments was elevated, but not significantly so, above initial concentrations. Percent water content (and porosity) for HL, HH, LL and LH surface (0-1 cm) were as follows: $68.5 \pm 6.4\%$ (0.84 ± 0.04), $79.2 \pm 2.1\%$ (0.90 ± 0.01), $71.4 \pm 2.9\%$ (0.86 ± 0.02), and $79.1 \pm 3.1\%$ (0.90 ± 0.02).

Pore water profiles

Fixed effects, single-factor ANOVAs identified significant treatment effects ($P \leq 0.05$) for all pore water constituents (NH_4^+, SRP, SO_4^{2-}, ΣH_2S, $Fe_{T(diss)}$) integrated for surface (0-2 cm) sediments. No significant effects due to treatment were identified for pore water concentrations of NH_4^+, SRP, SO_4^{2-}, or ΣH_2S integrated over the 10 cm core ($P = 0.7648$; $P = 0.6449$; $P = 0.2020$; $P = 0.1740$). Concentrations of dissolved Fe (II, III) were significantly different due to treatment (over 10 cm; $P < 0.0001$), with greater dissolved Fe (II, III) concentrations observed in low loading cores than La Trappe Creek sediments initially. No significant difference in total dissolved Fe concentrations were identified between low and high loading treatments ($P \geq 0.078$). Lack of significant treatment effects for core-integrated NH_4^+, SRP, SO_4^{2-}, and ΣH_2S were attributed to increases in the relative magnitude of concentrations with depth, similarities in the shape

of profiles below 2-4 cm, and variability among replicates. Statistical designation of treatments under multiple groupings (i.e., Tukey-Kramer least squares means) was likely associated with the use of minimal replication (n = 4) and the uncharacteristic shape of pore water profiles for one HL and one HH core. Decreased concentrations of NH_4^+, SRP, SO_4^{2-}, and dissolved Fe (II, III) were measured within the pore waters of sediments collected at depths of 1-4 cm for the HL core; whereas as the single HH core maintained a nearly constant concentration profile for NH_4^+, SRP, SO_4^{2-}, and ΣH_2S in the surface 10 cm. The shape of the dissolved Fe (II, III) profile for this core more closely resembled those typically observed for HL and LL sediments, with concentrations peaking at ~ 148 μmol Fe L^{-1}.

Pore water NH_4^+ concentrations for HL (7.5 ± 1.5 μmol N) were significantly different from LH (14.1 ± 4.1 μmol N; P = 0.0414) in the surface 2 cm; no significant differences between these two treatments and HH (14.7 ± 6.8 μmol N), LL (8.6 ± 2.1 μmol N), and Initials (13.9 ± 2.9 μmol N) were identified. Gradients (0-2 cm) of NH_4^+ for high loading treatments exceeded those of low loading cores and initial sediments (Figure 5.1, panel (a)). Concentrations at depth (7-10 cm) in all sediment cores were between 600 and ~ 700 μmol N L^{-1}. Surface sediment (0-0.5 cm) concentrations differed, such that concentrations increased with decreasing surface sediment irradiance (HL: 80 ± 22 μmol N L^{-1}; LL: 108 ± 48 μmol N L^{-1}) and increasing POM loading (HH: 200 ± 106 μmol N L^{-1}; LH: 246 ± 30 μmol N L^{-1}).

Depth-integrated (0-2 cm) concentrations of SRP were significantly different among treatments (P = 0.0052). Mean SRP concentrations for HH were not significantly different than LH cores (P = 0.9996), but these treatments did differ from HL and LL.

Cores receiving lower additions of POM (~ 1.5 g C m^{-2} d^{-1}) had a mean concentration of 1.76 ± 0.76 μmol P for the surface 2 cm, and surface pore water concentrations (μmol P L^{-1}) 4 to 8 times less than high loading treatments (Figure 5.2, panel (a)). Depth-integrated SRP for high loading treatments was 4.47 ± 1.38 μmol P. Cores receiving both levels of POM loading were not significantly different from Initials. Concentration gradients for all cores were indicative of a diffusive flux out of sediments; maximum gradients were observed for cores receiving high loading treatments.

A one-way ANOVA of dissolved Fe (II, III) in surface sediments (0-2 cm) identified significant differences in mean concentrations between HL and HH, LH, and Initials. No significant difference was identified between low loading treatments ($P = 0.1566$), or between LL and HH, LH, and initial conditions ($P > 0.07$). Pore water dissolved Fe (II, III) concentrations for high loading treatments decreased more than 10-fold within 10 cm cores, with the greatest dissolved Fe (II, III) concentrations (< 150 μmol Fe L^{-1}) occurring in the top 0.5 cm. Maximum concentrations (> 400 μmol Fe L^{-1}) for HL and LL were observed between 0.5 and 3 cm (Figure 5.2, panel (b)).

Concentrations of SO_4^{2-} for HL and LL treatments were significantly different than initial concentrations for La Trappe Creek sediments ($P = 0.0034$; $P = 0.0304$; Figure 5.2, panel (c)). No significant differences were identified among high loading treatments and low loading or initial conditions ($P > 0.10$). Estimated rates of SO_4^{2-} consumption suggested an increase in SO_4^{2-} reduction with decreased surface sediment irradiance and/or increased POM loading. Predicted fluxes of SO_4^{2-} for HL, HH, LL, LH, and Initials were -278 ± 222 μmol SO_4^{2-} m^{-2} h^{-1}; -462 ± 570 μmol SO_4^{2-} m^{-2} h^{-1}; -566 ± 130 μmol SO_4^{2-} m^{-2} h^{-1}; -777 ± 260 μmol SO_4^{2-} m^{-2} h^{-1}; and -322 ± 222 μmol SO_4^{2-} m^{-2} h^{-}

^{1}, respectively. Downward flux calculations followed Fick's first law of diffusion, assuming steady-state conditions and molecular diffusion. Salinity (10-14) of ambient, replacement waters was sufficient for replenishment of SO_4^{2-}. Profiles of Cl^- for all treatments decreased from surface sediment salinities between ~ 12 and 14 to ~ 9 at depth; profiles of Initials were more vertical in nature, with salinities at ~ 10. Ratios of SO_4^{2-} to Cl^- in La Trappe Creek sediments initially ranged from 0.004 to 0.041, with the greatest ratios occurring within surface sediments (Figure 5.1, panel (b)). Although an increase in SO_4^{2-} : Cl^- ratios were observed in profiles from all treatments, sediment cores receiving ~ 1.5 g C m^{-2} d^{-1} (HL, LL) exhibited the greatest increase in surface (0-0.5 cm) sediment ratios (0.043-0.049). The largest differences between Initial and highly loaded sediments occurred at depths below 2 cm.

Significant treatment effects were identified for ΣH_2S concentrations integrated over the surface 2 cm ($P = 0.0015$). The mean depth-integrated (0-2 cm) concentration of HH cores (8.70 ± 5.69 μmol) was significantly different than the means of cores receiving lower POM additions (0.32 ± 0.11 μmol; 0.15 ± 0.05 μmol) and sediments prior to treatment exposure (0.71 ± 0.45 μmol). LH (5.35 ± 3.35 μmol) was not determined to be statistically different from HH, HL, LL, or Initials. Subsurface peaks in dissolved sulfide were observed for six of the eight cores receiving high levels of POM. Elevated concentrations for low loading treatments were not observed until depths > 2 cm (Figure 5.2, panel (d)).

Solid-phase profiles

Model III, single-factor ANOVAs identified no significant treatment effects for depth-integrated (0-10 cm) concentrations of total, inorganic, and organic phosphorus ($P = 0.4353$; $P = 0.3379$; $P = 0.8937$). Mean (± standard deviation; $n = 16$) profiles of total phosphorus for the four treatments typically presented the greatest concentrations (29.5 ± 9.0 μmol P g^{-1} DW) in the surface 0.5 cm, with concentrations decreasing with depth to 11.4 ± 1.7 μmol P g^{-1} DW. Variability among cores (standard deviations < 2 μmol P g^{-1} DW) decreased below 2 cm. Subsurface peaks in total phosphorus were identified within the 1.5-2 cm depth-interval of duplicate HL cores (35.4 μmol P g^{-1} DW; 81.4 μmol P g^{-1} DW) and a single LL core (50.5 μmol P g^{-1} DW) but not within the profiles of other cores receiving treatment. Inorganic phosphorus comprised ~ 88% and 18% of these subsurface peaks in HL and LL cores, respectively. Percentages of total phosphorus in the organic fraction (40.1 ± 12.5%) were fairly consistent down core; whereas percent organic contents for all treatments generally decreased from a surface (0-1 cm) maximum to ~ 8.5% in the 7-10 cm fraction.

Significant differences due to treatment were identified for depth-integrated (0-2 cm, 0-10 cm) concentrations of HCl-extractable Mn ($P = 0.0005$; $P = 0.0003$), HCl-extractable Fe ($P = 0.0222$; $P = 0.0126$), and AVS ($P = 0.0002$; $P = 0.0004$). Concentrations of HCl-extractable Mn integrated over the 10 cm core for all treatments were significantly different than those for initial La Trappe Creek sediments ($P < 0.0325$). Treatment cores had a mean concentration of 1.04 ± 0.68 μmol Mn g^{-1} DW after 19 d of exposure; whereas Initials possessed a mean concentration of 0.66 ± 0.17 μmol Mn g^{-1} DW (Figure 5.3, panel (a)). Tukey-Kramer least squares means identified

that surface-integrated (0-2 cm) concentrations of HCl-extractable Mn for HH, LL, and LH were significantly different than Initials (16.1 ± 3.2 μmol Mn). No significant difference was identified for HL (24.2 ± 5.3 μmol Mn) and Initials (P = 0.2605), HH, or LL. HCl-extractable Mn concentrations integrated over the surface 2 cm for HH, LL, and LH were 30.8 ± 5.5 μmol Mn; 29.8 ± 4.8 μmol Mn; and 37.1 ± 10.1 μmol Mn, respectively

Depth-integrated concentrations (0-2 cm, 0-10 cm) of HCl-extractable Fe for LH cores were significantly different than initial sediment conditions (P = 0.01052; P = 0.0070). No significant differences were identified among HL, HH, and LL treatments or these treatments and LH or initial cores (P > 0.089). Mean HCl-extractable Fe concentrations for Initial and treatment profiles were: Initials: 73.8 ± 22.1 μmol Fe g^{-1} DW; HL: 88.2 ± 31.0 μmol Fe g^{-1} DW; HH: 88.5 ± 42.3 μmol Fe g^{-1} DW; LL: 92.5 ± 33.6 μmol Fe g^{-1} DW; and LH: 113.3 ± 52.4 μmol Fe g^{-1} DW (Figure 5.3, panel (b)). Minimum (41 μmol Fe g^{-1} DW) and maximum (291 μmol Fe g^{-1} DW) concentrations for all sediment cores (n = 22) differed seven-fold. Surface-integrated (0-2 cm) concentrations of HCl-extractable Fe were the least and greatest for Initials (1,928 ± 375 μmol Fe) and LH cores (3,453 ± 1,152μmol Fe), respectively, with all other treatments located between (~ 2,400 μmol Fe).

Tukey-Kramer least squares means identified the same statistical differences among treatments for 2 cm and 10 cm integrated concentrations of AVS. No significant differences were identified between high loading treatments (P = 0.0831; P = 0.1145), or between HL, HH, LL, and Initials (P > 0.08; P > 0.055). Mean 10 cm depth-integrated concentrations of AVS for low loading (HL: 324 ± 83 μmol S; LL: 299 ± 101 μmol S)

treatments were ~ 100 μmol S less than those for HH (414 ± 28 μmol S) and LH (584 ± 153 μmol S) cores. Surface (0-2 cm) sediment AVS concentrations for high loading cores exceeded those of HL, LL, and Initial cores two to three-fold (Figure 5.3, panel (c)). Similar increases in AVS concentrations were also observed when concentrations were integrated over the surface 2 cm.

No significant differences were identified among treatments or Initials for surface-integrated concentrations of Fe oxides ($P = 0.2825$). A significant treatment effect ($P = 0.0449$) was identified for core-integrated concentrations, but Tukey-Kramer least squares means identified no significant differences among paired treatments ($P > 0.05$). Mean Fe oxide concentrations for all treatments decreased two-fold along core profiles, with the greatest concentrations located in surface sediments (115 ± 20 μmol Fe g^{-1} DW). I measured section-integrated concentrations between 21 and 242 μmol Fe g^{-1} DW (Figure 5.3, panel (d)), and mean surface-integrated concentrations no less than ~ 1,100 μmol Fe.

Microelectrodes

Repeated measures analyses identified a significant treatment*time effect for dissolved O_2 penetration ($P = 0.0135$). Post hoc analysis, using differences of least squares means, determined no significant difference in O_2 penetration between HH and LH or between HL and LL after 3, 6, 9, 12, and 17 d of treatment exposure. Significant time effects ($P < 0.0001$) suggested no difference in dissolved O_2 penetration measured after 3, 6, and 9 d of loading. Mean penetration depths of dissolved O_2 (≥ 20 μmol O_2 L^{-1}) for low and high loading treatments were as follows: Initial: 0.83 ± 0.24 mm, 0.91 ±

0.39 mm; Day 3: 0.83 ± 0.39 mm, 0.28 ± 0.24 mm; Day 6: 0.83 ± 0.46 mm, 0.19 ± 0.16 mm; Day 9: 1.01 ± 0.38 mm, 0.28 ± 0.33 mm; Day 12: 0.58 ± 0.29 mm, 0.14 ± 0.39 mm; and Day 19: 1.54 ± 0.70 mm, 0.46 ± 0.25 mm. Concentrations of dissolved O_2 in overlying waters and, on occasion, in subsurface peaks often approached or exceeded O_2 saturation for ambient temperatures and salinities (~ 225 – 228 μmol O_2 L^{-1}), especially for low loading treatments (Figure 5.4, panels (a-c)). Dissolved O_2 concentrations for a few HL profiles exceeded saturating conditions after 6 (up to 391 μmol O_2 L^{-1}), 9 (up to 259 μmol O_2 L^{-1}), and 12 d (up to 281 μmol O_2 L^{-1}) of loading. Similarly high concentrations were observed for HH on Day 19 (up to 253 μmol O_2 L^{-1}).

A Kruskal-Wallis non-parametric (one-way) ANOVA identified a significant difference due to treatment ($P < 0.0001$) in the depth at which ΣH_2S exceeded 50 μmol L^{-1}. Rank sums (Wilcoxon Scores) for HL and LL treatments were identical; whereas scores for high loading treatments were reduced two- to three-fold. No ΣH_2S, determined from profiles of H_2S and pH, was measured in the surface 19.8 mm of any low loading core after 19 d of POM loading (Figure 5.5, panel (b)). ΣH_2S concentrations exceeded 50 μmol L^{-1} in LH and HH cores at depths between -0.2 and 19.8 mm (7.6 ± 9.2 mm) and 0.8 and 4.8 mm (2.4 ± 1.2 mm), respectively. Concentrations of H_2S in high loading cores often exceeded the linear calibration range (> 300 μmol L^{-1}) for H2S50 microsensors; where concentrations did not exceed this range, ΣH_2S concentrations were comparable to those determined following Cline (1969; Figure 5.2, panel (d)).

pH

After 19 d of loading, the pH of all treatments decreased from an initial mean of ~ 7.47 to ~ 6.9 in the surface 0.5 cm (Figure 5.4, panel (d)). A pH ≥ 7.2 was not observed in low loading cores until depths below the 3-4 cm section; whereas greater pHs were determined for high loading cores above this depth range. HH and LH cores had pH ≥ 7.2 in sediments beneath the surface 1.5 cm and 1 cm, respectively.

Discussion

Additions of *C. virginica* biodeposits supplied organic and inorganic particulates of carbon, nitrogen, phosphorus, and iron and manganese oxy(hydr)oxides to the sediment surface of incubated cores (Table 5.1), and thereby, enhanced depth-integrated concentrations within all cores after 19 d of treatment exposure (Table 5.2-5.3). Ratios of total carbon to nitrogen (8.05 ± 0.09) fell between those of phytoplankton (6.625) and freshly deposited marine organic matter (10); such similarity with these sources of organic matter was expected since *C. virginica* filter suspended particulates from the water column. Biodeposits in my study were collected from oysters reared in inflowing, mesohaline waters of the Choptank River, Chesapeake Bay, MD (38° 35.6' N, 76° 7.8' W) during summer. At this time of maximum oyster feeding, as much as 80 to 90% of filtered particles are voided as pseudofeces, readily supplying labile POM in the form of intact algal cells to sediments (Newell and Jordan 1983). Slight enrichment of phosphorus relative to nitrogen (13.01 ± 0.45) was likely associated with nitrogen limitation in eutrophic Choptank waters (Fisher et al. 1988; Fisher et al. 2006), preferential assimilation of nitrogen by *C. virginica* (Newell and Jordan 1983), and

adsorption of PO_4^{3-} onto iron-rich particles (e.g., Chen et al. 1973; Patrick and Khalid 1974; Krom and Berner 1980; Crosby et al. 1984; Froelich 1988; Parfitt 1989; Slomp and van Raaphorst 1993). Biodeposits are a source of chemical oxidants (and reduced organic carbon) which influence the interaction of manganese, iron, and sulfur and their joint influence on organic matter oxidation and sediment phosphorus dynamics.

Ratios of total carbon to nitrogen and to phosphorus (104.81 ± 41.18) within *C. virginica* biodeposits were less than those of surface sediments initially collected from La Trappe Creek (Table 5.4). Modifications of nutrient ratios within surface (0-1 cm) sediments were not merely associated with the dilution of sediment from additions of biodeposits, as ratios would have decreased for all combinations of carbon, nitrogen, and phosphorus within surface sediments. Total carbon to nitrogen ratios did decrease from initial conditions, with high loading treatments approaching the ratio maintained by *C. virginica* biodeposits. Similar decreases occurred for total carbon to nitrogen and total nitrogen to phosphorus ratios for HL and LL sediments. Ratios of total carbon and nitrogen to phosphorus in high loading treatments, however, increased with enhanced efflux of SRP to overlying waters (Chapter 4). Slightly lesser ratios for HL surface (0-1 cm) sediments coincided with a greater retention of phosphorus within shallow water sediments receiving higher levels of surface sediment irradiance (Cerco and Seitzinger 1997; Sundback and Graneli 1988; Chapter 4). Increased benthic oxygenic photosynthesis in HL sediments extended phosphorus retention to depths greater than 1 cm (Chapter 4); retention in LL sediments was predominately in the surface layer (Table 5.2-5.3). Analogous responses were not observed for HH and LH sediments, as sediments consistently maintained more reducing conditions (i.e., dark O_2 flux) and SRP

release in the dark (Chapter 4). Although mass balances indicate the retention and loss of organic and inorganic phosphorus, respectively, assimilation of inorganic phosphorus (e.g., PO_4^{3-}) and incorporation in benthic photoautotrophic biomass (i.e., increased sediment chlorophyll *a*; Chapter 4) was likely responsible for the observed retention of added organics (Table 5.2).

Discrepancies in surface- and core-integrated concentrations of total phosphorus occurred within treatments and, thereby, illustrated the importance of mobility and reoxidation in phosphorus retention in shallow water sediments (Table 5.2-5.3). High loading sediments retained less phosphorus than provided through additions of *C. virginica* biodeposits, and the greatest proportion of what was retained was found in surface (0-1 cm) sediments. Increases in pore water SRP in the upper ~ 3 cm, and decreased retention of solid-phase phosphorus within the 10 cm core relative to surface sediments, indicate an upward migration of phosphorus released from the reduction of oxy(hydr)oxides. Reduction of iron oxy(hydr)oxides was likely more influential in the release/migration of phosphorus than manganese given the relatively low concentrations of HCl-extractable manganese within La Trappe Creek sediments (Figure 5.3) and relative differences in the adsorptive capacity of manganese and iron oxy(hydr)oxides for phosphate. Enrichment in pore water SRP coincided with sub-surface and surface peaks in total dissolved sulfide and AVS, respectively (Figures 5.2-5.3); similar increases in pore water NH_4^+ were not observed. Low loading treatments incorporated all additional phosphorus supplied from *C. virginica* biodeposits and a proportion of pore water SRP (i.e., observed as a reduction in pore water concentrations in surface 3 cm) within the solid-phase fraction. No dissolved sulfide occurred within the surface ~ 2 cm of low

loading sediments, as sufficient iron was available to inhibit accumulation (Canfield 1989; Canfield et al. 1992).

Pore water concentrations of NH_4^+, not unlike SRP, were lower in the upper ~ 3 cm of sediments receiving lower levels of POM deposition (Figures 5.1-5.2). Incorporation of pore water SRP into the solid-phase, total phosphorus pool occurred through adsorption onto newly added or formed iron oxy(hydr)oxides. Increases in iron oxy(hydr)oxides in HL and LL cores exceeded additions from *C. virginica* biodeposits; maximum retention of iron, like total phosphorus, occurred in surface (0-1 cm) sediments and at depth for LL and HL cores, respectively (Table 5.2-5.3). Reductions in sediment uptake ratios of NH_4^+ to SRP in the upper ~ 2 cm (NH_4^+ : SRP; HL: 3.63 ± 0.89; LL: 3.09 ± 0.59) illustrate that assimilation was not the only mechanism responsible for decreases in dissolved phosphorus. Although loss of NH_4^+ may have been associated with oxidation to NO_2^- and NO_3^- by dissolved oxygen or added manganese oxy(hydr)oxides (Henriksen et al. 1981; Henriksen and Kemp 1988; Luther et al. 1997; Hulth et al. 1999; Anschutz et al. 2005), surface additions and minimal dissolved oxygen penetration would have likely restricted oxidation to the surface few mm. Changes in the exchangeable fraction of NH_4^+ adsorbed onto silts and clays seem unlikely given consistencies in pore water and water column salinity (Boatman and Murray 1982; Seitzinger et al. 1991; Rysgaard et al. 1999; Hou et al. 2003).

Further support for the role of iron oxy(hydr)oxides in sediment phosphorus dynamics was evident from relationships of pore water NH_4^+, SRP, and SO_4^{2-}. Increased gradients of pore water SO_4^{2-} were indicative of enhanced rates of sulfate reduction within sediments, but anaerobic degradation of organic matter was not solely responsible

for observed increases in pore water SRP or shifts in NH_4^+ to SRP ratios. If sulfate reduction were the only mechanism responsible for available SRP pools, especially in highly loaded sediments, pore water NH_4^+ concentrations would have also coincided with consumption of SO_4^{2-} (Figure 5.6; *See Figure 5.1*). Instead pore waters within all treatments and initial sediments were enriched in SO_4^{2-} relative to NH_4^+ concentrations (i.e., observed as an off-set of data from predicted 53 SO_4^{2-} : 16 NH_4^+ ratio). Separation of initial and treatment concentrations were due to increased concentrations of SO_4^{2-} (i.e., greater y-intercept) in overlying tank waters (Range: 7.8-10.2 mmol L^{-1}) relative to La Trappe Creek initially (7.6 mmol L^{-1}); slopes were comparable among treatments.

Differences in relationships for NH_4^+ and SRP concentrations with SO_4^{2-} suggest that reduction of iron oxy(hydr)oxides occurs through iron-sulfide mineral formation; shifts in iron-sulfide profiles were observed (e.g., AVS; Figure 5.3). Build-up of total dissolved sulfide in highly loaded surface sediments corresponds with loss of reactive iron for continued mineral formation from elevated rates of deposition (e.g., Rickard et al. 1999). Preservation of iron oxy(hydr)oxides at depth was likely associated with enhanced crystallinity (i.e., age, variability in susceptibility to reduction) and/or protection from reduction through surface coatings (Canfield et al. 1992; Postma 1993; Biber et al. 1994; Slomp et al. 1996). Release of phosphorus has been observed in sediments overlain by oxygenated waters during sulfate reduction and consequent iron monosulfide and pyrite production (Rozan et al. 2002).

Sediment consumption of SRP and release of iron-bound phosphorus in low and high loading treatments, respectively, led to shifts in NH_4^+ to SRP ratios within pore waters of surface (0-0.5 cm) sediments. Ratios at depths greater than 1.5 cm resembled

those within profiles from initial sediments (~ 3-5). Increased ratios in HL (14.18 ± 9.21) and LL sediments (12.95 ± 9.98) corresponded with continual, net effluxes of NH_4^+ relative to near-zero or minimal exchange of SRP (Chapter 4). High loading sediments maintained an enrichment of pore water SRP relative to NH_4^+ (HH: 3.26 ± 1.06; LH: 5.92 ± 1.51), and ratios were in proportion with ratios of measured, intermediary fluxes (Chapter 4). Pore water ratios provided some indication as to the relative release of NH_4^+ and SRP, but diffusive fluxes, calculated from concentration gradients, typically underestimated sediment exchange (Figure 5.7). Discrepancies in the magnitude of measured and diffusive fluxes may have been related to the depth-scale of pore water sectioning and biological advection (e.g., Aller 1980), but inaccurate estimates of porosity at the sediment-water interface, due to scale of measurement (0-1 cm), were likely responsible. Compaction and further dewatering of biodeposits led to no measurable change in sediment heights, as determined from periodic measurements of water column heights during flux incubations. Additions of biodeposits (volume: ~ 15 and 76 cm^3) had the potential to increase sediment heights between ~ 0.5 and 2.4 cm.

Pulsed additions of *C. virginica* biodeposits stimulated microbial respiration of non-refractory carbon and led to increases in surface (0-1 cm) sediment concentrations of total carbon (Table 5.2). Discrepancies within mass balances suggest that a fraction of the added carbon was lost to the water column (Table 5.1-5.2), and conversions of net ecosystem metabolism indicate that the dissolved inorganic carbon flux from aerobic respiration was insufficient to account for total losses (Figure 4.3; Figure 5.8). Iron and manganese reduction were most likely minor pathways for organic matter oxidation initially, as sediments exhibited low dissolved iron and HCl-manganese concentrations

and nearly constant profiles of iron oxy(hydr)oxides (Figures 5.1-5.2). Sulfate reduction, like in other coastal sediments, presumably contributed greatly to organic matter mineralization (e.g., Jorgensen 1977; Capone and Kiene 1988; Roden and Tuttle 1993; Kasten and Jorgensen 2000). Degradation through sub-oxic electron acceptors likely increased, however, with additions of *C. virginica* biodeposits, which were enriched in manganese and iron oxy(hydr)oxides relative to sediments (Table 5.1-5.2). Rates of sulfate reduction, estimated from gradients of pore water SO_4^{2-} concentrations, were maintained (HL) or increased within surface (0-2 cm) sediments (HH, LL, and LH). The proportion of organic matter oxidation that occurred through aerobic and anaerobic respiration, including metal reduction, cannot be resolved from my measurements. Further resolution of carbon not retained within sediments may have been established with flux estimates of dissolved organic carbon and pore water concentrations of dissolved organic and inorganic carbon (e.g., Burdige et al. 1992; Burdige et al. 1994; Middleboe et al. 1998; Alperin et al. 1999).

Additions of *C. virginica* biodeposits not only enhanced rates of microbial respiration, but they also prompted increases in oxidation-reduction cycling within sediments through enhanced benthic oxygenic photosynthesis and increased availability of manganese and iron oxy(hydr)oxides (Chapter 4; Table 5.1). Reoxidation of reduced chemical species, as identified by decreased pH, occurred at depth as great as ~ 4 cm within all treatments, and maximum reoxidation was observed within the 0-0.5 and 1-1.5 cm depth intervals for high and low loading treatments, respectively (Figure 5.4). Stepped increases in pH near the sediment-water interface in HL and LL sediments were associated with the development of a pH maximum at the depth of greatest dissolved O_2

concentrations and CO_2 consumption (*see* Revsbech et al. 1988). Similar increases in pH in highly loaded sediments were muted by metal and sulfate reduction, the relatively shallow penetration of dissolved O_2, and the scale of pH measurements. Although lesser values of pH within sediments do not necessarily coincide with greater reoxidation relative to other treatments (i.e., shifts in pH are a function of the balance between oxidative and reductive processes), increased ratios of SO_4^{2-} to Cl^- suggested that the greatest rates of reoxidation likely occurred in low loading sediments (HL, LL; Figure 5.1). Differences among treatments (for pH) were likely driven by the mode of iron liberation and degree of iron-sulfide precipitation (Boudreau and Canfield 1988).

Although direct coupling of redox-sensitive species cannot be determined from my measurements, discrepancies in mass balances and coincident profiles (i.e., O_2, dissolved Fe (II,III), ΣH_2S, AVS, pH) offered insights into interactions among cycles. Reoxidation within all treatments extended below the penetration depths of dissolved oxygen (Figure 5.1, 5.4), and peaks in reoxidation coincided with increasing concentrations of dissolved iron (II, III). Biological pumping and retention of O_2 within bubbles on microalgal mat surfaces may have expanded the depth- and time-scale of reoxidation by oxygen (e.g., Revsbech et al. 1980b; Revsbech et al. 1983), but additional oxidants, such as manganese and iron oxy(hydr)oxides, were likely more important at greater depths. Build-up of dissolved iron (II, III) within pore waters occurs through iron oxy(hydr)oxide reduction and/or liberation of iron from oxidation of sulfur in iron-sulfide minerals (e.g., FeS, FeS_2). Thermodynamics and frontier molecular orbital theory have been used to demonstrate that reactions of iron sulfides and dissolved sulfide (e.g., H_2S, HS^-) with dissolved oxygen are slow or unfavorable, respectively ($t_{1/2}$ = ~ 1 d for O_2;

Millero et al. 1987; Luther and Ferdelman 1993; Luther 1990). Proximities of dissolved oxygen with FeS and FeS_2 are uncertain, but microelectrode profiles verified the presumed separation of oxygen and ΣH_2S (Figures 5.4-5.5).

In contrast with dissolved oxygen, manganese oxy(hydr)oxides and iron (III) react quickly with reduced sulfur species, and $Mn^{2+/3+}$ and Fe^{2+} have been cited as potential catalysts between dissolved oxygen and reduced sulfur (Aller and Rude 1988, *see* Luther 2005a). Oxidation of aqueous Fe^{2+} and $Mn^{2+/3+}$ by dissolved oxygen requires the transfer of electrons to the metal d orbitals via an outer- and inner-sphere mechanism, respectively (Luther 2005b). At the pH in my sediments, abiological oxidation of Fe^{2+} occurs more rapidly than that of Mn^{2+} (pH < 9; Stumm and Morgan 1996). Biological mediation often enhances rates of manganese oxidation, but net loss of added manganese oxy(hydr)oxides suggests that slower, abiological reactions were primarily responsible for manganese retention within these sediments (Table 1-3). Mn^{2+} that escaped into the water column may have been short-lived, as water in tanks was exchanged regularly. Minimal retention of added manganese does not preclude recycling during the photoperiod, as NO_2^-, NO_3^-, Fe^{3+}, and iron oxy(hydr)oxides may have served as oxidants. Recycling or addition of manganese may have been responsible for the observed increase in iron oxy(hydr)oxides in low loading treatments through reoxidation of Fe^{2+} or sulfur in AVS or FeS_2. Reoxidation of AVS in the surface ~ 0.5 cm likely occurred after initial increases in sulfate reduction were met with continual additions of iron and manganese oxy(hydr)oxides. High concentrations of FeS_2 (i.e., chromium-reducible sulfur) have been shown to exist in the upper 10 cm of La Trappe Creek sediment (Range: 146-418 μmol S g^{-1} DW, Summer 2005; Chapter 2-3).

In summary, my laboratory experiment verified the importance of iron oxy(hydr)oxide reduction in sediment phosphorus mobility and availability for exchange at the sediment-water interface in shallow, illuminated sediments. Pulsed additions of *C. virginica* biodeposits supplied sufficient manganese and iron oxy(hydr)oxides to support the incorporation of added phosphorus and prevent exchange at the sediment-water interface in the absence of iron-sulfide mineral formation (Figure 5.9). Sediments receiving lower rates of organic matter loading were able to develop a reserve of iron oxy(hydr)oxides within surface sediments and, thereby, retain additional phosphorus from pore waters. Added manganese oxy(hydr)oxides were typically not incorporated within sediments and, as such, did not directly serve to increase the adsorptive capacity of sediments for phosphorus. Reoxidation of reduced iron and sulfur species by manganese oxy(hydr)oxides, however, likely aided enhanced surface retention of phosphorus. Although dissolved oxygen from benthic photosynthesis served to re-oxidize iron and manganese in surface sediments, I suspect that these fine-grained sediments would have retained less phosphorus in the absence of oxy(hydr)oxide additions, as might occur under different depositional conditions (e.g., senescent phytoplankton bloom). Shifts in the capacity of sediments to maintain existing and/or retain additional sources of phosphorus directly affect the availability and concentration relative to nitrogen of dissolved inorganic phosphorus and may, thereby, have consequences for benthic and pelagic communities.

Acknowledgements

This research was supported by the University of Maryland Center for Environmental Science, Horn Point Laboratory (HPL), through a student grant supplied to R. R. Holyoke from the HPL Education Committee. Cost of living allowance and tuition costs during preparation of this manuscript was provided by the National Ocean Service (Award No. NA04NOS4290250, Dr. Nancy Foster Scholarship). Nutrient flux data referred to here and presented in Chapter 4 were developed in conjunction with an on-going study supported by the Maryland Sea Grant Program, which intends to quantify the water quality value of benthic microalgal communities in Chesapeake Bay. I thank V. Adams and the Radiation Facility at the University of Maryland College Park for irradiating my samples of biodeposits, and D. Kimmel for advice on statistics. I thank E. Kiss, J. O'Keefe, and M. Owens for providing technical assistance in the Cornwell laboratory, and I especially thank L. Lane of HPL Analytical Services and R. I. E. Newell for assistance with sediment samples run on the CHN elemental analyzer. I also thank J. Seabrease, D. Meritt and C. Rounsaville, and E. Markin and A. Lazur for construction of incubation tanks, collection of eastern oyster biodeposits, and the use of incubation lighting.

Table 5.1 Solid-phase concentrations (μmol g^{-1} dry weight, mean ± standard deviation) of total C, N, and P and HCl-extractable Mn and Fe collected from subsamples (n = 17) of eastern oyster (*Crassostrea virginica*) biodeposits added to laboratory-incubated sediment cores and the total concentration (mmol m^{-2}, mean) of these nutrients added over 19 d for the two experimental loadings (low, high).

Solid-phase species	Solid-phase concentration (μmol g^{-1} DW biodeposits ± SD)	Total concentration added (mmol m^{-2})[a]	
		Low Loading	High Loading
Total C	6713.9 ± 86.5	2,369	11,846
Total N	833.9 ± 16.4	293	1,467
Total P	64.1 ± 3.1	23	113
Inorganic P	55.8 ± 2.7	20	98
Organic P	8.3 ± 3.8	3	15
HCl-extractable Mn	57.9 ± 3.1	20	102
HCl-extractable Fe[b]	174.1 ± 9.3	62	308

[a] Sediment cores possess an inner diameter of 6.35 cm, and thus, a surface area of approximately 0.003 m^2.

[b] Two additional 3.4 g of wet biodeposits (approximately 0.30 g DW) were collected from each irradiated bottle of biodeposits upon opening and discarding (after four days) the slurry. Subsamples were stored frozen until analyzed for acid-volatile sulfides (AVS). No measurable AVS (μmol g^{-1} DW) was detected in these subsamples (n = 9); mV readings for $PbClO_4$ titrations did, however, indicate a slight increase in AVS concentrations for sample bottles.

Table 5.2 Depth-integrated (0-1 cm) solid-phase and pore water concentrations (mmol m^{-2}, mean ± standard deviation) for the initial condition of La Trappe Creek sediments and the four experimental treatments after 19 days of loading. Depth-integrated concentrations are the summed concentrations of each pore water or solid-phase constituent, corrected for the total volume of water or mass of dry sediment, respectively, and the surface area of the core, over the top 1 cm of the core. Treatments are as described in the legend of Figure 5.1.

	Initial	HL	HH	LL	LH
Solid-phase constituents					
Total C	7,796 ± 898	8,462 ± 938	16,100 ± 3,644	9,456 ± 685	14,193 ± 2,087
Total N	682 ± 83	825 ± 113	1,986 ± 591	950 ± 97	1,694 ± 324
Total P	50 ± 7	66 ± 17	101 ± 17	83 ± 22	84 ± 11
Inorganic P	30 ± 7	40 ± 10	61 ± 12	56 ± 20	45 ± 8
Organic P	21 ± 4	25 ± 8	39 ± 7	27 ± 3	39 ± 5
HCl-Mn	2.7 ± 0.6	4.6 ± 2.1	6.5 ± 1.3	6.8 ± 1.6	6.7 ± 1.4
HCl-Fe	335 ± 72	354 ± 69	493 ± 77	430 ± 84	577 ± 115
AVS	54 ± 16	44 ± 14	148 ± 68	41 ± 16	180 ± 63
Fe oxides[a]	281 ± 60	310 ± 70	345 ± 38	347 ± 33	397 ± 110
Pore water constituents					
SRP	0.46 ± 0.19	0.12 ± 0.06	0.53 ± 0.16	0.14 ± 0.08	0.43 ± 0.15
Dissolved Fe	0.2 ± 0.1	1.8 ± 0.8	0.3 ± 0.3	1.0 ± 0.5	0.3 ± 0.3

Dissolved sulfide	0.09 ± 0.02	0.05 ± 0.02	1.21 ± 1.08	0.02 ± 0.02	0.76 ± 0.60
Sulfate	37 ± 7.7	61 ± 7.2	51 ± 4.4	61 ± 3.8	56 ± 11
NH_4^+	1.8 ± 0.4	0.7 ± 0.2	1.7 ± 0.9	0.9 ± 0.2	1.9 ± 0.5

[a] Iron oxide concentrations represent the difference between HCl-extractable Fe and acid-volatile sulfides.

Table 5.3 Depth-integrated (0-10 cm) solid-phase and pore water concentrations (mmol m^{-2}, mean ± standard deviation) for the initial condition of La Trappe Creek sediments and the four experimental treatments after 19 days of loading. Depth-integrated concentrations are the summed concentrations of each pore water or solid-phase constituent, corrected for the total volume of water or mass of dry sediment, respectively, and the surface area of the core, over the top 10 cm of the core. Treatments are as described in the legend of Figure 5.1.

	Initial	HL	HH	LL	LH
Solid-phase constituents					
Total P	444 ± 40	504 ± 44	474 ± 43	484 ± 64	475 ± 36
Inorganic P	261 ± 46	306 ± 49	295 ± 17	296 ± 49	280 ± 33
Organic P	183 ± 30	198 ± 21	179 ± 26	188 ± 36	195 ± 42
HCl-Mn	20 ± 2	25 ± 2	26 ± 1	26 ± 3	29 ± 4
HCl-Fe	2,062 ± 189	2,462 ± 280	2,253 ± 205	2,476 ± 353	2,819 ± 423
AVS	236 ± 66	324 ± 83	414 ± 28	299 ± 101	584 ± 153
Fe oxides[a]	1,826 ± 169	2,137 ± 208	1,839 ± 208	2,005 ± 192	2,235 ± 301
Pore water constituents					
SRP	10.2 ± 1.6	8.8 ± 1.1	9.5 ± 2.7	8.7 ± 1.3	10.2 ± 2.4
Dissolved Fe	0.4 ± 0.2	9.1 ± 4.0	1.0 ± 1.4	5.2 ± 3.3	0.6 ± 0.4
Dissolved sulfide	30 ± 10	15 ± 10	23 ± 14	15 ± 5	17 ± 10

Sulfate	190	± 51	293	± 65	342	± 128	280	± 26	256	± 122
NH_4^+	39	± 6	33	± 6	34	± 11	36	± 2	37	± 9

[a] Iron oxide concentrations represent the difference between HCl-extractable Fe and acid-volatile sulfides.

Table 5.4 Mean ratios (n = 4-6, standard deviations in parentheses) of total carbon, nitrogen, and phosphorus within surface (0-1 cm) sediments from La Trappe Creek initially and after 19 d of treatment exposure. Ratios were determined from solid-phase concentrations (μmol g^{-1} dry weight) of the surface 1 cm of sediment. Treatments are as described in the legend of Figure 5.1.

Treatment	C : N	C : P	N : P
Initial	11.46 (0.77)	158.23 (24.86)	13.78 (1.80)
HL	10.28 (0.45)	134.98 (43.60)	13.09 (4.08)
HH	8.25 (0.61)	166.89 (24.59)	20.36 (3.58)
LL	9.98 (0.35)	150.12 (40.09)	14.98 (3.71)
LH	8.44 (0.42)	169.19 (25.25)	20.20 (3.90)

Figure Legends

Fig. 5.1 Pore water profiles (mean ± standard deviation) of NH_4^+ (**a**) in μmol L^{-1} and SO_4^{2-} to Cl^- ratios (**b**) in mmol L^{-1} for the initial state of La Trappe Creek sediments (Initial, n = 6) and four treatments (n = 4) developed from two surface sediment irradiances (**L:** ~ 10 μmol photons m^{-2} s^{-1}, **H:** ~ 100 μmol photons m^{-2} s^{-1}) and two biodepositional loadings (**L:** ~ 1.5 g C m^{-2} d^{-1}, **H**: ~ 7.5 g C m^{-2} d^{-1}). Treatment identifications correspond to the light and then loading level. **HL:** high light, low loading. **HH:** high light, high loading. **LL:** low light, low loading. **LH:** low light, high loading. SO_4^{2-} to Cl^- ratios in seawater are typically 0.0517 (molality).

Fig. 5.2 Pore water profiles (mean ± standard deviation) of soluble reactive phosphorus (**a**), total dissolved iron (**b**), and total dissolved sulfide (**d**) in μmol L^{-1} and of sulfate (**c**) in mmol L^{-1}. Treatment identifications and number of observations correspond to those described within the legend of Figure 5.1.

Fig. 5.3 Solid-phase profiles (μmol g^{-1} dry weight, mean ± standard deviation) of HCl-extractable Mn (**a**), HCl-extractable Fe (**b**), acid-volatile sulfide (**c**), and iron oxy(hydr)oxides (**d**). Treatment identifications and number of observations correspond to those described within the legend of Figure 5.1.

Fig. 5.4 Dissolved O_2 (**a-c,** μmol L^{-1}, mean ± standard deviation) and pH (**d**) profiles for the initial state of La Trappe Creek sediments (**a**, **d**: Initial, n = 6) and four treatments (n = 4) developed from two surface sediment irradiances and two biodepositional loadings (HL, HH, LL, LH) as described within the legend of Figure 5.1. Two to three microelectrode profiles for dissolved O_2 were performed on each sediment core, using a Clark-type electrode with a 50 micron tip. Dissolved O_2 profiles shown in panels (a), (b), and (c) were observed prior to the start of the four treatments (**a**), after nine days of loading (**b**), and after 17 days of loading (**c**). Dissolved O_2 profiles were repeatedly measured on the same 16 sediment cores. Data identified as Initial for pH (**d**) profiles were measured on sediment cores (n = 6) collected from La Trappe on 31 August 2005 which did not undergo any of the treatments.

Fig. 5.5 ΣH_2S (μmol L^{-1}, mean ± standard deviation) profiles within surface (0-2 cm) sediments of incubated cores prior to the first (**a**) and 19th addition of POM (**b**), as determined with amperometric microsensors for $H_2S_{(g)}$ (Jeroschewski et al. 1996, **H2S50:** www.unisense.com) and pH. H2S50 microsensors are linear in the range of 0 to 300 μmol H_2S L^{-1} and curvilinear at concentrations > 300 μmol H_2S L^{-1}. Mean ΣH_2S concentrations including $H_2S_{(g)}$ concentrations exceeding 300 μmol H_2S L^{-1} are identified in **gray** (HH: 4 cores, LH: 1 core). Means (gray) were calculated assuming that $H_2S_{(g)}$ > 300 μmol H_2S L^{-1} were equal to 300 μmol H_2S L^{-1}. Treatments (n = 4) developed from two surface sediment irradiances and two biodepositional loadings (HL, HH, LL, LH) are as described within the legend of

Figure 5.1. Two to three microelectrode profiles for $H_2S_{(g)}$ were performed on each sediment core, and profiles were repeatedly measured on the same 16 sediment cores. Initial (**a**) and final (**b**) profiles were measured on 01 and 20 September 2005, respectively.

Fig. 5.6 Pore water NH_4^+ (**a**) and soluble reactive phosphorus (**b**) concentrations versus the corresponding SO_4^{2-} concentrations measured initially and upon conclusion of the experiment. Solid lines correspond to the expected stoichiometric ratios if all the available pore water NH_4^+ and soluble reactive phosphorus were generated from anaerobic mineralization (i.e., sulfate reduction) of organic matter. Intercepts were determined from linear regressions of all data points combined. Black and grey arrows along the axes correspond to the initial and final concentrations of these nutrients in the water column, respectively.

Fig. 5.7 Calculated pore water upward fluxes of NH_4^+ (**a**) and soluble reactive phosphorus (**b**) versus the corresponding sediment fluxes ($\mu mol\ m^{-2}\ h^{-1}$) measured in the dark upon conclusion of the experiment, after 19 d of loading, as presented in Chapter 4. Solid lines indicate the 1:1 ratio of measured versus predicted fluxes. Pore water upward flux calculations followed Fick's first law of diffusion, assuming steady-state conditions and molecular diffusion. Diffusion coefficients within sediments were estimated from the diffusion coefficient in free solution at ambient temperature (28°C) divided by the quantity of one minus the natural log of porosity squared. Porosity was approximated from measured

percent water content (0-1 cm). Treatment identifications correspond to those described within the legend of Figure 5.1, and methods of determining sediment fluxes are described in Chapter 4. Uncharacteristic shapes of pore water profiles for a single HL sediment corresponds to the occurrence of one HL data point within the range of NH_4^+ efflux for high loading treatments; see the *Pore water profiles* section within *Results*.

Fig. 5.8 Dissolved inorganic carbon (DIC, μmol C m^{-2} d^{-1}) fluxes estimated from stoichiometric conversions (138 O_2 : 106 C) of net ecosystem metabolism (NEM, Figure 4.3, panel (b)) for four treatments (HL, HH, LL, LH) developed from two surface sediment irradiances and two biodepositional loadings as described in the legend of Figure 5.1. Shading within bars corresponds to the number of days sediments have been receiving treatment.

Fig. 5.9 Potential interactions of oxidized and reduced forms of iron, manganese, and sulfur species and their combined influence on the retention and mobility of phosphorus within sediments. Reduction of iron oxy(hydr)oxides (represented by $Fe(III)_{ox}$) by dissolved sulfide may result in the release of dissolved iron (II) and phosphate (e.g., HPO_4^{2-}, PO_4^{3-}). Diffusion of Fe^{2+} may result in the formation of aqueous and/or solid phase iron-sulfides or newly formed, less crystalline iron (III) oxy(hydr)oxides with increased adsorptive capacities for phosphate. The adsorptive capacity of manganese oxy(hydr)oxides (represented by MnO_2) for phosphates is less than that of iron oxy(hydr)oxides and, as such, manganese

likely has minimal direct influence on phosphorus retention and mobility. Reduction of manganese oxy(hydr)oxides by Fe^{2+}, however, likely leads to the formation of new iron oxy(hydr)oxides and even greater retention of phosphate. Retention of manganese within sediments may be limited due to the slow abiological process of oxidation between Mn^{2+} and O_2.

Fig. 5.1

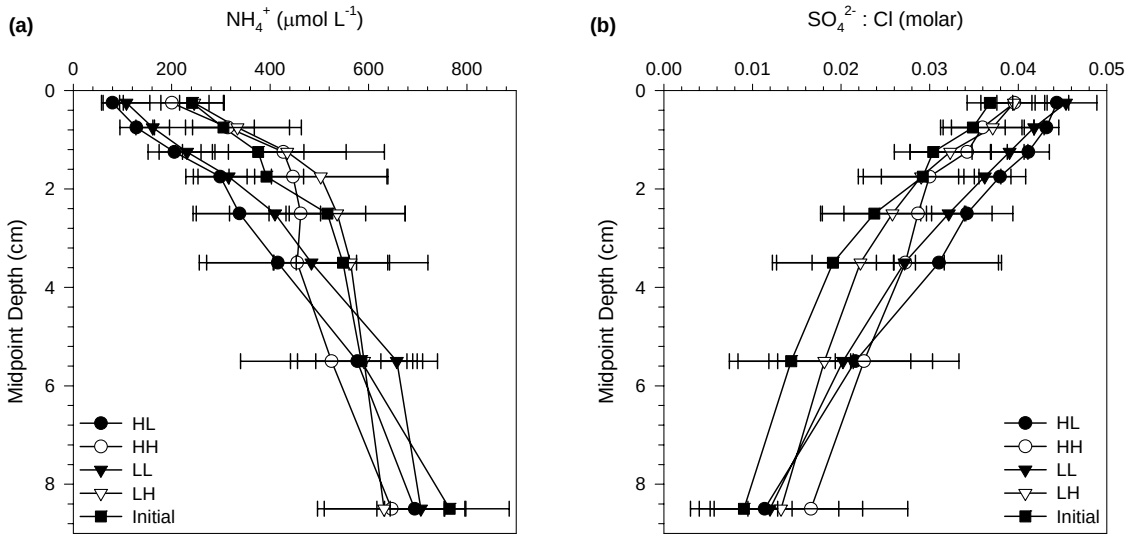
(a)
NH4+ (μmol L-1)
0
200
400
600
800
Midpoint Depth (cm)
0
2
4
6
8
HL
HH
LL
LH
Initial
(b)
SO4 2- : Cl (molar)
0.00
0.01
0.02
0.03
0.04
0.05
Midpoint Depth (cm)
HL
HH
LL
LH
Initial

Fig. 5.2

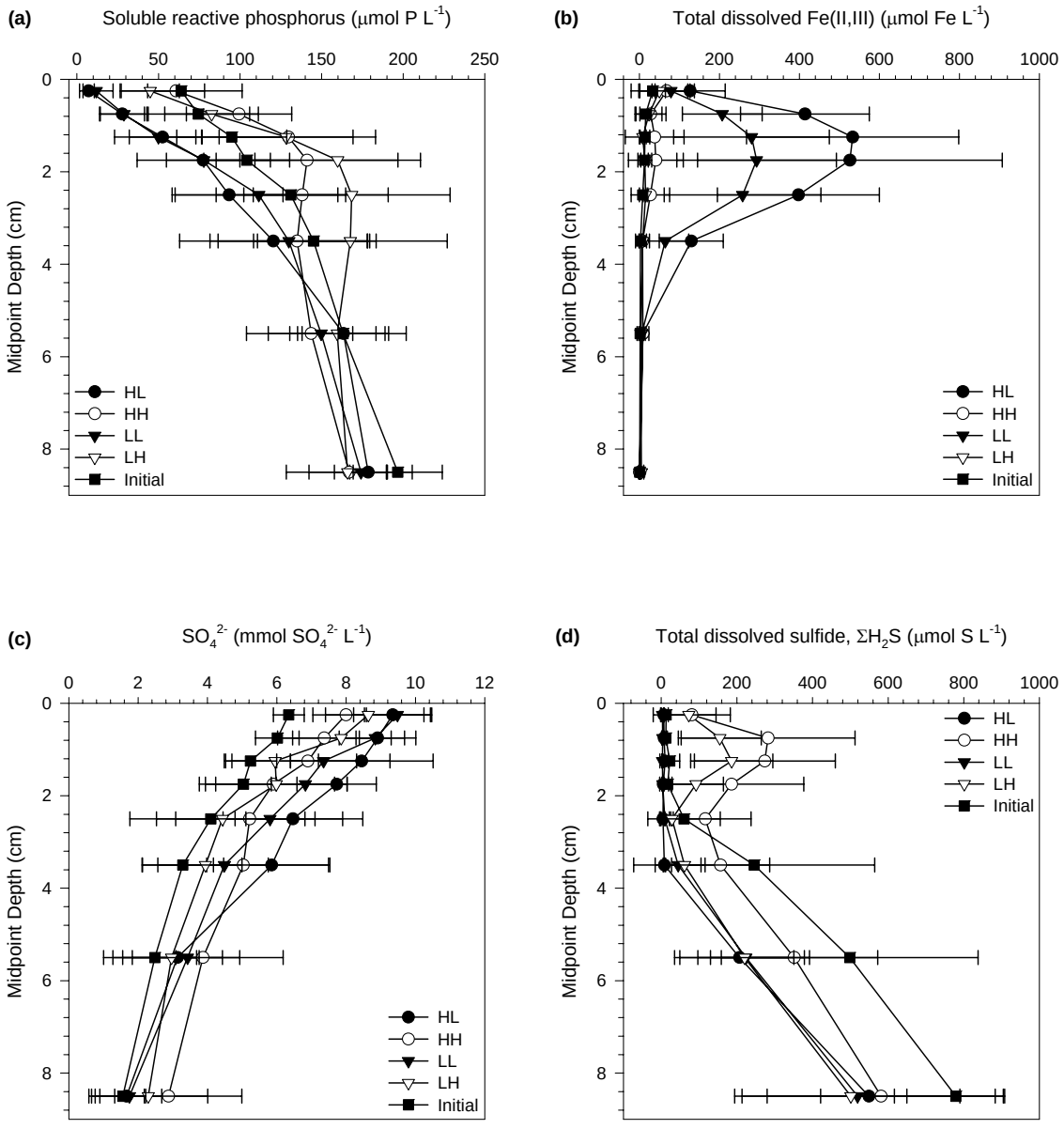
(a)
Soluble reactive phosphorus (μmol P L-1)
Midpoint Depth (cm)
HL
HH
LL
LH
Initial
(b)
Total dissolved Fe(II,III) (μmol Fe L-1)
(c)
SO4 2- (mmol SO4 2- L-1)
(d)
Total dissolved sulfide, ΣH2S (μmol S L-1)

Fig. 5.3

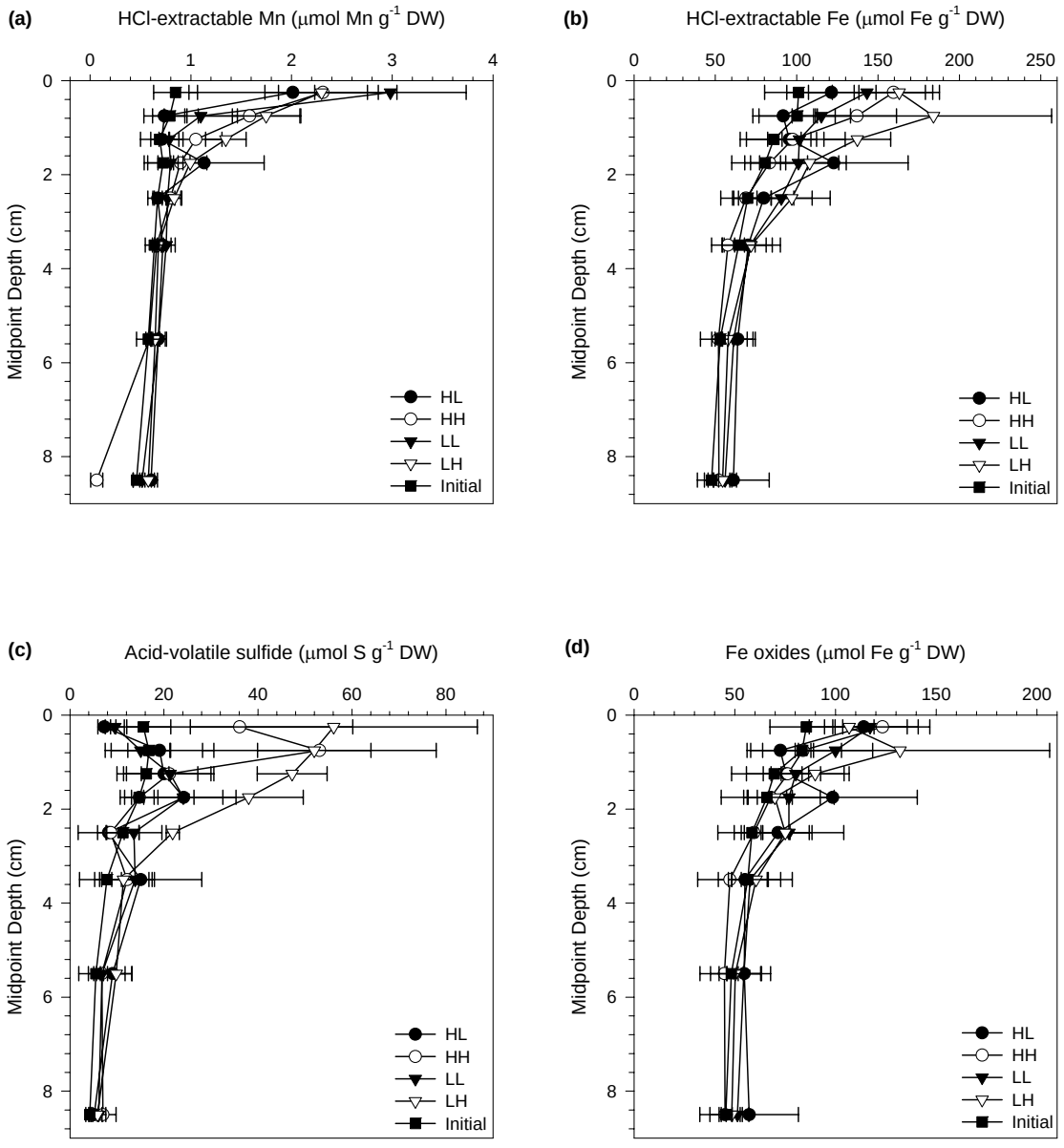
(a)
HCl-extractable Mn (μmol Mn g-1 DW)
(b)
HCl-extractable Fe (μmol Fe g-1 DW)
(c)
Acid-volatile sulfide (μmol S g-1 DW)
(d)
Fe oxides (μmol Fe g-1 DW)
Midpoint Depth (cm)
HL
HH
LL
LH
Initial

Fig. 5.4

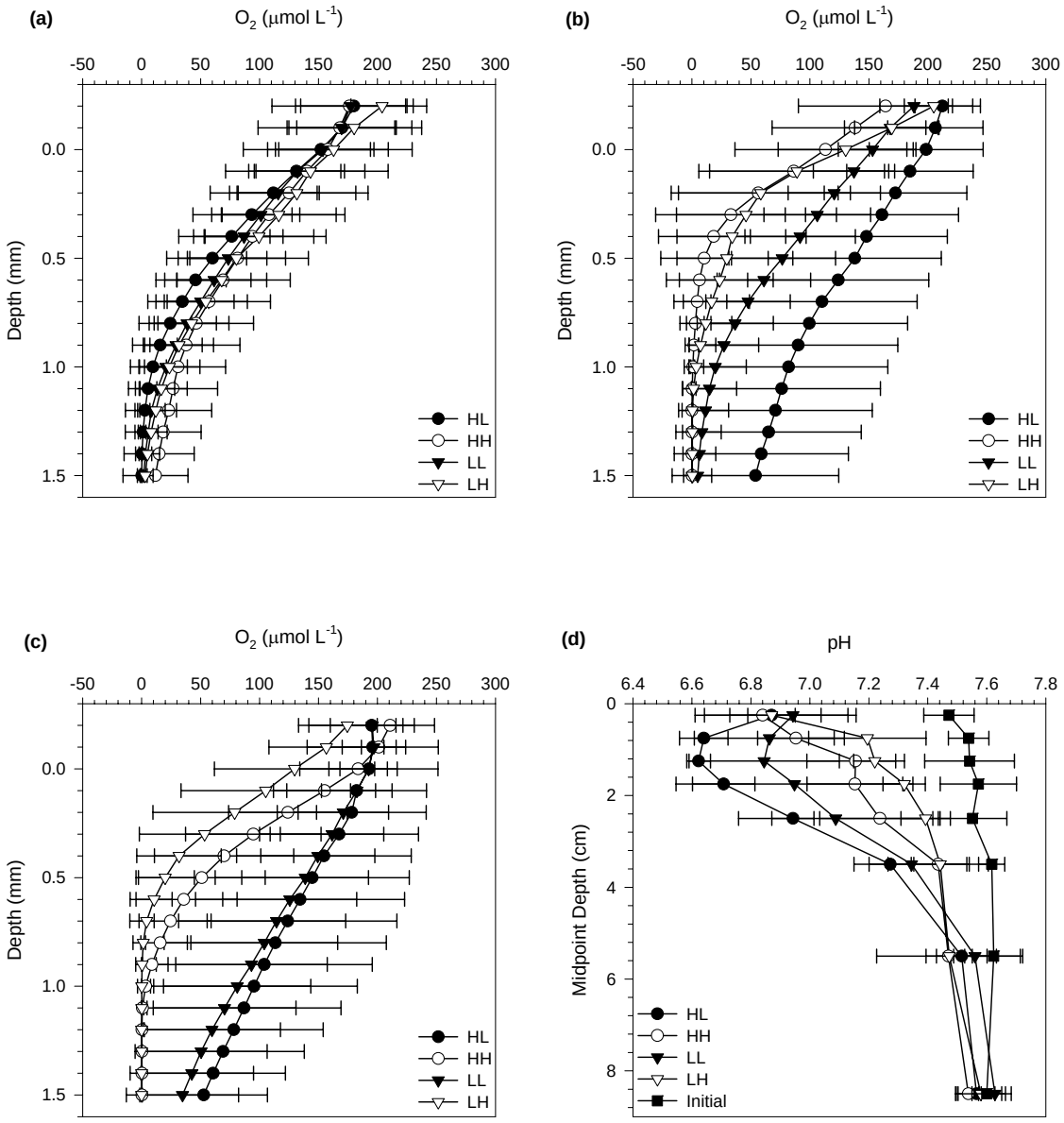
(a)
O2 (μmol L-1)
-50 0 50 100 150 200 250 300
Depth (mm)
0.0 0.5 1.0 1.5
HL
HH
LL
LH
(b)
O2 (μmol L-1)
-50 0 50 100 150 200 250 300
Depth (mm)
0.0 0.5 1.0 1.5
HL
HH
LL
LH
(c)
O2 (μmol L-1)
-50 0 50 100 150 200 250 300
Depth (mm)
0.0 0.5 1.0 1.5
HL
HH
LL
LH
(d)
pH
6.4 6.6 6.8 7.0 7.2 7.4 7.6 7.8
Midpoint Depth (cm)
0 2 4 6 8
HL
HH
LL
LH
Initial

Fig. 5.5

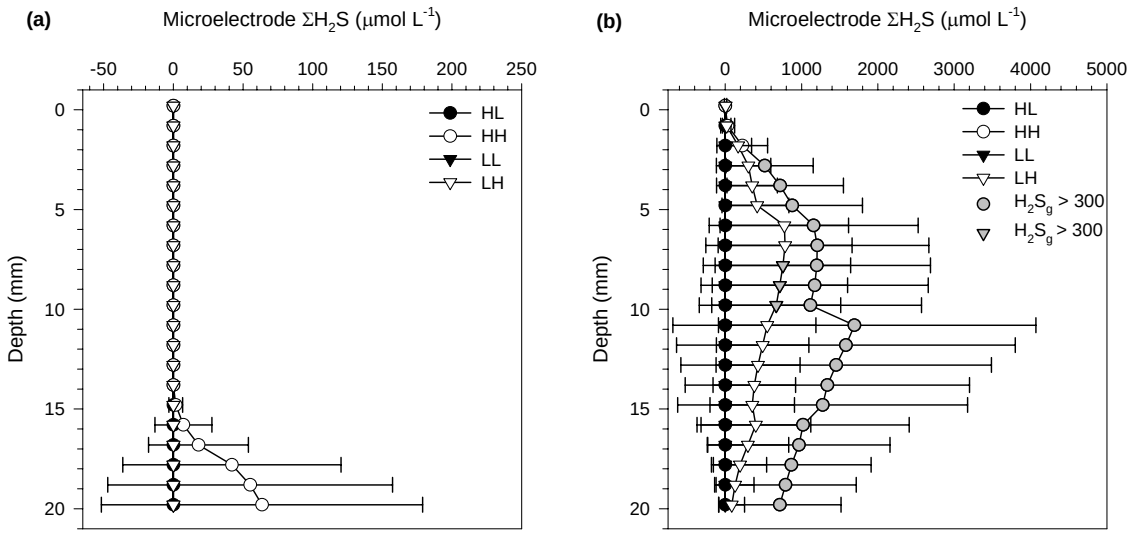
(a)
Microelectrode ΣH2S (μmol L-1)
-50
0
50
100
150
200
250
Depth (mm)
0
5
10
15
20
HL
HH
LL
LH
(b)
Microelectrode ΣH2S (μmol L-1)
0
1000
2000
3000
4000
5000
Depth (mm)
HL
HH
LL
LH
H2Sg > 300
H2Sg > 300

Fig. 5.6

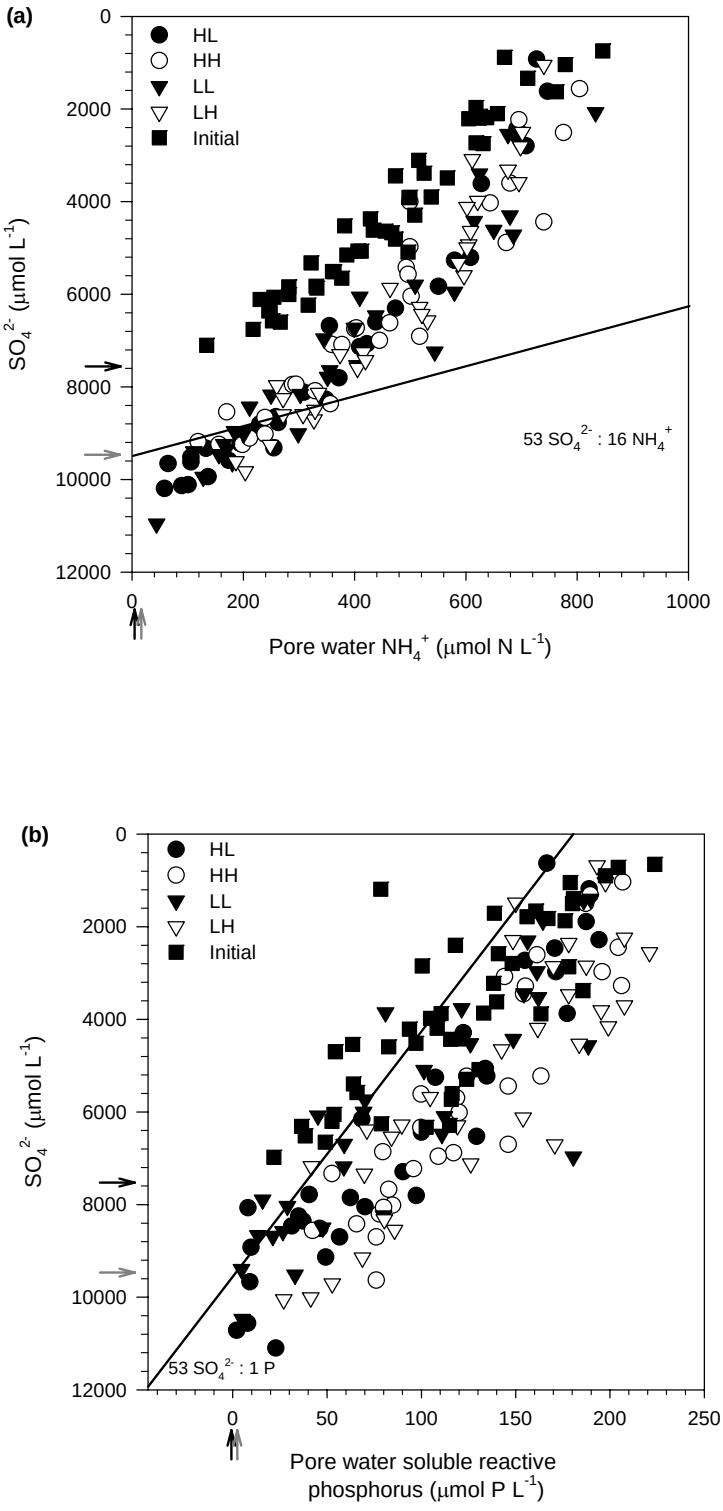
(a)
HL
HH
LL
LH
Initial
SO_4^{2-} (μmol L^{-1})
0
2000
4000
6000
8000
10000
12000
53 SO_4^{2-} : 16 NH_4^+
0
200
400
600
800
1000
Pore water NH_4^+ (μmol N L^{-1})
(b)
HL
HH
LL
LH
Initial
SO_4^{2-} (μmol L^{-1})
0
2000
4000
6000
8000
10000
12000
53 SO_4^{2-} : 1 P
0
50
100
150
200
250
Pore water soluble reactive phosphorus (μmol P L^{-1})

Fig. 5.7

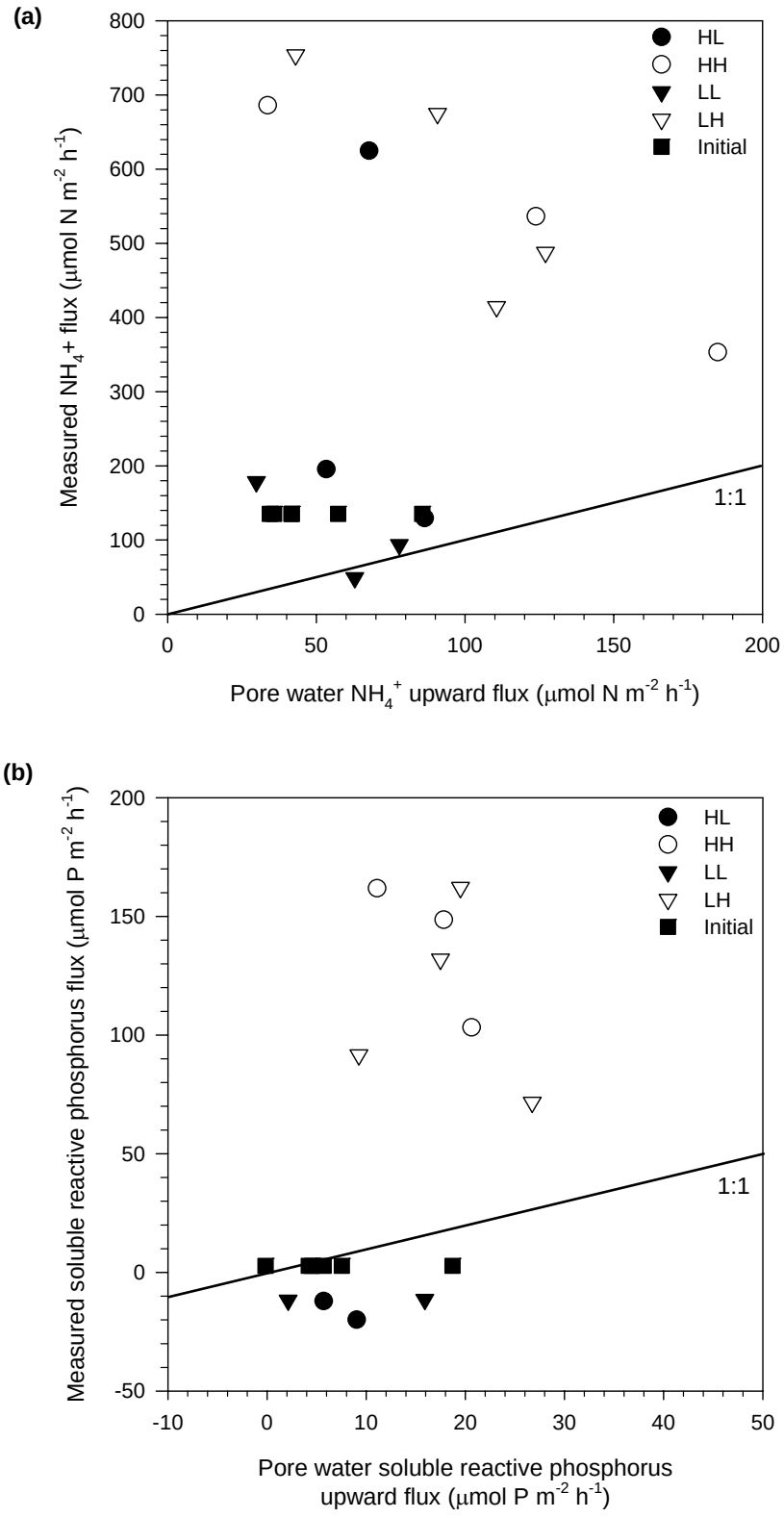
(a)
HL
HH
LL
LH
Initial
1:1
Measured NH4+ flux (μmol N m-2 h-1)
Pore water NH4+ upward flux (μmol N m-2 h-1)
0
100
200
300
400
500
600
700
800
0
50
100
150
200
(b)
HL
HH
LL
LH
Initial
1:1
Measured soluble reactive phosphorus flux (μmol P m-2 h-1)
Pore water soluble reactive phosphorus upward flux (μmol P m-2 h-1)
-50
0
50
100
150
200
-10
0
10
20
30
40
50

Fig. 5.8

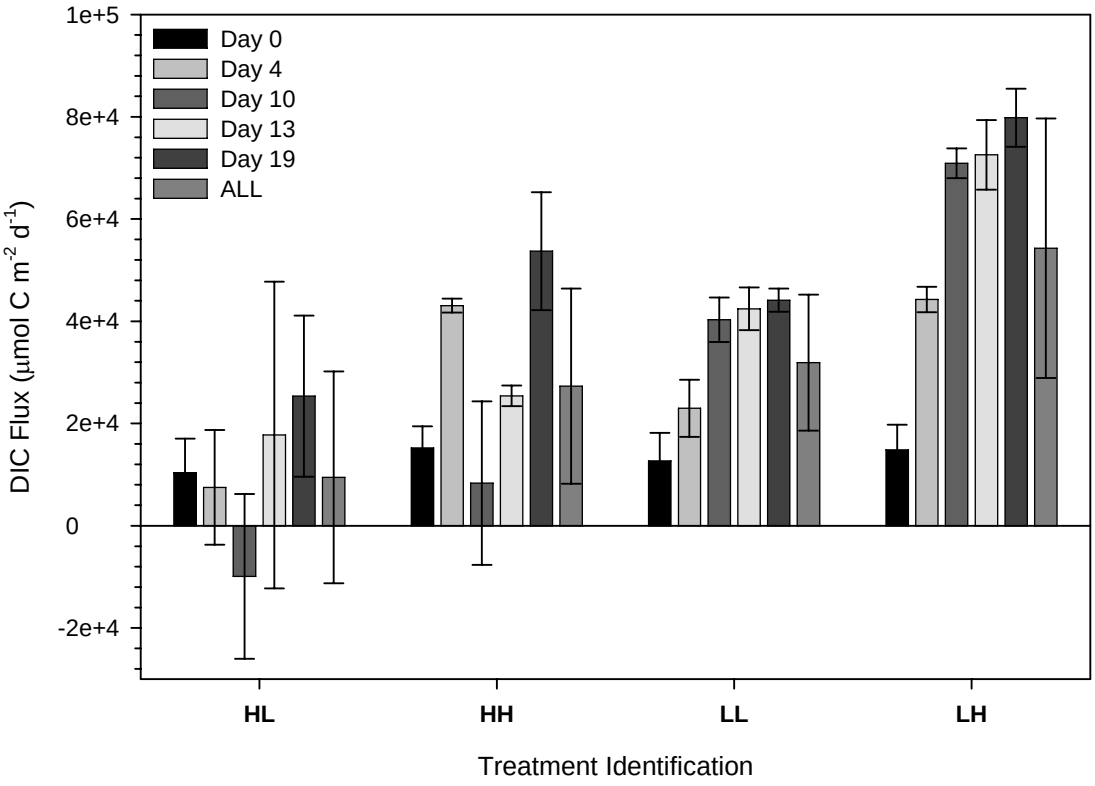
1e+5
8e+4
6e+4
4e+4
2e+4
0
-2e+4
DIC Flux (µmol C m-2 d-1)
Day 0
Day 4
Day 10
Day 13
Day 19
ALL
HL
HH
LL
LH
Treatment Identification

Fig. 5.9

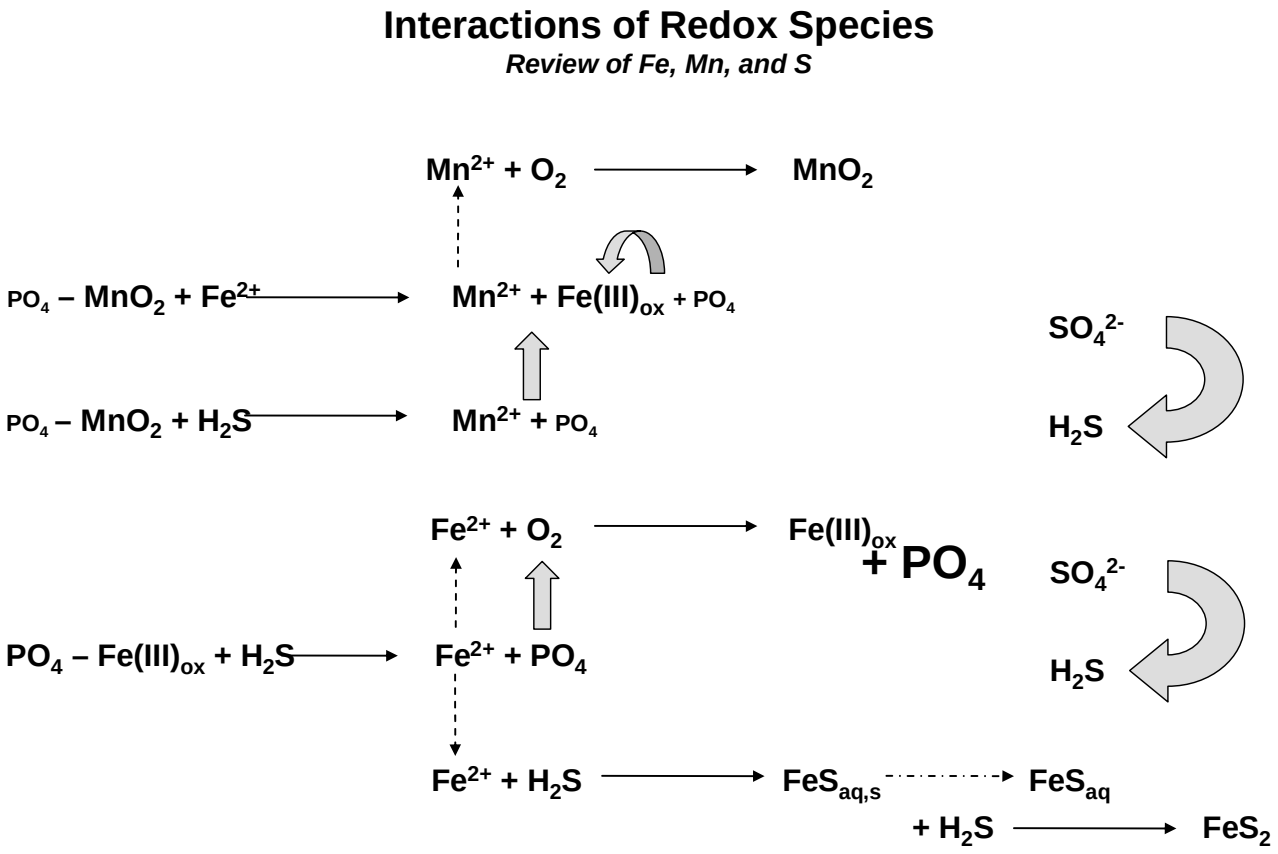
Interactions of Redox Species
Review of Fe, Mn, and S
Mn2+ + O2
MnO2
PO4 – MnO2 + Fe2+
Mn2+ + Fe(III)ox + PO4
SO42-
PO4 – MnO2 + H2S
Mn2+ + PO4
H2S
Fe2+ + O2
Fe(III)ox
+ PO4
SO42-
PO4 – Fe(III)ox + H2S
Fe2+ + PO4
H2S
Fe2+ + H2S
FeSaq,s
FeSaq
+ H2S
FeS2

Appendix A: Critical erosion threshold of eastern oyster (*Crassostrea virginica*, Gmelin) biodeposits: influence of feces, pseudofeces, and incorporation within sediments

Objectives and Hypotheses

Throughout this dissertation, field and laboratory studies indicate that the quantity and quality of *Crassostrea virginica* (Gmelin 1791) biodeposits (feces and pseudofeces) influence the biogeochemical response of sediments and, ultimately, the exchange of nitrogen and phosphorus at the sediment-water interface. Research presented in the following two appendices evaluates how the relative amount of *C. virginica* biodeposits deposited at the sediment surface may be influenced by resuspension events. The following hypotheses were addressed to assess the likelihood of *C. virginica* feces and pseudofeces being eroded if deposited on fine-grained sediments of Chesapeake Bay.

Hypothesis 1 There is no difference in the critical shear stress necessary to erode feces and pseudofeces produced by *C. virginica*.

Hypothesis 2 The proportion of *C. virginica* biodeposits that erode decreases with duration at the sediment surface (i.e., age of biodeposits).

Materials and Methods

Sandpaper 1-6 (BDR03-08)

A total of 46 market-size (~ 7.6 cm, Horn Point brood-stock) *C. virginica* were scrubbed with a domestic sodium hypochlorite and freshwater solution (< 1% volume : volume) to eliminate *Polydora* spp. from shells on 24 April 2006. After rinsing individuals with freshwater, *C. virginica* were placed in individual holding trays, positioned within four shallow pans under inflowing water from the Choptank sub-estuary, Chesapeake Bay (Figure A.1). Flow in pans was maintained so as to supply

adequate food to *C. virginica*, while preventing transport of biodeposits (feces and pseudofeces). Individual *C. virginica* (and trays) were cleaned every 4-5 d from 24 April through 11 May 2006, with freshwater cleanings occurring within 18-24 h of fecal and pseudofecal collections. Biodeposits were collected twice per day from 09 through 11 May 2006 (Sandpaper 1-6, BDR03-08).

Feces and pseudofeces were collected separately with graduated, disposable glass pipettes (VWR serological 10 in 1/10 TD-EX 20°C) with the tips removed. Pipette tips were removed (and flamed) to increase bore size and, thereby, minimize breakage of biodeposits. Separate fecal and pseudofecal collections were possible since *C. virginica* expel feces and pseudofeces to the right- and left-side of the umbo, respectively. Upon collection, biodeposits were allowed to settle in pipettes until accurate volume estimates could be determined. Volumes collected totaled 2.5 ml, 4.4 ml, and 10.6 ml, with the exception of the pseudofecal treatment in Sandpaper 3 (BDR05, 10.8 ml).

PVC discs, with dual O-rings for stabilization, were covered with electro-coated 320A wet and dry silicon carbide abrasive paper (sandpaper) and positioned 10 cm from the top of polycarbonate (9.525 cm ID, 10.16 cm OD) cores. Sandpaper, attached to PVC discs with a thin layer (spread with a razor blade) of DAP silicon rubber sealant, served to mimic fine-grained sediment (36 μm, average particle diameter). PVC push-pins were inserted into the top of sandpaper-discs to eliminate the area of central suction (for the erosion microcosm) and, thereby, reduced the effective core area to 68.337 cm^2. Core headspaces (10 cm, 712.6 ml) were filled with ambient estuarine water (17.5-20.2°C) prior to placement of equal volumes of feces and pseudofeces on sandpaper-discs in separate cores. Each type (feces, pseudofeces) and volume (2.5 ml, 4.4 ml, 10.6 ml)

combination were run twice, and combinations systematically alternated with the turbidimeters and erosion heads. Modified-Gust microcosms (9.525 cm ID, Gust and Müller 1997) were used to expose feces and pseudofeces separately to the following applied shear stresses (Pa, mean ± standard deviation): 0.01 ($0.0100 \pm 3.14 \times 10^{-5}$), 0.05 ($0.0497 \pm 8.90 \times 10^{-5}$), 0.10 ($0.0996 \pm 1.00 \times 10^{-4}$), 0.15 ($0.1495 \pm 2.75 \times 10^{-4}$), 0.20 ($0.1996 \pm 8.69 \times 10^{-5}$), 0.30 ($0.2988 \pm 1.80 \times 10^{-4}$), and 0.45 ($0.4487 \pm 1.85 \times 10^{-4}$).

Sediment 1-15 (BDR09-23)

Ninety-six market-size (≥7.6 cm) *C. virginica* were selected from Horn Point brood-stock and dredged from portions of the Patuxent sub-estuary, Chesapeake Bay, on 16 May 2006. Patuxent *C. virginica* were scrubbed immediately and the following day with a domestic sodium hypochlorite and freshwater solution (< 1% volume : volume), and all *C. virginica* were scrubbed with freshwater every 2-3 d thereafter through 23 May 2006. Feces and pseudofeces were collected with graduated, wide-mouth pipettes and homogenized through placement in glass funnels within 30-34 h of the final freshwater rinse. A total of 63 ml of *C. virginica* biodeposits, 31.5 ml of feces and pseudofeces, were collected for 7 ml additions (0.417 g or 0.061 kg m^{-2}, Figure A.5, panel (A), Figure B.1) to Treatment cores for Sediment 7-15 (BDR09-17). Forty-eight *C. virginica* were maintained through 04 June, with a second sodium hypochlorite cleaning occurring on 30 May 2006. Individual *C. virginica* (and trays) were cleaned 14-28 h before collections of biodeposits for Sediment 1-6 (BDR18-23). *C. virginica* were held in individual holding trays, positioned within four to eight shallow pans, under inflowing estuarine water from

the Choptank. Flow in pans was maintained so as to supply adequate food to *C. virginica*, while preventing transport of biodeposits (feces and pseudofeces).

Thirty sediment cores were collected within the mesohaline portion (salinity, 12.2-12.3) of the Choptank sub-estuary between 38° 37.152'N 76° 08.135 W and 38° 38.187'N 76° 08.148'W on 24 May and 02 June 2006. Cores (9.525 cm ID) were collected by pressing polycarbonate tubes (45 cm in length, 10.16 OD) into sediments retrieved with a box corer. Core tubes were inserted into box-cored sediment so as to maintain a level sediment surface. Water depths varied from 7.5 to 8.5 m during core collection, and surface water temperatures were 18.6 to 24°C.

Upon returning to the laboratory, the 18 and 12 sediment cores collected on 24 May and 02 June, respectively, were randomly designated into Treatment and Control cores. Additions of *C. virginica* biodeposits (7 ml, 3.5 ml of each) were added to Treatment cores (n = 9) from Sediment 7-15 (BDR09-17) on 24 May and allowed to settle in cores for ~ 1 h. Treatment and Control cores were divided and systematically alternated within three MEERC mesocosms (B1-3, 51.4 cm ID, 76.2 cm tall) filled with inflowing 2-μm filtered estuarine water. Treatment and Control cores for Sediment 1-6 (BDR18-23) were immediately submerged in two MEERC mesocosms (B1-2) containing 2-μm filtered water. Additions of biodeposits to these Treatment cores (n = 6) occurred within 20 min and 6 h of erosion experiments on 03 and 04 June 2006. T-bubblers (12.7 cm wide) were positioned approximately 8 cm from the sediment surface for aeration in all cores, and flow within tanks was maintained between 13.2 and 19.8 ml s^{-1}. Cores were aerated continuously, except during additions of *C. virginica* biodeposits (<1 h). Measurements of photosynthetically active radiation with LiCor (2π) light sensors in the

field indicated that no light was available at the sediment surface to support benthic photosynthesis (bottom, <0 μmol photons m^{-2} s^{-1}); tanks were covered with black plastic to maintain these conditions.

Treatment and Control cores for each erosion experiment were randomly selected from the same incubation tank and alternated systematically with the turbidimeters and erosion heads. Cores were adjusted such that the sediment surface was positioned 10 cm from the top of the polycarbonate tube (and level), and PVC push-pins were inserted into the center of surface sediments. Filtered (2 μm) water from the Choptank sub-estuary served as replacement water and, thereby, maintained the headspace within cores. Pairs of Treatment and Control cores were analyzed in triplicate immediately (i.e., <20 min) and within ~ 6 h, 1 d, 4 d, and 7 d of adding *C. virginica* biodeposits. Core analyses for incorporation of biodeposits after 1-7 d (Sediment 7-15, BDR09-17) were staggered approximately every 3 h; additions of *C. virginica* biodeposits were staggered for Sediment 1-6 (BDR18-23). Modified-Gust microcosms (9.525 cm ID, Gust and Müller 1997) were used to expose Treatment and Control cores separately to the following applied shear stresses (Pa, mean ± standard deviation): 0.01 ($0.0099 \pm 5.18 \times 10^{-5}$), 0.05 ($0.0494 \pm 2.36 \times 10^{-4}$), 0.10 ($0.0992 \pm 4.79 \times 10^{-4}$), 0.20 ($0.1986 \pm 9.61 \times 10^{-4}$), and 0.45 ($0.4466 \pm 2.21 \times 10^{-3}$). Problems were identified for three sediment cores (BDR13 T4.2: T-bubbler struck sediment surface; BDR 12 T4.1 and BDR13 C4.2: aeration needed to be reduced).

Field validation with benthic microalgae (Sediment 16-17, Trap 1-4)

A total of four sediment cores were collected from underneath off-bottom aquaculture of *C. virginica* (Mainstem Oyster) and at a corresponding reference site (Mainstem Reference) in the upper reaches of La Trappe Creek on 02 October 2003 (Chapter 3). Off-bottom aquaculture had been established on 29 July 2003 and was maintained through core collection (Table 3.2). Sediment cores were collected in the same manner as those for Sediment 1-15 (BDR09-23), using polycarbonate tubes and box coring. Surface waters (~ 20°C) were collected in three 20 L carboys and used to maintain the headspace (10 cm) during erosion experiments performed later that afternoon and evening. Modified-Gust microcosms (9.525 cm ID, Gust and Müller 1997) were used to expose Oyster and Reference cores separately to the following applied shear stresses (Pa, mean ± standard deviation): 0.01 ($0.0108 \pm 1.33 \times 10^{-5}$), 0.05 ($0.0508 \pm 2.47 \times 10^{-4}$), 0.10 ($0.1033 \pm 7.18 \times 10^{-5}$), 0.15 ($0.1578 \pm 7.06 \times 10^{-5}$), 0.20 ($0.2147 \pm 4.30 \times 10^{-5}$), 0.30 ($0.3376 \pm 5.99 \times 10^{-5}$), and 0.45 ($0.4214 \pm 8.94 \times 10^{-4}$).

Modified-Gust microcosm

Modified-Gust microcosms (Gust and Muller 1997) were used to expose sandpaper and sediment cores to applied shear stresses (τ_b) for the determination of the critical shear stress (τ_c) necessary to erode *C. virginica* biodeposits (Figure A.3). The 9.525-cm microcosms were designed to generate controllable, nearly uniform shear stress using spinning disks within an erosion head and central suction (manufactured at Horn Point Laboratory, P. Dickhudt). A data logger calculates the revolutions per minute (RPM) at which discs should spin and the pumping rate necessary to achieve desired

shear stresses. Replacement water is pumped through individual microcosms (2 per experiment), while effluent with eroded *C. virginica* biodeposits or sediment is passed through a turbidimeter and collected in 1-2 L square, wide-mouth high-density polyethylene (HDPE) bottles. HDPE bottles with collected effluent were stored on ice (in coolers) until transport to dark temperature-controlled chambers (5°C).

All effluent was filtered onto pre-rinsed and ashed (450°C) 47 mm and 142 mm Whatman GF/F filters (0.7 μm) within 1-2 d of collection. Filters were rinsed immediately with UltraPur deionized water before drying to a constant weight (80°C). Total suspended solid (TSS) concentrations, determined from filtering, were used to formulate a calibration of nephelometric turbidity units (NTU) provided by turbidimeters. Formulation of erosion rates (kg m^{-2} s^{-1}), erosion rate constants (M, kg m^{-2} s^{-1} Pa^{-1}), cumulative eroded mass (kg m^{-2}), and critical shear stress (τ_c) followed Sanford and Maa (2001). Filters from each applied shear stress (step interval, τ_b) for Sandpaper 1-6 and Sediment 1-15, not La Trappe Creek, were ashed in a muffle furnace (450°C) for the determination of percent organic content (%, loss on ignition).

Statistical analyses

Statistical analyses of cumulative eroded mass (kg m^{-2}) and loss on ignition (%) were conducted in SAS version 9.1.2 for Windows using Proc Mixed. Output from Sanford and Maa (2001), conducted in MatLab R2006a, provided cumulative eroded masses (kg m^{-2}) for each applied shear stress (τ_b) at slightly different critical shear stresses (*see* Figure A.4). In order to provide comparisons of cumulative eroded mass between treatment (feces, pseudofeces, biodeposits) and control cores, I conducted linear

interpolations of eroded mass (kg m^{-2}) between critical shear stresses (τ_c) encompassing a selected set of shear stresses. Defined shear stresses were 0.05 and 0.10 Pa for Sandpaper 1-6 (BDR03-09), and 0.10, 0.20, and 0.30 Pa for Sediment 1-17. Percent organic contents (%) were compared for step intervals, without corrections or interpolation.

This experimental design was a randomized complete block with repeated measures. Each treatment combination – volume (2.5 ml, 4.4 ml, 10.6 ml) and treatment (feces, pseudofeces) or time (immediate, 6 h, 1-7 d) and treatment (control, treatment) – constituted a main plot within which the levels of shear stress (τ_b, τ_c) were subsequently applied. Because shear stresses (τ_b, τ_c) were not random, but in sequence (0.01-0.45 Pa), they constituted a repeated rather than a split-plot factor. Fit statistics (AIC model) were used to determine the appropriate covariance model for each repeated measure, and statistical tests relied on autoregressive, compound symmetry, and unstructured models. Turbidimeters and incubation tanks (for Sediment 1-15) served as their own blocks. Plots of residuals were used to identify departures from ideal conditions regarding variance homogeneity; residuals were uniformly distributed around the zero line. Comparisons of the simple effects of treatment combinations and of the least squares means of one factor at the levels of other factors were conducted for significant interactions. When no interactions were significant, least squares means of the main effects for each treatment factor were compared. Significant difference and effects determined for $P \leq 0.05$.

Acknowledgements

Financial support for this research was provided through The Keith Campbell Foundation for the Environment (4-35309) as part of a study modeling the ecological

benefit of *Crassostrea virginica* restoration in Chesapeake Bay. Educational costs for R.R.H. during the research were provided through the Dr. Nancy Foster Scholarship Program of the National Oceanic Atmospheric Administration (Award No. NA04NOS4290250). I thank E. Kiss for her assistance in the laboratory, and J. Seabrease for equipment construction and design. I thank A. Padeletti and D. Meritt for providing *C. virginica* for the collection of feces and pseudofeces, and P. Dickhudt for assistance with La Trappe Creek experiments in 2003. I especially thank S. Suttles for his technical support throughout the 2006 experiments and with MatLab programming. Additional gratitude goes out to B. Momen, R. Newell, and L. Sanford for their assistance with statistics, context, and data interpretation.

Table A.1 Cumulative eroded mass (kg m^{-2}, mean ± standard deviation) at critical shear stress (τ_c) values of 0.10, 0.20, and 0.30 Pa for sediment cores collected from La Trappe Creek (Sediment 16-17, Trap1-4). Treatment cores were collected from sediments located beneath aquaculture floats of the eastern oyster, *Crassostrea virginica*, after ~ 9 weeks of deployment. Control cores were collected at a corresponding reference site away from any aquaculture influence, but otherwise similar to the treatment site (Chapter 3, Mainstem). Differences between Control and Treatment were not significant at an alpha of 0.05, though a trend toward more erodible mass in treatment cores at higher stresses was suggested.

RAW Data

Critical shear stress (Pa)	Cumulative eroded mass (kg m^{-2})		Sample size (n)	
	Control	Treatment	Control	Treatment
0.10	0.016 ± 0.012	0.016 ± 0.004	2	2
0.20	0.036 ± 0.033*	0.042 ± 0.024	2	2
0.30	0.057 ± 0.051*	0.076 ± 0.053	2	2

* Problems arose with the filtered (142 mm, GF/F) masses for the fifth step interval (τ_b = 0.215 Pa) for Trap3 and the fourth (τ_b = 0.157 Pa) and fifth step intervals (τ_b = 0.215 Pa) for Trap4. Filters for these applied shear stresses (τ_b) were damaged during filtering and, as such, the eroded masses were reconstructed from the nephelometric turbidity units (NTU) provided by the turbidimeter and the a-coefficients (kg m^{-3} * NTU) for the preceding and following step intervals.

Figure Legends

Fig. A.1 Schematic of the experimental design for Sandpaper 1-6 (BDR03-08), conducted from 09 May through 11 May 2006. Inflowing estuarine water from the Choptank River was pumped into shallow pans, holding individual trays, with one *Crassostrea virginica* per tray. Settled feces and pseudofeces were collected separately with graduated, 10 ml pipettes with the tips removed and allowed to settle within pipettes until accurate volume estimates could be determined. PVC discs covered with 320A wet and dry silicon carbide waterproof abrasive paper were positioned 10 cm from the top of polycarbonate (9.525 cm I.D.) cores. Ambient estuarine water from the Choptank River filled the 10 cm headspace. Equal volumes (2.5 ml, 4.4 ml, 10.6 ml) of feces and pseudofeces were placed in separate cores on the sandpaper-discs, and the cores were immediately sealed with an erosion head designed to generate a shear stress at the disc surface. Each type (feces, pseudofeces) and volume combination was run twice. Combinations systematically alternated with the turbidimeters and erosion heads.

Fig. A.2 Schematic of the experimental design for Sediment 1-15 (BDR09-23), conducted from 25 May through 04 June 2006. Sediment cores were collected from a mesohaline portion of the Choptank River, Chesapeake Bay, Maryland (between 38° 37.152'N 76° 08.135'W and 38° 38.187'N 76° 08.148'W) on 24 May and 02 June 2006. Inflowing estuarine water from the Choptank River was pumped into shallow pans holding individual trays, with one *Crassostrea*

virginica per tray. Settled feces and pseudofeces were collected separately with graduated, 10 ml pipettes with the tips removed and allowed to settle in sealed funnels until sufficient material was collected to add 3.5 ml each of feces and pseudofeces (7 ml total, 0.061 kg m^{-2}) to each of 15 Treatment cores; no additions were made to Control cores. Sediment cores were incubated in the dark until analysis, except for cores analyzed immediately (Day 0). T-shaped bubblers, positioned ~ 8 cm from the sediment surface, and flow (13.2 – 19.8 ml s^{-1}) within tanks maintained aerobic conditions within cores. All sediment cores were incubated in 2 μm filtered Choptank estuarine water. Treatment and Control cores for each erosion experiment were randomly selected from the same incubation tank and alternated systematically with the turbidimeters and erosion heads.

Fig. A.3 Schematic of the modified-Gust microcosms (9.525 cm I.D.) used to expose *Crassostrea virginica* biodeposits and sediment cores to defined shear stresses (0.01-0.45 Pa). Erosion microcosms were designed to generate controllable, nearly uniform shear stress using spinning discs (within the erosion head) and central suction. A data logger calculated the RPM at which discs should spin and the pumping rate (Q) necessary to achieve desired shear stresses. Replacement water was pumped through the microcosm, while effluent with eroded sediment was passed through a turbidimeter. Turbidimeter readings were transmitted to the datalogger in nephelometric turbidity units (NTU). Filtered effluent (GF/F 0.7

μm, 47 and 142 mm diameter filters) was used to calibrate NTU to total suspended solids.

Fig. A.4 Erosion rates (kg m^{-2} s^{-1}) in time (s) for (A) Control and (B) Treatment sediment cores from a representative Sediment experiment, conducted 87.7 h (~ 7 d) after the addition of biodeposits (7 ml, 0.061 kg m^{-2}) to Treatment cores (Sediment 14, BDR16). Solid black lines indicate the exponential fits for observed erosion rates, while red stair-steps show the applied shear stress (τ_b, Pa) time series. Profiles of (C) critical shear stress (τ_c, Pa) and (D) the erosion rate constant (M, kg m^{-2} s^{-1} Pa^{-1}) were calculated as functions of the cumulative eroded mass of sediment eroded (kg m^{-2}).

Fig. A.5 (A) Cumulative eroded mass (g) for each volume (ml) of feces and pseudofeces positioned on 320A grit (36 μm) wet-dry silicon carbide abrasive paper in Sandpaper 1-6 (BDR03-08) experiments. Solid lines indicate significant ($P < 0.05$) regressions, with R^2 as shown, for feces and pseudofeces data. For these experiments, standard erosion test protocols (Fig. A.4) were followed, but the experiments were terminated when all of the added biodeposits were eroded. Cumulative eroded masses (g) include material suspended in the water within the core upon conclusion of the final step (τ_b) interval. (B) Cumulative eroded mass (kg m^{-2}, mean ± standard deviation) of feces and pseudofeces at 0.05 and 0.10 Pa (τ_c). Differences between feces and pseudofeces were significant at these specific critical shear stresses ($P = 0.0076$).

Fig. A.6 Cumulative eroded mass (kg m^{-2}, mean ± standard deviation) versus the age of biodeposits (days) at three defined (0.10, 0.20, 0.30 Pa) critical shear stresses (τ_c, Pa). Cumulative eroded masses are for Treatment and Control cores combined (Sediment 1-15, BDR09-23). Differences of least squares means for the significant Age * Critical shear stress interaction (P = 0.0098) identified significant differences between the cumulative eroded masses (kg m^{-2}) after 1 d of aging and 4 -7 d at 0.20 Pa and all other ages at 0.30 Pa ($P < 0.05$).

Fig. A.7 Loss on ignition (%, mean ± standard deviation) at 450°C for (A) applied shear stresses (τ_b, Pa) and (B) the age of biodeposits (days) for Treatment and Control cores combined (Sediment 1-15 (BDR09-23)). Lower-case letters positioned above bars indicate significant differences between mean values; bars with the same letter are not significantly different from one another ($P > 0.05$).

Fig. A.8 Profiles of critical shear stress (τ_c, Pa) with cumulative eroded mass (kg m^{-2}) for Treatment and Control cores from (A) Sediment 8 (BDR10), conducted 16.75 h (~ 1 d) after additions of biodeposits (7 ml, 0.061 kg m^{-2}), and from a (B) La Trappe Creek experiment (Sediment 17, Trap2-4), conducted on 02 October 2003. Cores from La Trappe Creek were collected from sediments located beneath aquaculture floats of the eastern oyster, *Crassostrea virginica*, after ~ 9 weeks of deployment and at a corresponding reference site (Chapter 3, Mainstem). Cores from Sediment 8 (BDR10) had no benthic microalgae present, whereas cores

collected from La Trappe Creek (Sediment 17, Trap2-4) were influenced by the presence of benthic microalgal communities.

Fig. A.1

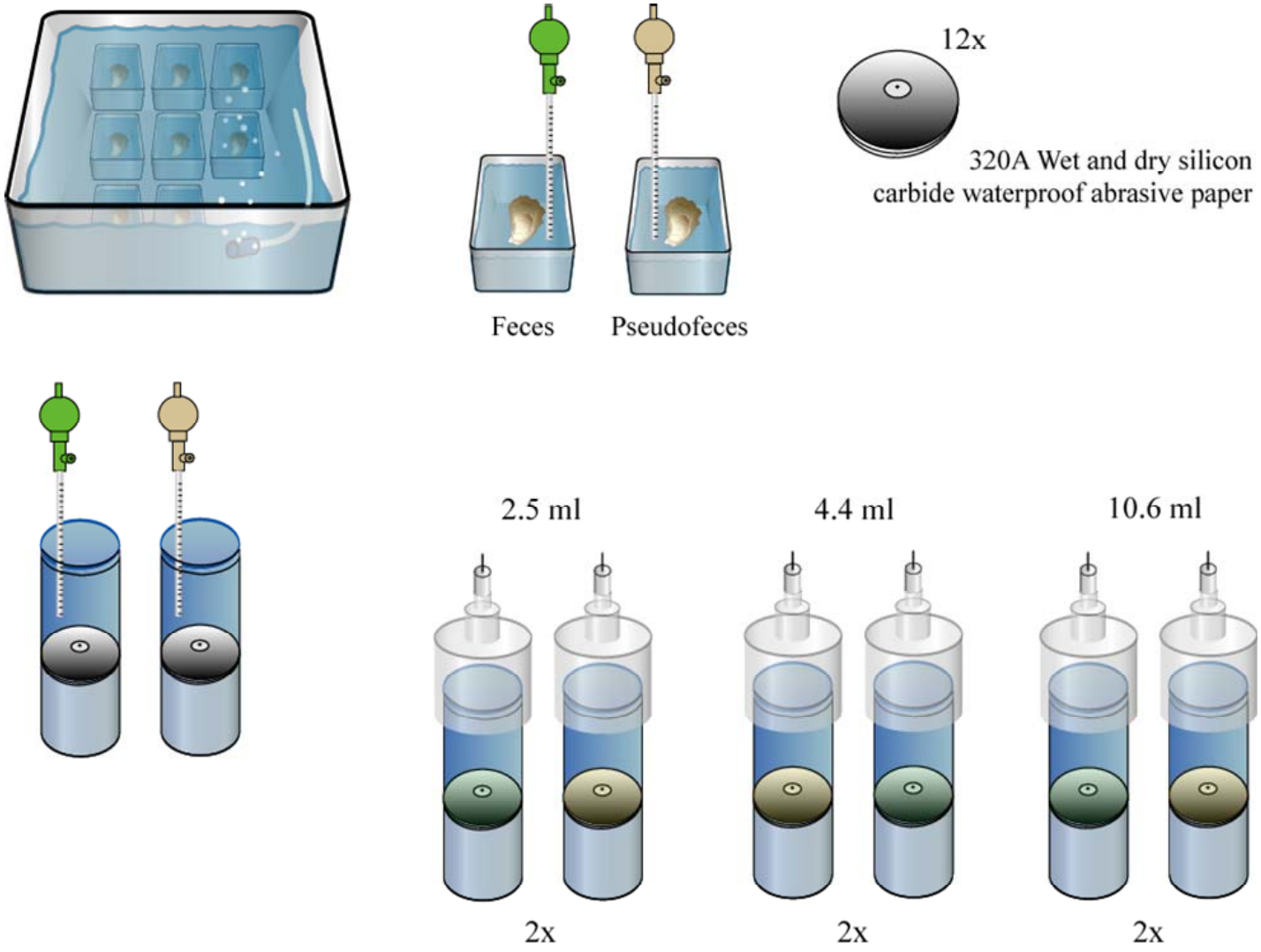
12x
320A Wet and dry silicon carbide waterproof abrasive paper
Feces
Pseudofeces
2.5 ml
4.4 ml
10.6 ml
2x
2x
2x

Fig. A.2

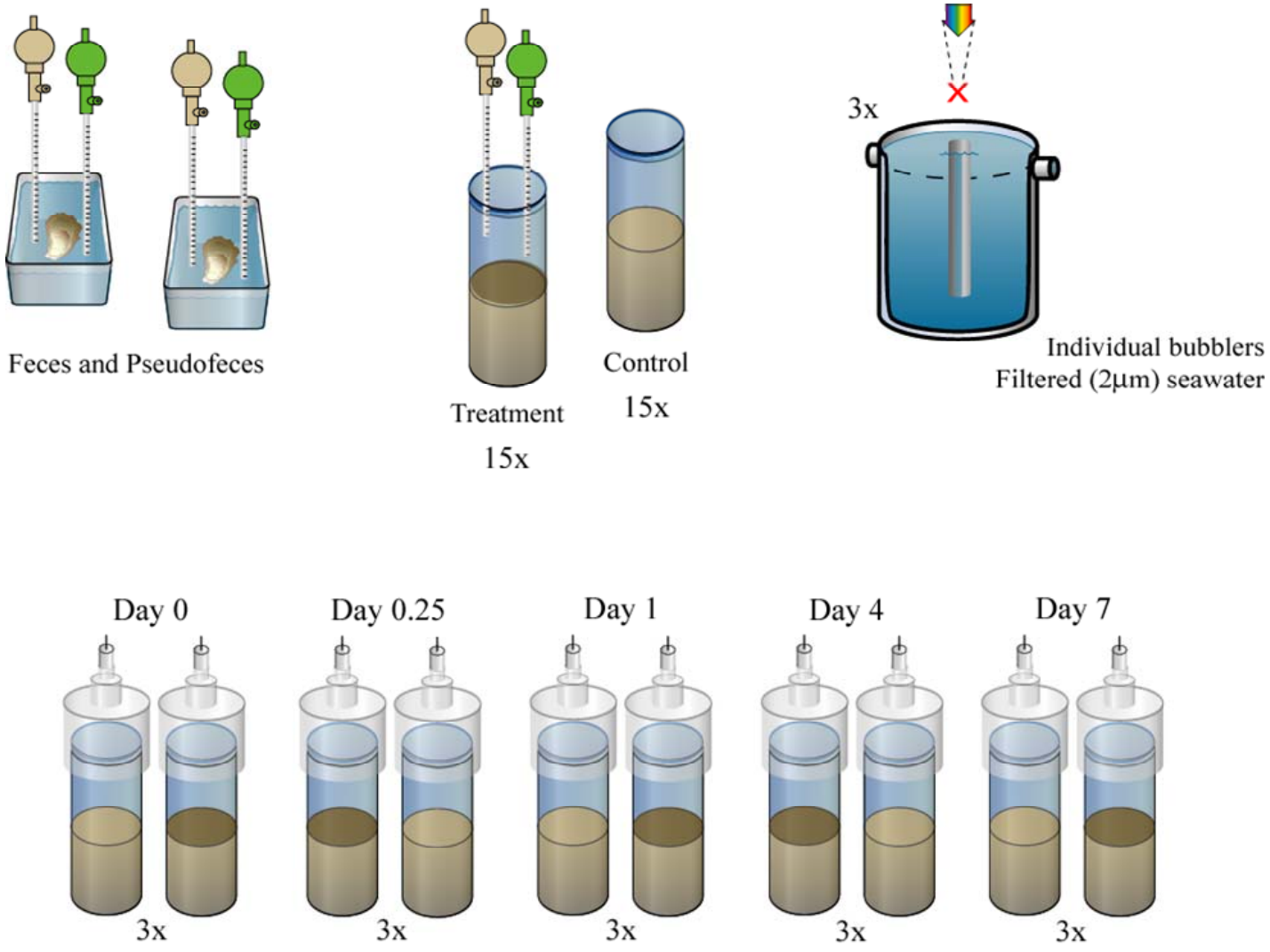
Feces and Pseudofeces
Treatment
15x
Control
15x
3x
Individual bubblers
Filtered (2µm) seawater
Day 0
Day 0.25
Day 1
Day 4
Day 7
3x
3x
3x
3x
3x

Fig. A.3

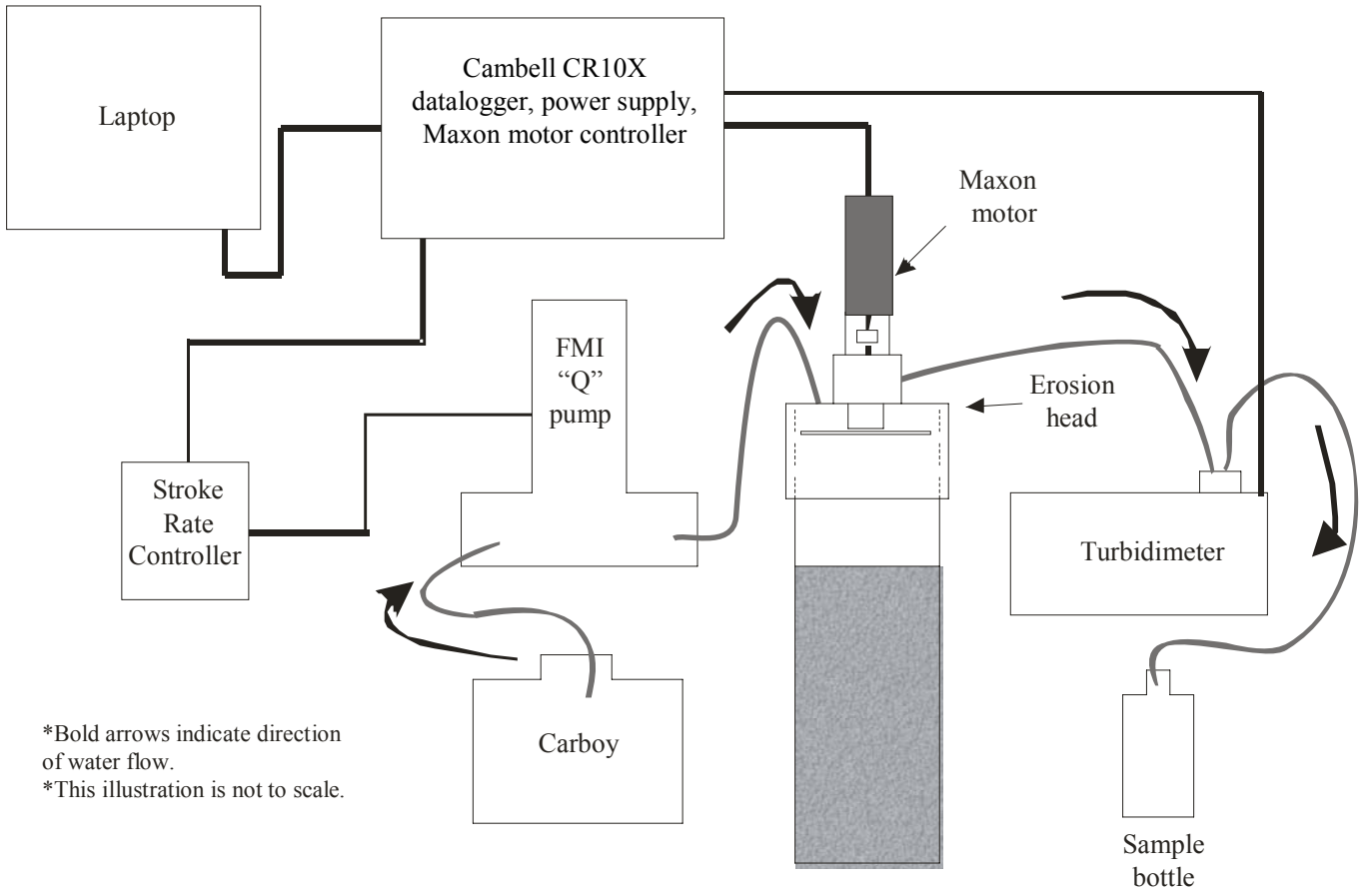

Illustration provided by S.E. Suttles
(Revised by P. Dickhudt)

Fig. A.4

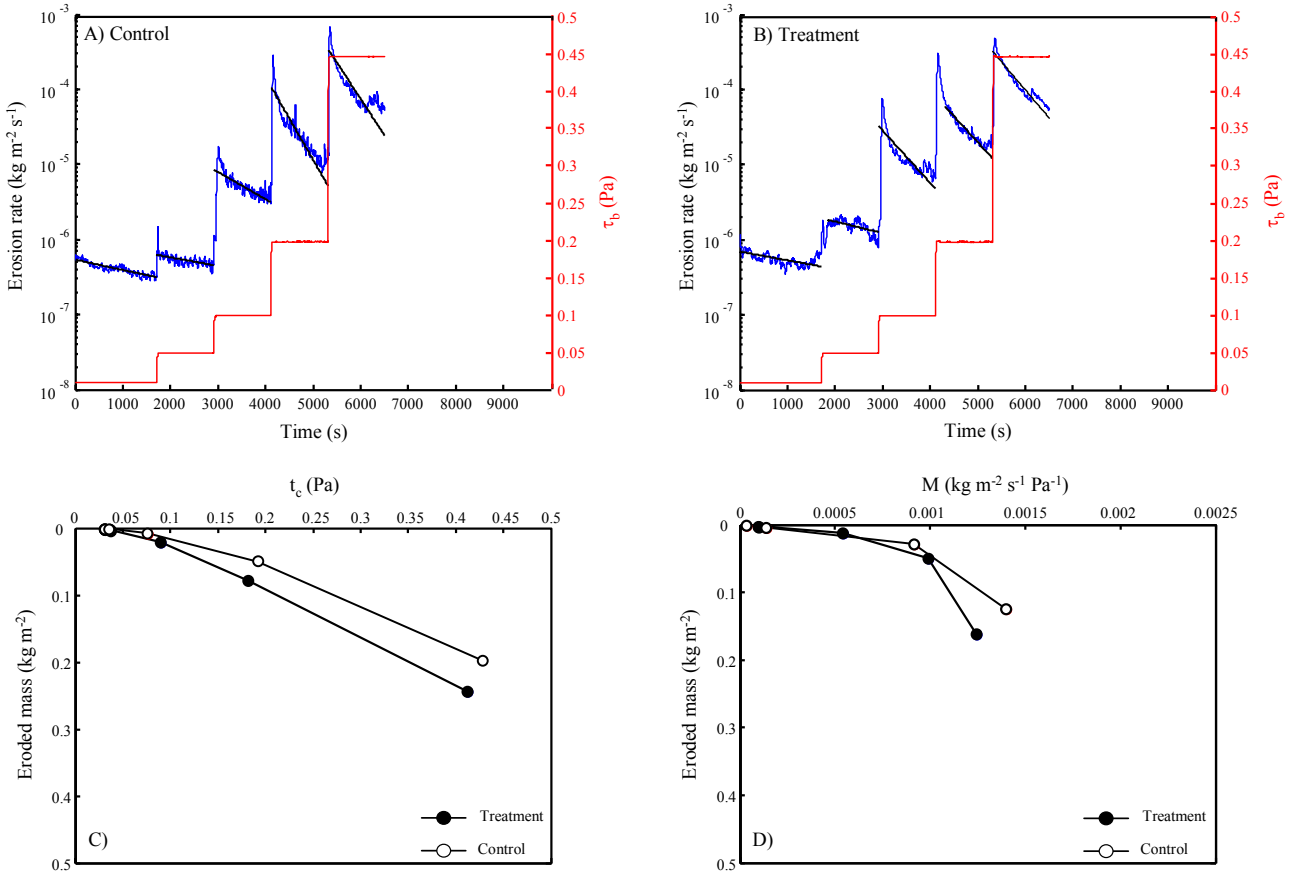
A) Control
B) Treatment
Erosion rate (kg m-2 s-1)
τb (Pa)
Time (s)
tc (Pa)
M (kg m-2 s-1 Pa-1)
Eroded mass (kg m-2)
C)
D)
Treatment
Control

Fig. A.5

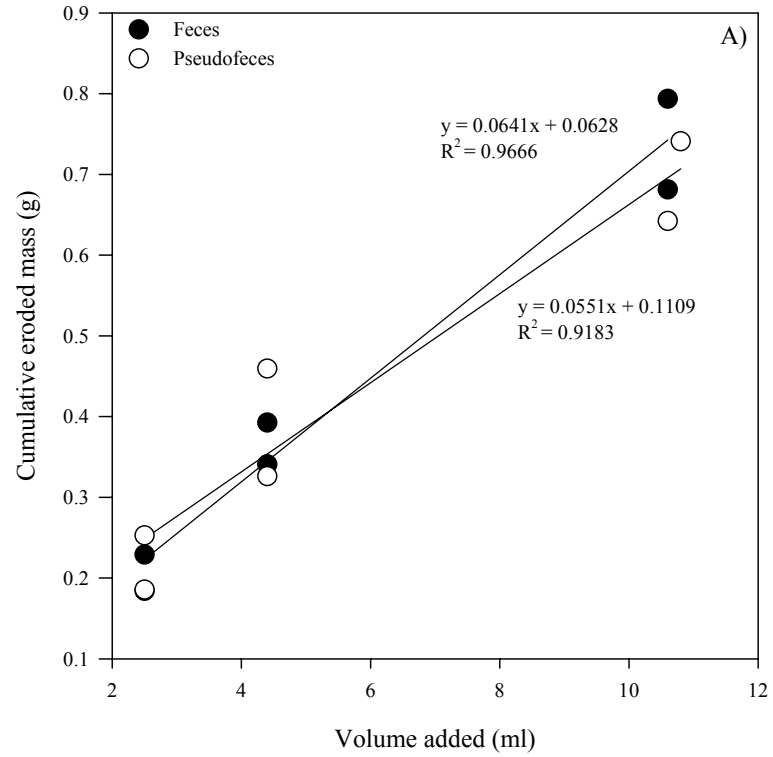
Feces
Pseudofeces
A)
y = 0.0641x + 0.0628
R2 = 0.9666
y = 0.0551x + 0.1109
R2 = 0.9183
Cumulative eroded mass (g)
Volume added (ml)
0.1
0.2
0.3
0.4
0.5
0.6
0.7
0.8
0.9
2
4
6
8
10
12

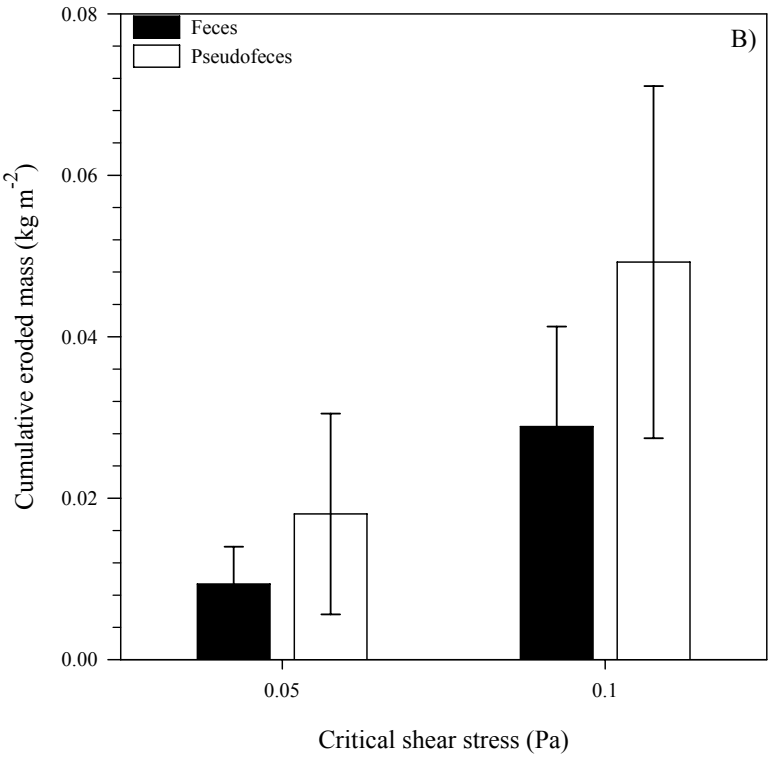
Feces
Pseudofeces
B)
Cumulative eroded mass (kg m-2)
Critical shear stress (Pa)
0.00
0.02
0.04
0.06
0.08
0.05
0.1

Fig. A.6

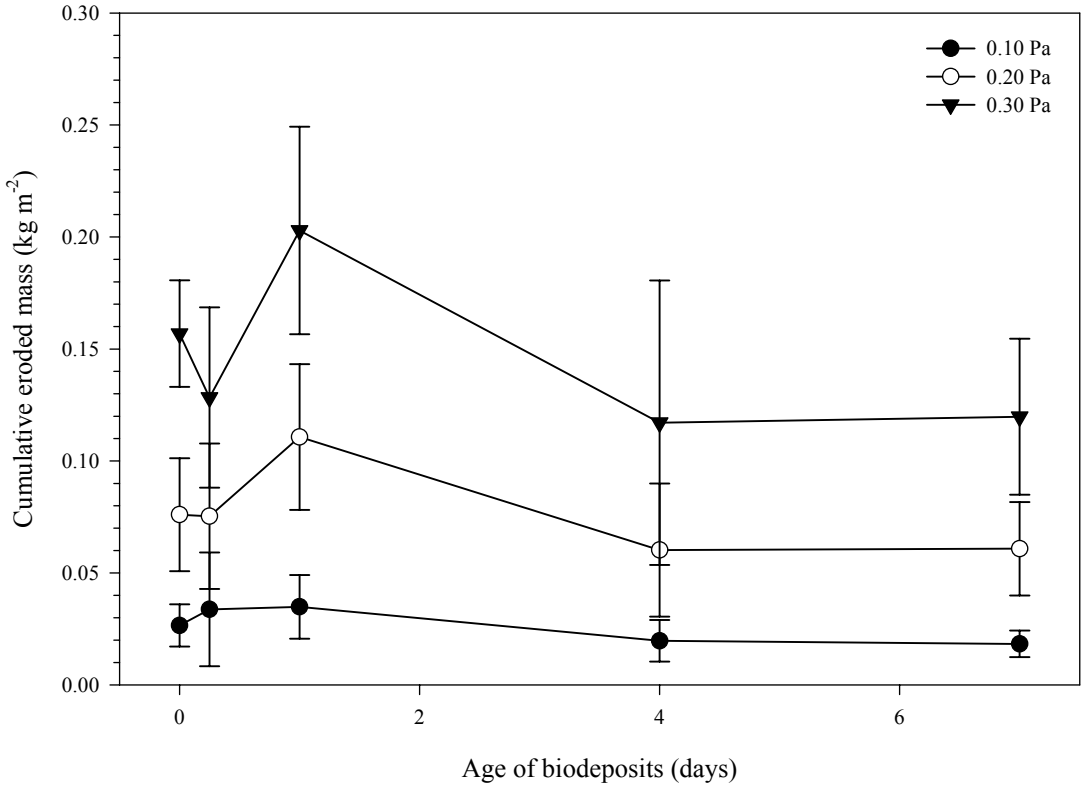
0.10 Pa
0.20 Pa
0.30 Pa
Cumulative eroded mass (kg m-2)
0.00
0.05
0.10
0.15
0.20
0.25
0.30
0
2
4
6
Age of biodeposits (days)

Fig. A.7

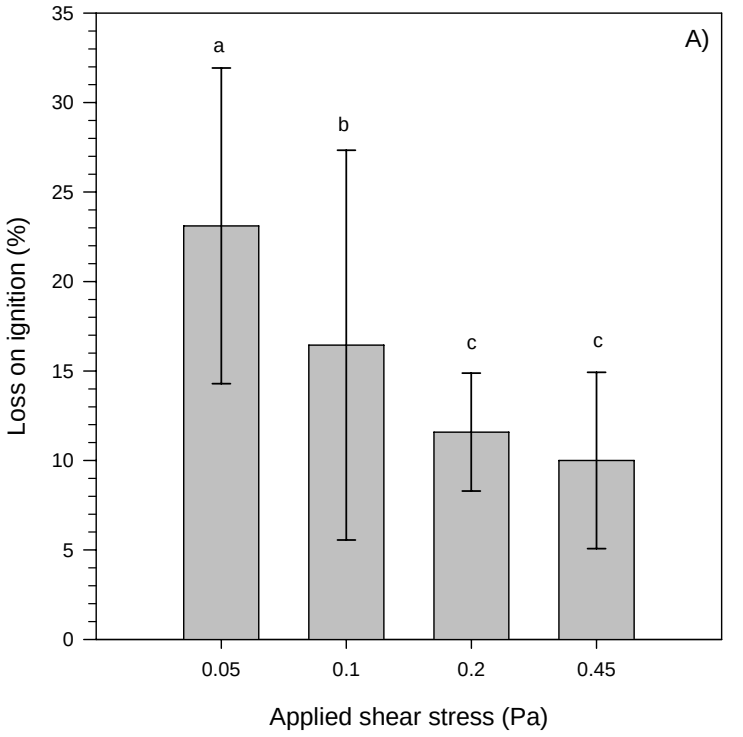
A)
a
b
c
c
Loss on ignition (%)
0
5
10
15
20
25
30
35
0.05
0.1
0.2
0.45
Applied shear stress (Pa)

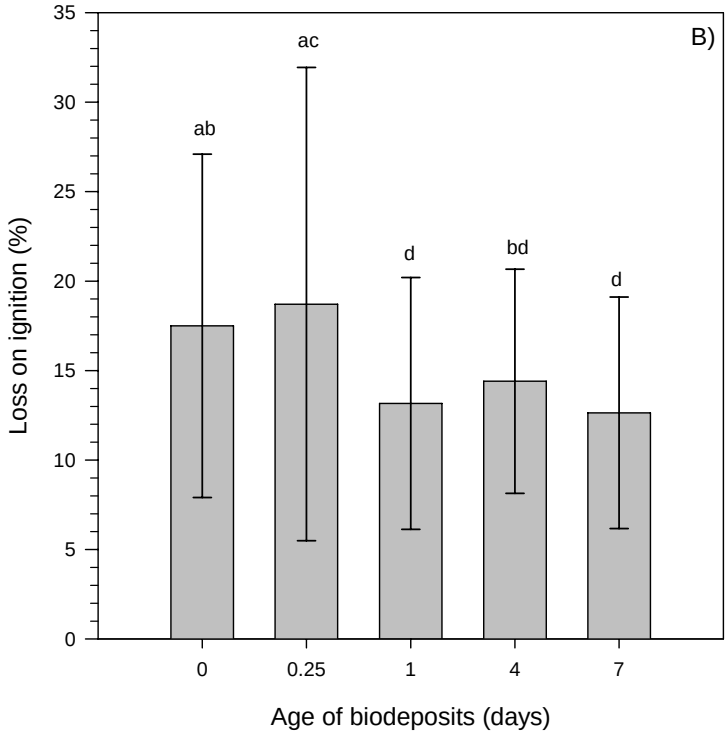
B)
ab
ac
d
bd
d
Loss on ignition (%)
0
5
10
15
20
25
30
35
0
0.25
1
4
7
Age of biodeposits (days)

Fig. A.8

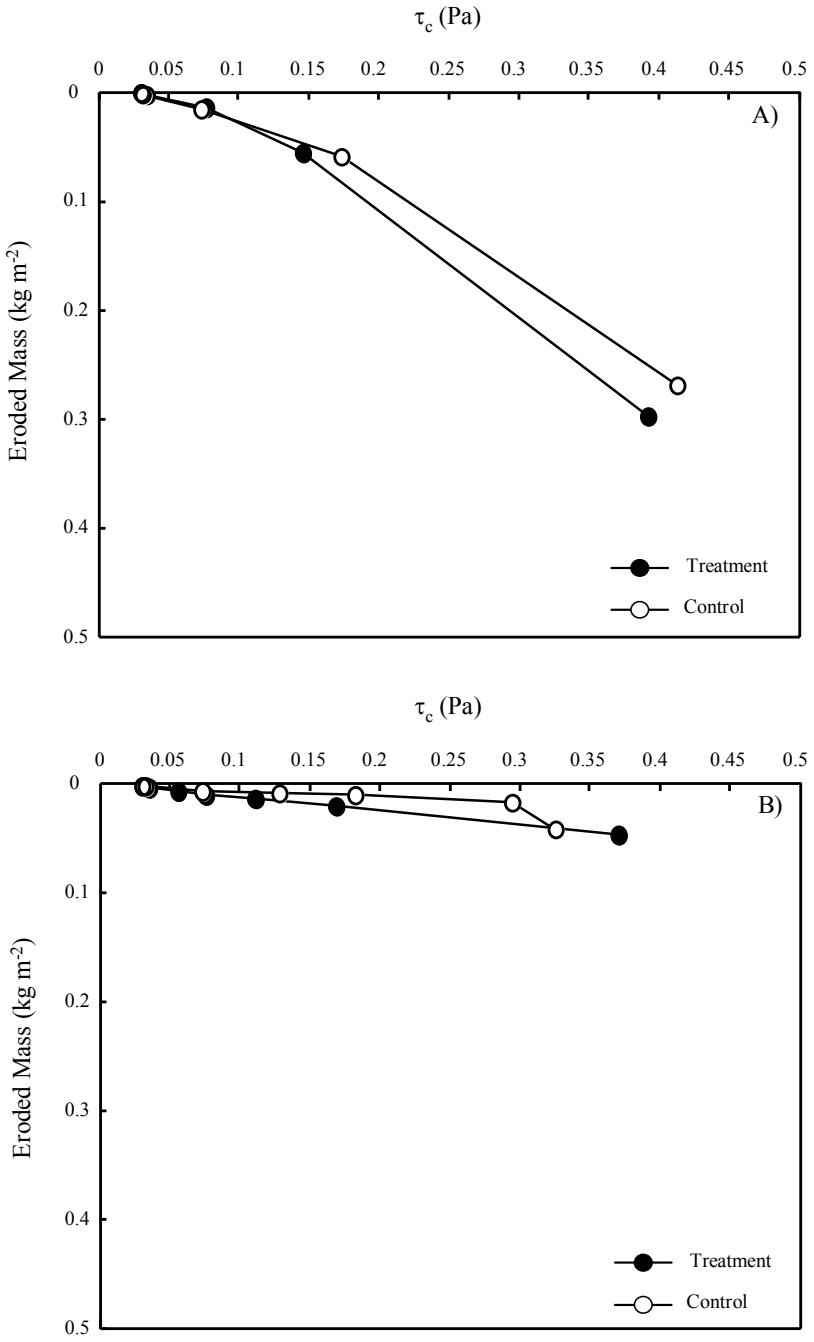
τc (Pa)
0
0.05
0.1
0.15
0.2
0.25
0.3
0.35
0.4
0.45
0.5
Eroded Mass (kg m-2)
A)
Treatment
Control
τc (Pa)
B)
Treatment
Control

Appendix B: Raw data (mean ± standard deviation) and the comparison of least squares means for significant ($P < 0.05$) main effects, and additional figures for Appendix A

Table B.1 Background total suspended solid (TSS) concentrations (kg m^{-3}) determined for replacement water (raw or 2 μm filtered) pumped through sandpaper and sediment cores. Background TSS concentrations for each core were calculated from exponential best fits (at 4500 s) for TSS, converted from nephelometric turbidity units (NTU), during the 0.01 Pa flushing step (30 min). The lowest calculated TSS for cores analyzed with the same replacement water (**in bold**) was manually selected for all cores that day, except on 02 October 2003 (La Trappe Creek). Background TSS concentrations for La Trappe Creek sediments were maintained for individual cores.

Date	Experiment	Volume (ml)	Background TSS (kg m^{-3}) Feces	Pseudofeces
09 May 2006				
	Sandpaper 1 (BDR03)	4.4	0.01281	**0.00693**
	Sandpaper 2 (BDR04)	2.5	0.00777	0.00805
10 May 2006				
	Sandpaper 3 (BDR05)	10.6*	0.00570	**0.00440**
	Sandpaper 4 (BDR06)	4.4	0.00885	0.00652
11 May 2006				
	Sandpaper 5 (BDR07)	10.6	0.00534	**0.00258**
	Sandpaper 6 (BDR08)	2.5	0.01162	0.00898
		Age (d)	Control	Treatment
03 June 2006				
	Sediment 1 (BDR18)	0	0.00250	0.00611
	Sediment 2 (BDR19)	0	0.00347	**0.00040**
	Sediment 3 (BDR20)	0	0.00126	0.00045

04 June 2006			
Sediment 4 (BDR21)	0.25	**0.00007**	0.00056
Sediment 5 (BDR22)	0.25	0.00172	0.00019
Sediment 6 (BDR23)	0.25	n.d.†	0.00304
25 May 2006			
Sediment 7 (BDR09)	1	**0.00083**	0.00284
Sediment 8 (BDR10)	1	0.00398	0.00468
Sediment 9 (BDR11)	1	0.00090	0.00480
28 May 2006			
Sediment 10 (BDR12)	4	0.00140	**0.00027**
Sediment 11 (BDR13)	4	0.00014	0.00500
Sediment 12 (BDR14)	4	0.00621	0.00966
31 May 2006			
Sediment 13 (BDR15)	7	**0.00012**	0.00169
Sediment 14 (BDR16)	7	0.00133	0.00257
Sediment 15 (BDR17)	7	0.00025	0.00104

	Aquaculture Deployment (d)	Control	Treatment
02 October 2003			
Sediment 16 (Trap1-3)	63	0.0118‡	0.00884
Sediment 17 (Trap2-4)	63	0.0100‡	0.00783

* Collected volume (ml) of pseudofeces was 10.8 ml for Sandpaper 3 (BDR05).

† No exponential fit could be determined for the flushing (0.01 Pa) step for the Control core in Sediment 6 (BDR23). The slope (- λ) for this step was a positive value (0.00075), which is indicative of Type II erosion (i.e., erosion was growing).

‡ Background TSS concentrations for La Trappe Creek Control cores were manually selected, as exponential fits provided negative values.

Table B.2 Cumulative eroded mass (kg m^{-2}, mean ± standard deviation) for each combination of treatment, volume (ml), and defined (0.05, 0.10 Pa) critical shear stress (τ_c, Pa) established in Sandpaper experiments 1-6 (BDR03-08), and the comparison of least squares means for significant ($P < 0.05$) main effects.

RAW Data

Volume (ml)	Critical shear stress (Pa)	Cumulative eroded mass (kg m^{-2})		Sample size (n)	
		Feces	Pseudofeces	Feces	Pseudofeces
2.5	0.05	0.006 ± 0.002	0.009 ± 0.001	2	2
2.5	0.10	0.017	0.027	1	1
4.4	0.05	0.007 ± 0.001	0.018 ± 0.005	2	2
4.4	0.10	0.022 ± 0.001	0.037 ± 0.004	2	2
10.6	0.05	0.015 ± 0.000	0.014	2	1
10.6	0.10	0.042 ± 0.005	0.066	2	1
10.8	0.05	n.d.*	0.042	0	1
10.8	0.10	n.d.*	0.078	0	1

STATISTICALLY SIGNIFICANT Data

	Critical shear stress (Pa)	Cumulative eroded mass (kg m^{-2})	Sample size (n)	Differences of Least Squares Means (Pr > |t|)	
Treatment * Critical shear stress				**0.0076**	
Feces	0.05	0.009 ± 0.005	6	No estimates for differences of least squares means for the significant Treatment * Critical shear stress interaction	
Pseudofeces	0.05	0.018 ± 0.012	6		
Feces	0.10	0.029 ± 0.012	5		
Pseudofeces	0.10	0.049 ± 0.022	5		
Volume (ml) * Critical shear stress				**0.0027**	
2.5	0.05	0.007 ± 0.002	4	2.5 vs. 4.4 ml / 0.05 Pa	0.0660
4.4	0.05	0.012 ± 0.007	4	**2.5 vs. 10.6 ml / 0.05 Pa**	**0.0245**
10.6	0.05	0.015 ± 0.001	3	4.4 vs. 10.6 ml / 0.05 Pa	0.3931
10.8	0.05	0.042	1		
2.5	0.10	0.022 ± 0.007	2	**2.5 vs. 4.4 ml / 0.10 Pa**	**0.0197**
4.4	0.10	0.030 ± 0.009	4	**2.5 vs. 10.6 ml / 0.10 Pa**	**<0.0001**
10.6	0.10	0.050 ± 0.015	3	**4.4 vs. 10.6 ml / 0.10 Pa**	**<0.0001**
10.8	0.10	0.078	1		

* No data available for this volume (ml) of feces.

Table B.3 Loss on ignition at 450 °C (%, mean ± standard deviation) for each combination of treatment, volume (ml), and applied shear stress (τ_b, Pa) established in Sandpaper experiments 1-6 (BDR03-08), and the comparison of least squares means for significant (P <0.05) main effects.

RAW Data

Volume (ml)	Applied shear stress (Pa)	Loss on ignition (%)		Sample size (n)	
		Feces	Pseudofeces	Feces	Pseudofeces
2.5	0.05	23.812 ± 2.966	23.286 ± 0.417	2	2
2.5	0.10	27.160 ± 0.620	15.511 ± 1.192	2	2
2.5	0.15	27.581 ± 1.355	27.621 ± 1.088	2	2
4.4	0.05	30.758 ± 1.980	20.506 ± 5.776	2	2
4.4	0.10	31.706 ± 2.816	16.128 ± 1.011	2	2
4.4	0.15	31.696 ± 2.103	24.395 ± 4.478	2	2
10.6	0.05	35.013 ± 2.862	28.687	2	1
10.6	0.10	48.231 ± 21.137	17.377	2	1
10.6	0.15	31.187 ± 0.418	37.459	2	1
10.8	0.05	n.d.*	17.461	0	1
10.8	0.10	n.d.*	16.163	0	1
10.8	0.15	n.d.*	18.977	0	1

STATISTICALLY SIGNIFICANT Data

	Applied shear stress (Pa)	Loss on ignition (%)	Sample size (n)	Differences of Least Squares Means (Pr > |t|)
Treatment * Applied shear stress				**0.0057**
Feces	0.05	29.861 ± 5.455	6	No estimates for differences of least squares means for the significant Treatment * Applied shear stress interaction
Pseudofeces	0.05	22.289 ± 4.607	6	
Feces	0.10	35.729 ± 13.794	6	
Pseudofeces	0.10	16.136 ± 0.976	6	
Feces	0.15	30.155 ± 2.305	6	
Pseudofeces	0.15	26.745 ± 6.464	6	

* No data available for this volume (ml) of feces.

Table B.4 Cumulative eroded mass (kg m^{-2}, mean ± standard deviation) for each combination of treatment, time (d), and defined (0.10, 0.20, 0.30 Pa) critical shear stress (τ_c, Pa) established in Sediment core experiments 1-15 (BDR09-23), and the comparison of least squares means for significant ($P < 0.05$) main effects.

RAW Data

Time (d)	Critical shear stress (Pa)	Cumulative eroded mass (kg m^{-2})		Sample size (n)	
		Control	Treatment	Control	Treatment
0	0.10	0.026 ± 0.004	0.028 ± 0.014	3	3
0	0.20	0.066 ± 0.014	0.083 ± 0.032	2	3
0	0.30	0.158	0.156 ± 0.034	1	2
0.25	0.10	0.044 ± 0.033	0.024 ± 0.016	3	3
0.25	0.20	0.071 ± 0.026	0.078 ± 0.042	2	3
0.25	0.30	0.127 ± 0.017	0.129 ± 0.056	2	3
1	0.10	0.028 ± 0.001	0.041 ± 0.020	3	3
1	0.20	0.096 ± 0.024	0.125 ± 0.038	3	3
1	0.30	0.182 ± 0.046	0.224 ± 0.043	3	3
4	0.10	0.019 ± 0.006	0.020 ± 0.014	3	3
4	0.20	0.057 ± 0.023	0.063 ± 0.041	3	3
4	0.30	0.107 ± 0.046	0.127 ± 0.088	3	3

7	0.10	0.014 ± 0.005	0.022 ± 0.005	3	3
7	0.20	0.047 ± 0.014	0.075 ± 0.016	3	3
7	0.30	0.096 ± 0.032	0.144 ± 0.018	3	3

STATISTICALLY SIGNIFICANT Data

	Critical shear stress (Pa)	Cumulative eroded mass (kg m^{-2})	Sample size (n)	Differences of Least Squares Means (Pr > |t|)	
Time (d) * Critical shear stress				**0.0098**	
0	0.10	0.027 ± 0.009	6	0 vs. 0.25 d / 0.10 Pa	0.4771
0.25	0.10	0.034 ± 0.025	6	0 vs. 1 d / 0.10 Pa	0.6398
1	0.10	0.035 ± 0.014	6	0 vs. 4 d / 0.10 Pa	0.7936
4	0.10	0.020 ± 0.009	6	0 vs. 7 d / 0.10 Pa	0.7424
7	0.10	0.018 ± 0.006	6	0.25 vs. 1 d / 0.10 Pa	0.2784
				0.25 vs. 4 d / 0.10 Pa	0.3102
				0.25 vs. 7 d / 0.10 Pa	0.2798
				1 vs. 4 d / 0.10 Pa	0.4344
				1 vs. 7 d / 0.10 Pa	0.3936
				4 vs. 7 d / 0.10 Pa	0.9425
0	0.20	0.076 ± 0.025	5	0 vs. 0.25 d / 0.20 Pa	0.5591
0.25	0.20	0.075 ± 0.032	5	0 vs. 1 d / 0.20 Pa	0.0805
1	0.20	0.111 ± 0.033	6	0 vs. 4 d / 0.20 Pa	0.5408
4	0.20	0.060 ± 0.030	6	0 vs. 7 d / 0.20 Pa	0.5597

7	0.20	0.061 ± 0.021	6	0.25 vs. 1 d / 0.20 Pa	0.2784
				0.25 vs. 4 d / 0.20 Pa	0.2247
				0.25 vs. 7 d / 0.20 Pa	0.2351
				1 vs. 4 d / 0.20 Pa	**0.0113**
				1 vs. 7 d / 0.20 Pa	**0.0123**
				4 vs. 7 d / 0.20 Pa	0.9751
0	0.30	0.157 ± 0.024	3	0 vs. 0.25 d / 0.30 Pa	0.5327
0.25	0.30	0.128 ± 0.040	5	**0 vs. 1 d / 0.30 Pa**	**0.0504**
1	0.30	0.203 ± 0.046	6	0 vs. 4 d / 0.30 Pa	0.0970
4	0.30	0.117 ± 0.063	6	0 vs. 7 d / 0.30 Pa	0.1213
7	0.30	0.120 ± 0.035	6	**0.25 vs. 1 d / 0.30 Pa**	**0.0058**
				0.25 vs. 4 d / 0.30 Pa	0.2872
				0.25 vs. 7 d / 0.30 Pa	0.3456
				1 vs. 4 d / 0.30 Pa	**<0.0001**
				1 vs. 7 d / 0.30 Pa	**<0.0001**
				4 vs. 7 d / 0.30 Pa	0.8895

Table B.5 Loss on ignition at 450 °C (%, mean ± standard deviation) for each combination of treatment, time (d), and applied shear stress (τ_b, Pa) established in Sediment cores experiments 1-15 (BDR09-23), and the comparison of least squares means for significant ($P < 0.05$) main effects.

RAW Data

Time (d)	Applied shear stress (Pa)	Loss on ignition (%)		Sample size (n)	
		Control	Treatment	Control	Treatment
0	0.05	32.801 ± 18.606	21.173 ± 2.626	3	3
0	0.10	21.355 ± 7.657	16.275 ± 0.597	3	3
0	0.20	14.672 ± 6.671	13.615 ± 1.063	3	3
0	0.45	9.723 ± 1.269	10.379 ± 1.464	3	3
0.25	0.05	19.291 ± 12.326	28.329 8.638	3	3
0.25	0.10	34.558 ± 28.722	15.699 3.152	3	3
0.25	0.20	12.295 ± 1.828	13.349 4.566	3	3
0.25	0.45	16.060 ± 13.012	10.091 0.995	3	3
1	0.05	24.008 ± 4.634	22.885 ± 9.457	3	3
1	0.10	10.443 ± 0.624	12.992 ± 0.885	3	3
1	0.20	8.828 ± 0.773	10.749 ± 0.537	3	3
1	0.45	7.482 ± 0.098	7.886 ± 0.739	3	3

4	0.05	17.297 ± 6.167	22.862 ± 7.725	3	3
4	0.10	14.592 ± 3.743	17.649 ± 9.026	3	3
4	0.20	12.300 ± 4.253	12.081 ± 2.035	3	3
4	0.45	8.893 ± 0.844	9.545 ± 2.025	3	3
7	0.05	23.731 ± 1.010	18.673 ± 6.900	3	3
7	0.10	11.279 ± 3.246	9.614 ± 0.932	3	3
7	0.20	9.567 ± 1.450	8.342 ± 0.871	3	3
7	0.45	7.308 ± 0.542	12.562 ± 8.841	3	3

STATISTICALLY SIGNIFICANT Data

	Loss on ignition (%)	Sample size (n)	Differences of Least Squares Means (Pr > |t|)	
Time (d)			**0.0142**	
0	17.499 ± 9.596	24	0 vs 0.25 d	0.5631
0.25	18.709 ± 13.228	24	**0 vs. 1 d**	**0.0405**
1	13.160 ± 7.039	24	0 vs. 4 d	0.1411
4	14.402 ± 6.267	24	**0 vs. 7 d**	**0.0220**
7	12.632 ± 6.472	24	**0.25 vs. 1 d**	**0.0094**
			0.25 vs. 4 d	**0.0420**
			0.25 vs. 7 d	**0.0046**
			1 vs. 4 d	0.5527
			1 vs. 7 d	0.8005
			4 vs. 7 d	0.3980

Applied shear stress (Pa)			**0.0001**	
0.05	23.105 ± 8.821	30	**0.05 vs. 0.10 Pa**	**0.0006**
0.10	16.446 ± 10.892	30	**0.05 vs. 0.20 Pa**	**<0.0001**
0.20	11.579 ± 3.293	30	**0.05 vs. 0.45 Pa**	**<0.0001**
0.45	9.993 ± 4.930	30	**0.10 vs. 0.20 Pa**	**0.0108**
			0.10 vs. 0.45 Pa	**0.0009**
			0.20 vs. 0.45 Pa	0.3972

Figure Legends

Fig. B.1 Cumulative eroded mass in (A) kg and (B) kg m^{-2} for each volume (ml) of feces and pseudofeces positioned on 320A grit (36 μm) wet-dry silicon carbide abrasive paper in Sandpaper 1-6 (BDR03-08) experiments. Solid lines indicate significant trends, with R^2 as shown, for feces and pseudofeces data combined.

Fig. B.2 Erosion rates (kg m^{-2} s^{-1}) in time (s) for 2.5 ml of (A) feces and (B) pseudofeces positioned on abrasive paper in a representative Sandpaper experiment, conducted on 09 May 2006 (Sandpaper 2, BDR04). Solid lines indicate the exponential decay constant of the erosion rate ($-\lambda$, s^{-1}), while solid stair-steps illustrate the applied shear stress (τ_b, Pa) for each step interval. Profiles of (C) critical shear stress (τ_c, Pa) and (D) the erosion rate constant (M, kg m^{-2} s^{-1} Pa^{-1}) were calculated for the cumulative mass of feces and pseudofeces eroded (kg m^{-2}).

Fig. B.3 Erosion rates (kg m^{-2} s^{-1}) in time (s) for 10.6 ml of (A) feces and (B) pseudofeces positioned on abrasive paper in a representative Sandpaper experiment, conducted on 11 May 2006 (Sandpaper 5, BDR07). Solid lines indicate the exponential decay constant of the erosion rate (λ), while solid stair-steps illustrate the applied shear stress (τ_b, Pa) for each step interval. Profiles of (C) critical shear stress (τ_c, Pa) and (D) the erosion rate constant (M, kg m^{-2} s^{-1} Pa^{-1}) were calculated for the cumulative mass of feces and pseudofeces eroded (kg m^{-2}).

Fig. B.4 (A) Comparison of critical shear stresses (τ_c, Pa) for Sandpaper 1-6 (BDR03-08) as determined with a modified version of the erosion formulation of Sanford and Maa (2001, MatLab τ_{ce}) and a new formulation, which assumes that applied (τ_b) and critical (τ_c) shear stresses remain constant (Constant τ_c). (B) Relationship of β/df, the erosion rate coefficient (where τ_c is constant) dependent on the thickness of the flocculent layer, and the cumulative eroded mass (kg m^{-2}) of feces and pseudofeces.

Fig. B.5 Photographs illustrating (A) the placement of individual eastern oysters (*Crassostrea virginica*) in submerged holding trays; (B) the collection of pseudofecal material within a graduated, 10 ml pipette with the tip removed; (C) a dual O-ring PVC disc covered with 320A (36 μm) wet and dry silicon carbide waterproof abrasive paper; (D) an adjustable PVC disc used to level the sediment or sandpaper surface within cores; (E) the erosion microcosm system (*see Fig. A.3*); and (F) the filtering rigs for 47 and 142 mm GF/F filters.

Fig. B.6 Photographs illustrating (A) 10.8 ml of pseudofeces and (B) 10.6 ml of feces within cores prior to the start of the 0.01 Pa flushing interval (Sandpaper 3, BDR05). Photographs C-F illustrate the behavior of the fecal material during the (C) 0.10 Pa, (D) 0.15 Pa, (E) 0.20 Pa, and (F) 0.30 Pa step intervals.

Fig. B.7 Photographs illustrating (A) Control and (B) Treatment cores from Sediment 4 (BDR21), conducted 6 h (~ 0.25 d) after additions of biodeposits (7 ml, 0.061 kg

m^{-2}), prior to the start of the 0.01 Pa flushing interval. Photographs C-D illustrate these (C) Control and (D) Treatment cores during the 0.20 Pa step interval.

Fig. B.8 Photograph of a Treatment core (Sediment 1, BDR18) within a few minutes of adding biodeposits (7 ml, 0.061 kg m^{-2}) to the sediment surface. An unclassified polychaete emerged from its burrow and consumed a proportion of added biodeposits (while moving across the sediment surface) until it retreated into a different burrow.

Fig. B.1

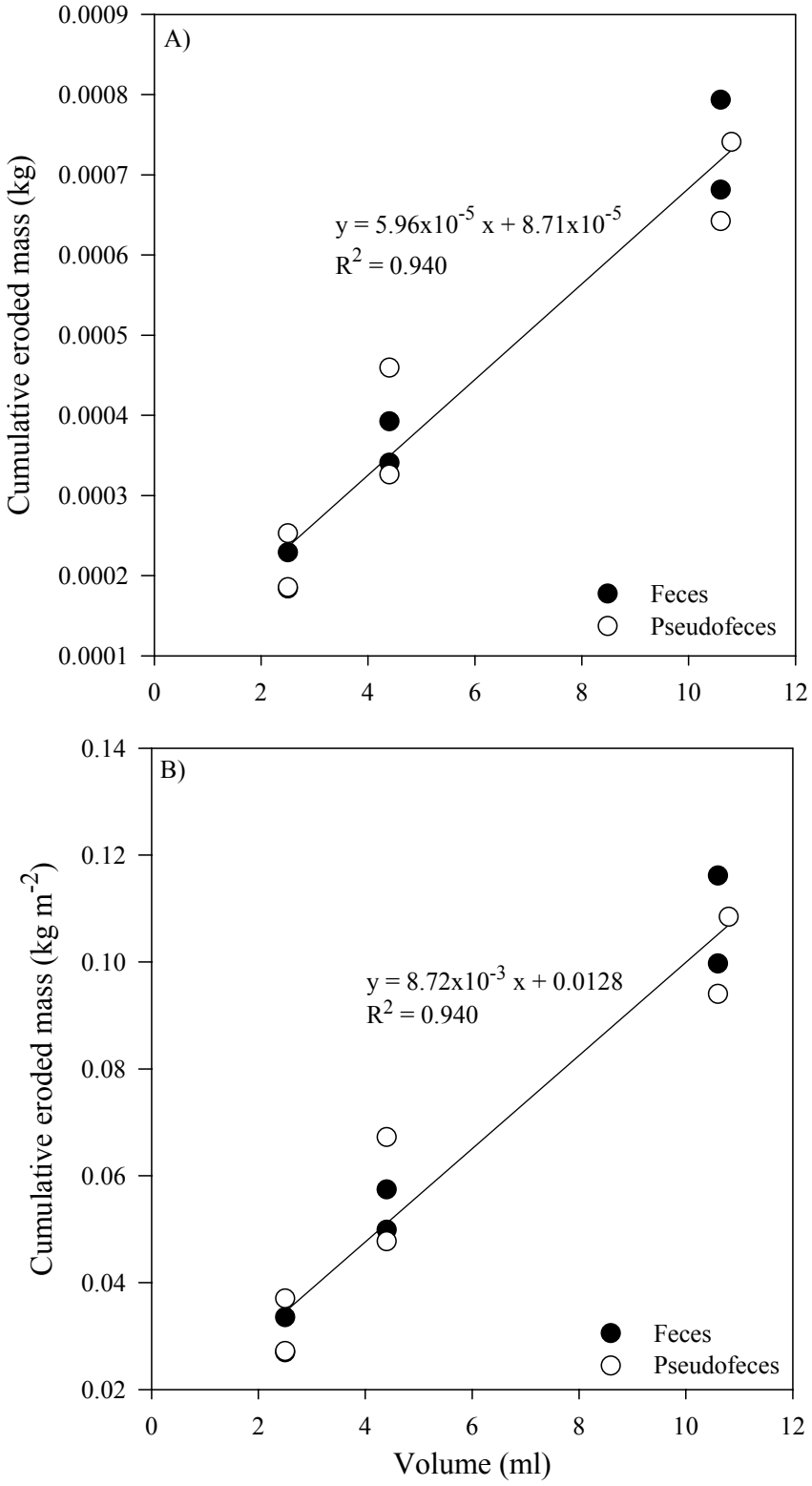
A)
Cumulative eroded mass (kg)
0.0009
0.0008
0.0007
0.0006
0.0005
0.0004
0.0003
0.0002
0.0001
y = 5.96x10-5 x + 8.71x10-5
R2 = 0.940
Feces
Pseudofeces
0
2
4
6
8
10
12
B)
Cumulative eroded mass (kg m-2)
0.14
0.12
0.10
0.08
0.06
0.04
0.02
y = 8.72x10-3 x + 0.0128
R2 = 0.940
Feces
Pseudofeces
Volume (ml)

Fig. B.2

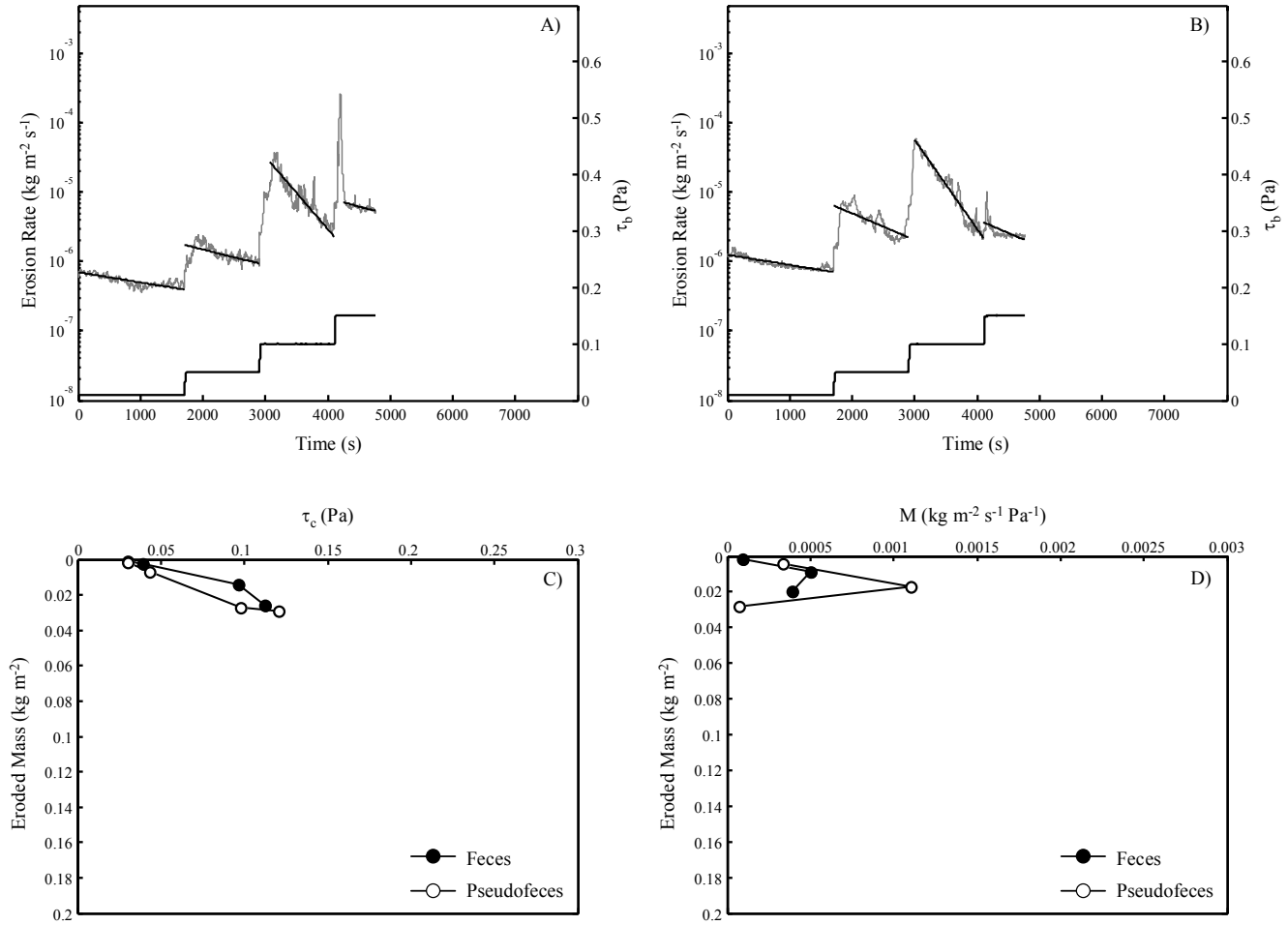
A)
B)
C)
D)
Erosion Rate (kg m-2 s-1)
τb (Pa)
Time (s)
τc (Pa)
M (kg m-2 s-1 Pa-1)
Eroded Mass (kg m-2)
Feces
Pseudofeces

Fig. B.3

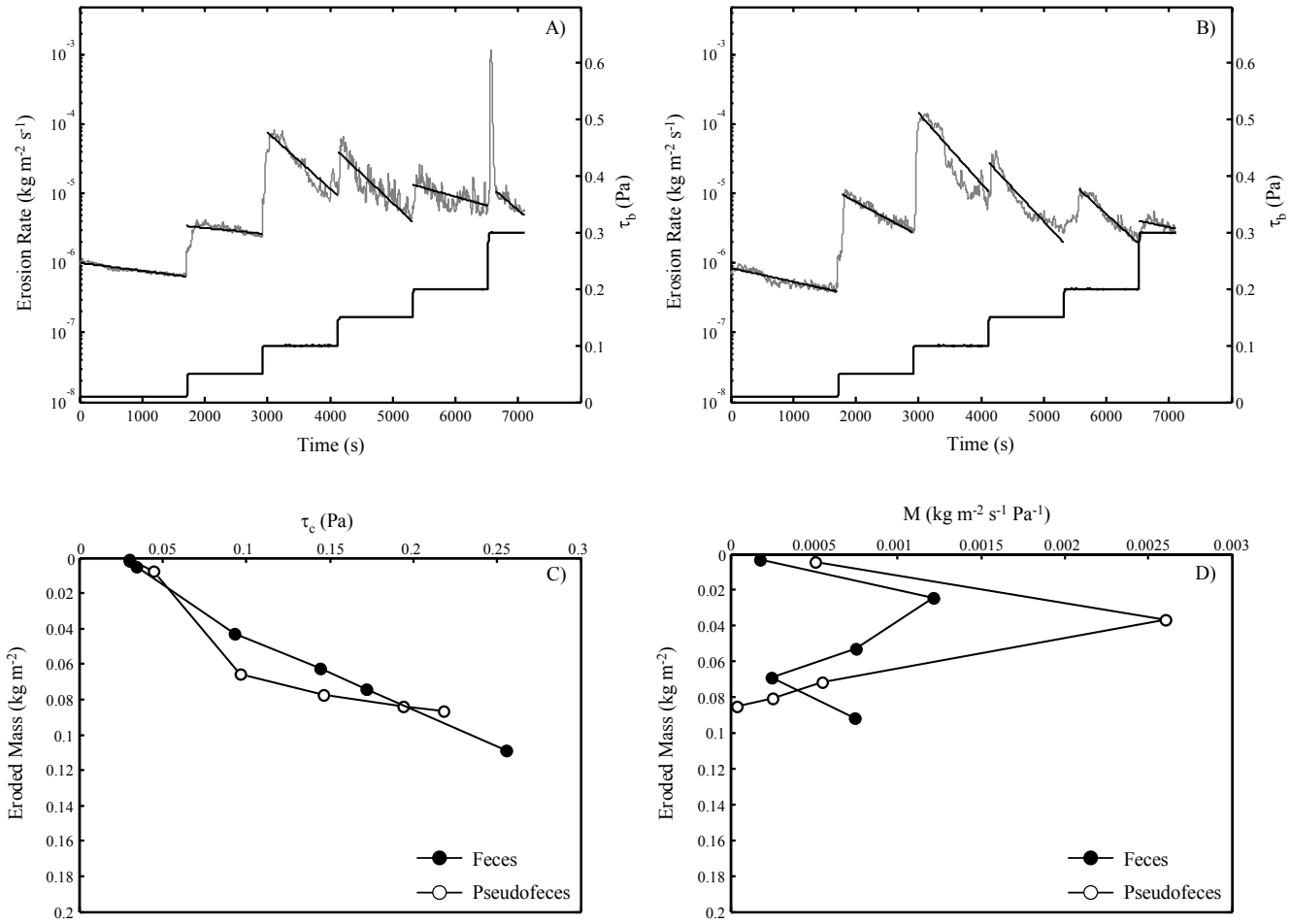
A)
B)
C)
D)
Erosion Rate (kg m-2 s-1)
τb (Pa)
Time (s)
τc (Pa)
M (kg m-2 s-1 Pa-1)
Eroded Mass (kg m-2)
Feces
Pseudofeces

Fig. B.4

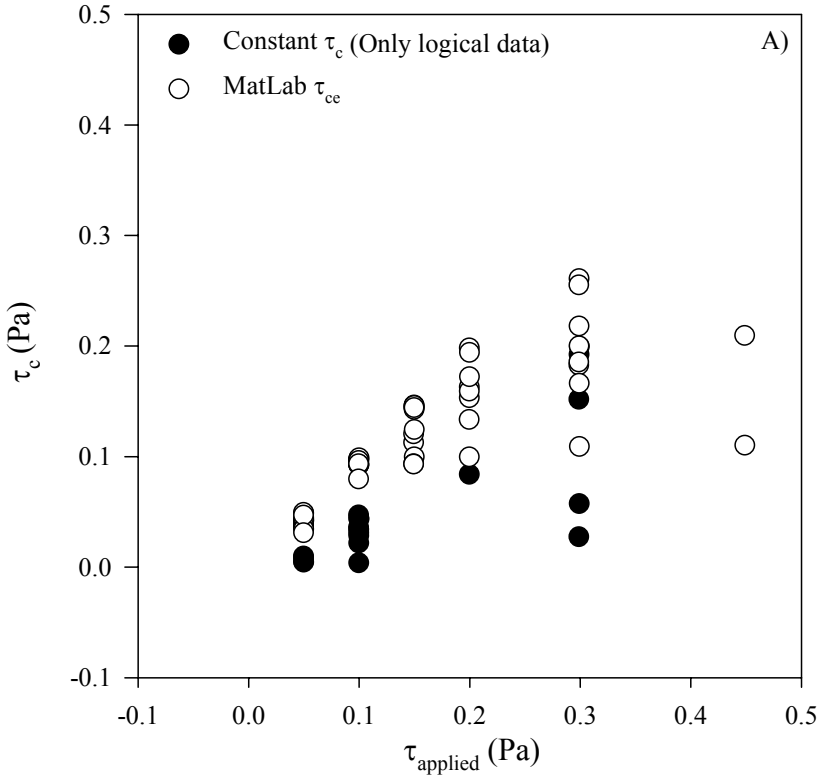
Constant τ_c (Only logical data)
MatLab τ_{ce}
A)
τ_c (Pa)
$\tau_{applied}$ (Pa)
0.5
0.4
0.3
0.2
0.1
0.0
-0.1
-0.1
0.0
0.1
0.2
0.3
0.4
0.5

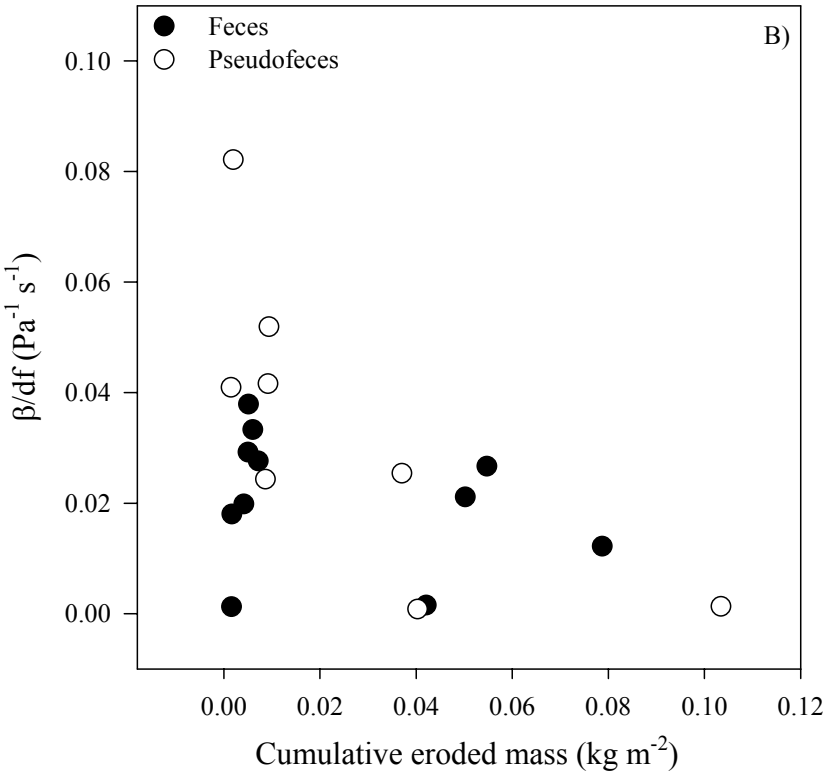
Feces
Pseudofeces
B)
β/df (Pa^{-1} s^{-1})
Cumulative eroded mass (kg m^{-2})
0.10
0.08
0.06
0.04
0.02
0.00
0.00
0.02
0.04
0.06
0.08
0.10
0.12

Fig. B.5

Fig. B.6

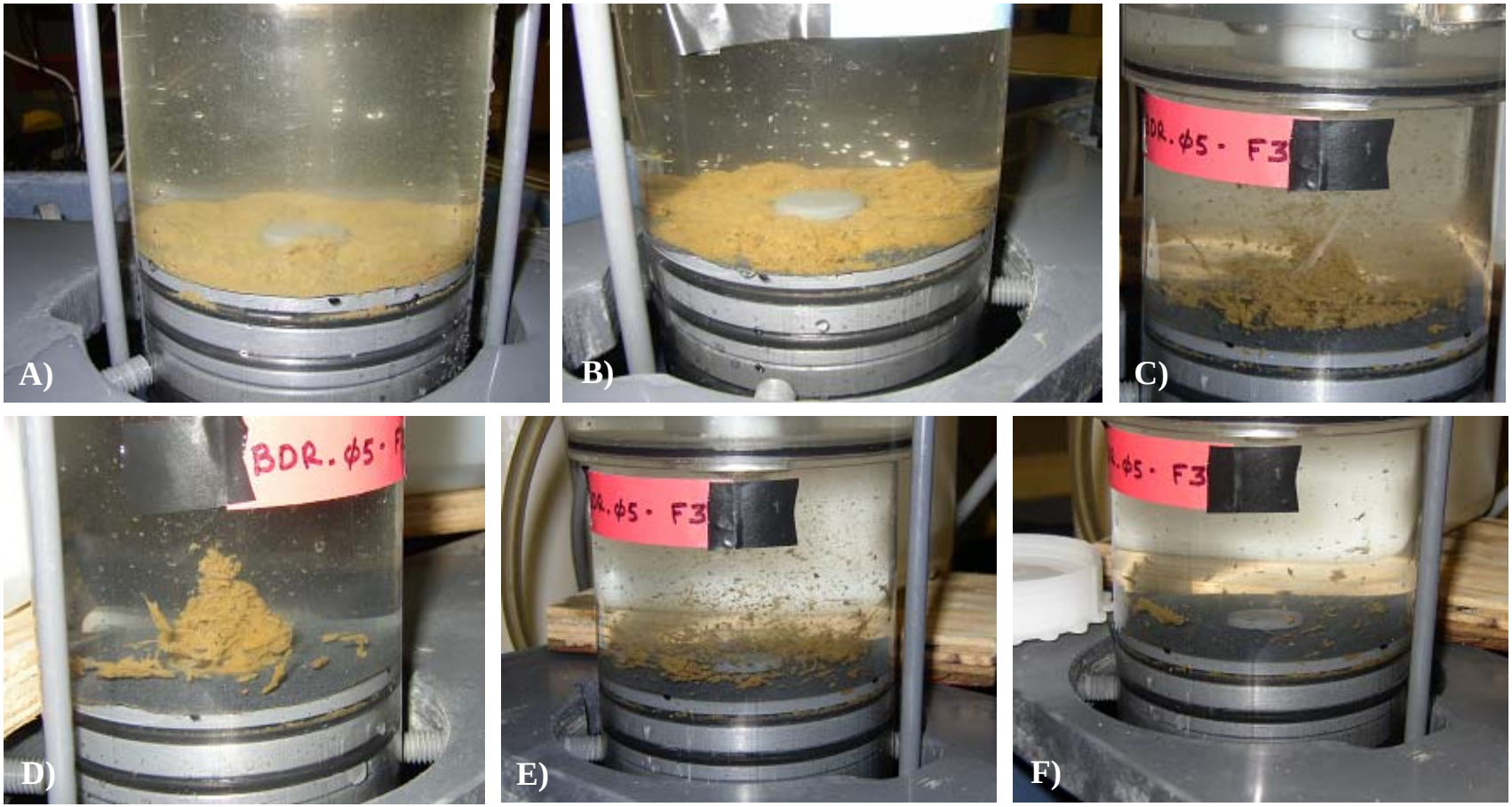

Fig. B.7

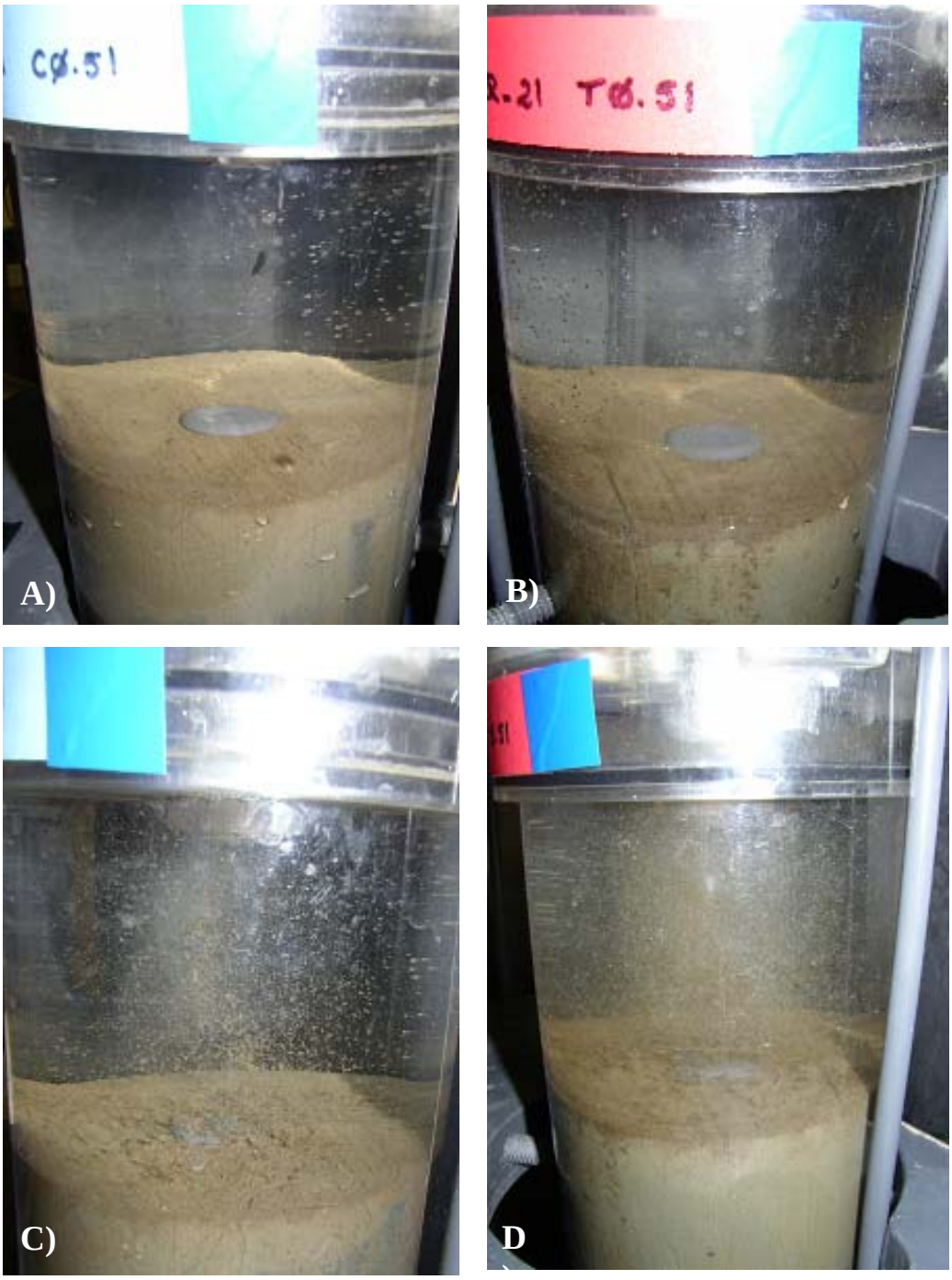

Fig. B.8

References

Aller, R. C. 1994. Bioturbation and remineralization of sedimentary organic matter: effects of redox oscillation. Chemical Geology, *114*, 331-345.

Aller, R. C. 1988. Complete oxidation of solid phase sulfides by manganese and bacteria in anoxic marine sediments. Geochimica et Cosmochimica Acta, *52*, 751-765.

Alperin, M. J., C. S. Martens, D. B. Albert, I. S. Suayak, L. K. Benninger, N. E. Blair and R. A. Jahnke. 1999. Benthic fluxes and pore water concentration profiles of dissolved organic carbon in sediments from the North Carolina continental slope. Geochimica et Cosmochimica Acta, *63*, 427-448.

An, S. and S. B. Joye. 2001. Enhancement of coupled nitrification-denitrification by benthic photosynthesis in shallow estuarine sediments. Limnology and Oceanography, *46*, 62-74.

Anschutz, P., S. Zhong and B. Sundby. 1998. Burial efficiency of phosphorus and the geochemistry of iron in continental margin sediments. Limnology and Oceanography, *43*, 53-64.

Anschutz, P., K. Dedieu, F. Desmazes and G. Chaillou. 2005. Speciation, oxidation state, and reactivity of particulate manganese in marine sediments. Chemical Geology, *218*, 265-279.

Aspila, K. I., H. Agemian and A. S. Y. Chau. 1976. A semi-automated method for determination of inorganic, organic and total phosphate in sediments. Analyst, *101*, 187-197.

Barranguet, C. 1997. The role of microphytobenthic primary production in a Mediterranean mussel culture area. Estuarine, Coastal and Shelf Science, *44*, 753-765.

Bartoli, M., D. Nizzoli and P. Viaroli. 2003. Microphytobenthos activity and fluxes at the sediment-water interface: interactions and spatial variability. Aquatic Ecology, *37*, 341-349.

Biber, M. V., M. Dos Santos Afonso and M. Stumm. 1994. The coordination chemistry of weathering: IV. Inhibition of the dissolution of oxide minerals. Geochimica et Cosmochimica Acta, *58*, 1999-2010.

Bloesch, J. and N. M. Burns. 1980. A critical-review of sediment trap techniques. Swiss Journal of Hydrology, *42*, 15-55.

Blomqvist, S. and C. Kofoed. 1981. Sediment trapping – a sub-aquatic in situ experiment. Limnology and Oceanography, *36*, 585-590.

Boatman, C. D. and J. W. Murray. 1982. Modeling exchangeable NH4+ adsorption in marine sediments: process and controls of adsorption. Limnology and Oceanography, *27*, 99-110.

Borsuk, M. E., S. P. Powers and C. H. Peterson. 2002. A survival model of the effects of bottom-water hypoxia on the population density of an estuarine clam (*Macoma balthica*). Canadian Journal of Fisheries and Aquatic Sciences, *59*, 1266-1274.

Boudreau, B. P. 1997. Diagenetic models and their implementation: Modeling transport and reactions in aquatic sediments. Springer, New York.

Boudreau, B. P. and D. E. Canfield. 1988. A provisional diagenetic model for pH in anoxic porewaters: Application to the FOAM sites. Journal of Marine Research, *46*, 429-455.

Boynton, W. R. and W. M. Kemp. 1985. Nutrient regeneration and oxygen consumption by sediments along an estuarine salinity gradient. Marine Ecology Progress Series, *23*, 45-55.

Burdige, D. J. and J. Homstead. 1994. Fluxes of dissolved organic-carbon from Chesapeake Bay sediments. Geochimica et Cosmochimica Acta, *58*, 3407-3424.

Burdige, D. J., M. J. Alperin, J. Homstead and C. Martens. 1992. The role of benthic fluxes of dissolved organic-carbon in oceanic and sedimentary carbon cycling. Geophysical Research Letters, *19*, 1851-1854.

Caffrey, J. M., J. E. Cloern and C. Grenz. 1998. Changes in production and respiration during a spring phytoplankton bloom in San Francisco Bay, California, USA: Implications for net ecosystem metabolism. Marine Ecology Progress Series, *172*, 1-12.

Canfield, D. E. 1989. Reactive iron in marine sediments. Geochimica et Cosmochimica Acta, *53*, 619-632.

Canfield, D. E., R. Raiswell, J. T. Westrich, C. M. Reaves and R. A. Berner. 1986. The use of chromium reduction in the analysis of reduced inorganic sulfur in sediments and shales. Chemical Geology, *54*, 149-155.

Canfield, D. E., R. Raiswell and S. Bottrell. 1992. The reactivity of sedimentary iron minerals toward sulfide. American Journal of Science, *292*, 659-683.

Capone, D. G. and R.P. Kiene. 1988. Comparison of microbial dynamics in marine and freshwater sediments: contrasts in anaerobic carbon catabolism. Limnology and Oceanography, *33*, 725-749.

Carignan, R. and R. J. Flett. 1981. Postdepositional mobility of phosphorus in lake sediments. Limnology and Oceanography, *26*, 361-366.

Cerco, C. F., and S. P. Seitzinger. 1997. Measured and modeled effects of benthic algae on eutrophication in Indian River-Rehoboth Bay, Delaware. Estuaries, *20*, 231-248.

Chambers, R. M., J. T. Holligbaugh, and S. M. Vink. 1994. Sulfate reduction and sediment metabolism in Tomales Bay, California. Biogeochemistry, *25*, 1-18.

Chen, Y. S. R., J. N. Butler and W. Stumm. 1973. Kinetic study of phosphate reaction with aluminum oxide and kaolinite. Environmental Science and Technology, *7*, 327-332.

Christensen, K. K., F. O. Andersen and H. S. Jensen. 1997. Comparison of iron, manganese, and phosphorus in freshwater littoral sediment with growth of *Littorella uniflora* and benthic microalgae. Biogeochemistry, *38*, 149-171.

Cline, J. D. 1969. Spectrophotometric determination of hydrogen sulfide in natural waters. Limnology and Oceanography, *14*, 454-458.

Cognie, B. and L. Barille. 1999. Does bivalve mucus favor the growth of their main food source, microalgae? Oceanologica Acta, *22*, 441-450.

Cornwell, J. C., and J. W. Morse. 1987. The characterization of iron sulfide minerals in anoxic marine sediments. Marine Chemistry, *22*, 193-206.

Cornwell, J. C., and P. J. Sampou. 1995. Environmental controls on iron sulfide mineral formation in a coastal plain estuary. Geochemical Transformations of Sedimentary Sulfur. ACS Symposium Series, pp. 224-242.

Cornwell, J. C., D. J. Conley, M. Owens, and J. C. Stevenson. 1996. A sediment chronology of the eutrophication of Chesapeake Bay. Estuaries, *19*, 488-499.

Cowan, J. L. W., and W. R. Boynton. 1996. Sediment-water oxygen and nutrient exchanges along the longitudinal axis of Chesapeake Bay: Seasonal patterns, controlling factors and ecological significance. Estuaries, *19*, 562-580.

Crosby, S. A., G. E. Millward, E. I. Butler, D. R. Turner and M. Whitfield. 1984. Kinetics of phosphate adsorption by iron oxyhydroxides in aqueous systems. Estuarine, Coastal and Shelf Science, *19*, 257-270.

Dalsgaard, T. 2003. Benthic primary production and nutrient cycling in sediments with benthic microalgae and transient accumulation of macroalgae. Limnology and Oceanography, *48*, 2138-2150.

Dame R. F., R. G. Zingmark and E. Haskin. 1984. Oyster reefs as processors of estuarine materials. Journal of Experimental Marine Biology and Ecology, *83*, 239-247.

Dame R. F., J. D. Spurrier and T. G. Wolaver. 1989. Carbon, nitrogen and phosphorus processing by an oyster reef. Marine Ecology Progress Series, *54*, 249-256.

Dame R. F., Spurrier J. D. and R. G. Zingmark. 1992. In situ metabolism of an oyster reef. Journal of Experimental Marine Biology and Ecology, *164*, 147-159.

Dame R. and S. Libes. 1993. Oyster reefs and nutrient retention in tidal creeks. Journal of Experimental Marine Biology and Ecology, *171*, 231-238.

Diaz, R. J. and R. Rosenberg. 1995. Marine benthic hypoxia: a review of its ecological effects and the behavioral responses of benthic macrofauna. Oceanography and Marine Biology Annual Review, *33*, 245-303.

Epping E. H. G., V. Schoemann, H. de Heji. 1998. Manganese and iron oxidation during benthic oxygenic photosynthesis. Estuarine, Coastal and Shelf Science, *47*, 753-767.

Eyre, B. D. and A. J. P. Ferguson. 2005. Benthic metabolism and nitrogen cycling in a subtropical east Australian Estuary (Brunswick): Temporal variability and controlling factors. Limnology and Oceanography, *50*, 81-96.

Fear, J. M., S. P. Thompson, T. E. Gallo and H. W. Paerl. 2005. Denitrification rates measured along a salinity gradient in the eutrophic Neuse River estuary, North Carolina, USA. Estuaries, *38*, 608-619.

Ferguson, A. J. P., B. D. Eyre and J. M. Gay. 2003. Organic matter and benthic metabolism in euphotic sediments along shallow sub-tropical estuaries, northern New South Wales, Australia. Aquatic Microbial Ecology, *33*, 137-154.

Ferguson, A. J. P., B. D. Eyre and J. M. Gay. 2004. Benthic nutrient fluxes in euphotic sediments along shallow sub-tropical estuaries, northern New South Wales, Australia. Aquatic Microbial Ecology, *37*, 219-235.

Fisher, T. R., L. W. Harding, D. W. Stanley and L. G. Ward. 1988. Phytoplankton, nutrients, and turbidity in the Chesapeake, Delaware, and Hudson Estuaries. Estuarine, Coastal and Shelf Science, *27*, 61-93.

Fisher, T. R., J. D. Hagy III, W. R. Boynton and M. R. Williams. 2006. Cultural eutrophication in the Choptank and Patuxent estuaries of Chesapeake Bay. Limnology and Oceanography, *5*, 435-447.

Ford S. E. and M. R. Tripp. 1996. Diseases and defense mechanisms, *in* The Eastern Oyster, Crassostrea virginica, V. S. Kennedy, R. I. E. Newell and A. Eble, eds., Maryland Sea Grant Publication, College Park, 581-660.

Froelich, P. N. 1988. Kinetic control of dissolved phosphate in natural rivers and estuaries: A primer on the phosphate buffer mechanism. Limnology and Oceanography, *33*, 649-668.

Gardner, W. D. 1980a. Sediment trap dynamics and calibration – a laboratory evaluation. Journal of Marine Research, *38*, 17-39.

Gardner, W. D. 1980b. Field assessment of sediment traps. Journal of Marine Research, *38*, 41-52.

Gibb, M. M. 1979. A simple method for the rapid determination of iron in natural waters. Water Research, *13*, 295-297.

Gibbs M., F. Funnel, S. Pickmere, A. Norkko and J. Hewitt. 2005. Benthic nutrient fluxes along an estuarine gradient: influence of the pinnid bivalve Atrina zelandica in summer. Marine Ecology Progress Series, *288*, 151-164.

Gilbert F., P. Souchu, M. Bianchi, P. Bonin. 1997. Influence of shellfish farming activities on nitrification, nitrate reduction to ammonium and denitrification at the water-sediment interface of the Thau lagoon, France. Marine Ecology Progress Series, *151*, 143-153.

Gowen, R. J., P. Tett and K. J. Jones. 1992. Predicting marine eutrophication: The yield of chlorophyll from nitrogen in Scottish coastal waters. Marine Ecology Progress Series, *85*, 152-161.

Graneli, E. and K. Sundback. 1985. The response of planktonic and microbenthic algal assemblages to nutrient enrichment in shallow coastal waters, southwest Sweden. Journal of Experimental Marine Biology and Ecology, *85*, 253-268.

Green, M. A., R. C. Aller, J. K. Cochran, C. Lee, and J. Y. Aller. 2002. Bioturbation in shelf/slope sediments off Cape Hatteras, North Carolina: the use of 234 Th, Chl-a, and Br- to evaluate rates of particle and solute transport. Deep-Sea Research II, *49*, 4627-4644.

Gust, G. and V. Müller. 1997. Interfacial hydrodynamics and entrainment functions of currently used erosion devices, *in* Cohesive Sediments, N. Burt, W. R. Parker and J. Watts, eds., John Wiley & Sons, New York, 149-174 .

Hancke, K. and R. N. Glud. 2004. Temperature effects on respiration and photosynthesis in three diatom-dominated benthic communities. Aquatic Microbial Ecology, *37*, 265-281.

Hargrave, B. T. and N. M. Burns. 1979. Assessment of sediment trap collection efficiency. Limnology and Oceanography, *24*, 1124-1136.

Haven, D. S. and R. Morales-Alamo. 1966. Aspects of biodeposition by oysters and other invertebrate filter feeders. Limnology and Oceanography, *11*, 487-498.

Haven, D. S. and R. Morales-Alamo. 1968. Occurrence and transport of faecal pellets in suspension in a tidal estuary. Sedimentary Geology, *2*, 141-151.

Haven, D. S. and R. Morales-Alamo. 1970. Filtration of particles from suspension by the American oyster Crassostrea virginica. Biological Bulletin, Marine Biology Lab, Woods Hole, *139*, 248-264.

Henriksen, K., J. I. Hansen and T. H. Blackburn. 1981. Rates of nitrification, distribution of nitrifying bacteria and nitrate fluxes in different types of sediment from Danish waters. Marine Biology, *61*, 299-304.

Henriksen, K. and W. M. Kemp. 1988. Nitrification in estuarine and coastal marine sediments, *in* Nitrogen Cycling in Coastal Marine Environments, T. H. Blackburn and J. Sorensen, eds., Wiley and Sons, Chichester, 205-249.

Holland, A. F., A. T. Shaughnessy and M. H. Hiegel. 1987. Long-term variation in mesohaline Chesapeake Bay macrobenthos: Spatial and temporal patterns. Estuaries, *10*, 227-245.

Hou, L. J., M. Liu, H. Y. Jiang, S. Y. Xu, D. N. Oui, Q. M. Liui and B. L. Zhang. 2003. Ammonium adsorption by tidal flat surface sediments from the Yangtze estuary. Environmental Geology, *45*, 72-78.

Hulth, S., R. C. Aller and F. Gilbert. 1999. Coupled anoxic nitrification/manganese reduction in marine sediments. Geochimica et Cosmochimica, *63*, 49-66.

Ingall, E. and R. Jahnke. 1997. Influence of water column anoxia on the elemental fractionation of carbon and phosphorus during sediment diagenesis. Marine Geology, *139*, 219-229.

Ito, S. and T. Imai. 1955. Ecology of oyster bed. I. On the decline of productivity due to repeated cultures. Tohoku Journal of Agricultural Research, *4*, 9-26.

Jensen, H. S., P. Kristensen, E. Jeppesen and A. Skytthe. 1992. Iron:phosphorus ratio in surface sediment as an indicator of phosphate release from aerobic sediments in shallow lakes. Hydrobiologia, *235*, 731-743.

Jensen, H. S., P. B. Mortensen, F. O. Andersen, E. Rasmussen and A. Jensen. 1995. Phosphorus cycling in a coastal marine sediment, Aarhus Bay, Denmark. Limnology and Oceanography, *40*, 908-917.

Jeroshewski, P., C. Steuckart and M. Kuhl. 1996. An amperometric microsensor for the determination of H2S in aquatic environments. Analytical Chemistry, *68*, 4351-4357.

Jorgensen, B. B. 1977. The sulfur cycle of a coastal marine sediment (Limfjorden, Denmark). Limnology and Oceanography, *22*, 814-832.

Joye, S. B. and J. T. Hollibaugh. 1995. Influence of sulfide inhibition of nitrification on nitrogen regeneration in sediments. Science, *270*, 623-625.

Kana, T. M., O. C. Darkangel, M. D. Hunt, J. B. Oldham, G. E. Bennett and J. C. Cornwell. 1994. Membrane inlet mass-spectrometer for rapid high-precision determination of N-2, O-2, and Ar in environmental water samples. Analytical Chemistry, *66*, 4166-4170.

Kana,, T. M., M. B. Sullivan, J. C. Cornwell, and K. Groszkowski. 1998. Denitrification in estuarine sediments determined by membrane inlet mass spectrometry. Limnology and Oceanography, *43*, 334-339.

Kana, T. M. and D. L. Weiss. 2004. Comment on "Comparison of isotope pairing and N-2 : Ar methods for measuring sediment denitrification" by B. D. Eyre, S. Rysgaard, T. Dalsgaard, and P. Bondo Christensen. 2002. Estuaries, *25*, 1077-1087. Estuaries, *27*, 173-176.

Kaspar H. F., P. A. Gillespie, I. C. Boyer and A. L. MacKenzie. 1985. Effects of mussel aquaculture on the nitrogen cycle and benthic communities in Kenepuru Sound, Marlborough Sounds, New Zealand. Marine Biology, *85*, 127-136.

Kasten, S. and B. B. Jorgensen. 2000. Sulfate reduction in marine sediments, *in* Marine Geochemistry, H. D. Schulz and M. Zable, eds., Springer, Berlin, 263-282.

Kemp, W. M., P. Sampou, J. Caffrey, M. Mayer, K. Henriksen and W. R. Boynton. 1990. Ammonium recycling versus denitrification in Chesapeake Bay sediments. Limnology and Oceanography, *35*, 1545-1563.

Kemp, W. M., S. Puskaric, A. Fageneli, E. Smith, and W. Boynton. 1999. Pelagic-benthic coupling and nutrient cycling, i*n* Ecosystems at the land-sea margin: drainage

basin to coastal sea, T. Malone, A. Malej, L. Harding, N. Smodlaka and R. Turner, eds., American Geophysical Union, Washington, D. C., 295-339.

Kemp, W. M., W. R. Boynton, J. E. Adolf, D. F. Boesch, W. C. Boicourt, G. Brush, J. C. Cornwell, T. R. Fisher, P. M. Glibert, J. D. Hagy, L. W. Harding, E. D. Houde, D. G. Kimmel, W. D. Miller, R. I. E. Newell, M. R. Roman, E. M. Smith and J. C. Stevenson. 2005. Eutrophication of Chesapeake Bay: historical trends and ecological interactions. Marine Ecology Progress Series, *303*, 1-29.

Kennedy V. S. and L. L. Breisch. 1981. Maryland's oysters, research and management. Maryland Sea Grant, University of Maryland, College Park, 286 p.

Kerhin, R. T., et al. 1988. The surficial sediments of Chesapeake Bay, Maryland: Physical characteristics and sediment budget. Maryland Geological Survey, digital map series 05.1 version 3 (1997).

Kostka, J. E. and G. W. Luther III. 1995. Seasonal cycling of Fe in saltmarsh sediments. Biogeochemistry, *29*, 159-181.

Kreeger, D. A. and R. I. E. Newell. 2001. Seasonal utilization of different seston carbon sources by the ribbed mussel, Geukensia demissa (Dillwyn) in a mid-Atlantic salt marsh. Journal of Experimental Marine Biology and Ecology, *260*, 71-91.

Krom, M. D. and R. A. Berner. 1980. Adsorption of phosphate in anoxic marine sediments. Limnology and Oceanography, *25*, 797-806.

Krom, M. D. and R. A. Berner. 1981. The diagenesis of phosphorus in a nearshore marine sediment. Geochimica et Cosmochimica Acta, *45*, 207-216.

Lee, K.-Y., T. R. Fisher, and E. Rochelle-Newall. 2001. Modeling the hydrochemistry of the Choptank River basin using GWLF and Arc/Info: 2. Model Application. Biogeochemistry, *56*, 311-348.

Leon, I., G. Mendez and B. Rubio. 2004. Geochemical phases of Fe and degree of pyritization in sediments from Ria de Pontevedra (NW Spain): Implications of mussel raft culture. Ciencias Marina, *30*, 585-602.

Leventhal, J. and C. Taylor. 1990. Comparison of methods to determine degree of pyritization. Geochimica et Cosmochima Acta, *54*, 2621-2625.

Lijklema, L. 1980. Interaction of orthophosphate with iron (III) and aluminum hydroxides. Environmental Science and Technology, *14*, 537-541.

Luckenback, M. W., F. X. O'Beirn and J. Taylor. 1999. An introduction to culturing oysters in Virginia. Virginia Sea Grant, Gloucester Point, 24 p.

Luther, III, G. W. 1990. The frontier molecular orbital theory approach in geochemical processes, *in* Aquatic Chemical Kinetics, W. Stumm, ed., John Wiley & Sons, New York, 173-198.

Luther, III, G. W. 2005a. Acid volatile sulfide – A comment. Marine Chemistry, *97*, 198-205.

Luther, III, G. W. 2005b. Manganese(II) oxidation and Mn(IV) reduction in the environment-Two one-electron transfer steps versus a single two-electron step. Geomicrobiology Journal, *22*, 195-203.

Luther, III, G. W. and T. G. Ferdelman. 1993. Voltammetric characterization of iron (II) sulfide complexes in laboratory solutions and in marine waters and porewaters. Environmental Science and Technology, *27*, 1154-1163.

Luther, III, G. W., B. Sundby, B. L. Lewes, P. J. Brendel and N. Silverberg. 1997. Interactions of manganese with the nitrogen cycle: Alternative pathways to dinitrogen. Geochimica et Cosmochimica Acta, *61*, 4043-4052.

Ma, S., A. Noble, D. Butcher, R. E. Trouwborst and G. W. Luther III. 2006. Removal of H2S via an iron catalytic cycle and iron sulfide precipitation in the water column of dead end tributaries. Estuarine, Coastal and Shelf Science, *70*, 461-472.

MacIntyre, H. L., R. J. Geider and D. C. Miller. 1996. Microphytobenthos: The ecological role of the "secret garden" of unvegetated, shallow-water marine habitats. I. Distribution, abundance and primary production. Estuaries, *19*, 186-201.

Mackin, J. E., R. C. Aller and J. Y. Aller. 1988. The effects of iron reduction and non steady-state diagenesis on iodine, ammonium, and boron distributions in sediments from the Amazon continental shelf. Continental Shelf Research, *8*, 363-386.

Marvin-DiPasquale, M. C., and D. G. Capone. 1998. Benthic sulfate reduction along the Chesapeake Bay central channel. I. Spatial trends and controls. Marine Ecology Progress Series, *168*, 213-228.

Mazouni, N. 2004. Influence of suspended oyster cultures on nitrogen regeneration in a coastal lagoon (Thau, France). Marine Ecology Progress Series, *276*, 103-113.

Mazouni, N., J-C. Gaertner, J-M. Deslou-Paoli, S. Landrein and M. G. d'Oedenberg. 1996. Nutrient and oxygen exchanges at the water-sediment interface in a shellfish farming lagoon (Thau, France). Journal of Experimental Marine Biology and Ecology, *205*, 91-113.

McManus, J., W. M. Berelson, K. H. Coale, K. S. Johnson and T. E. Kilgore. 1997. Phosphorus regeneration in continental margin sediments. Geochimica et Cosmochimica Acta, *61*, 2891-2907.

Meyers, P. A. 1994. Preservation of elemental and isotopic identification of sedimentary organic matter. Chemical Geology, *144*, 289-302.

Meyers, P. A. 1997. Organic geochemical proxies of paleoceanographic, paleolimnologie, and paleoclimatic processes. Organic Geochemistry, *27*, 213-250.

Middelboe, M., N. Kroer, N. O. G. Jorgensen and D. Pakulski. 1998. Influence of sediment on pelagic carbon and nitrogen turnover in a shallow Danish estuary. Aquatic Microbial Ecology, *14*, 81-90.

Miles, A. and K. Sundback. 2000. Diel variation in microphytobenthic productivity in areas of different tidal amplitude. Marine Ecology Progress Series, *205*, 11-22.

Millero, F. J., S. Hubinger, M. Fernandez and S. Garnett. 1987. Oxidation of H2S in seawater as a function of temperature, pH and ionic strength. Environmental Science and Technology, *21*, 439-443.

Millero, F. J., T. Plese and M. Fernandez. 1988. The dissociation of hydrogen sulfide in seawater. Limnology and Oceanography, *33*, 269-274.

Miura, T. and T. Yamashiro. 1990. Size selective feeding of *Anodonta calipygos* a phytoplanktivorous freshwater bivalve, and viability of egested algae. Japanese Journal of Limnology, *51*, 73-78.

Mohlenberg, F. and H. U. Riisgard. 1978. Efficiency of particle retention in 13 species of suspension feeding bivalves. Ophelia, *17*, 239-246.

Morse, J. W. and J. C. Cornwell. 1987. Analysis and distribution of iron sulfide minerals in recent anoxic marine sediments. Marine Chemistry, *22*, 55-69.

Muller, P. J. and E. Suess. 1979. Productivity, sedimentation rate, and sedimentary organic matter in the oceans – Organic carbon preservation. Deep-Sea Research, *26*, 1347-1362.

Murphy, J. and J. P. Riley. 1962. A modified single solution method for determination of phosphate in natural waters. Analytica Chimica Acta, 27, 31-36.

Murray, L. and R. L. Wetzel. 1987. Oxygen production and consumption associated with the major autotrophic components in two temperate seagrass communities. Marine Ecology Progress Series, *38*, 231-239.

Murray, T. J., M. J. Oesterling, Virginia Sea Grant Marine Advisory Program. 2007. Virginia shellfish aquaculture. Situation and outlook report. Results of Virginia shellfish aquaculture crop, reporting survey 2005-2007. Virginia Sea Grant, Gloucester Point, 10 pp.

National Marine Fisheries Service. Fisheries Statistics Division, Silver Spring, Maryland. http://www.st.nmfs.gov/st1/commercial/landings/annual-landings.html.

National Research Council. 2004. Nonnative Oysters in the Chesapeake Bay. The National Academies Press, Washington, District of Columbia.

Nelson, K. A., L. A. Leonard, M. H. Posey, T. D Alphin and M. A. Mallin. 2004. Using transplanted oyster (Crassostrea virginica) beds to improve water quality in small tidal creeks: a pilot study. Journal of Experimental Marine Biology and Ecology, *298*, 347-368.

Newell, R. I. E. 1988. Ecological changes in Chesapeake Bay, Are they the result of overharvesting the American oyster, Crassostrea virginica? *In* Understanding the Estuary, M. P. Lynch and E. C. Krome, eds., Gloucester Point, Virginia, 536-546.

Newell, R. I. E. 2004. Ecosystem influences of natural and cultivated populations of suspension-feeding bivalve mollusks: a review. Journal of Shellfish Research, *23*, 51-61.

Newell, R. I. E. and S. J. Jordan. 1983. Preferential ingestion of organic material by the American oyster Crassostrea virginica. Marine Ecology Progress Series, *13*, 47-53.

Newell, R. I. E. and C. J. Langdon. 1996. Mechanisms and physiology of larval and adult feeding, *in* The Eastern Oyster, Crassostrea virginica, V. S. Kenneday, R. I. E. Newell and A. Eble, eds., Maryland Sea Grant Publication, 185-230.

Newell, R. I. E., J. C. Cornwell and M. S. Owens. 2002. Influence of simulated bivalve biodeposition and microphytobenthos on sediment nitrogen dynamics: a laboratory study. Limnology and Oceanography, *47*, 1367-1379.

Newell, R. I. E. and E. W. Koch. 2004. Modeling seagrass density and distribution in response to changes in turbidity stemming from bivalve filtration and seagrass sediment stabilization. Estuaries, *27*, 793-806.

Newell, R. I. E., T. R. Fisher, R. R. Holyoke and J. C. Cornwell. 2005. Influence of eastern oysters on nitrogen and phosphorus regeneration in Chesapeake Bay, USA, *in* The Comparative Roles of Suspension-feeders in Ecosystems, R. F. Dame and S. Olenin, eds., Dordrecht, Springer, 93-120.

Nilsson, P., B. Jonsson, I. L. Swanberg and K. Sundback. 1991. Response of a marine shallow-water sediment system to an increased load of inorganic nutrients. Marine Ecology Progress Series, *71*, 275-290.

O'Connor, B. D. S., J. Costelloe, B. F. Keegan and D. C. Rhoads. 1989. The use of REMOTS technology in monitoring coastal enrichment resulting from mariculture. Marine Pollution Bulletin, *20*, 384-390.

Odum, H. T. and C. M. Hoskin. 1958. Comparative studies on the metabolism of marine waters. Publications of the Institute of Marine Science, Texas, 5, 16-46, *in* A metabolism-based trophic index for comparing the ecological values of shallow-water sediment habitats, W. M. Rizzo, et al. 1996. Estuaries, *19*, 247-256.

Odum, H. T. and R. F. Wilson. 1962. Further studies on the reaeration and metabolism of Texas bays, 1958-1960. Publications of the Institute of Marine Science, Texas, 8, 23-55, *in* A metabolism-based trophic index for comparing the ecological values of shallow-water sediment habitats, W. M. Rizzo, et al. 1996. Estuaries, *19*, 247-256.

Olafsson, E., J. Ullberg and N-L. Arroyo. 2005. The clam *Macoma balthica* prevents *in situ* growth of microalgal mats: implications for meiofaunal assemblages. Marine Ecology Progress Series, *298*, 179-188.

Parfitt, R. L. 1989. Phosphate reactions with natural allophone, ferrihydrite and goethite. Journal of Soil Science, *40*, 359-369.

Parsons, T. R., Y. Maita, and C. M. Lalli. 1984. A manual of chemical and biological methods for seawater analysis. Pergamon Press, New York. 173 pp.

Patrick, Jr., W. H. and R. A. Khalid. 1974. Phosphate release and sorption by soils and sediments: Effect of aerobic and anaerobic conditions. Science, *186*, 53-55.

Peterson, B. J., B. Fry. 1987. Stable isotopes in ecosystem studies. Annual Review of Ecology and Systematics, *18*, 293-320.

Pietros, J. M. and M. A. Rice. 2003. The impacts of aquacultured oysters, Crassostrea virginica (Gmelin, 1791) on water column nitrogen and sedimentation: results of a mesocosm study. Aquaculture, *220*, 407-422.

Porter, E. T., J. C. Cornwell and L. P. Sanford. 2004. Effect of oysters Crassostrea virginica and bottom shear velocity on benthic-pelagic coupling and estuarine water quality. Marine Ecology Progress Series, *271*, 61-75.

Postma, D. 1993. The reactivity of iron oxides in sediments: a kinetic approach. Geochimica et Cosmochimica Acta, *57*, 5027-5034.

Reay, W. G., D. L. Gallagher and G. M. Simmons, Jr. 1995. Sediment-water column oxygen and nutrient fluxes in nearshore environments of the lower Delmarva Peninsula, USA. Marine Ecology Progress Series *118*, 215-227.

Revsbech, N. P. 1989. An oxygen microelectrode with a guard cathode. Limnology and Oceanography, *34*, 472-476.

Revsbech, N. P., B. B. Jorgensen and T. H. Blackburn. 1980a. Oxygen in the sea bottom measured with a microelectrode. Science, *207*, 1355-1356.

Revsbech, N. P., J. Sorensen, T. H. Blackburn and J. P. Lomholt. 1980b. Distribution of oxygen in marine sediments measured with microelectrodes. Limnology and Oceanography, *25*, 403-411.

Revsbech, N. P. and B. B. Jorgensen. 1983. Photosynthesis of benthic microflora measured with high spatial resolution by the oxygen microprofile method: capabilities and limitations of the method. Limnology and Oceanography, *28,* 749-756.

Revsbech, N. P., B. B. Jorgensen, T. H. Blackburn, and Y. Cohen. 1983. Microelectrode studies of the photosynthesis and O2, H2S, and pH profiles of a microbial mat. Limnology and Oceanography, *28*, 1062-1074.

Revsbech, N. P., J. Nielsen and P. K. Hansen. 1988. Benthic primary production and oxygen profiles, *in* Nitrogen cycling in coastal marine environments, T. H. Blackburn and J. Sorensen, eds., John Wiley & Sons, 69-83.

Richard, M., P. Archambault, G. Thouzean and G. Desrosiers. 2007. Summer influence of 1 and 2 yr old mussel cultures on benthic fluxes in Grande-Entrée lagoon, Iles-de-la-Madeleine (Quebec, Canada). Marine Ecology Progress Series, *338*, 131-143.

Rickard, D., A. Oldroyd and A. Cramp. 1999. Voltammetric evidence for soluble FeS complexes in anoxic estuarine muds. Estuaries, *22*, 693-701.

Risgaard-Petersen, N. 2003. Coupled nitrification-denitrification in autotrophic and heterotrophic estuarine sediments: On the influence of benthic microalgae. Limnology and Oceanography, *48*, 93-105.

Risgaard-Petersen, N., S. Rysgaard, L. Nielsen and N. P. Revsbech. 1994. Diurnal variation of denitrification and nitrification in sediments colonized by benthic microphytes. Limnology and Oceanography, *39*, 573-579.

Risgaard-Petersen, N., M. H. Nicolaisen, N. P. Revsbech and B. A. Lomstein. 2004. Competition between ammonia-oxidizing bacteria and benthic microalgae. Applied Environmental Microbiology, *70*, 5528-5537.

Risgaard-Petersen, N., R. L. Meyer and N. P. Revsbech. 2005. Denitrification and anaerobic ammonium oxidation in sediments: effects of microphytobenthos and NO3-. Aquatic Microbial Ecology, *40*, 67-76.

Rizzo, W. M. 1990. Nutrient exchanges between the water column and a subtidal benthic microalgal community. Estuaries, *13*, 219-226.

Rizzo, W. M. and R. L. Wetzel. 1985. Intertidal and shoal benthic community metabolism in a temperate estuary: Studies of spatial and temporal scales of variability. Estuaries, *8*, 343-351.

Rizzo, W. M. and R. L. Wetzel. 1986. Temporal variability in oxygen metabolism of an estuarine shoal sediment, *in* Estuarine Variability, D. A. Wolfe, ed., Academic Press, 227-239. *In* A metabolism-based trophic index for comparing the ecological values of shallow-water sediment habitats, W. M. Rizzo, et al. 1996. Estuaries, *19*, 247-256.

Rizzo, W. M., G. J. Lackey and R. R. Christian. 1992. Significance of euphotic, subtidal sediments to oxygen and nutrient cycling in a temperate estuary. Marine Ecology Progress Series, *86*, 51-61.

Rizzo, W. M., B. E. Berry, R. L. Wetzel, S. K. Dailey, G. J. Lackey and R. R. Christian. 1996. A metabolism-based trophic index for comparing the ecological values of shallow-water sediment habitats. Estuaries, *19*, 247-256.

Roden, E. E., and J. H. Tuttle. 1993. Inorganic sulfur cycling in mid and lower Chesapeake Bay sediments. Marine Ecology Progress Series, *93*, 101-118.

Rothschild, B. J., J. S. Ault, P. Goulletquer and M. Heral. 1994. Decline of the Chesapeake Bay oyster population: a century of habitat destruction and overfishing. Marine Ecology Progress Series, *111*, 29-39.

Rozan, T. F., M. Taillefert, R. E. Trouwborst, B. T. Glzaer, S. Ma, J. Herszage, L. M. Valdes, K. S. Price and G. W. Luther III. 2002. Iron-sulfur-phosphorus cycling in

sediments of a shallow coastal bay: implications for sediment nutrient release and benthic microalgal blooms. Limnology and Oceanography, *47*, 1346-1354.

Rullkötter, J. 2000. Organic matter: The driving force for early diagenesis, *in* Marine Geochemistry, H. D. Schulz and M. Zabel, eds., Springer, New York, 129-172.

Ruttenberg, K. and R. A. Berner. 1993. Authigenic apatite formation and burial in sediments from non-up-welling continental margin environments. Geochimica et Cosmochimica Acta, *57*, 991-1007.

Rysgaard, S., P. B. Christensen and L. P. Nielsen. 1995. Seasonal variation in nitrification and denitrification in estuarine sediment colonized by benthic microalgae and bioturbating infauna. Marine Ecology Progress Series, *126*, 111-121.

Rysgaard, S., P. Thastum, T. Dalsgaard, P. B. Christensen, N. P. Sloth. 1999. Effects of salinity on NH4+ adsorption capacity, nitrification, and denitrification in Danish estuarine sediments. Estuaries, *22,* 21-30.

Sanford, L. P. and J. P.-Y. 2001. A unified erosion formulation for fine sediments. Marine Geology, *179*, 9-23.

Schreiber, R. A. and J. R. Pennock. 1995. The relative contribution of benthic microalgae to total microalgal production in a shallow sub-tidal estuarine environment. Ophelia, *42*, 335-352.

Schluter, M., E. Sauter, H-P. Hansen, and E. Suess. 2000. Seasonal variations of bioirrigation in coastal sediments: Modelling of field data. Geochimica et Cosmochimica Acta, *64*, 821-834.

Schulz, H. D. 2000. Quantification of early diagenesis: Dissolved constituents in marine pore water, *in* Marine Geochemistry, H. D. Schulz and M. Zabel, eds., Springer, New York, 455 pp.

Seitzinger, S. P., W. S. Gardner and A. K. Spratt. 1991. The effect of salinity on ammonium sorption in aquatic sediments: Implications for benthic nutrient recycling. Estuaries, *14*, 167-174.

Simon, N. S. 1988. Nitrogen cycling between sediment and the shallow-water column in the transition zone of the Potomac River and estuary. I. Nitrate and ammonium fluxes. Estuarine, Coastal and Shelf Science *26*, 483-497.

Slomp, C. P. and W. van Raaphorst. 1993. Phosphate adsorption in oxidized marine sediments. Chemical Geology, *107*, 477-480.

Slomp, C. P., E. H. Epping, W. Helden and W. V. Raaphorst. 1996. A key role for iron-bound phosphorus in authigenic apatite formation in North Atlantic continental platform sediments. Journal of Marine Research, *54*, 1179-1205.

Sloth, N. P., H. Blackburn, L. S. Hansen, N. Risgaard-Petersen and B. A. Lomstein. 1995. Nitrogen cycling in sediments with different organic loadings. Marine Ecology Progress Series, *116*, 163-170.

Smith, G. F., E. B. Roach and D. G. Bruce. 2003. The location, composition, and origin of oyster bars in mesohaline Chesapeake Bay. Estuarine, Coastal and Shelf Science, *56*, 391-409.

Smith, G. F., D. G. Bruce, E. B. Roach, A. Hansen, R. I. E. Newell and A. M. McManus. 2005. Habitat conditions of mesohaline oyster bars in the Maryland Chesapeake Bay: An

assessment of 40 years of oyster management. North American Journal Fisheries Management, *25*, 1569-1590.

Solorzano, L. 1969. Determination of ammonia in natural waters by the phenolhypochlorite method. Limnology and Oceanography, *14*, 799-801.

Stumm, W. and J. J. Morgan. 1996. Aquatic chemistry, 3rd edition. John Wiley & Sons, New York, 1022 pp.

Sun, M.-Y., C. Lee and R. C. Aller. 1993. Laboratory studies of oxic and anoxic degradation of chlorophyll-a in Long Island Sound sediments. Geochimica et Cosmochimica Acta, *57*, 147-157.

Sundback, K. and W. Graneli. 1988. Influence of microphytobenthos on the nutrient flux between sediment and water: a laboratory study. Marine Ecology Progress Series, *43*, 63-69.

Sundback, K., V. Enoksson, W. Graneli, and K. Pettersson. 1991. Influence of sublittoral microphytobenthos on the oxygen and nutrient flux between sediment and water: a laboratory continuous-flow study. Marine Ecology Progress Series, *74*, 263-279.

Sundback, K., P. Nilsson, C. Nilsson and B. Jonsson. 1996. Balance between autotrophic and heterotrophic components and processes in microbenthic communities of sandy sediments: A field study. Estuarine, Coastal and Shelf Science, *43*, 689-706.

Sundback, K. and A. Miles. 2000. Balance between denitrification and microalgal incorporation of nitrogen in microtidal sediments, NE Kattegat. Aquatic Microbial Ecology, *22*, 291-300.

Sunback, K., A. Miles, and E. Goransson. 2000. Nitrogen fluxes, denitrification and the role of microphytobenthos in microtidal shallow-water sediments: an annual study. Marine Ecology Progress Series, *300*, 59-76.

Sundback, K., A. Miles, S. Hulth, L. Pihl, P. Engstrom, E. Selander, and A. Svenson. 2003. Importance of benthic nutrient regeneration during initiation of macroalgal blooms in shallow bays. Marine Ecology Progress Series, *246*, 115-126.

Sundback, K., F. Linares, F. Larson, and A. Wulff. 2004. Benthic nitrogen fluxes along a depth gradient in a microtidal fjord: The role of denitrification and microphytobenthos. Limnology and Oceanography, *49*, 1095-1107.

Sundby, B., C. Gobeil, N. Silverburg and A. Mucci. 1992. The phosphorus cycle in coastal marine sediments. Limnology and Oceanography, *37*, 1129-1145.

Sutton, A. J., T. R. Fisher and A. B. Gustafson. Submitted. Effects of restored stream buffers (CREP) on water quality in non-tidal streams in the Choptank River Basin. Submitted to Journal of Environmental Quality.

Tenore, K. R., L. F. Boyer and R. M. Cal. 1982. Coastal upwelling in the Rias Bajas, NW Spain. Contrasting the benthic regimes of the Rias de Arosa and de Muros. Journal of Marine Research, *40*, 701-768.

Thamdrup, B., H. Fossing and B. B. Jorgensen. 1994. Manganese, iron, and sulfur cycling in a coastal marine sediment, Aarhus Bay, Denmark. Geochimica et Cosmochimica Acta, *58*, 5115-5129.

Tiedje, J. M., S. Simkins and P. M. Groffman. 1989. Perspectives on measurement of denitrification in the field including recommended protocols for acetylene based methods. Plant And Soil, *115*, 261-284.

Tobias, C., A. Giblin, J. McClelland, J. Tucker, and B. Peterson. 2003. Sediment DIN fluxes and preferential recycling of benthic microalgal nitrogen in a shallow macrotidal estuary. Marine Ecology Progress Series, *257*, 25-36.

Tuttle, J. H. and R. B. Jonas. 1992. Influence of rafted oyster aquaculture on sediment processes. Final Report to Maryland Department of Natural Resources Tidewater Administration, Maryland Coastal Research Division, 112 pp.

Tyler, A. C. and K. J. McGlathery. 2003. Benthic algae control sediment-water column fluxes of organic and inorganic nitrogen compounds in a temperate lagoon. Limnology and Oceanography, *48*, 2125-2137.

Unisense A/S (1998) Microsensor technology for research. http://www.unisense.com. Cited 08 March 2007

United States Environmental Protection Agency. 1983a. Methods for chemical analysis of water and wastes. USEPA, Cincinnati (EPA 353.2).

United States Environmental Protection Agency. 1983b. Methods for chemical analysis of water and wastes. USEPA, Cincinnati (EPA 300.00).

United States Geological Survey. Stream flow data for the Choptank River, Greensboro, Maryland (01491000), http://waterdata.usgs.gov/.

University of California, Davis. Stable isotope data for duplicate Lowry Cove sediments, http://stableisotopefacility.ucdavis.edu.

Valiela, I., J. McClelland, J. Hauxwell, P. J. Behr, D. Hersh and K. Foreman. 1997. Macroalgal blooms in shallow estuaries: Controls and ecophysical and ecosystem consequences. Limnology and Oceanography, *42*, 1105-1118.

Van Heukelem, L., A. J. Lewitus, T. M. Kana and N. E. Craft. 1994. Improved separations of phytoplankton pigments using temperature-controlled high performance liquid chromatography. Marine Ecology Progress Series, *114*, 303-313.

Welker, C., E. Sdrigotti, S. Covelli and J. Faganeli. 2002. Microphytobenthos in the Gulf of Trieste (Northern Adriatic Sea): Relationship with labile sedimentary organic matter and nutrients. Estuarine, Coastal and Shelf Science, *55*, 259-273.

Williams, J. D. H., J. K. Syers, S. S. Shukla and R. F. Harris. 1971. Levels of inorganic and total phosphorus in lake sediments as related to other sediment parameters. Environmental Science and Technology, *5*, 1113-1120.

Source of Unpublished Materials

Cornwell, J.C. University of Maryland Center for Environmental Science, Horn Point Laboratory, P.O. Box 775, Cambridge, Maryland. E-mail: cornwell@hpl.umces.edu, tele: 410.221.8445.

Cornwell, J.C. and M.S. Owens. University of Maryland Center for Environmental Science, Horn Point Laboratory, P.O. Box 775, Cambridge, Maryland. E-mail: cornwell@hpl.umces.edu, tele: 410.221.8445.

Fisher, T.R. University of Maryland Center for Environmental Science, Horn Point Laboratory, P.O. Box 775, Cambridge, Maryland. E-mail: fisher@hpl.umces.edu, tele: 410.221.8432.